CHARACTERIZATION, CONTROL AND MODELING OF PHASE SEPARATION IN MIXED PHOSPHOLIPID-PERFLUORINATED FATTY ACID MONOLAYERS

A Thesis Submitted to the
College of Graduate Studies and Research
In Partial Fulfillment of the Requirements
For the Degree of Doctor of Philosophy
In the Department of Chemistry
University of Saskatchewan
Saskatoon, Saskatchewan

By

Ala' Fakhri Eftaiha

PERMISSION TO USE

In presenting this thesis in partial fulfillment of the requirements for a Postgraduate degree from the University of Saskatchewan, I agree that the Libraries of this University may make it freely available for inspection. I further agree that permission for copying of this thesis in any manner, in whole or in part, for scholarly purposes may be granted by the professor or professors who supervised my thesis work or, in their absence, by the Head of the Department or the Dean of the College in which my thesis work was done. It is understood that any copying or publication or use of this thesis or parts thereof for financial gain shall not be allowed without my written permission. It is also understood that due recognition shall be given to me and to the University of Saskatchewan in any scholarly use which may be made of any material in my thesis.

Requests for permission to copy or to make other use of material in this thesis in whole or part should be addressed to:

Head of the Department of Chemistry

University of Saskatchewan

110 Science Place

Saskatoon, Saskatchewan (S7N 5C9)

ABSTRACT

The overall objective of this PhD thesis research is to understand and control phase separation in mixed perfluorinated fatty acid-phospholipid surfactant systems that have applications as pulmonary surfactant (PS) mixtures, with an ultimate view of controlling film composition, morphology and mechanical properties. In this context the interaction between perfluorooctadecanoic acid (C18F), 1,2-dipalmitoyl-sn-glycero-3-phosphocholine (DPPC), the major component of native PS extract, and 1,2-dipalmitoyl-sn-glycero-3-phosphoglycerol (DPPG) has been explored in Langmuir monolayers and Langmuir–Blodgett (LB) films using a combination of atomic force microscopy (AFM), fluorescence microscopy (FM) and Brewster angle microscopy (BAM) measurements.

Thermodynamic and morphological studies of binary and ternary mixed films made of C18F, DPPC and DPPG indicated that both the phospholipids and C18F were miscible over a wide range of compositions. The mixed phospholipid-C18F films contained multimolecular aggregates that were highly enriched in the phospholipids. Furthermore, it was found that the magnitude of the DPPC-C18F interaction could be modulated by altering the concentration of sodium ions in the underlying subphase. Using a highly simplified lung mimic fluid (pH 7.4, 150mM NaCl), DPPC and C18F became fully immiscible. Moreover, the performance characteristics of the mixed films demonstrated the usefulness of C18F as an additive for PS formulations.

The effectiveness of a PS protein mimicking peptide was evaluated against DPPC to allow comparison with previous measurements of DPPC-C18F mixed system. The mixing thermodynamics of the peptide and DPPC in Langmuir monolayer implied a repulsive interaction between the film components. The hysteresis response of the mixed monolayer films

indicated that the lipid-protein mixture improved the re-spreading of DPPC films. Moreover, molecular-level organization of the mixed films explored by both FM and BAM confirmed the formation of liquid-expanded DPPC domains in the presence of minute amount of the peptide.

In order to obtain a thorough understanding of the effect of the deposition process and surfactant tail polarities on the interfacial behavior of perfluorocarbon-hydrocarbon mixed monolayer films, both BAM and AFM measurements of arachidic acid (C20) with perfluorotetradecanoic acid (C14F) and palmitic acid (C16) with C18F mixed monolayer were performed. These measurements revealed that film morphology was minimally perturbed upon its deposition onto solid substrates. Coarse grained molecular dynamics (MD) simulations of films comprised of DPPC molecules with tails of various polarities suggested that the phase separation between the monolayer components could be controlled by varying surfactant tail polarities.

ACKNOWLEDGMENTS

I would like to express my profound gratitude to my supervisor Dr. Matthew Paige for his invaluable support, useful suggestions and encouragement throughout this research work. I want to express my deep appreciation to Dr. Surajith Wanasundara and Dr. Richard Bowles for their supervision throughout the simulation project. I am grateful to Dr. Sophie Brunet for the microscopy measurements, to Marie Laurence-Tremblay and Dr. Jan Rainey (Dalhousie University) for the peptide synthesis, to Ken Thoms for the mass spectrometric measurements and to Dr. Keith Brown for his assistance with the NMR measurements.

I would also like to thank my committee members, Dr. David Palmer, Dr. Stephen Urquhart, Dr. Steve Reid and Dr. Susan Kaminskyj for their guidance during my PhD program.

I would like to acknowledge the Department of Chemistry and the Herzberg Fund for financial support, the past and the present staff of the Department of Chemistry as well as the members of Dr. Paige's group.

Last but not least, I am most grateful to my parents and to my sisters, Reem, Ola, Ruba and Ameera for their support and encouragement throughout the hard times.

To the soul of my father, Fakhri
To my mother, Ghada, with love

TABLE OF CONTENTS

LIST OF TABLES

LIST OF FIGURES

List of Abbreviations

AFM: Atomic Force Microscope

BAM: Brewster Angle Microscopy

Bodipy-PC: (2-(4,4-difluoro-5-methyl-4-bora-3a,4a-diaza-s-indacene-3-dodecanoyl)-1 hexadecanoyl-sn-glycero-3 phosphocholine)

C18F: Perfluorooctadecanoic, $C_{17}F_{35}COOH$

C_s: Isothermal compressibility

CFM : Confocal Fluorescence Microscopy

DPPC: 1,2-dipalmitoyl-sn-glycero-3-phosphocholine, $C_{40}H_{80}NO_8P$

DPPG: 1,2-dipalmitoyl-sn-glycero-3-phosphoglycerol, $C_{38}H_{74}O_{10}PNa$

FLIM: Fluorescence Lifetime Imaging

Hel 13-5: An α-Helical peptide made of 13 hydrophobic and 5 hydrophilic amino acids respectively

κ: Isothermal elasticity

LB: Langmuir Blodgett

LC: liquid-condensed

LE: liquid-expanded

NBD-PG: (1-palmitoyl-2-{12-[(7-nitro-2-1,3-benzoxadiazol-4-yl)amino]lauroyl}-sn-glycero-3-[phospho-rac-(1-glycerol)] (ammonium salt))

PC: Phosphatidyl choline

PG: Phosphatidyl glycerol

PL: Phospholipids

PS: Pulmonary surfactant

SP: Surfactant protein

CHAPTER 1 INTRODUCTION

1.1 Gas-Liquid Interface

An interface is defined as the region that separates two different phases of matter such as solid-liquid, solid–gas, and gas-liquid interfaces. For the gas-liquid interface, molecules at the phase boundary have different properties than those molecules buried in the bulk because their potential energies are significantly different. Understanding the properties of liquids at interfaces is important to elucidate the behavior of molecules that tend to adsorb to the interface, particularly surface active agents (surfactants).[1]

1.1.1 Surface Tension

The attractive forces between molecules in a bulk liquid are uniform in all directions. However, they are directed both laterally and toward the bulk liquid for molecules located on the gas side, because the number of nearest neighbor molecules is smaller in the surface than in the bulk. This makes the energy of surface molecules higher than bulk molecules.[2] Thus, to expand a liquid surface, work has to be done to overcome cohesive interactions between bulk molecules in order to bring them to the interface. Mathematically, this work is expressed as:[3]

$$dw = \gamma\, dA \qquad (1.1)$$

where dw corresponds to the work required to increase surface area, dA is the change in area and the proportionality constant γ is the surface tension.

The positive free energy associated with the surface molecules can be minimized through adsorption of surfactants under certain conditions. The basic chemical structure of surfactants consists of two portions, one a lyophobic or solvent repelling part and the other a lyophilic or solvent attracting part. The unfavorable interaction between the surfactants' lyophobic portion

and solvent molecules induce their adsorption to the interface, thereby reducing the free energy of the system.[4]

1.1.2 Thermodynamics of Interfaces: Fundamental Relationships

Gibbs described an ideal interface that separate two bulk phases (α and β) that have uniform thermodynamic properties by an infinite thin layer (σ). According to this model,[3] the total volume of the system (V) is

$$V = V^{\alpha} + V^{\beta}, \text{ where } V^{\sigma} = 0 \qquad (1.2)$$

By combining the first and second law of thermodynamics, one can obtain an equation that describes the change in internal energy in a closed system, in the absence of non-expansion work:

$$dU = TdS - PdV \qquad (1.3)$$

Here, dU corresponds to an infinitesimal change in internal energy of the system, TdS is the heat flow under reversible conditions and PdV is the expansion work. For the previously described Gibbs model, the internal energy expression becomes

$$dU = dU^{\alpha} + dU^{\beta} + dU^{\sigma} = TdS^{\alpha} - P^{\alpha}dV^{\alpha} + TdS^{\beta} - P^{\beta}dV^{\beta} + \gamma dA + TdS^{\sigma} + \sum \mu_i^{\alpha} dN_i^{\alpha} + \sum \mu_i^{\beta} dN_i^{\beta} + \sum \mu_i^{\sigma} dN_i^{\sigma} \qquad (1.4)$$

where γdA represents the surface expansion work and $\sum \mu_i dN_i$ is the contribution of the chemical potential μ_i of the i^{th} component in different phases to the total internal energy.

Equation (1.4) can be simplified by substituting dV^{α} in term of dV^{β} (equation (1.2)) and summing up the entropy terms to the following:

$$dU = TdS - P^{\alpha}dV - \left(P^{\beta} - P^{\alpha}\right)dV^{\beta} + \gamma dA + \sum \mu_i^{\alpha} dN_i^{\alpha} + \sum \mu_i^{\beta} dN_i^{\beta} + \sum \mu_i^{\sigma} dN_i^{\sigma} \qquad (1.5)$$

Using the Clausius inequality, the differential form of Helmholtz energy, dF is defined as

$$dF = dU - TdS - SdT \qquad (1.6)$$

By substituting the internal energy expression (equation (1.5)) in equation (1.6) at constant temperature and volume (i.e. dV and $dT = 0$) , the Helmholtz expression becomes

$$dF = \left(P^{\beta} - P^{\alpha}\right)dV^{\beta} + \gamma dA + \sum \mu_i^{\alpha} dN_i^{\alpha} + \sum \mu_i^{\beta} dN_i^{\beta} + \sum \mu_i^{\sigma} dN_i^{\sigma} \qquad (1.7)$$

According to this equation, the thermodynamic definition of surface tension is obtained from the variation in the Helmholtz free energy as a function of surface area at constant temperature, total volume, volume of phase β and total numbers of all components:

$$\left(\frac{\partial F}{\partial A}\right)_{T,V,V^{\beta},N_i} = \gamma \qquad (1.8)$$

By the same analogy, surface tension is defined as the change in Gibbs free energy (G) with surface area at constant temperature, pressure and total numbers of all components as follows

$$\left(\frac{\partial G}{\partial A}\right)_{T,P,N_i} = \gamma \qquad (1.9)$$

1.2 Langmuir Monolayers

Surfactant monolayers can be formed either by adsorption of water soluble amphiphiles to create a Gibbs monolayer or by spreading insoluble amphiphiles directly to the interface to form a Langmuir monolayer.[5] Figure 1-1 is a schematic representation that shows the formation of both monolayer types. The accumulation of surfactants at the air-water interface decreases the water surface tension. The difference in surface tension between a bare water surface (γ_o) and a monolayer covered surface (γ) is often defined in terms of a surface pressure (π):

$$\pi = \gamma_o - \gamma \qquad (1.10)$$

The adsorption process adopted by Gibbs relates the reduction in the surface tension to the amount of surfactant adsorbed from the bulk solution.[6] For Langmuir monolayers, the surface tension is varied as a function of area occupied per molecule at the interface by compressing or expanding the monolayer using a Langmuir trough (discussed later). Langmuir monolayer

describes surfactant film, as a two-dimensional analogous to an ideal gas. Similarly to pressure and volume, surface pressure varies with the area per molecule.[7]

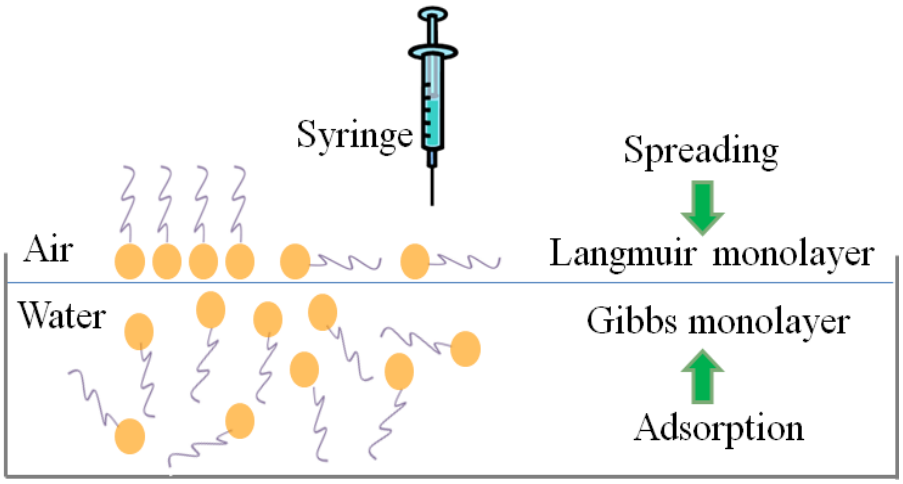

Figure 1-1 Schematic presentation of Gibbs (adsorbed) and Langmuir monolayers (this Figure has been redrawn from reference [5]).

1.2.1 Phases of Insoluble Monomolecular Films

Monomolecular insoluble films at the air-liquid interface, often referred to as Langmuir monolayers, are well-suited to explore the interfacial behavior of surfactants under controlled conditions. A broadly useful type of measurement for these systems is the surface pressure-area isotherm, in which the surface pressure of the system is measured as a function of mean molecular area at constant temperature. This measurement can provide useful thermodynamic information about the system.[8] Figure 1-2 shows a generalized surface pressure-mean molecular area isotherm of a Langmuir monolayer.

Analogous to three dimensional systems, monolayer films exhibit different phases (gaseous, liquid and solid) depending upon temperature, surface pressure, surfactant packing densities and chemical structure. Low packing densities of surfactant molecules at the air-water interface results in a gaseous phase, where surfactant molecules are distant from each other, with

an area per molecule in the range of hundreds square angstroms. The extent of attraction between molecules is negligible.[1,7,9]

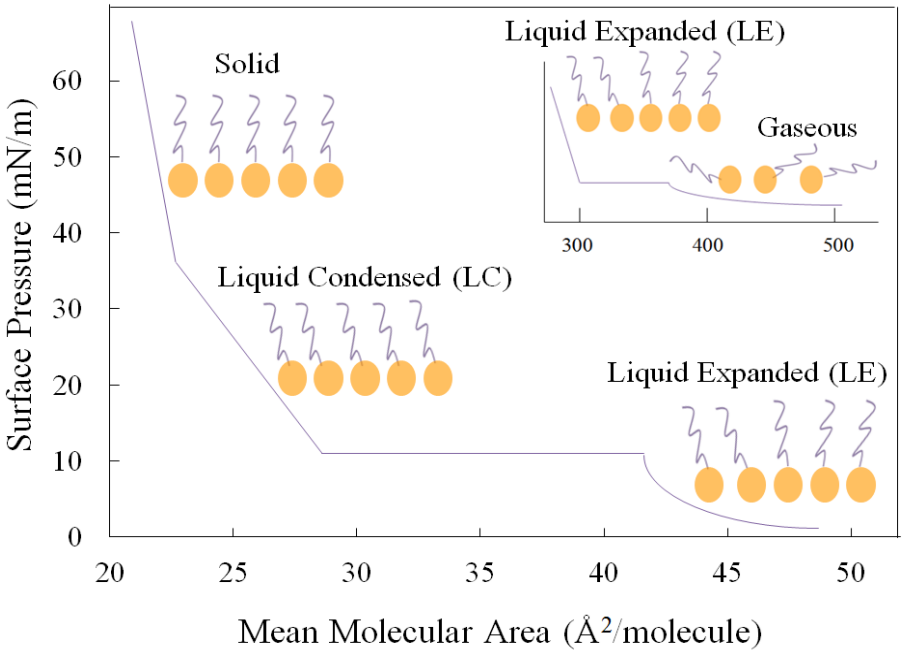

Figure 1-2 A schematic diagram of surface pressure-mean molecular area isotherm of a Langmuir monolayer. Not all the surfactant film may exhibit all of the indicated states and transitions (this Figure has been redrawn from reference [8]).

Increasing the molecular density of the monolayer, either by depositing additional surfactant or by compressing the monolayer, will lead to a detectable increase in surface pressure which signifies the onset of the liquid expanded (LE) phase. Although the lateral interaction between the amphiphilic molecules in the LE phase is increased, they remain mobile and show no lateral order. A further compression of the monolayer gives rise to the formation of a liquid condensed (LC) phase via a plateau or a constant pressure region that involves the coexistence of two phases. Here, the surfactant molecules become more closely packed and show a smaller tilt angle from the surface normal in comparison to those in the LE phase. Also, the monolayer becomes less compressible than the LE phase.[1,7,9]

As the film is further compressed, the surfactant side chains orient themselves perpendicular to the surface and the gaps between the closely packed vertical molecules vanish to form a solid phase. This phase is much less compressible than the LC phase. Extrapolation of the mean molecular area of the solid phase to zero surface pressure gives the cross-sectional area of a molecule under close-packed conditions. The highest surface pressure at which a solid monolayer can be compressed with enough room still available to accommodate all of the molecules in a single layer corresponds to the collapse pressure. If the monolayer film is compressed beyond this point, it becomes unstable and collapses.[1,7,9]

1.2.2 Mixed Monolayers

Mixed monolayer films are useful model systems to explore complex phenomena that take place in multicomponent surfactant systems such as biological membranes. Analogous to the thermodynamics of mixed gases and liquids, for a mixed monolayer system made of two surfactants A and B, if the intermolecular forces between A and B are same to those between A-A and B-B molecules, then the mixture is deemed to be ideal. The Gibbs energy of mixing of a multicomponent ideal film is calculated according to:[10]

$$\Delta G_{mix} = nRT \sum_{i=1}^{N} \chi_i ln\chi_i \qquad (1.11)$$

where ΔG_{mix} corresponds to the Gibbs energy of mixing, n is the total number of moles and χ_i is the mole fraction of the i^{th} component. Therefore, the entropy of mixing, ΔS_{mix} is:[2]

$$\Delta S_{mix} = -(\frac{\partial \Delta G_{mix}}{\partial T})_{p,N_i} = -nR \sum_{i=1}^{N} \chi_i ln\chi_i \qquad (1.12)$$

From equations (1.11) and (1.12), the enthalpy of mixing, ΔH_{mix}, is zero ($\Delta G = \Delta H - T\Delta S$). This is expected for ideal systems in which there are no additional interactions between A

and B molecules. It is concluded here that spontaneous mixing is driven by the increase in the entropy of the system, because $ln\chi_i$ is negative, which implies positive ΔS_{mix} for all compositions.

For non-ideal mixtures, A-A, B-B and A-B interactions are all different. In these cases, it is often useful to define thermodynamic excess functions, which are equal to the difference between the observed thermodynamic function of mixing and the function of the ideal system.[2]

This provides a convenient way of describing the properties of non-ideal mixtures. Positive values of excess Gibbs energy of mixing indicate that the film components are immiscible or are at least partially miscible, while negative values are an indication of intimate association between the film constituents.

Domain shapes and sizes in immiscible or phased separated mixed monolayers are mainly governed by a competition between line tension and dipole-dipole interaction between the monolayer forming components.[11,12] Line tension is defined as the energy per unit length exerted on the one-dimensional interface between two coexisting phases. Dipolar repulsive interactions take place between dipole components that are perpendicular to the plane of monolayers. These counteracting forces should lead to a minimum overall free energy for a particular system; monolayers tend to decrease high edge energies by reducing the total boundary length between segregated domains through formation of compact, often circular domains. This competes with dipolar repulsion that favors formation of domains and/or domains with extended shapes.[11,13]

1.2.3 Langmuir Trough

The Langmuir trough is an important tool for studying insoluble surfactant monolayers at the air-water interface. It can be integrated with a variety of surface characterization techniques

such as Brewster angle microscopy and fluorescence microscopy to investigate molecular structure and domain formation at the air–water interface.[14] As shown in Figure 1-3, the Langmuir trough is typically constructed of a polytetrafluoroethylene (Teflon) trough and contains two barriers that are parallel to the walls of the trough and in contact with the top of an aqueous subphase. A Langmuir monolayer is generally prepared by spreading a known amount of dilute surfactant solution, dissolved in volatile organic solvent or solvent mixtures, onto the subphase surface. The area occupied by each molecule at the surface is generally described in terms of the following expression:[7]

$$MMA = \frac{AM}{cN_A V} \qquad (1.13)$$

where MMA is the surfactant mean molecular area, A is trough area, M is surfactant molecular weight, c is surfactant concentration (g/L), N_A is Avogadro's number and V is the volume of surfactant solution that spreads on the liquid surface.

After allowing the solvent to evaporate for several minutes, the film area is controlled by the movable barrier(s). The change in surface tension as a result of compressing or expanding the film is measured by a Wilhelmy electro-balance, equipped with a Wilhelmy plate (typically made from a piece of absorbent paper or platinum) suspended in the subphase. One of the major concerns regarding the plate is that it should be completely wetted before the measurement to ensure a zero contact angle between the plate and the water. This is often overcome by using a roughened plate. The major merit of using a Wilhelmy plate to determine surface tension (or pressure) is that the plate is easily cleaned and maintained.[1,15] The movable barriers are made either of hydrophilic or hydrophobic materials. Although hydrophilic barriers prevent the leakage of aqueous subphase and surfactants, they may potentially adsorb the film materials. This can be avoided by using hydrophobic or specifically Teflon-made barriers.[16] Both film leakage and

surfactant adsorption should be taken in consideration, as they limit the ability to attain high surface pressure values even for a highly compressed monolayer. In addition, these effects can result in errors in measured molecular areas.

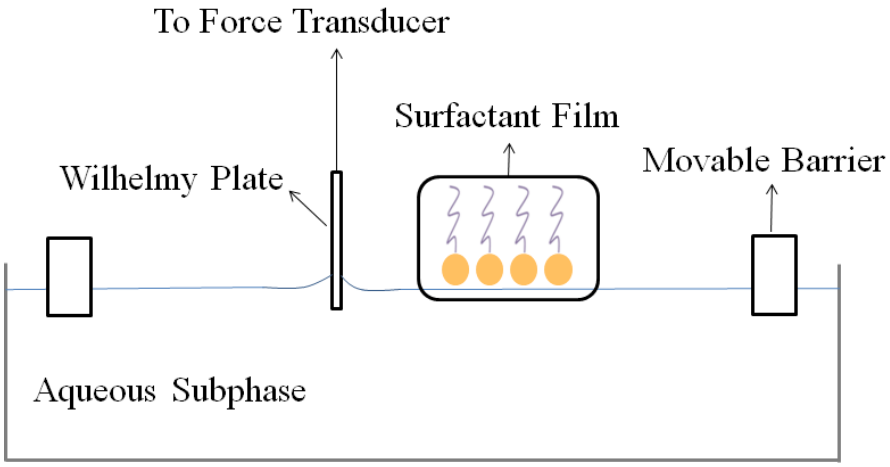

Figure 1-3 Schematic illustration of a Langmuir trough.

1.2.4 Langmuir-Blodgett Films

Insoluble monolayers can be transferred from the air-water interface onto the air-solid interface by a vertical movement of a solid substrate through the monolayer using the Langmuir–Blodgett (LB) technique. To facilitate the deposition process, the Langmuir trough is often equipped with a dipping well to accommodate the solid substrate below the Langmuir film. In principle, after compressing a surfactant film to a fixed surface pressure, the upward movement of a hydrophilic substrate through the film will result in depositing surfactant molecules with headgroups oriented towards the solid substrate and the tails exposed to the air.[17] A subsequent immersion and emersion of the substrate can result in multilayer deposition in a head-to-head configuration, known as Y-type. The surfactant molecules deposited on the upstroke orient their polar heads towards the substrate, while those deposited on the down stroke orient their tails facing the substrate.[7] Other configuration such as head-to-tail or tail-to-head structure may form

depending on the substrate hydrophilicity, its direction of movement (down or up-stroke), as well as the subphase pH and temperature.[18]

The quality of deposition is measured semi-quantitatively by a parameter called the transfer ratio, which is defined as the ratio of the change in the area occupied by the monolayer at constant surface pressure to the area of the substrate that is covered by the monolayer. A unity transfer ratio is often taken as a criterion for good deposition. Ratios above 1.05 or below 0.95 suggest poor film homogeneity.[1]

The ease of construction of both supported lipid monolayers and bilayers with a controlled molecular density by this class of techniques offers the possibility of engineering model systems for biomembranes with the aid of understanding the features of freestanding membranes. Moreover, the diversity of the film imaging techniques in terms of spatial resolution and mechanism of contrast makes LB films appealing to explore structure, orientation, domain formation and topography of mixed film systems. However, caution must also be taken that the LB deposition process itself does not alter the surfactant film structure, as has been seen in a number of surfactant systems.[19]

A variety of solid substrates can be used to prepare LB films. The choice of substrate depends to a great extent on the characterization techniques that will be used to investigate the deposited film. The most convenient substrate is one that provides optical transparency, flatness, ease of cleaning and causes no perturbation to the film morphology. During this PhD thesis, mica and glass substrates have been used to prepare LB films, because they are compatible with atomic force microscopy and fluorescence microscopy (discussed in details in the subsequent section). Mica is a clay mineral of the formula $KAl_2Si_3AlO_{10}(OH)_2$. It is semi-transparent, easy to cleave by scotch tape and to cut with scissors, and is well-suited for atomic force microscopy

studies because it cleaves to give large, atomically flat layers. However, the semitransparent nature of mica limits its usefulness for fluorescence microscopy measurements. For optical measurements, glass slides are generally preferable. These slides must be cleaned extensively, typically by a plasma-cleaner, to remove production impurities. It is worth noting that the total charge of mica surface depends on both the pH of the aqueous media and the ion exchange properties of mica. In general, the dissolution of cations such as $Si^{4+}$and Al^{3+} will result in a negatively charged surface, similarly to the charge acquired by the glass surface.[3,20]

1.3 Fundamentals of Pulmonary Surfactant

Lungs are essential respiration organs in animals. Their principal function is to transport oxygen from the atmosphere into the bloodstream, and to release carbon dioxide outside the body. This gas exchange is accomplished through millions of tiny, thin-walled air sacs called alveoli. A typical pair of human lungs contains several hundred million alveoli that are lined with a thin aqueous layer, covered by a film of pulmonary surfactant (PS). The major function of this film is to reduce the surface tension at the alveolar surface to maintain normal respiratory mechanics and function. Deficiency and/or dysfunction of PS can cause severe respiratory diseases. Exogenous surfactants therapeutics are standard intervention for such diseases. The development of effective therapeutics requires collaboration between diverse research fields with common interests in the surfactant system. In this context, biophysics, surface chemistry and thermodynamics are important to explore the interfacial molecular behavior of natural and synthetic additives that might be able to mimic the biophysical properties of the endogenous surfactant.[21]

1.3.1 Surfactant Composition

Endogenous PS is a mixture of lipids and proteins, approximately 90% and 10% by weight respectively (presumably this varies from species to species), that forms an insoluble monomolecular film at the gas exchange interface in the lung alveoli. Phospholipids (PL) are the major constituent of the lipids (~90–95 wt%), where the most abundant constituent is dipalmitoyl phosphatidylcholine (DPPC, Figure 1-4, ~35% of the total PL). DPPC is comprised of two fully saturated, sixteen carbon chains fatty acyl chains esterified at C-1 and C-2 of glycerol and a zwitterionic head group attached to the third carbon of the glycerol backbone via a phosphate moiety, which is connected to a choline head group. Anionic, unsaturated phosphatidylglycerols are the other prominent PL components, in addition to small amounts of other lipids such as phosphatidylethanolamines.[9]

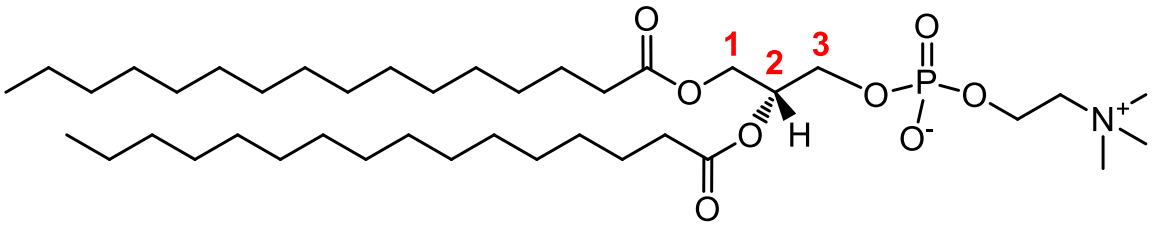

Figure 1-4 Chemical structure of dipalmitoyl phosphatidylcholine (DPPC).

Four pulmonary surfactant proteins (SPs) are often found associated with the previously described lipids.[9,21] The SPs have been named SP-A, B, C and D. Both, SP-A and D are large and hydrophilic glycoproteins, while SP-B and C are smaller and extremely hydrophobic proteins. Functionally, no role has been definitively determined for SP-D in the surface activity of lung surfactant, however, along with SP-A, it is believed to participate in host-defense mechanism(s) of the lungs. It have been reported that SP-A, B and C play a substantial role in increasing surface activity of endogenous lung surfactant and also play an important role in enhancing surfactant respreading.[9,21]

1.3.2 Biophysical Properties of Pulmonary Surfactant

Alveoli are spherical structures at the terminal ends of the respiratory airways, with a diameter ranging from about 75 to 300 micrometers in adults.[22] In the absence of PS, the surface tension across the alveolar interface is ~ 70 mN/m. According to the Young-Laplace equation, which relates the pressure gradient across a curved interface to its radius and surface tension, a high pressure is required either to inflate or to maintain stable alveoli structures. However, the presence of surfactants reduces the surface tension at the aqueous surface of the alveoli, which reduces the work of breathing and stabilizes alveolar inflation and deflation.[9]

This ability of PS to decrease surface tension to remarkably low values upon film compression is attributed to the interfacial behavior of saturated PL, particularly DPPC, which tends to pack tightly in a highly compressed monolayer by directing its fatty acid chains perpendicular to the surface. In contrast, unsaturated PL has a large cross sectional area that disrupts packing in condensed films, which prevents low surface tensions from being reached. However, not all PL have a similar behavior to DPPC, which highlights the influence of the headgroup on surfactant phase behavior. Theoretically, the phosphotidylcholine headgroup of DPPC tends to dehydrate at high degrees of compression which contributes toward the formation of highly packed molecular structures. This gives it performance superiority over the other PL in PS.[9,21]

In addition to achieving low surface tension values upon film compression, PS should be able to absorb rapidly to the air-water interface and replenish surface films upon subsequent film re-expansion. However, DPPC films exhibit a large hysteresis and poor re-spreading on successive compression-expansion cycles. This might be explained by the limited molecular movement of DPPC molecules in the interfacial region of highly compressed film, which may

constrain its ability to reorient and reorganize. However, the presence of compounds that disrupt surfactant packing such as unsaturated phospholipids, particularly, phosphatidyl glycerol or cholesterol, increases dynamic re-spreading and decreases the stability of post-collapse films.[9,23]

No single PS constituent is rigid enough to sustain near-zero surface tension and yet fluid enough to re-spread rapidly. The selective squeeze-out hypothesis suggests the ejection of fluid lipids upon monolayer compression to leave behind a film that is highly enriched in saturated lipids, particularly DPPC, to allow reduction of surface near zero value.[9,21] At high compression, the rigid film collapses to form both surface and subsurface aggregates. Upon subsequent expansion, surface associated proteins (SP-B and C) promote and facilitate the re-spreading of the squeezed-out surfactant back into the interface.[21,23]

The Langmuir trough is one of the most popular techniques to measure surface tension lowering, re-spreading, and hysteresis properties of both endogenous and exogenous PS. It provides an approach to examine film morphologies in-situ or ex-situ through LB films. However, it has a number of drawbacks for studying PS. In addition to film leakage and surfactant adsorption described previously, it requires a large subphase volume to fill the trough, which makes it not ideal for studying surfactant adsorption, since the average thickness of the alveoli lining layer is about 0.14 μm.[9] Also, it allows for relatively slow cycling rates that are below the range in normal respiration.

1.4 Perfluorinated Surfactants

Fluorinated surfactants are synthetic amphiphilic molecules, obtained by replacement of hydrogen atoms along the carbon backbone of the hydrophobic tail by fluorine atom(s). The outstanding chemical inertness and thermal stability of these surfactants in comparison with their hydrogenated counterparts make them convenient for multiple applications in material science

such as cookware, clothing and firefighting foams. There are significant concerns relating to the bioaccumulation and potential toxicity of some fluorinated molecules, but there are nonetheless numerous valuable biomedical applications for these materials such as blood substituents and as additives in lung replacement therapeutics.[24,25]

The useful surface properties of fluorinated compounds come from both the extreme electronegativity and the large size of fluorine atom. A comparison of some basic properties of fluorinated and hydrogenated compounds is presented in Figure 1-5. The larger radius fluorine atom compared to hydrogen atoms (1.47 vs. 1.20 Å) results in fluorinated chains being more bulky than their hydrogenated counterparts with a cross sectional area of about 27-30 $Å^2$ for the former and 18-21 $Å^2$ for the latter.[26] This also causes the chain conformation to change from zigzag (adopted by hydrocarbon chains) to helical structure in order to alleviate the steric hindrance between the CF_2 groups along the carbon chain. In addition, the lower polarizability of fluorine compared to hydrogen results in weaker intermolecular interactions between the fluoroalkyl chains compared to aliphatic chains. As a result, fluorinated surfactants tend to be more volatile and to have lower cohesive and surface energies than the analogous hydrocarbon surfactants. Consequently, the mixing of fluorinated surfactant, particularly fully fluorinated (perfluorinated) surfactants with hydrocarbon amphiphiles may yield a fully miscible, partially miscible or phase separated system based on the precise chemical nature of the compounds under investigation. Here, particular attention should be paid to head group interactions and any factor that may modulate it, since these effects contribute heavily to the overall miscibility of the system.[26-28]

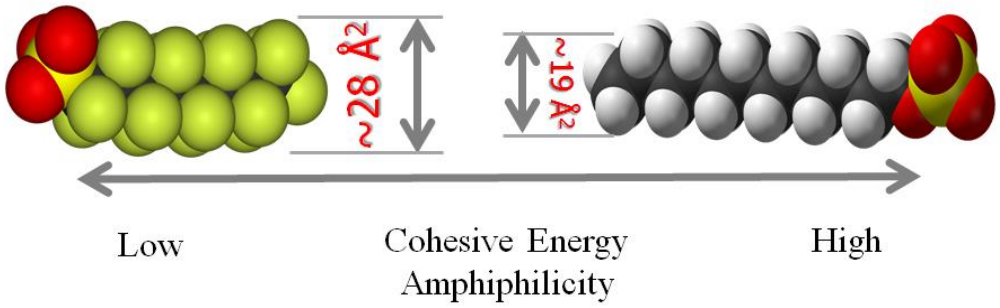

Figure 1-5 A schematic representation showing differences in cross sectional area, amphiphilicity and cohesive energy between fluorinated (left) and hydrogenated (right) surfactant molecules (this Figure has been redrawn from reference [26]).

The significance of surfactant immiscibility in mixed hydrogenated-fluorinated Langmuir monolayer arises from the ability of surfactant molecules to reorganize upon film compression, which is functionally important for PS application, especially if the one component has a lower collapse pressure and higher tendency to adsorb at the air-water interface after repeated compression expansion cycles.[29] In a phase separated film, molecules or patches of surfactant with lower affinity for the interface will tend to be excluded preferentially from the film during compression, which will refine the surface composition. This is considered the most important concept of the previously described squeezing out hypothesis. In addition to this, surfactant immiscibility will be helpful to control surface patterns and to engineer robust and stable films.

1.5 Monolayer Characterization Techniques

A wide range of surface-sensitive microscopy techniques, namely atomic force microscopy, confocal fluorescence microscopy and Brewster angle microscopy have been used to examine the morphology, composition and the underlying molecular-level organization of mixed lipid monolayers throughout this research project. While none of these techniques provide all of the information necessary to characterize the surfactant system thoroughly, they can give complementary information in terms of spatial resolution and mechanism of contrast to monitor

the surfactant structures, domain formation and phase coexistence both at air-water or air solid interfaces.[14,30]

1.5.1 Brewster Angle Microscopy

Brewster angle microscopy (BAM) is a reflectance-based technique that can provide real-time imaging of lipid monolayers in a Langmuir trough.[3,14,30] When a ray of light passes an interface between two media of different refractive index, part of the ray is reflected and the remaining is refracted. Snell's law describes the relationship between the angles of incidence and refraction, measured with respect to the surface normal, according to the following formula:

$$\frac{sin\theta_i}{sin\theta_t} = \frac{n_t}{n_i} \qquad (1.14)$$

where θ_i and θ_t represent the angle of incidence and refraction respectively and n_i and n_t are the refractive index of the respective medium. If $n_t > n_i$, i.e., the light is initially traveling within the lower refractive index medium, then the refracted ray will bend toward the surface normal. The law of refraction indicates that the refracted ray lies on the opposite side of the normal from the incident ray and both rays lie in the same plane.

If a parallel polarized light, i.e. its electric field component parallel to the plane of incidence, goes from a lower to a higher index medium, the ratio of the amplitude of the reflected electrical field component to that of the incident component decrease gradually over the entire range of θ_i until it equals zero and the incident beam is completely transmitted. This takes at a particular value of incidence angle, namely the Brewster angle, at which the angle between the reflected and refracted beams is 90°.[31] Accordingly, equation (1.14) becomes:

$$tan\,\theta_1 = \frac{n_2}{n_1} \qquad (1.15)$$

Because, $sin\theta_2 = sin(90^\circ - \theta_1) = cos\theta_1$. The general of principle of BAM is presented schematically in Figure 1-6. Illuminating the air-water interface by a parallel polarized light at the Brewster angle (around 53°), no reflection occurs and the surface appears as a dark area. However, in the presence of an insoluble monolayer at the interface, the light will be reflected and the film will appear as a bright region.

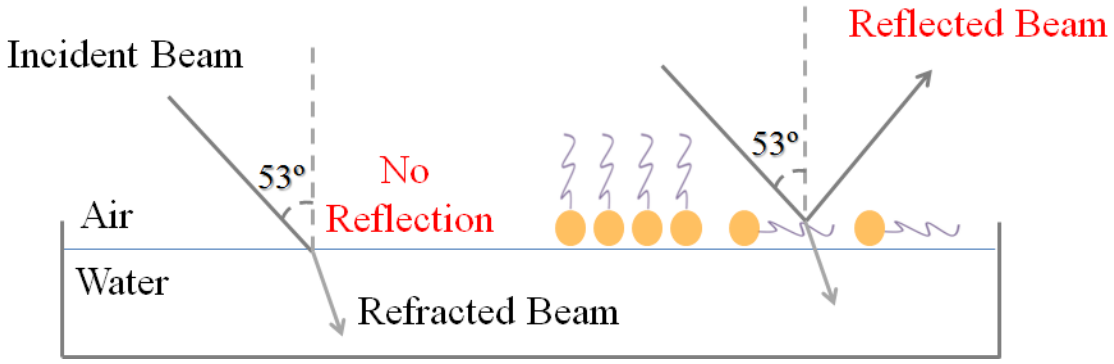

Figure 1-6 Physical principle of Brewster angle microscopy (this Figure has been redrawn from reference [32]).

In a typical configuration, a Brewster angle microscope is mounted to a Langmuir trough and coupled with a CCD camera. This allows collection of images of monolayer film structure at different molecular densities directly at the air-water interface with video frame rates to explore gross film morphology and dynamics. This approach allows monolayer visualization with a micrometer spatial resolution. While the spatial resolution limits the ability to extract molecular-scale information, BAM does not require the addition of probe molecules to the surfactant film to generate a contrast as in fluorescence microscopy.[30,33]

1.5.2 Atomic Force Microscopy

Atomic force microscopy (AFM) is a variation of scanning probe microscopy based on interaction between a probe tip and sample. It can provide morphological information about various types of samples, ranging from soft biological materials such as DNA and proteins, to

hard surfaces, with micrometer to nanometer length-scale resolution. These properties make it a well-suited approach for morphological imaging of LB films.[3,14]

The operational principle of AFM is schematically illustrated in Figure 1-7A. It operates by raster scanning a sharp probe tip over a surface of interest. The deflection of the cantilever resulting from interactions between the tip and the surface is correlated to surface morphology by monitoring displacement of a laser beam reflected off the back of the cantilever.

The atomic force microscope can be operated in a number of different modes, the most common being contact and tapping modes (Figure 1-7B). In contact mode AFM, the tip is brought in contact with the surface and the deflection of the cantilever is kept constant during scanning by a feedback loop that adjusts the z position of the tip. In order to avoid potential sample damage or dislodging of adsorbed species due to the contact between the tip and sample surface during scanning, AFM can also be operated in tapping mode, in which the tip hits the surface for a short time intervals governed by the resonance frequency of the cantilever. Again, electronic feedback control is used to maintain stable imaging.[3]

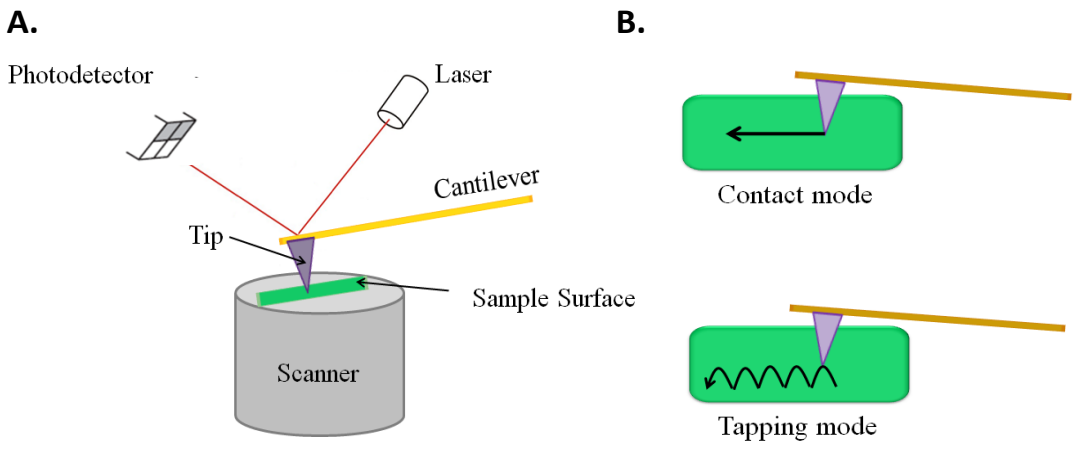

Figure 1-7 A: Schematic diagram of a scanned-sample AFM, B: Illustration of tip movement in contact and tapping mode (this Figure has been redrawn from reference [3]).

AFM imaging provides excellent spatial resolution (typically several nanometers in the lateral direction), limited primarily by convolution of surface features with the finite-sized tip, and less than a nanometer in the vertical direction, generally limited by electronic or vibrational noise. However, AFM images intrinsically lack chemical information and combined morphological - compositional mapping with the microscope can be challenging, even when using more exotic variations of AFM imaging. Further, it must also be noted that AFM imaging is only applicable to solid-supported films, and, as noted, the deposition process itself might result in a possible distortion of the monolayer structure.[19]

1.5.3 Fluorescence Microscopy

Confocal fluorescence microscopy (CFM) is of great utility for imaging mixed surfactant films, since fluorescence microscopes are both well-developed and commonly available in many research labs. CFM can be used to visualize the lateral organization of surfactant monolayers either at the air-water interface in a Langmuir trough or at the air-solid interface in LB films. Image contrast is generated by doping the film with trace amounts of fluorescent probes (concentrations typically less than one mole percent). Some fluorescent probes can accumulate preferentially into one particular phase of the monolayer. For example, some probes are expelled from liquid condensed and solid phases, so these domains appear as dark regions, while liquid expanded phases correspond to bright patterns. This is useful for investigating single component monolayers. However, this is a primary shortcoming for studying mixed LB film, since non-fluorescent regions can be attributed to either the presence of a specific component or the occurrence of a liquid-condensed region that has "squeezed out" the fluorescent probe, thereby complicating analysis of CFM images for these systems.[3,14,30]

1.6 Computer Simulations

Computer simulations are a powerful approach for studying the properties of surfactant films since they provide information with a high temporal and spatial resolution that may not be feasible experimentally. Monte Carlo (MC) and Molecular Dynamics (MD) simulations are the most popular approaches to measure molecular properties of surfactant film systems. While MC relies on random sampling, MD solves the classical equations of motion of many interacting particles to calculate properties of interest.[14]

1.6.1 Molecular Dynamics

MD simulations are commonly used methods to examine surfactant films. These approaches solve Newton's equations of motion of microscopic systems that contain a limited number of interacting particles (N). The net force acting on each particle is described as the following:[34]

$$F_i = m_i \frac{\partial^2 r_i}{\partial t^2} = -\frac{\partial V}{\partial r_i}, i = 1,2, \dots \dots, N \qquad (1.16)$$

Here, t is the time, V the potential energy, m_i is the mass, r_i is the displacement and F_i is the forces acting of the i^{th} particle. Generally, the interactions between particles are described by a set of parameters and equations, namely the force field. These parameters are obtained either by quantum mechanical calculations or by fitting various properties to experiment.[14]

In brief, the particles that comprise the system to be simulated are placed in a box under periodic boundary conditions, which are applied to mimic bulk conditions by surrounding the simulation box with translated copies of the box self. As an input, initial coordinates and velocities are assigned to all energy minimized particles. Then, a velocity is attributed to each particle drawn from the system velocity distribution. After that, the equations of motion are integrated for a short time step, to measure the force acting on every particle in order to update

the system configuration. This procedure is repeated millions of times until the properties of the system no longer change with time, i.e. the system reaches equilibrium. This will end with a trajectory for each particle that describes its coordinates as a function of time. This can be used to obtain various thermodynamic, structural and dynamic properties of the system of interest.[14]

The well-suited setups to simulate surfactant monolayers are either two symmetric monolayers sandwiching a water slab (Figure 1-8A) or a single monolayer at one side of the water slab (Figure 1-8B). Although the single monolayer setup is more close to the real monolayer system and it requires a shorter simulation time, the sandwich setup provides more particles for sampling and hence, more robust statistics.[14]

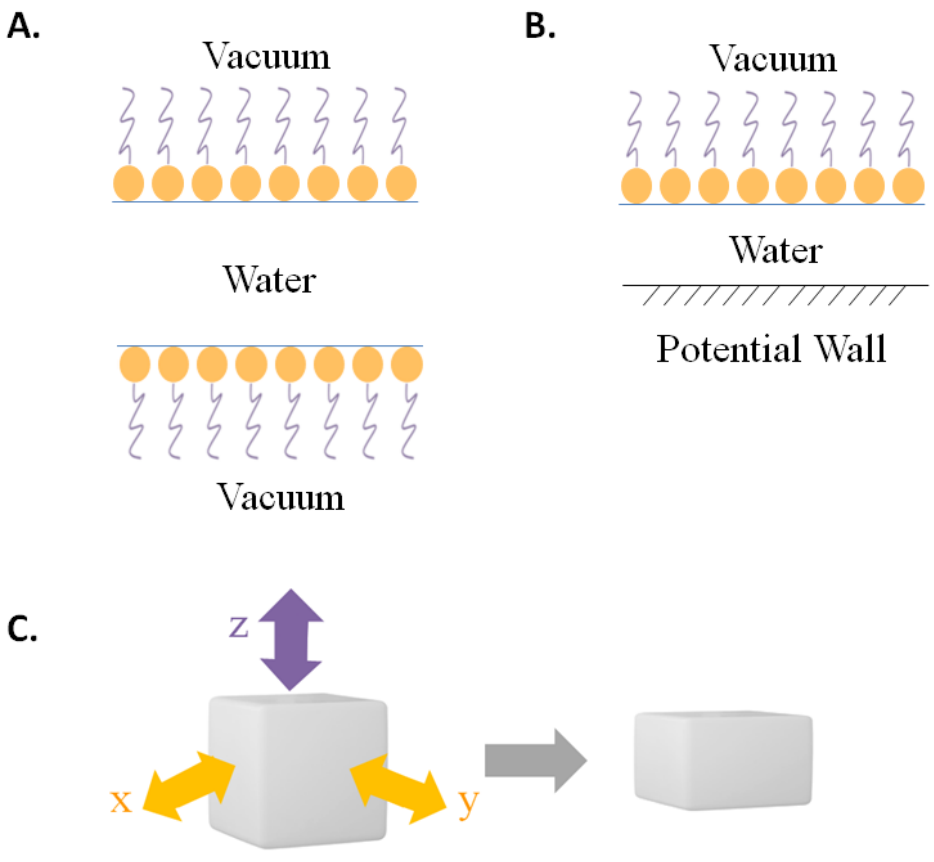

Figure 1-8 System setup of surfactant monolayers consists of A: Two monolayers sandwiching a water slab, B: A single monolayer at the top of a water slab and C: Constant surface pressure coupling scheme**.** (Figure A and B have been redrawn from reference [36] and C from reference [35]).

Most MD simulations are carried out at constant temperature and pressure (i.e., isothermal and isobaric ensemble), because this resembles typical laboratory environments. However, the presence of an interface requires selecting an ensemble that includes either the surface tension or interfacial area. For the simulation project presented in Chapter 6, we chose constant surface tension pressure coupling (Figure 1-8C),[35] in which equal pressures are applied in the lateral directions and decoupled from the normal pressure. To avoid any contact between the two monolayers, we have applied zero pressure in the z-direction. Compression or expansion a monolayer is conducted in a similar fashion to Langmuir trough, by increasing or decreasing the lateral pressure. This will change the x and y dimensions of the box, thereby changing the area occupied per molecule.

1.6.2 MARTINI Force Field

Direct investigations of the structure and dynamics of lipid monolayers via MD simulation have been reported in the literature using both atomistic and coarse-grained (CG) models.[23,37,38] Atomistic MD simulations can provide information about both the structure and dynamics of monolayer systems since atomistic models represent all atoms explicitly. However, these kind of simulations are restricted to relatively short time scales, which prevent the study of many phase transition process, as well as they would be prohibitively expensive in terms of computing time for systems contain a large number of species. This has led to the development of more computationally efficient CG simulation models, in which groups of atoms are represented by a single interaction site. CG simulations have been able to treat patches of bilayer membranes up to a few tens of nanometers in lateral extent, over timescales of a few tens of nanoseconds.[39]

The choice of which CG force field is used to simulate surfactant monolayers depends on the phenomena of interest. In principle, a good choice of CG force field should result in obtaining a match with atomistic simulations. A typical example of a CG force field used for surfactant film simulations is the MARTINI force field,[40] developed by Marrink and coworkers. Initially this force field was developed for lipid simulations,[41] but later it was extended to include other molecules such as proteins.[42] The MARTINI force field uses a four-to-one mapping strategy to represent molecules; where on average four heavy atoms are represented by a single interaction center (hydrogen atoms are excluded). This rule is not strict, as sometimes it is appropriate to map three, five, or more atoms into one interaction center. Four main interaction sites are defined by the MARTNI field. They are named polar (P), nonpolar (N), apolar (C), and charged (Q). Apolar sites represent hydrophobic moieties such as butane, while nonpolar sites are used for mixed groups which are partly polar and apolar like propanol. This mapping was further tuned by adding subtypes denoting the hydrogen-bonding capabilities (donor (d), acceptor (a), both (da) and none (0)), and the degree of polarity (from 1 to 5, where 1 indicates low polarity and 5 represents high polarity species).[40]

The parameterization of various MARTNI CG particles are based on the free energy of hydration, the free energy of vaporization, and the partitioning free energies between water and a number of organic phases. Non-bonded interactions are described either by (6-12) Lennard-Jones (LJ) potentials or via electrostatic coulombic potential. The bonded interactions are described primarily by a weak harmonic potential, with equilibrium angle at 180° and 120° for both saturated and unsaturated systems respectively.[40] As described in Chapter 6, we chose to perform MARTINI CG model simulations to explore the role played by side-chain polarity on phase separation. We have focused on investigations of dipalmitoylphosphatidylcholine (DPPC,

Figure 1-4); because Larson[43] and coworker indicated that the MD simulations of CG DPPC monolayers yield results that are in reasonable agreement with some of the experimental isotherms. The CG representation of DPPC is shown in Figure 1-9. Based on the previously described nomenclature, the positively charged choline and the negatively charged phosphate group are assigned as Q_0 and Q_a respectively. The glycerol ester moiety is represented by two non-polar sites (N_a) and each tail is modeled by four hydrophobic particles (C_1), corresponding to 16 methylene units.

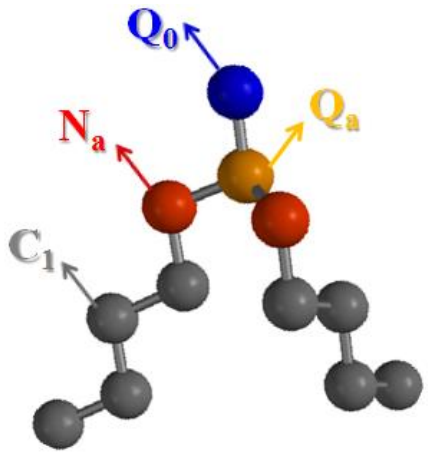

Figure 1-9 Mapping between chemical structure and MARTINI coarse grained model for DPPC.

1.7 Research Objectives

The ultimate objective of this research project is to understand and control factors that affect surfactant miscibility and domain formation in mixed hydrocarbon-fluorocarbon systems that have applications as pulmonary lung surfactant mixtures. This objective was accomplished through measuring miscibility, mechanical rigidity and morphology of mixed phospholipid-perfluorinated fatty acid films at both liquid-air and solid-air interfaces as well as by investigating the performance characteristics of these films as a simple model of pulmonary surfactant mixture in terms of surfactant spreading rate and films hysteresis response to repeated expansion-contraction cycles. Furthermore, the effect of the deposition process on the film

structure and surfactant tail polarities on the interfacial behavior of mixed lipid films were examined both experimentally and computationally.

The overall approach used in this thesis was to investigate mixing thermodynamics, film structures and PS performance parameters for different hydrogenated-fluoroinated mixed surfactant systems. Measurements performed on Langmuir monolayers, using surface pressure-area isotherms in combination with Brewster angle microscopy, atomic force microscopy and fluorescence microscopy. Computationally, CG MD simulations were used to investigate the self-assembly of lipid monolayers at the air-water interface using the MARTINI force field.

These studies were performed through inter-related topics, in some cases in collaboration with researcher from Chemistry Cepartment at University of Saskatchewan as well as with other researchers outside of the University.

1.8 References

1. Adamsonm, A. W.; Gast, A. P. *Physical Chemistry of Surfaces, Sixth Edition;* John Wiley & Sons, Inc.: New York, USA, 1997.

2. Fawcett, W. R. *Liquids, Solutions, and Interfaces: From Classical Macroscopic Descriptions to Modern Microscopic Details;* Oxford University Press, Inc.: New York, USA, 2004.

3. Butt, H.; Graf, K.; Kappl, M. *Physics and Chemistry of Interfaces;* Wiley-VCH Verlag & Co. KGaA: Weinheim, 2003.

4. Myers, D. *Surfaces, Interfaces, and Colloids: Principles and Applications, Second Edition;* John Wiley & Sons, Inc.: New York, USA, 1999.

5. Vollhardt, D.; Fainerman, V. B. Characterisation of phase transition in adsorbed monolayers at the air/water interface. *Adv. Colloid Interface Sci.* **2010**, *154*, 1-19.

6. Butt, H.; Kappl, M. *Surface and Interfacial Forces;* Wiley-VCH Verlag GmbH & Co. KGaA: Weinheim, 2010.

7. Petty, M. C. *Langmuir-Blodgett Films: An Introduction;* Cambridge University Press: New York, USA, 1996.

8. Kaganer, V.; Mohwald, H.; Dutta, P. Structure and phase transitions in Langmuir monolayers. *Reviews of Modern Physics* **1999**, *71*, 779-819.

9. Zuo, Y. Y.; Veldhuizen, R. A. W.; Neumann, A. W.; Petersen, N. O.; Possmayer, F. Current perspectives in pulmonary surfactant - Inhibition, enhancement and evaluation. *Biochimica Et Biophysica Acta-Biomembranes* **2008**, *1778*, 1947-1977.

10. Goodrich, F. C. In *In Molecular interaction in mixed monolayers; Proceeding of the Second International Congress of Surface Activity*; 1957; .

11. McConnell, H. Structures and Transitions in Lipid Monolayers at the Air-Water-Interface. *Annu. Rev. Phys. Chem.* **1991**, *42*, 171-195.

12. Sriram, I.; Schwartz, D. K. Line tension between coexisting phases in monolayers and bilayers of amphiphilic molecules. *Surface Science Reports* **2012**, *67*, 143-159.

13. Israelachvili, J. N. *Intermolecular and Surface Forces: Revised Third Edition;* Elsevier Inc.: USA, 2011; .

14. Baoukina, S.; Marrink, S. J.; Tieleman, D. P. In *Structure and Dynamics of Lipid Monolayers: Theory and Applications;* Faller, R., Jue, T., Longo, M. L. and Risbud, S. H., Eds.; Biomembrane Frontiers: Nanostructures, Models and the Design of Life; Humana Press: New York, USA, 2009; Vol. 2, .

15. Birdi, K. S. *Self-Assembly Monolayer Structures of Lipids and Macromolecules at Interfaces* Kluwer Academic Publishers: USA, 2002; .

16. Nakahara, H.; Lee, S.; Sugihara, G.; Shibata, O. Mode of interaction of hydrophobic amphiphilic alpha-helical peptide/dipalmitoylphosphatidylcholine with phosphatidylglycerol or palmitic acid at the air-water interface. *Langmuir* **2006**, *22*, 5792-5803.

17. Matsumoto, M.; Tachibana, H.; Azumi, R. Control of the structures and functions of Langmuir-Blodgett films using supramolecular architecture. *Materials Science & Engineering C-Biomimetic Materials Sensors and Systems* **1997**, *4*, 255-261.

18. Blodgett, K. Films built by depositing successive monomolecular layers on a solid surface. *J. Am. Chem. Soc.* **1935**, *57*, 1007-1022.

19. Gleiche, M.; Chi, L.; Fuchs, H. Nanoscopic channel lattices with controlled anisotropic wetting. *Nature* **2000**, *403*, 173-175.

20. Simonsen, A. C. In *Spatiotemporal Organization of Spin-Coated Supported Model Membranes;* Faller, R., Jue, T., Longo, M. L. and Risbud, S. H., Eds.; Biomembrane Frontiers: Nanostructures, Models and the Design of Life; Humana Press: New York, USA, 2009; Vol. 2, .

21. Notter, R. H. *Lung Biology in Health and Disease;* Lung surfactants: Basic Science and Clinical Applications; Marcel Dekker: New York, USA, 2000; Vol. 149.

22. Norman, R. G. In *The Airway and Mechanics of Breathing;* Butkov, N., Lee-Chiong, T. L., Eds.; Fundamentals of Sleep Technology: Endorsed by the American Association of Sleep echnologists; Lippincott Williams & Wilkins: USA, 2007.

23. Duncan, S. L.; Dalal, I. S.; Larson, R. G. Molecular dynamics simulation of phase transitions in model lung surfactant monolayers. *Biochimica Et Biophysica Acta-Biomembranes* **2011**, *1808*, 2450-2465.

24. Knepper, T.; Lange, F., Eds.; In *Polyfluorinated Chemicals and Transformation Products;* Barceló, A., Kostianoy, A. G., Eds.; The Handbook of Environmental Chemistry 17; Springer-Verlag Berlin Heidelberg: Germany, 2012; Vol. 17.

25. Thomas, R. R. In *Fluorinated Surfactants;* Farn, Richard J., Eds.; Chemistry and Technology of Surfactants; Blackwell Publishing Ltd: Oxford, UK, 2006.

26. Krafft, M. P.; Riess, J. G. Chemistry, Physical Chemistry, and Uses of Molecular Fluorocarbon-Hydrocarbon Diblocks, Triblocks, and Related Compounds-Unique "Apblar" Components for Self-Assembled Colloid and Interface Engineering. *Chem. Rev.* **2009**, *109*, 1714-1792.

27. Riess, J. G. Highly fluorinated amphiphilic molecules and self-assemblies with biomedical potential. *Current Opinion in Colloid & Interface Science* **2009**, *14*, 294-304.

28. Krafft, M. P. Highly fluorinated compounds induce phase separation in, and nanostructuration of liquid media. Possible impact on, and use in chemical reactivity control. *Journal of Polymer Science Part A-Polymer Chemistry* **2006**, *44*, 4251-4258.

29. Nakahara, H.; Lee, S.; Krafft, M. P.; Shibata, O. Fluorocarbon-Hybrid Pulmonary Surfactants for Replacement Therapy - A Langmuir Monolayer Study. *Langmuir* **2010**, *26*, 18256-18265.

30. Eftaiha, A. F.; Brunet, S. M. K.; Paige, M. F., Eds.; In *A Comparison of Atomic Force Microscopy,Confocal Fluorescence Microscopy and Brewster Angle Microscopy for Characterizing Mixed Monolayer Surfactant Films;* Méndez-Vilas, A., Ed.; Current Microscopy Contributions to Advances in Science and Technology; Formatex: Spain, 2012; Vol. 2.

31. Hecht, E. *Optics*, Fourth Edition*;* Pearson, Education, Inc.: USA, 2002.

32. KSV NIMA-Biolin Scientific Brewster Angle Microscope. *http://www.ksvnima.com /brewster-angle-microscope* (accessed March-1st, 2013).

33. Giner-Casares, J. J.; Brezesinski, G., Eds.; In *Brewster Angle Microscopy (BAM) for In Situ Characterization of Ultrathin Films at Air/Lliquid Interfaces;* Méndez-Vilas, A., Ed.; Current Microscopy Contributions to Advances in Science and Technology; Formatex: Spain, 2012; Vol. 2.

34. Frenkel, D.; Smit , B. *Understanding Molecular Simulation: From Algorithms to Applications;* Academic Press: California, USA, 2002; .

35. Tieleman, D. P. In *Methods and Parameters for Membrane Simulations;* Sansom, M. S. P., Biggin, P. C., Eds.; Molecular Simulations and Biomembranes: From Biophysics to Function; Royal Society of Chemistry: UK, 2010.

36. Kaznessis, Y.; Kim, S.; Larson, R. Simulations of zwitterionic and anionic phospholipid monolayers. *Biophys. J.* **2002**, *82*, 1731-1742.

37. Mohammad-Aghaie, D.; Mace, E.; Sennoga, C. A.; Seddon, J. M.; Bresme, F. Molecular Dynamics Simulations of Liquid Condensed to Liquid Expanded Transitions in DPPC Monolayers. *J Phys Chem B* **2010**, *114*, 1325-1335.

38. Giner-Casares, J. J.; Camacho, L.; Martin-Romero, M. T.; Cascales, J. J. L. A DMPA Langmuir monolayer study: From gas to solid phase. An atomistic description by molecular dynamics simulation. *Langmuir* **2008**, *24*, 1823-1828.

39. Frischknecht, A. L.; Frink, L. J. D. In *Molecular Theory Applied to Lipid Bilayers and Lipid–Protein Interactions;* Faller, R., Jue, T., Longo, M. L. and Risbud, S. H., Eds.; Biomembrane Frontiers: Nanostructures, Models and the Design of Life; Humana Press: New York, USA, 2009; Vol. 2.

40. Marrink, S. J.; Risselada, H. J.; Yefimov, S.; Tieleman, D. P.; de Vries, A. H. The MARTINI force field: Coarse grained model for biomolecular simulations. *J Phys Chem B* **2007**, *111*, 7812-7824.

41. Marrink, S.; de Vries, A.; Mark, A. Coarse grained model for semiquantitative lipid simulations. *J Phys Chem B* **2004**, *108*, 750-760.

42. Monticelli, L.; Kandasamy, S. K.; Periole, X.; Larson, R. G.; Tieleman, D. P.; Marrink, S. The MARTINI coarse-grained force field: Extension to proteins. *Journal of Chemical Theory and Computation* **2008**, *4*, 819-834.

43. Duncan, S. L.; Larson, R. G. Comparing experimental and simulated pressure-area isotherms for DPPC. *Biophys. J.* **2008**, *94*, 2965-2986.

CHAPTER 2 THERMODYNAMIC AND STRUCTURAL CHARACTERIZATION OF A MIXED PERFLUOROCARBON-PHOSPHOLIPID TERNARY MONOLAYER SURFACTANT SYSTEM

2.1 Description

This chapter is a verbatim copy of a paper published in the Journal of Colloid and Interface Science. [Reproduced with permission from *Journal of Colloid and Interface Science*, (368) 356–365, 2012.]

Mixed monolayer films provide a simple model system to investigate the interfacial behavior of perfluorocarbon-hydrocarbon surfactant mixtures that have potential biomedical applications. This contribution explored miscibility, elasticity and morphology of binary and ternary mixtures of perfluorooctadecanoic acid (C18F), 1,2-dipalmitoyl-sn-glycero-3-phosphocholine (DPPC) and 1,2-dipalmitoyl-sn-glycero-3-phosphoglycerol (DPPG), the main phospholipid constituents of pulmonary lung surfactant, through a combination of surface pressure-area isotherm measurements, atomic force microscopy (AFM) and fluorescence microscopy (FM). Mixing thermodynamics indicated that the film forming materials were miscible with each other's. Isothermal elasticity data denoted that the addition of C18F led to minimal changes in the mechanical behavior of the mixed films. Microscopic measurements, both AFM and FM (steady state and time resolved measurements) confirmed the miscibility between the phospholipids and the C18F and indicated the formation of surface-associated reservoirs that were highly enriched in DPPC. These surface structures are of potential importance for pulmonary surfactant applications as they may be used to replenish the surfactant film upon monolayer expansion.

The experimental section for this study is provided in the paper. Detailed descriptions of the techniques used are provided in Chapter 1.

2.2 Description of the Candidate's Contribution

For this contribution, I prepared the samples, performed the isotherm and atomic force microscopy measurements, carried out data analysis, played a major role in interpreting the results, wrote the initial draft of the work and participated in the subsequent editing in response to collaborators and editors. Dr. Sophie Brunet carried out the confocal fluorescence and the fluorescence lifetime measurements and was involved in editing the paper. Dr. Matthew Paige provided extensive guidance throughout the experimental work and was greatly involved in results interpretation, writing and editing the paper.

2.3 Relation of Contribution towards Research Objectives

This contribution was solely performed towards the overall objective of the thesis research. It was important to examine the miscibility of binary and ternary mixed monolayers containing C18F and the two phospholipids, to assess its potential utility as a PS additive. Thermodynamic measurements indicated the presence of attractive interactions between C18F and the both phospholipids. The interaction of the perfluorocarboxylic acid with the DPPC was stronger than that of DPPG. Microscopy data revealed the formation of surface aggregate that are useful for PS application. A full discussion of the results of this study and its implications for the thesis research as a whole is provided in Chapter 8.

Thermodynamic and structural characterization of a mixed perfluorocarbon-phospholipid ternary monolayer surfactant system

Ala'a F. Eftaiha, Sophie M.K. Brunet and Matthew F. Paige

Department of Chemistry, University of Saskatchewan, 110 Science Place, Saskatoon, Saskatchewan, Canada, S7N 5C9

Received 16 August 2011, Accepted 1 October 2011

2.4.1 Abstract

Pulmonary lung surfactant is a mixture of surfactants that reduces surface tension during respiration. Perfluorinated surfactants have potential applications for artificial lung surfactant formulations, but the interactions that exist between these compounds and phospholipids in surfactant monolayer mixtures are poorly understood. We report here, for the first time, a detailed thermodynamic and structural characterization of a minimal pulmonary lung surfactant model system that is based on a ternary phospholipid-perfluorocarbon mixture. Langmuir and Langmuir–Blodgett monolayers of binary and ternary mixtures of the surfactants 1,2-dipalmitoyl-sn-glycero-3-phosphocholine (DPPC), 1,2-dipalmitoyl-sn-glycero-3-phosphoglycerol (DPPG) and perfluorooctadecanoic acid (C18F) have been studied in terms of miscibility, elasticity and film structure. The extent of surfactant miscibility and elasticity has been evaluated via Gibbs excess free energies of mixing and isothermal compressibilities. Film structure has been studied by a combination of atomic force microscope and fluorescence microscopy. Combined thermodynamic and microscopy data indicate that the ternary monolayer films were fully miscible, with the mixed films being more stable than their pure individual components alone, and that film compressibility is minimally improved by the addition of perfluorocarbons to the phospholipids. The importance of these results is discussed in context of these mixtures' potential applications in pulmonary lung surfactant formulations.

2.4.2 Introduction

Pulmonary lung surfactant (PS) is a mixture of lipids (90%) and proteins (10%) that forms a thin molecular film at the air–liquid alveolar (lung) interface in order to reduce surface tension during lung inflation and to prevent alveolar collapse upon lung deflation.[1-5] Phosphatidylcholines (PC) and phosphatidylglycerols (PG) are the major chemical constituents of pulmonary surfactant phospholipids, with the most abundant component of the PC being zwitterionic 1,2-dipalmitoylphosphatidylcholine (DPPC). The ability of PS to attain low surface tension has largely been attributed to the formation of surfactant films that are highly enriched in DPPC. However, DPPC adsorbs very slowly to the air-water interface and has a limited capacity to replenish the surfactant film upon alveolar expansion. Additional phospholipids with superior adsorption and spreading properties (e.g. anionic phospholipids such as PG), often working in conjunction with proteinaceous components, are generally needed to offset these shortcomings.[5] In short, there is no single component of PS that has the entire range of surface properties considered essential for assisting normal respiratory function and the multiple components of PS act synergistically in order to achieve the desired physiological performance. Improper performance (or a deficiency) of PS has been linked to a number of severe respiratory diseases, including respiratory distress syndrome, and the development of exogenous PS replacement therapy to treat these diseases is an active area of research. While a number of commercial exogenous PS mixtures have been developed from both animal (typically bovine and porcine extracts) as well as semi-synthetic sources, there is still considerable interest in improving the efficacy, safety and cost of these formulations.

Fluorocarbon-based surfactants have recently become a target of potential interest for PS applications as these molecules have a number of highly useful physicochemical properties at the

air-water interface, including low surface tension, high film elasticity and high oxygen solubility.[6-8] Use of perfluorinated or partially fluorinated molecules for scientific and biomedical applications is a controversial one, as these molecules have a well-documented biological and environmental persistence.[9] Nonetheless, the topic is a potentially important one, and the use of fluorinated molecules for such applications is an active area of research. A variety of perfluorocarbon surfactants (e.g. carboxylic acids, alcohols) form highly stable monolayers at the air-water interface and when mixed with hydrogenated surfactants, can result in the formation of films that are either miscible or immiscible and contain diverse (and controllable) structural features at the micron and nanometer length-scales.[10-18] Fluorocarbons in general have significant potential for use in PS applications. Gerber et al.[19,20] have reported that perfluorooctyl bromide gas significantly inhibits the crystallization of DPPC Langmuir monolayers upon compression and facilitates its re-spreading upon film decompression. Nakahara et al.[21] have observed that the surface pressure and the hysteresis behavior (surfactant recovery) of DPPC monolayers can be enhanced through the addition of partially fluorinated alcohols.

Our group and others have been investigating the miscibility, composition and morphology of Langmuir and Langmuir-Blodgett monolayer films prepared from mixtures of hydrogenated surfactants (typically fatty acids and phospholipids) and perfluorinated fatty acids, with an ultimate goal of controlling the mechanical, chemical and morphological properties of these films.[12-15, 22-24] The additional degree of control over mixed film properties that can be obtained through the addition of perfluorocarbons warrants further investigation for potential PS applications, and we view the development of a fundamental understanding of the thermodynamic, mechanical and morphological properties of these mixed films as an integral part of using them for clinical applications. In effect, we view these mixtures as simple, minimal

models of PS mixtures that allow us to investigate the underlying intermolecular interactions in a tractable system.

Studies directed at characterizing properties of binary mixed films involving simple fatty acids or phospholipids with fluorocarbon surfactants are plentiful in the literature. In the case of fatty acids, mixtures with perfluorocarbons are commonly immiscible when the surfactants have sufficiently large differences in surfactant chain lengths (see Qaqish et al.[14] for example), with the resulting films undergoing phase-separation and forming a diverse range of morphological structures. Interactions of DPPC with fluorocarbons in binary mixtures are also well-studied; key results have been reported by Lehmler et al.[25] and Nakamura et al.[26] in which the degree miscibility of full and partially fluorinated surfactants and DPPC was also found to depend strongly on chain length differences. Research carried out in our own group (Eftaiha et al.[27]) has revealed that perfluorooctadecanoic acid ($CF_3(CF_2)_{16}COOH$) and DPPC are miscible under a wide range of mixing conditions, though the properties of the films could be tuned through the addition of univalent cations to the underlying subphase.

While a mixture of PGs are found in native lung surfactant, many model lung surfactant mixtures reported in the literature have made use of dipalmitoylphosphatidylglycerol, which typically accounts for 10-40% of the total PG content,[28] as a representative PG. The miscibility of dipalmitoylphosphatidylglycerol with perfluorocarboxylic acids is much less well-studied than that for DPPC, though some information can be found; Yokoyama et al.[18] have investigated the miscibility of DPPG with $CF_3(CF_2)_nCOOH$ perfluorocarboxylic acids, and found the systems to be miscible for n = 10, 12 acids and immiscible with n = 14, 16 acids in the monolayer state when using an acidified (pH = 2) sub-phase. It was found that the key driving forces that regulate monolayer miscibility in these systems are a combination of attractive forces between polar

headgroups balanced by interaction forces between the tail groups of the two different surfactants.[18, 29, 30]

While the studies described above have provided important insight into the interactions which exist in binary phospholipids-fluorinated surfactant systems, significant improvements in the properties of surfactant mixtures with potential PS applications might be realized through the use of more complex ternary surfactant mixtures comprised of DPPC, DPPG and perfluorocarboxylic acids. In this study, we have investigated the mixing thermodynamics, film elasticity and morphology of a ternary surfactant system comprised of DPPC, DPPG and perfluorooctadecanoic acid. A number of binary phospholipid-perfluorocarbon systems have been reported in the literature (see above), but this is, to our knowledge, the first detailed characterization of a ternary mixed system. While data for wide range of film compositions has been collected, emphasis has been placed on measurements of 4DPPC:1DPPG mole ratio mixtures (with varying fractions of C18F), as the relative ratio of DPPC to DPPG in these films is a reasonable approximation of the phospholipid composition found in PS systems. We note that other researchers in this field have used phospholipid mixtures of similar composition as minimal models for lung surfactant mixtures.[31-33] Thermodynamic properties for the mixed monolayers (Gibbs excess mixing energies and isothermal compressibilities) have been measured via compression isotherms, while film morphology has been studied by a combination of atomic force microscope, confocal fluorescence imaging and fluorescence lifetime imaging (FLIM) of solid-supported monolayer films.

2.4.3 Experimental

2.4.3.1 Chemicals

Dipalmitoylphosphatidylcholine was purchased from Sigma–Aldrich Corporation, dipalmitoylphosphatidylglycerol was purchased from Avanti Polar Lipids, and perfluorooctadecanoic acid was purchased from Alfa Aesar. The fluorescent lipids 2-(4,4-difluoro-5-methyl-4-bora-3a,4a-diaza-s-indacene-3-dodecanoyl)-1-hexadecanoyl-sn-glycero-3 phosphocholine (Bodipy-PC) and 1-palmitoyl-2-{12-[(7-nitro-2-1,3-benzoxadiazol-4-yl)amino]lauroyl}-sn-glycero-3-[phospho-rac-(1 glycerol)] (ammonium salt) (NBD-PG) were purchased from Invitrogen Corp. and Avanti Polar Lipids, respectively. The chemical structures of the surfactants and the fluorescent probes are presented in Figure 2-1.

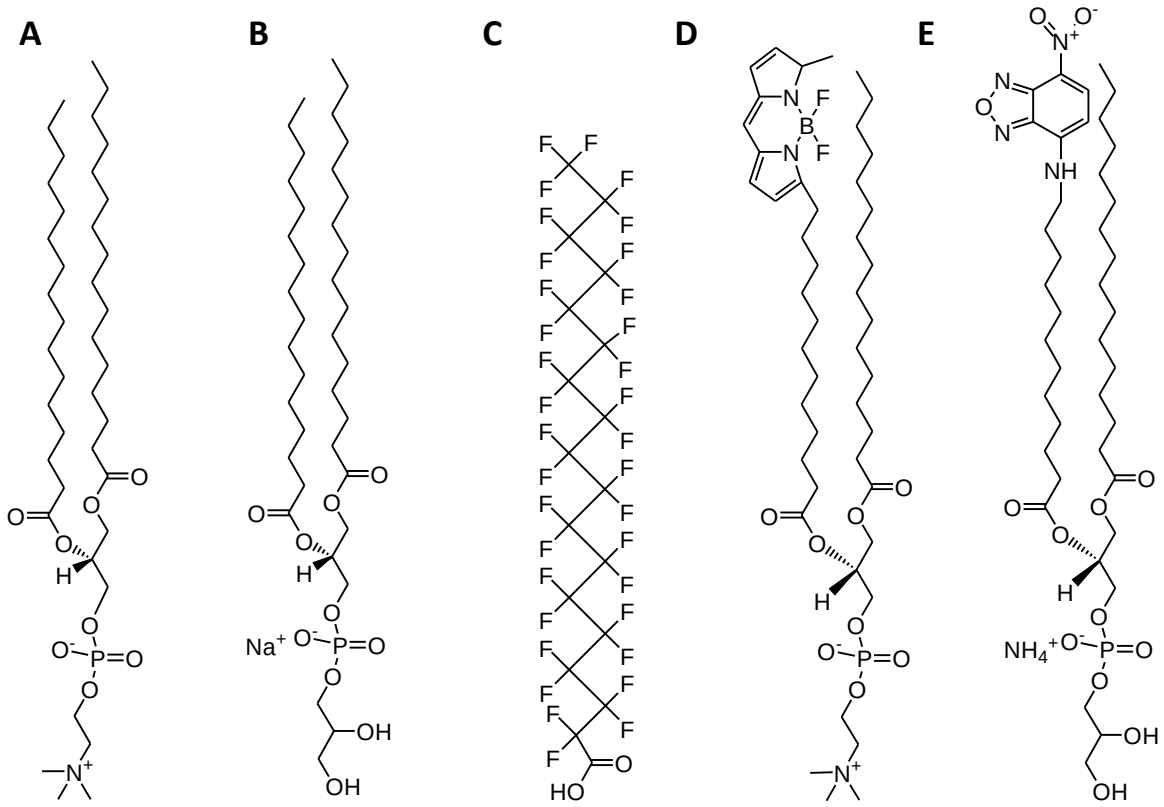

Figure 2-1 Chemical structures of A: 1,2-dipalmitoyl-sn-glycero-3-phosphocholine (DPPC), B: (1,2-dipalmitoyl-sn-glycero-3-phospho-(1'-rac-glycerol) (sodium salt)) (DPPG), C: perfluorooctadecanoic acid (C18F), D: (2-(4,4-difluoro-5-methyl-4-bora-3a,4a-diaza-s-indacene-3-dodecanoyl)-1-hexadecanoyl-sn-glycero-3 phosphocholine) (Bodipy-PC) and E: (1-palmitoyl-2-{12-[(7-nitro-2-1,3-benzoxadiazol-4-yl)amino]lauroyl}-sn-glycero-3-[phospho-rac-(1-glycerol)] (ammonium salt)) (NBD-PG).

The solvents n-hexane (HPLC grade), chloroform, methanol and ethanol were purchased from Merck KGaA or Sigma-Aldrich. All reagents were used as received without additional purification. Microscope cover glass (No. 1.5, VWR International) was rinsed thoroughly with ethanol and dried under nitrogen gas. The slides were then placed in a plasma cleaner (PDC-32G, Harrick Plasma) for ~20 minutes at high power to remove any residual contaminants.

2.4.3.2 Isotherm Measurements and Langmuir-Blodgett Film Deposition

Stock solutions of DPPC, DPPG and C18F (1.25 mM) were prepared by dissolving DPPC and C18F in *n*-hexane:methanol (9:1) (v/v), while DPPG was dissolved in *n*-hexane:chloroform:methanol (8:1:1) (v/v/v). Appropriate volumes of the stock solutions were mixed to prepare binary and ternary mixtures of DPPC, DPPG and C18F. Herein, the composition of the ternary mixtures has been described by the molar ratio of DPPC:DPPG:C18F.

Langmuir and LB film preparation of the binary and the ternary mixtures was performed using a KSV 2000 Langmuir trough at 25.0 ± 0.5°C by spreading 80 μL of the surfactant mixtures on a water subphase (Millipore, pH 5.5, resistivity 18 MΩ.cm). The spreading solvent was allowed to evaporate for 10 minutes prior to compression. The surface pressure (π) of the monolayers was measured using a Wilhelmy balance equipped with a roughened platinum Wilhelmy plate. For isotherm measurements, the rate of compression was 20 mm/min (~0.10 $Å^2 \cdot molecule^{-1} \cdot minute^{-1}$), while for deposition it was 10 mm/min (~0.05 $Å^2 \cdot molecule^{-1} \cdot minute^{-1}$). For deposition measurements, films were compressed to π = 30 mN/m and the film was allowed to stabilize for 10 minutes before the glass substrate was pulled upward through the water-air interface in a single stroke. The film was left to dry at room temperature for several hours before imaging either in the AFM or the fluorescence microscope.

For the fluorescent probe-doped samples, stock solutions of the fluorescent probes (Bodipy-PC and NBD-PG) were prepared in *n*-hexane:chloroform:methanol (8:1:1) (v/v/v). Aliquots of the stock solutions were added to the surfactant mixtures to prepare $2.5x10^{-3}$ % and $2.0x10^{-2}$ % mole % Bodipy-PC and / or NBD-PG to the total amount of surfactant in solution (moles of dye per 100 moles of total surfactant).

2.4.3.3 Atomic Force Microscope and Fluorescence Microscope Imaging

The Bodipy-PC and NBD-PG doped LB films on glass were imaged using a Zeiss LSM410 laser scanning confocal microscope (LSM Tech). Samples were excited with 458 nm (Bodipy-PC) or 488 nm (NBD-PG) laser light from a multiline argon ion laser. Emission was passed through a 500 nm longpass emission filter.

AFM images of LB films were obtained using a Dimension Hybrid Nanoscope system (Veeco Metrology Group). Intermittent contact imaging "Tapping Mode" was used to collect topographical images. AFM probes (Veeco Instruments) with a resonance frequency of ~240-280 KHz and a nominal spring constant of ~10-100 N/m were used. Samples were typically imaged with a scan size of 10 μm x 10 μm, a scan rate of 1.00 Hz and a resolution of 512 pixels per line. No tip-induced damage of films was observed under these operating conditions.

FLIM images were acquired using a modified version of the confocal microscope described above. Excitation was carried out with a pulsed laser system set at 457 nm and the system was operated through a SPC-830 (Becker and Hickl, Berlin, Germany) FLIM data acquisition board. The emission filter in the confocal path was a 505 nm longpass filter. Fluorescence emission was directed onto a single photon counting photomultiplier tube (PMC-100-4, Becker and Hickl), and the output signal from this was used as the constant fraction discriminator input to the SPC-830. The pulsed laser was a Mira 900-D laser system (Coherent)

operating in femtosecond mode, and a harmonic generator was used to adjust the output to the desired wavelength. A pick off optic was used to trigger the fast photodiode (PHD-400, Becker and Hickl) and send a synchronization pulse to the SPC-830.

2.4.4 Results and Discussion

Figure 2-2A shows π–*A* isotherms for pure DPPC, DPPG and C18F monolayers on the air-water interface (pH 5.5), at 25.0 ± 0.5°C. Isotherms for these films were comparable with those reported elsewhere in the literature,[18, 27, 29] where C18F forms the most condensed monolayer, followed by DPPG and then DPPC. The isotherm for the DPPC film consisted of a characteristic gaseous phase at low compression, a transition region (~9-11 mN/m) between a liquid-expanded (LE) and liquid-condensed (LC) phases and a film collapse pressure of ~70 mN/m. Isotherms for DPPG and C18F monolayers underwent a direct transition from the gaseous phase to the liquid-condensed phase and had collapse pressures of ~56 and 62 mN/m, respectively. The shape of the π–*A* isotherm for pure DPPG has been shown to be strongly affected by the subphase pH, temperature and composition (presence of salt) as well as the ionization state of the DPPG headgroup.[34] At low subphase pH, a pronounced liquid expanded-liquid condensed phase transition is observed, but under the conditions used here (no salts and at pH 5.5), the DPPG film does not undergo a transition between the expanded and condensed phases. Figure 2-2B shows π–*A* isotherms for a series of mixed surfactant films of general composition 4:1:X (ratio refers to DPPC:DPPG:C18F). The characteristic LE-LC transition for DPPC became difficult to discern upon mixing with DPPG, and upon addition of C18F, disappeared entirely. This result is consistent with previous reports in which perfluorocarbon addition results in solubilization of the DPPC monolayer and disruption of the liquid phase transition. The collapse pressure of the mixed film ranged from ~ 65-72 mN/m and, with the

exception of the 4:1:10 mixture, decreased with increasing mole fraction of C18F. Variations in collapse pressure as a function of film composition correlate with the existence of interactions between components in mixed monolayers,[35] and to further explore this effect, the applicability of the additivity relationship for the ternary mixtures was examined. In brief, for a ternary system in which the film components behave ideally (i.e. no net difference in interaction energies between the various film components), mean molecular areas of the film components should behave in a purely additive fashion described as:

$$A_{123} = A_1\chi_1 + A_2\chi_2 + A_3\chi_3 \qquad (2.1)$$

where A_{123} is the mean molecular area (MMA) for the mixed film, A_i is the mean molecular area for the i^{th} component (determined from isotherms of the pure components) and χ_i is the mole fraction of the i^{th} component. Mixtures whose behavior rigorously obeys equation (2.1) are either perfectly miscible or perfectly immiscible and further measurements are needed to distinguish the two, whereas mixtures whose behavior does not follow equation (2.1) are miscible. Furthermore, net attractive or repulsive interactions between different film components result in deviations (negative deviations from equation (2.1) for attractive and positive deviations for repulsive) from additivity. The additivity relationship for the 4:1:X mixtures collected at π = 30 mN/m is shown in Figure 2-2C, along with the ideal additivity behavior predicted from equation (2.1) for reference. For the 4:1:X mixtures, the mixed films showed increasingly negative deviations from ideality with increasing C18F content. This is indicative of miscibility and of attractive interactions between C18F and the other components of the mixed film. Deviations from ideality were larger for ternary mixtures that had a higher content of DPPC than DPPG (data not shown), suggesting that the DPPC-C18F interaction plays a dominant role in the attractive interactions that were observed. We note that stabilization of surfactant films,

particularly at high surface compression, is a potentially desirable property for PS formulations,[5] and as such, we have explored this property in greater detail in the discussion below.

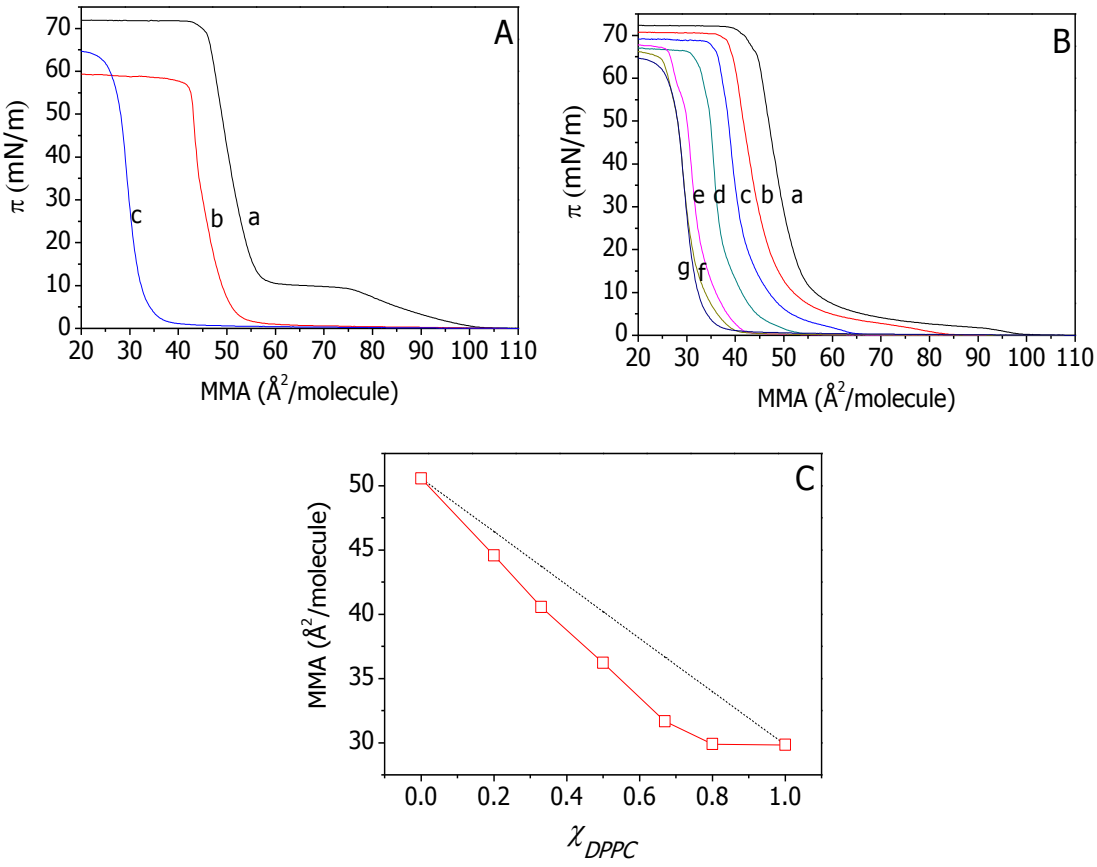

Figure 2-2 Surface pressure–mean molecular area isotherms of, A: Pure components, a: DPPC, b: DPPG and c: C18F, B: 4:1:X mixtures, a: 4:1:0, b: 4:1:1.25, c: 4:1:2.5, d: 4:1:5, e: 4:1:10, f: 4:1:20, g: C18F, at the air-water interface, C: Plot showing mean molecular area as a function of mole fraction of C18F for the ternary surfactant films. The boxes are experimental data points, the dashed line represents the ideal behavior predicted by the additivity relationship (equation (2.1)) and the solid line is included as a guide to the eye.

To explore the nature of the phospholipid-perfluorinated acid interaction, the thermodynamic stability of the mixed monolayers were examined via the excess free energy of mixing (ΔG_{ex}^{π}), defined as follows for a ternary mixture:

$$\Delta G_{ex}^{\pi} = \int_0^{\pi} [A_{123} - (\chi_1 A_1 + \chi_2 A_2 + \chi_3 A_3)] d\pi \qquad (2.2)$$

(Note, the corresponding expression for binary mixtures simply contains two $\chi_i A_i$ terms) Negative ΔG_{ex}^{π} values indicate that the mixed film is more thermodynamically stable than the

constituent single-component films. Plots of ΔG_{ex}^{π} as a function of surface pressure and monolayer composition for a selection of binary and ternary surfactant mixtures are shown in Figure 2-3(A-D). As shown in Figure 2-3 (A and B), binary mixtures of C18F with both phospholipids are more thermodynamically stable than the pure films of the individual components. For mixtures of DPPC and C18F, values for ΔG_{ex}^{π} became increasingly negative with increasing mole fraction of C18F over the entire range of film compositions measured, and, with a few minor fluctuations for the films that contain the lowest mole fraction of C18F, became increasingly negative with increasing surface pressures. The largest magnitude mixing energies (taken as absolute values of ΔG_{ex}^{π} at π = 50 mN/m) were ~1.9 kJ/mol, indicating strong film cohesion. These results are consistent with those reported earlier in our previous study of DPPC-C18F miscibility,[27] in which it was observed that, under the same subphase conditions, DPPC (zwitterionic under the conditions used here) and C18F (negatively charged) mix intimately and that the C18F effectively dissolves the pure phospholipid film. Similar trends and mixing energy magnitudes were observed for the DPPG-C18F mixtures, though for DPPG (negatively charged), a maximum cohesive interaction (~1.6 kJ/mol) was found at 1:2 DPPG-C18F; at higher C18F content, a minor decrease in film stability was detected.

It is worth exploring the source of the increased film stability in further thermodynamic detail. Following the approach of Goodrich[36], the total Gibbs free energy of mixing (ΔG_{ex}^{π}) for a mixture of i^{th} components can be written as a sum of an ideal mixing term and an excess Gibbs free energy term:

$$\Delta G_{mix} = \Delta G_{ex}^{\pi} + \Delta G_{id-mix}^{\pi} = \Delta G_{ex}^{\pi} + RT(\sum_{i=1}^{n} \chi_i ln\chi_i) \qquad (2.3)$$

where the ideal mixing term G_{id-mix}^{π} is the product of temperature and the entropy associated with the formation of an ideal mixture (the ideal enthalpy of mixing is zero). The G_{id-mix}^{π} term can simply be calculated from the appropriate mole fractions of the mixed solutions. By definition, ΔG_{ex}^{π} is the free energy contribution to film stabilization that arises from interactions between molecules. It should be noted, however, that the entropic contribution to ΔG_{mix} is of the same order of magnitude as ΔG_{ex}^{π} for both the binary (values range from 0 to -1.7 kJ/mol) and ternary mixtures (values range from 0 to -2.4 kJ/mol) shown in Figure 2-3. This indicates that in addition to the attractive interactions between the different film components, statistical entropy of mixing is of comparable importance in driving the spontaneous mixing of the films.

While the attractive interaction between the negatively charged carboxylate of the C18F head group and the positive charge of the zwitterionic DPPC head group might nominally be used to rationalize their mutual attraction, the same principle is not applicable for the interaction between negatively charged DPPG and C18F. While there are significant differences in estimated pK_a values for DPPG in monolayer systems found in the literature (values ranging from 1-5 can be found, though these values are likely strongly dependent on the exact subphase conditions used), we can reasonably expect DPPG monolayers to be negatively charged for the experiments described here. Under these conditions, it appears that dispersion interactions between the DPPG and C18F sidechains alone are sufficient to generate a net attractive interaction between film components (and overcome the repulsion between the negatively charged headgroups). Given that the sidechains for DPPC and DPPG are essentially identical (see Figure 2-1), we can use the difference in the Gibbs mixing energies at high compression pressure to provide a crude upper-limit estimate of the degree of additional film stabilization provided by the attraction between the zwitterionic head group of DPPC and C18F; based on the

values reported above, we take this to be ~ 250 J/mol. To our knowledge, this is the first reported estimate of the magnitude of film stabilization energy provided purely from headgroup interactions in these mixed systems.

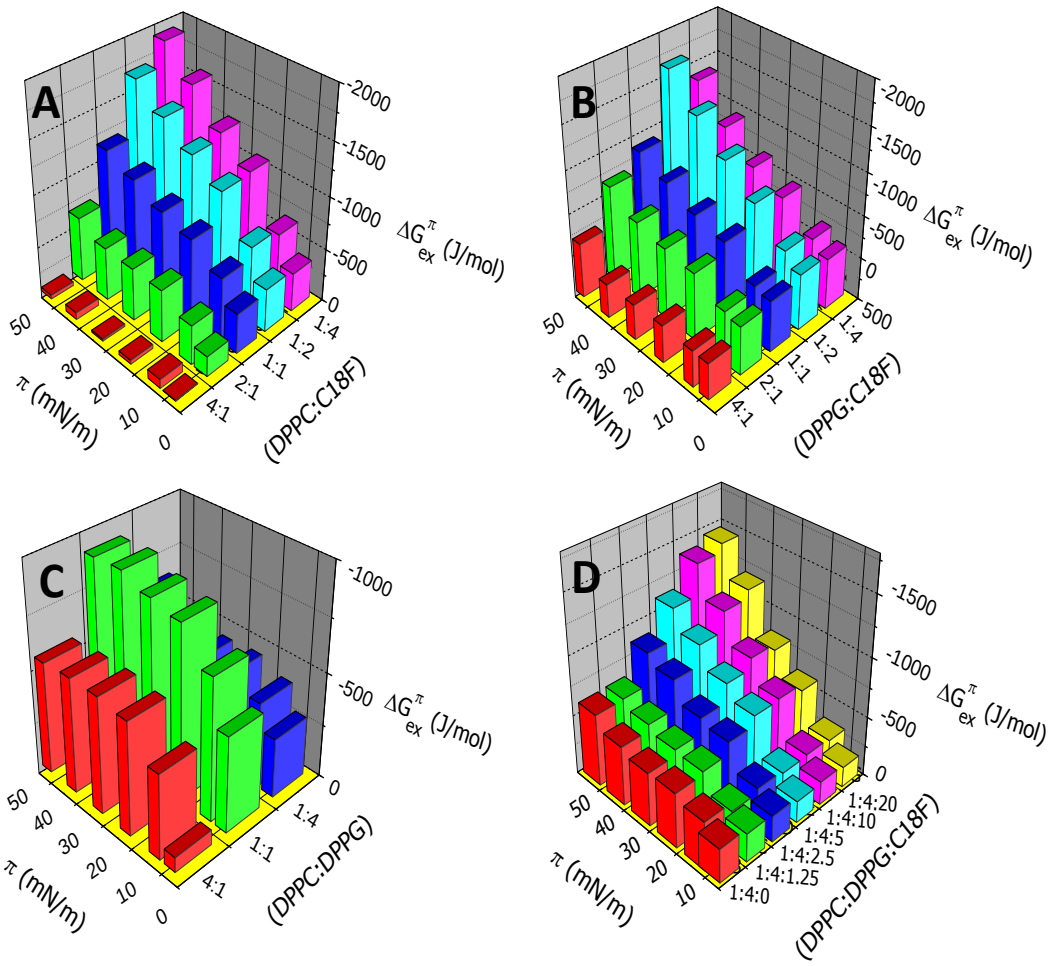

Figure 2-3 Plots of ΔG^{π}_{ex} as a function of surface pressure and monolayer composition for a series of binary and ternary surfactant mixtures. A, DPPC:C18F binary mixtures. B, DPPG:C18F binary mixtures. C, DPPC:DPPG binary mixtures. D, DPPC:DPPG:C18F mixtures at fixed 4:1 DPPC:DPPG mole ratio.

As shown in Figure 2-3C, the mixed DPPC-DPPG monolayers also show negative ΔG^{π}_{ex} values (absolute values ranging from 70 to 900 J/mol), indicating a modest cohesive interaction between film components. The film cohesion displayed a maximum at equimolar 1:1 mixtures of the two phospholipids. These mixtures are reasonably well-studied (see Koppenol et al.[37], and others), and our results are in good agreement with reports that can be found in the literature.

The attractive interaction between film components has generally been attributed to the zwitterion-negative ion interaction between the two phospholipids under the experimental conditions used here, and our results are consistent with this.

The 4:1:X ternary mixtures (Figure 2-3D) showed similar trends to those observed for the binary mixed films, with ΔG_{ex}^{π} values increasing in magnitude with surface pressure and, for the majority of film compositions, increasing with the amount of C18F content. In all cases, the values for ΔG_{ex}^{π} for the ternary mixtures fell between the maximum and minimum values seen for the binary mixtures. As seen by the significant increase in magnitude of ΔG_{ex}^{π} upon changing film composition from zero C18F content to the 4:1:1.25 mixture, addition of a small amount of perfluorocarbon to the mixed film results in a significant overall film stabilization (on the order of ~250 J/mol). This value is of the same order as the additional stabilization energy gained from the interaction between the DPPC and C18F headgroups (recall, the acyl sidechains are chemically identical), suggesting that the primary stabilizing influence of C18F arises from this interaction. Supporting evidence comes from similar measurements of the 1:4 DPPC:DPPG mixture; upon addition of perfluorocarbon to films of that contain only a small amount of DPPC (see Appendix A), there is a negligible change in overall film stability, indicating that the DPPC-C18F headgroup interaction is the key chemical factor that leads to enhanced film stabilization. It is also worth noting that if the total C18F content is too high, a decrease in ΔG_{ex}^{π} with C18F content is observed (i.e. ΔG_{ex}^{π} is smaller in magnitude for the 4:1:20 mixture than for the 4:1:10 mixture), providing further support for this argument.

To assess the influence of the attractive interactions on the mechanical rigidity of the monolayer films (and hence their predicted response to expansion-contraction cycles during

respiration), isothermal compressional moduli were calculated from the π–*A* isotherms. The compressional modulus of a surfactant monolayer is defined as:

$$\kappa = -A\left(\frac{d\pi}{dA}\right)_T \qquad (2.4)$$

where *A* is the experimentally measured mean molecular area. Table 2-1 summarizes κ values measured at π = 30 mN/m for the pure films as well as the mean value measured for ternary mixtures of composition 4:1:X (X ranged from 0 to 20). We note that there were significant variations in the measured κ values as a function of C18F content for the ternary films (as well as control samples of the binary mixtures) and these details are necessarily lost through the averaging process. While it was not practical to interpret all of the effects that were observed, several salient points stand out. Of the pure components, the C18F monolayer had a higher modulus (slightly less compressible) than the two phospholipid monolayers, which had values that were comparable with each other. The overall elasticity of the ternary mixed film was minimally increased by the addition of the perfluorocarbon over a wide range of compositions, despite the significant degree of film stabilization imparted by the headgroup interactions involving C18F. In terms of potential applications for use of C18F in artificial PS formulations, this can be viewed as a beneficial overall property. PS generally requires elastic modulus values of > 100 mN/m (sometimes cited as κ^{-1} values of 0.01(mN/m)$^{-1}$) in order to achieve very low surface tension values with a comparatively small amount of compression during normal respiration.[5] While the elastic modulus values for the individual film components achieve this degree of compressibility by themselves, the addition of C18F does lead to minor improvements in the compressive properties of the film. This factor, in combination with the improved film stability (particularly at high surface pressures), suggests some significant potential for perfluorocarbon additives in PS treatments.

Table 2-1 Monolayer elasticity and associated standard deviations (σ_{n-1}; n = 3 samples for each of the pure films) for the pure monolayer films and for the mixed (4:1:X) ternary films averaged over C18F content ranging from X = 1 to 20 (five different film compositions). Measurement conditions: π = 30 mN/m, pH 5.5, 25.0 $\pm$ 0.5 ^{0}C.

Surfactant mixture	***κ (mN/m)***	***σ_{n-1}***
Pure Component		
DPPC	2.8×10^2	$\pm 0.1 \times 10^2$
DPPG	2.9×10^2	$\pm 0.2 \times 10^2$
C18F	3.6×10^2	$\pm 0.2 \times 10^2$
Ternary Mixtures(4:1:X mean)		
DPPC:DPPG:C18F	3.2×10^2	$\pm 0.7 \times 10^2$

To assess film morphology and the spatial distribution of surfactants in the mixed systems, a combination of atomic force microscope and fluorescence microscope (both steady-state and time-resolved) imaging of deposited (LB) films has been carried out. Steady-state confocal fluorescence images of different binary and ternary mixtures of phospholipid(s) with C18F doped with either Bodipy-PC or NBD-PG (fluorescent analogues of DPPC and DPPG, respectively) are shown in Figure 2-4 (A-D). For these images, contrast corresponds to the presence (bright) or absence (dark) of the fluorescent probe. The bulky fluorescence probes used here partition preferentially into liquid expanded regions of the films and are excluded from condensed regions[38-42] and hence fluorescence images will contain 'voids' due to this partitioning, even for single component films.

As shown in Figure 2-4A, fluorescence images of 1:1 DPPC-C18F (Bodipy-PC) consisted of three regions with distinct brightness levels: first, dark voids that were free of fluorescent material; second, a continuous film with moderate fluorescence; and third, small, highly fluorescent aggregates. We assign the non-fluorescent voids to condensed regions of the monolayer from which the fluorescence probes are excluded. While we do not have a fluorescent analog probe for C18F and cannot directly locate the perfluorinated surfactant in these mixtures, the location of the C18F can be inferred. Because the DPPC and C18F are miscible as shown in the thermodynamic measurements described above, we can reasonably identify the continuous

film as consisting of an intimate mixture of DPPC and C18F. The highly fluorescent aggregates are regions of the sample that are enriched in fluorescent probe in comparison with the continuous film. It is unclear whether this is due to local regions of the film in which there is a higher density of DPPC over that of the continuous film (but not sufficiently high to result in dye partitioning), or a labeling artifact (perhaps a tendency for the probe to preferentially aggregate with other probe molecules, or to accumulate in pinhole defects in the monolayer). We have previously observed the formation of similar aggregates in the mixed DPPC-C18F binary systems[27] via AFM imaging experiments in which no fluorescent probe was used, suggesting that the aggregates are areas of the film that are enriched in DPPC. This is an issue that cannot be easily resolved, though we note that these aggregates were observed for all conditions investigated, regardless of the fluorescent probe that was used. To our knowledge, aggregates of this type have not been reported for fluorescence studies of closely-related monolayer films where fluorescence imaging was performed directly at the air-water interface, which suggests that these aggregates may result from the deposition and monolayer drying process.

For the 1:1 DPPG-C18F mixtures (Figure 2-4B; NBD-PG label), the films again consisted of three different regions, including non-fluorescent voids, discrete, micron length-scale patches with moderate fluorescence and occasional highly-fluorescent aggregates. The non-fluorescent voids occupied a larger fraction of the total image area than for the DPPC-C18F mixtures, which is expected because the DPPG-C18F films are more condensed at the deposition pressures used (35$Å^2$/molecule for DPPG-C18F versus 38 $Å^2$/molecule for DPPC-C18F) and a larger fraction of liquid condensed monolayer will be found. The moderately fluorescence patches contained occasional bright aggregates that were similar to those found for the DPPC-C18F mixtures. Again, films that contain patches of moderate fluorescence are the expected

result for a thermodynamically miscible system, with the patches consisting of an intimate mixture of the phospholipid and perfluorocarbon, which is consistent with our earlier measurements.

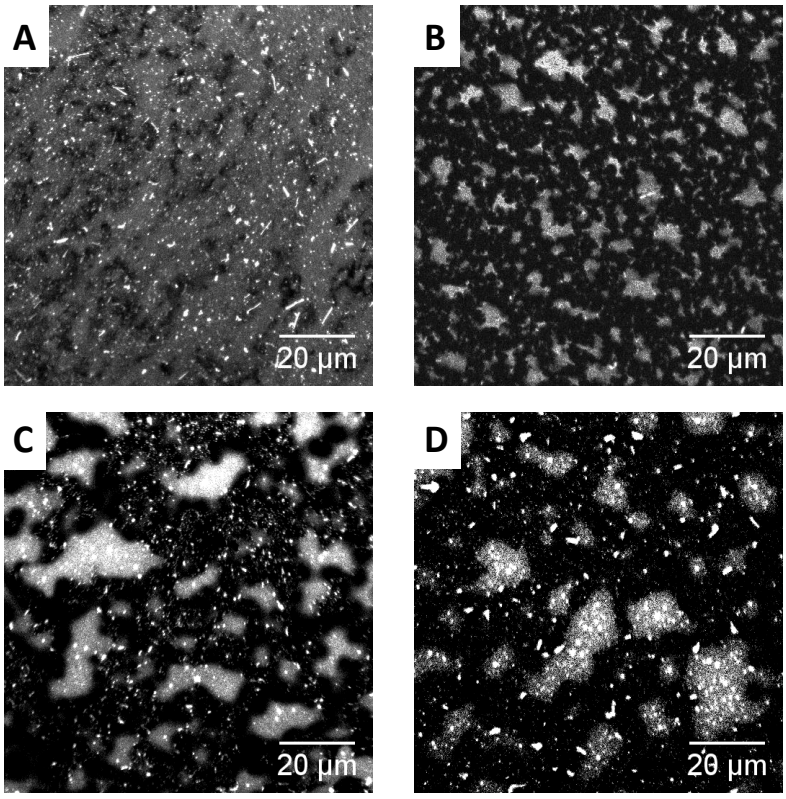

Figure 2-4 Confocal fluorescence images (100 µm x 100 µm) of LB films doped with either Bodipy-PC or NBD-PG and deposited on glass substrate using water as a subphase. A: 1:1 DPPC:C18F (Bodipy-PC), B: 1:1 DPPG:C18F (NBD-PG), C: 4:1:5 (Bodipy-PC) , D: 4:1:5 (NBD-PG).

Mixed ternary (4:1:5) films were imaged using two approaches: first, with a single-probe confocal fluorescence microscope imaging experiment (Figure 4C for a 4:1:5 Bodipy-PC label, Figure 4D for a 4:1:5 NBD-PG label) and second, with a dual-probe confocal fluorescence lifetime imaging experiment (Figure 2-5). Steady-state fluorescence images of ternary mixtures were qualitatively similar to those observed for the DPPG-C18F mixtures, with images containing void regions, patches and aggregates. At this deposition pressure, the mixed film occupied a mean area of 36 $Å^2$/molecule and a similar fraction of condensed phase (void regions) as seen for the DPPG-C18F films was observed. The patches for the 4:1:5 mixtures were

comparable in size and spatial distribution regardless of the fluorescent probe that was used; images of films labeled with Bodipy-PC were qualitatively indistinguishable from those labeled with NBD-PG. Taken in conjunction with the thermodynamic data, this suggests that in the ternary mixture, all three of the DPPC, DPPG and C18F are co-mixed in the same patches. While we do not have a fluorescently labeled perfluorinated probe, the spatial distribution of the two phospholipids can simultaneously be determined in a single fluorescence experiment. To accomplish this, we have used dual-labeled samples containing both fluorescent probes, with contrast provided by fluorescence lifetime (Figure 2-5).

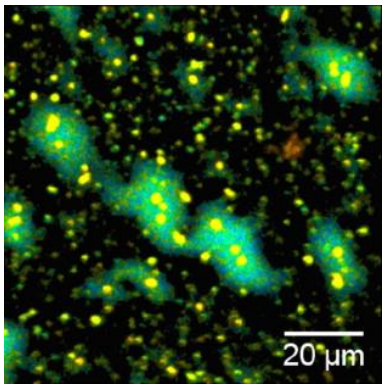

Figure 2-5 False color (averaged lifetime) fluorescence lifetime image (64µm x 64µm) for 4:1:5 ternary mixture. Color in the image reflects the weighting of the 2.7 ns (Bodipy-PC) lifetime component compared with the weighting of the 5.4 ns component, with blue-green-red corresponding to low, medium and high fractional contribution to the amplitude of the 2.7 ns component.

Differences in fluorescence lifetimes for the two probes can be used to distinguish DPPC from DPPG; literature sources list the lifetime for Bodipy-PC at ~ 4 ns in solution[43] and NBD-PG at ~ 10 ns in membranes[44] (values ranging from 7-11 ns from other model membrane systems can be found elsewhere in the literature). Measurements of control samples of mixed films containing either Bodipy-PC or NBD-PG alone gave a distribution of lifetimes, which complicates the analysis. Based on the single-component control sample measurements, Bodipy-PC was taken to have a lifetime of ~ 2.7 $\pm$ 0.5 ns in the mixed films, and NBD-PG ~ 5.4 $\pm$ 0.8 ns.

The values were slightly lower (quenched) than those obtained for solution-based experiments, which is consistent with the expected result for dry samples on glass substrates.

For the ternary mixture, image data was fit using two constrained lifetimes (2.7 ns and 5.4 ns) and the amplitudes of these two components was allowed to vary. Using the false color scheme defined by the relative weight of the two lifetime components in Figure 2-5, the blue and red regions correlate to regions of the sample that primarily consist of NBD-PG and Bodipy-PC, respectively. For the 4:1:5 monolayer, the micron-sized patches were a mixture of both DPPC and DPPG, with patches varying widely in overall composition. The patches surrounded a number of scattered aggregates (yellow) that were enriched in DPPC (~80%). Outside of the patches, large numbers of heterogeneous aggregates were observed which showed varying amounts of DPPC and DPPG content, and on only very rare occasions were pure DPPC (red) patches detected. However, a large fraction of these aggregates were highly enriched in DPPC, providing further support of the hypothesis that the highly luminescent aggregates observed in the steady-state fluorescent measurements were regions of the film that were locally enriched in DPPC. In short, all luminescent regions of the sample, patches and aggregates, were co-mixtures of DPPC and DPPG, and the dark regions contain large quantities of dispersed phospholipid in the form of aggregates. Again, while we cannot definitively determine the location of the C18F using microscopy approaches alone, the combined data indicate the films are co-mixtures of DPPC, DPPG and C18F.

While fluorescence-based imaging provides information about the spatial distribution of surfactant in the mixed system, the approach cannot provide morphological information about surfaces at length-scales below the diffraction limit of light (~300 nm for the experiments described here), nor does it provide information about the height of film above the underlying

substrate. Film morphology is of particular interest for model PS systems, as it has been proposed that the ability of PS to form surfactant multilayers at high film compression and to form nanometer-sized domains ('nanodomains') is important for its function.[5,45] In particular, the ability to form surfactant multilayers has been linked to the formation of a surface-associated surfactant reservoir (excess surfactant beyond a monolayer) that can be readily incorporated into the PS monolayer during respiration. To assess film morphology, AFM images were used to examine the binary and ternary mixtures at the nanometer length-scale. Figure 2-6 (A-D) shows AFM images as well as the corresponding cross-sectional analysis of different binary and ternary surfactant mixtures.

As shown Figure 2-6A, AFM images of binary (1:1) DPPC-C18F mixed films consisted of a uniform flat surface dotted with circular protrusions with heights ranging from ~2-6 nm and diameters ranging from ~30-450 nm. Based on the dimensions of the protrusions, these must be multi-molecular aggregates and it is reasonable to assume that these are the highly-fluorescence DPPC-rich aggregates that were observed in the confocal fluorescence images. These observations agree with our previous AFM measurements[27] which indicate a high degree of attraction between film components can favor the formation of multi-molecular aggregates over a simple continuous monolayer on the substrate. For comparison, Figure 2-6B shows a similar image for a binary (1:1) DPPG-C18F mixture. These films also contained circular protrusions (in this case, the protrusions were surrounded by an indentation) as well as occasional cracks in the deposited films. The protrusions had heights of ~0.2-12 nm, with diameters in the range of ~ 10-40 nm, with this size being an overestimate because of tip convolution effects, again indicating that these were multimolecular aggregates. In conjunction with the results from the confocal

fluorescence imaging experiments, these results also suggest that the phospholipid tends to form multimolecular aggregates when mixed with C18F.

AFM images of the ternary films (ratios 4:1:5 and 1:4:5) are shown in Figure 2-6 (C and D). In general, these films had morphologies that were comparable with the DPPG-C18F binary films, and contained an abundant number of phospholipid aggregates (based on the FLIM images, these aggregates were a heterogeneous mixture of phospholipids) distributed over the entire surface. As noted previously, we cannot entirely dismiss the possibility that depositing the surfactants from the air-water interface onto a solid substrate may alter the overall film structure. Future experiments involving Brewster angle microscopy may help resolve this issue. However, based on the assumption that deposition causes negligible alterations to overall film structure, the observation of multimolecular phospholipid aggregates in the mixed films is of potential importance and value for future PS applications. As noted previously, the formation of multilayer deposits in PS mixtures has been related to the formation of phospholipid reservoirs which enhance the surfactant film's performance. It has been recognized that the formation of phospholipid reservoirs in real PS is associated with the presence of various surfactant proteins (SP-A, SP-B and SP-C), although the precise mechanism and nature of this association remains unclear.[5] The mixed system described here is capable of producing multimolecular aggregates that are highly enriched in both DPPC and DPPG without the need for additional surfactant proteins. Given the relatively large preparation, storage and handling costs associated with protein-containing pharmaceutical materials, the use of simple ternary mixtures of this type holds significant potential for practical PS formulations with excellent performance and low-costs.

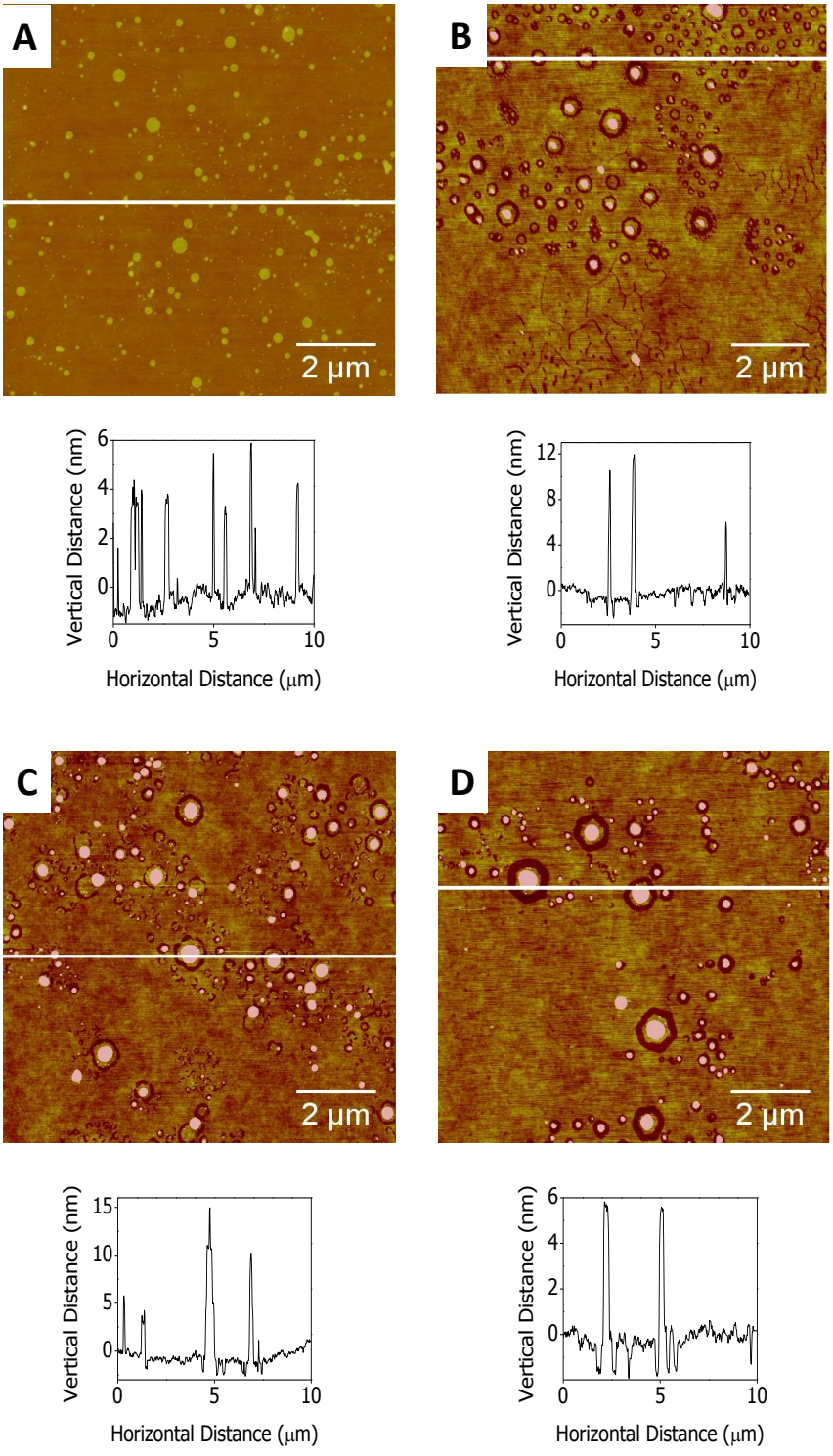

Figure 2-6 AFM height mode images (10µm x 10µm) and the cross-sectional analysis of LB films deposited on glass substrate using water as a subphase A: 1:1 DPPC:C18F, B: 1:1 DPPG:C18F, C: 4:1:5 DPPC:DPPG:C18F, D: 1:4:5 DPPC:DPPG:C18F.

2.4.5 Conclusion

The miscibility and film-forming abilities of binary and ternary mixtures of the surfactants DPPC, DPPG and C18F have been investigated at the air-water and solid-air interfaces by a combination of thermodynamic and structural characterization approaches. The addition of the perfluorinated surfactant to phospholipids results in enhanced overall film stability. While all three film components were macroscopically miscible under all conditions investigated, and a strong attractive interaction between components was observed, the strongest surfactant-surfactant interaction took place between DPPC and C18F. This additional film stabilization resulted from the interaction between the zwitterionic headgroup of DPPC and the negatively-charged headgroup of C18F. Film compressibility was slightly improved by the presence of the perfluorocarbon surfactant. Mixed films deposited onto solid substrates contained multimolecular aggregates, likely enriched in DPPC, and the formation of such "nanodomains" has significant potential value for prospective PS formulations as a phospholipid reservoir for enhanced surfactant adsorption during respiration cycles.

2.4.6 Acknowledgments

Funding for this work was provided by the Natural Sciences and Engineering Research Council of Canada (NSERC), the Canada Foundation for Innovation (CFI), the Province of Saskatchewan and by the University of Saskatchewan. The Saskatchewan Structural Sciences Centre (SSSC) is acknowledged for providing access to fluorescence microscopy instrumentation.

2.4.7 Appendix A. Supplementary Material

Table 2-2 Tabulated values of ΔG_{ex}^{π} for 1:4:X ternary mixtures at low mole fraction of C18F.

	ΔG_{ex}^{π} *(J/mol)*	
π (mN/m)	*1:4:0*	*1:4:1.25*
5	-281	-235
10	-404	-328
20	-456	-481
30	-446	-495
40	-497	-546
50	-606	-610

2.4.8 References

1. Engelskirchen, S. The pseudo-binary pulmonary surfactant system. *Current Opinion in Colloid & Interface Science* **2007**, *12*, 68-74.

2. Notter, R. H. *Lung Biology in Health and Disease;* Lung surfactants: Basic Science and Clinical Applications; Marcel Dekker: New York, USA, 2000; Vol. 149.

3. Perez-Gil, J.; Keough, K. Interfacial properties of surfactant proteins. *Biochimica Et Biophysica Acta-Molecular Basis of Disease* **1998**, *1408*, 203-217.

4. Rugonyi, S.; Biswas, S. C.; Hall, S. B. The biophysical function of pulmonary surfactant. *Respiratory Physiology & Neurobiology* **2008**, *163*, 244-255.

5. Zuo, Y. Y.; Veldhuizen, R. A. W.; Neumann, A. W.; Petersen, N. O.; Possmayer, F. Current perspectives in pulmonary surfactant - Inhibition, enhancement and evaluation. *Biochimica Et Biophysica Acta-Biomembranes* **2008**, *1778*, 1947-1977.

6. Kissa, E., Ed.; In *Fluorinated Surfactants and Repellents, Second Edition;* Marcel Dekker Inc.: New York,USA, 1997; Vol. 97.

7. Krafft, M. Fluorocarbons and fluorinated amphiphiles in drug delivery and biomedical research. *Adv. Drug Deliv. Rev.* **2001**, *47*, 209-228.

8. Krafft, M.; Goldmann, M. Monolayers made from fluorinated amphiphiles. *Current Opinion in Colloid & Interface Science* **2003**, *8*, 243-250.

9. Lau, C.; Anitole, K.; Hodes, C.; Lai, D.; Pfahles-Hutchens, A.; Seed, J. Perfluoroalkyl acids: A review of monitoring and toxicological findings. *Toxicological Sciences* **2007**, *99*, 366-394.

10. Matsumoto, M.; Tanaka, K.; Azumi, R.; Kondo, Y.; Yoshino, N. Structure of phase-separated Langmuir-Blodgett films of hydrogenated and perfluorinated carboxylic acids investigated by IR spectroscopy, AFM, and FFM. *Langmuir* **2003**, *19*, 2802-2807.

11. Matsumoto, M.; Watanabe, S.; Tanaka, K.; Kimura, H.; Kasahara, M.; Shibata, H.; Azumi, R.; Sakai, H.; Abe, M.; Kondo, Y.; Yoshino, N. Control of two-dimensional nanopatterns by adjusting intermolecular interactions. *Adv Mater* **2007**, *19*, 3668-3671.

12. Matsumoto, Y.; Nakahara, H.; Moroi, Y.; Shibata, O. Langmuir monolayer properties of perfluorinated double long-chain salts with divalent counterions of separate electric charge at the air-water interface. *Langmuir* **2007**, *23*, 9629-9640.

13. Qaqish, S. E.; Paige, M. F. Mechanistic insight into domain formation and growth in a phase-separated langmuir-blodgett monolayer. *Langmuir* **2007**, *23*, 10088-10094.

14. Qaqish, S. E.; Paige, M. F. Structural and compositional mapping of a phase-separated Langmuir-Blodgett monolayer by atomic force microscopy. *Langmuir* **2007**, *23*, 2582-2587.

15. Qaqish, S. E.; Urquhart, S. G.; Lanke, U.; Brunet, S. M. K.; Paige, M. F. Phase Separation of Palmitic Acid and Perfluorooctadecanoic Acid in Mixed Langmuir-Blodgett Monolayer Films. *Langmuir* **2009**, *25*, 7401-7409.

16. Rontu, N.; Vaida, V. Miscibility of perfluorododecanoic acid with organic acids at the air-water interface. *Journal of Physical Chemistry C* **2007**, *111*, 9975-9980.

17. Shibata, O.; Krafft, M. Mixed Langmuir monolayers made from single-chain perfluoroalkylated amphiphiles. *Langmuir* **2000**, *16*, 10281-10286.

18. Yokoyama, H.; Nakahara, H.; Shibata, O. Miscibility and phase behavior of DPPG and perfluorocarboxylic acids at the air-water interface. *Chem. Phys. Lipids* **2009**, *161*, 103-114.

19. Gerber, F.; Krafft, M.; Vandamme, T.; Goldmann, M.; Fontaine, P. Preventing crystallization of phospholipids in monolayers: A new approach to lung-surfactant therapy. *Angewandte Chemie-International Edition* **2005**, *44*, 2749-2752.

20. Gerber, F.; Krafft, M.; Vandamme, T.; Goldmann, M.; Fontaine, P. Fluidization of a dipalmitoyl phosphatidylcholine monolayer by fluorocarbon gases: Potential use in lung surfactant therapy. *Biophys. J.* **2006**, *90*, 3184-3192.

21. Nakahara, H.; Lee, S.; Krafft, M. P.; Shibata, O. Fluorocarbon-Hybrid Pulmonary Surfactants for Replacement Therapy - A Langmuir Monolayer Study. *Langmuir* **2010**, *26*, 18256-18265.

22. Qaqish, S. E.; Paige, M. F. Rippled domain formation in phase-separated mixed Langmuir-Blodgett films. *Langmuir* **2008**, *24*, 6146-6153.

23. Qaqish, S. E.; Paige, M. F. Characterization of domain growth kinetics in a mixed perfluorocarbon-hydrocarbon Langmuir-Blodgett monolayer. *J. Colloid Interface Sci.* **2008**, *325*, 290-293.

24. Lehmler, H.; Bummer, P. Mixing of perfluorinated carboxylic acids with dipalmitoylphosphatidylcholine. *Biochimica Et Biophysica Acta-Biomembranes* **2004**, *1664*, 141-149.

25. Nakamura, S.; Nakahara, H.; Krafft, M. P.; Shibata, O. Two-component Langmuir monolayers of single-chain partially fluorinated amphiphiles with dipalmitoylphosphatidylcholine (DPPC). *Langmuir* **2007**, *23*, 12634-12644.

26. Eftaiha, A. F.; Paige, M. F. The influence of salinity on surfactant miscibility in mixed dipalmitoylphosphatidylcholine-perfluorooctadecanoic acid monolayer films. *J Colloid Interface Sci* **2011**, *353*, 210-219.

27. Yu, S. H.; Possmayer, F. Lipid compositional analysis of pulmonary surfactant monolayers and monolayer-associated reservoirs. *J. Lipid Res.* **2003**, *44*, 621-629.

28. Nakahara, H.; Nakamura, S.; Kawasaki, H.; Shibata, O. Properties of two-component Langmuir monolayer of single chain perfluorinated carboxylic acids with dipalmitoylphosphatidylcholine (DPPC). *Colloids and Surfaces B-Biointerfaces* **2005**, *41*, 285-298.

29. Yokoyama, H.; Nakahara, H.; Nakagawa, T.; Shimono, S.; Sueishi, K.; Shibata, O. Miscibility behavior of two-component monolayers at the air-water interface: Perfluorocarboxylic acids and DMPE. *J. Colloid Interface Sci.* **2009**, *337*, 191-200.

30. Saad, S. M. I.; Policova, Z.; Acosta, E. J.; Hair, M. L.; Neumann, A. W. Mixed DPPC/DPPG Monolayers at Very High Film Compression. *Langmuir* **2009**, *25*, 10907-10912.

31. vonNahmen, A.; Schenk, M.; Sieber, M.; Amrein, M. The structure of a model pulmonary surfactant as revealed by scanning force microscopy. *Biophys. J.* **1997**, *72*, 463-469.

32. Wang, L.; Cai, P.; Galla, H. J.; He, H. X.; Flach, C. R.; Mendelsohn, R. Monolayer-multilayer transitions in a lung surfactant model: IR reflection-absorption spectroscopy and atomic force microscopy. *European Biophysics Journal with Biophysics Letters* **2005**, *34*, 243-254.

33. Maltseva, E.; Shapovalov, V. L.; Mohwald, H.; Brezesinski, G. Ionization state and structure of L-1,2-dipalmitoylphosphatidylglycerol monolayers at the liquid/air interface. *J Phys Chem B* **2006**, *110*, 919-926.

34. Gaines, G. L. *Insoluble Monolayers at Liquid – Gas Interfaces*; Interscience Publishers: New York, USA, 1966; .

35. Goodrich, F. C. In *In Molecular interaction in mixed monolayers; Proceeding of the Second International Congress of Surface Activity*; **1957**, 85–91.

36. Koppenol, S.; Yu, H.; Zografi, G. Mixing of saturated and unsaturated phosphatidylcholines and phosphatidylglycerols in monolayers at the air/water interface. *J. Colloid Interface Sci.* **1997**, *189*, 158-166.

37. McConnell, H.; Tamm, L.; Weis, R. Periodic Structures in Lipid Monolayer Phase-Transitions. *Proceedings of the National Academy of Sciences of the United States of America-Physical Sciences* **1984**, *81*, 3249-3253.

38. Moore, B.; Knobler, C. M.; Broseta, D.; Rondelez, F. Studies of Phase-Transitions in Langmuir Monolayers by Fluorescence Microscopy. *Journal of the Chemical Society-Faraday Transactions II* **1986**, *82*, 1753-1761.

39. Peters, R.; Beck, K. Translational Diffusion in Phospholipid Monolayers Measured by Fluorescence Microphotolysis. *Proceedings of the National Academy of Sciences of the United States of America-Biological Sciences* **1983**, *80*, 7183-7187.

40. vonNahmen, A.; Post, A.; Galla, H. J.; Sieber, M. The phase behavior of lipid monolayers containing pulmonary surfactant protein C studied by fluorescence light microscopy. *European Biophysics Journal with Biophysics Letters* **1997**, *26*, 359-369.

41. Yuan, C.; Johnston, L. J. Phase evolution in cholesterol/DPPC monolayers: atomic force microscopy and near field scanning optical microscopy studies. *Journal of Microscopy-Oxford* **2002**, *205*, 136-146.

42. Haugland, R. P. *Molecular Probes - Handbook, Ninth Edition;* Molecular Probes, Inc.: Eugene, OR, 2002.

43. Kramer, B.; Koberling, F.; Ortmann, U.; Wahl, M.; Kapusta, P.; Bulter, A.; Erdmann, R. Time-resolved laser scanning microscopy with FLIM and advanced FCS capability. *Multiphoton Microscopy in the Biomedical Sciences V* **2005**, *5700*, 138-143.

44. Zuo, Y. Y.; Keating, E.; Zhao, L.; Tadayyon, S. M.; Veldhuizen, R. A. W.; Petersen, N. O.; Possmayer, F. Atomic force microscopy studies of functional and dysfunctional pulmonary surfactant films. I. Micro- and nanostructures of functional pulmonary surfactant films and the effect of SP-A. *Biophys. J.* **2008**, *94*, 3549-3564.

CHAPTER 3 THE INFLUENCE OF SALINITY ON SURFACTANT MISCIBILITY IN MIXED DIPALMITOYLPHOSPHATIDYLCHOLIE – PERFLUOROOCTADECANOIC ACID MONOLAYER FILMS

3.1 Description

This chapter is a verbatim copy of a paper published in the Journal of Colloid and Interface Science. [Reproduced with permission from Journal of Colloid and Interface Science, (353) 210–219, 2011.]

In this chapter the miscibility of mixed films systems comprised of perfluorooctadecanoic acid (C18F) and dipalmitoyl-sn-glycero-3-phosphocholine (DPPC) was explored as a function of subphase salinity. At the air-water interface, additivity measurements, excess Gibbs free energies of mixing and isothermal compressibility data derived from surface pressure-area isotherms showed that the specific adsorption of sodium ion to the negatively charged carboxylate group of C18F decrease the extent of the attractive interaction between the DPPC and the perfluorocarboxylic acid. This reduction in the overall film cohesion was further verified by the atomic force microscopy (AFM) images of the mixed LB films that indicated the multimolecular aggregates formation was diminished in the presence of sodium chloride as expected from the isotherm measurements.

The experimental section for this study is provided in the paper. A detailed description of the techniques used is provided in Chapter 1.

3.2 Description of the Candidate's Contribution

For this contribution, I carried out all experimental work, including preparation of samples and measurement of the isotherm and atomic force microscopy images. I played a major role in interpreting the results, wrote the initial draft of the work and participated in the subsequent editing in response to reviewers. Dr. Matthew Paige provided extensive guidance

throughout the experimental work and was greatly involved in results interpretation, writing and editing of the paper.

3.3 Relation of Contribution towards Research Objectives

This contribution was solely performed towards the objectives of the thesis research. In Chapter 2, we illustrated that the electrostatic attractive interaction between surfactant head group are crucial in controlling the miscibility of binary and ternary mixed monolayers made of C18F, DPPC and DPPG. These measurements were conducted using a Millipore water subphase (resistivity is about 18.2 ΩM.cm). For real-life applications such as pulmonary lung surfactant, it is important to consider the composition of extracellular fluid, with particular emphasis on ionic strength. Therefore, we chose to examine the impact of surfactant head group - ion interactions, particularly sodium (Na^+) and chloride (Cl^-) ions as they are the major inorganic ionic species found in the extracellular fluid, on the miscibility of mixed DPPC-C18F monolayer films at air-water and air-solid interfaces. Thermodynamic and microscopic data indicated that the specific adsorption of Na^+ to the negatively charged carboxylate head group of C18F reduced the extent of interaction between DPPC and C18F. A full discussion of the results of this study and its implications for the thesis research as a whole of is provided in Chapter 8.

The influence of salinity on surfactant miscibility in mixed dipalmitoylphosphatidylcholine – perfluorooctadecanoic acid monolayer films

Ala'a F. Eftaiha, Sophie M.K. Brunet and Matthew F. Paige

Department of Chemistry, University of Saskatchewan, 110 Science Place, Saskatoon, Saskatchewan, Canada, S7N 5C9

Received 7 July 2011, Accepted 17 September 2011

3.4.1 Abstract

The miscibility, mechanical and morphological properties of mixed Langmuir and Langmuir Blodgett monolayers prepared from the phospholipid 1,2-dipalmitoyl-sn-glycero-3-phosphocholine and the perfluorinated fatty acid perfluorooctadecanoic acid have been studied as a function of film composition and subphase salinity. It was demonstrated here, for the first time, that the extent of surfactant miscibility in mixed phospholipid-perfluoroacid monolayers, and hence the resulting mechanical properties of the monolayer film, can be controlled by altering the concentration of sodium ions in the underlying subphase. Elevated sodium ion concentrations resulted in lower net attractive interactions between film components, likely through specific ion adsorption to the negatively charged perfluoroacid, along with decreased film elasticities. These results differ significantly from conventional fatty acid-carboxylate monolayer systems in which film cohesion is typically enhanced through adsorption of cations to the surfactant headgroups. Atomic force microscope images of films deposited onto solid mica substrates revealed that the films deposited from pure water formed multimolecular aggregates of surfactant, which could be attributed to the highly cohesive nature of the films, but the use of salt in the subphase diminished aggregate formation and resulted in the production of homogeneous monolayer films.

3.4.2 Introduction

Fluorinated molecules possess a number of useful physical properties, such as low surface tension, chemical (and biological) stability and high oxygen-carrying capacity that make them well-suited for a variety of important technological applications. Applied materials that make use of the properties of these molecules include liquid ventilation media, temporary blood substitutes, drug-delivery media and emulsifiers for low surface-energy liquids.[1] Of particular recent interest for technological applications are partially or fully-fluorinated surfactants. Because of their lipophobicity, many of these surfactants are highly immiscible with structurally similar alkyl surfactants and, under appropriate conditions, will undergo phase-separation at the air-water interface. While such effects play key roles in emulsification and micellization processes, phase-separation has also been demonstrated as a viable approach for controlling the composition and morphology of solid films and liquid surfaces,[2-5] and because of this, there have been significant efforts made to both understand and control factors that regulate miscibility of mixed surfactant systems containing fluorinated amphiphiles.

Recent developments in this area of research have focused primarily on understanding phase-separation phenomena and monolayer film morphology in simple, immiscible binary mixtures of perfluorinated (or partially fluorinated) fatty acids and their hydrogenated counterparts (see the work by Broniatowski et al.[6] and others[7-9] for some recent examples). The film morphology and composition in these immiscible systems is regulated by a combination of inter-related factors, including dipole-dipole repulsion between charged surfactant headgroups, line-tension, kinetics of surface domain growth, substrate-mediated condensation and hydrodynamic flow effects.[2, 5, 7, 8, 10, 11] Further control of film morphology has been demonstrated by exploiting solubility of the components in an aqueous subphase, as well as

through kinetic control of the phase-separation process.[10,11] Through careful manipulation of these factors, a wide range of different film morphologies can be prepared, ranging from circular domains to nanoscale wires and lines.[3] While these studies of simple surfactant systems have helped provide a detailed fundamental understanding of miscibility and phase-separation phenomena, our group has a significant interest in extending this work into mixed phospholipid systems, with an ultimate goal of exploiting phase-separation (and miscibility in general) to control composition and morphology of physicologically relevant membrane monolayer and bilayer systems. The work described here seeks to examine factors that affect miscibility of binary mixtures of a simple dipalmitoylphosphatidylcholine (DPPC) phospholipid and a perfluorinated fatty acid. We are particularly interested in developing a rigorous understanding of the influence of cation binding on surfactant-surfactant interactions in these systems, as any potential biological / biomedical applications will likely take place in environments of high ionic strength, and the area of research is poorly developed.

A significant body of work exists on interactions between biological surfactants and fluorinated surfactants, in part because of the potential deleterious effects surfactant miscibility can have on lung-surfactant mixtures when fluorinated substances are respirated (see the work by Arora et al.[12] and others[13-21]). Lehmler et al.[17, 22, 23] have carried out a number of investigations of miscibility on binary mixtures of partially fluorinated surfactants and phosphatidylcholines of varying chain length and reported that these monolayer mixtures are often partially miscible (negative deviations from ideal mixing) at the air-water interface, with film components most typically exhibiting an attractive interaction. However, the extent of miscibility had a strong dependence on surfactant chain length (even versus odd carbon chain length alters miscibility, increasing chain lengths beyond a certain length result in increased immiscibility), headgroup

charge (opposite charge leads to enhanced miscibility) as well as the surface pressure of the measurement (increasing miscibility was observed with increasing pressure). Results of a similar nature have been reported in mixed vesicle (bilayer) systems.[24] Shibata et al. have also reported on surfactant miscibility in a number of mixed perfluorocarbon-phospholipid systems.[9, 15, 16, 25] Of particular interest are investigations of a series of perfluorocarboxylic acids ($CF_3(CF_2)_nCOOH$) with DPPC on high-salinity (0.2M NaCl) aqueous subphases. These systems varied from miscible (n = 10), to partially miscible (n = 12, 14; miscibility depends on relative mole fraction of perfluorocarbon in the mixture) to immiscible (n = 16), and that the perfluorcarbon surfactant had the capability to soften and dissolve solid DPPC domains upon sufficient monolayer compression.

While the work by Shibata represents important progress in understanding miscibility in these simple binary systems, further research in this area is required, particularly in understanding the role of subphase salinity in component miscibility. This is a particularly important issue for biomedical applications of surfactant mixtures, as the dissolved salts that are present in physiological environments have the potential to greatly affect phase-behaviour, miscibility and mechanical properties of the film. There is also abundant evidence in the literature that binding of ions to the zwitterionic headgroups of phospholipids (negatively charged phosphate, positively charged ammonium at neutral pHs), typically through Coulombic forces, can play a significant role in controlling lipid aggregation and film stability (see [26] and related references), and ion-binding of this type may provide a useful chemical "handle" to promote or disable miscibility in mixed surfactant films. In this work, we study, in further detail, the miscibility of perfluorooctadecanoic acid ($C_{17}F_{35}COOH$, abbreviated C18F) with DPPC under various conditions of subphase salinity, with a view towards understanding and

quantifying the influence of subphase salinity on miscibility in mixed binary monolayers. Miscibility of film components was investigated through measurements of Langmuir and Langmuir-Blodgett (LB) films, including the measurement of pressure-area isotherms, isothermal elasticities, Gibbs mixing energies, as well as atomic force microscope (AFM) characterization of monolayer film morphologies. Under the conditions investigated, it was found that the two surfactants were miscible, though the degree of miscibility, mechanical properties of the films and the mixing energetics was a strong function of sodium ion concentration and compression pressure. A wide variety of film morphologies were observed under the deposition conditions observed, and the results are discussed in comparison with those obtained in closely-related binary surfactant systems.

3.4.3 Materials and Methods

3.4.3.1 Chemicals

Perfluorooctadecanoic acid (97%) was purchased from Alfa Aesar and dipalmitoylphosphatidylcholine (1,2-Dipalmitoyl-sn-glycero-3-phosphocholine, semisynthetic, 99%) was purchased from Sigma-Aldrich Corporation. Sodium chloride, hexanes (HPLC grade) and absolute ethanol (99%) were purchased from EMD or Alfa Aesar. All reagents were used as received without additional purification. Muscovite mica (Structure Probe Inc.) was cut into ~12 mm x 12 mm squares and freshly cleaved with adhesive tape prior to film deposition.

3.4.3.2 Surface Pressure Isotherms and Langmuir-Blodgett Film Deposition

Stock solutions of the surfactants C18F and DPPC (1.25 mM) were prepared in an *n*-hexane/ethanol mixture (9:1 by volume). Appropriate volumes of the stock solutions were mixed to give a range of solution compositions (molar ratios of DPPC to C18F of 3:1, 2:1, 1:1, 1:2, and 1:3). Ultrapure water (Millipore, pH 5.5, resistivity 18MΩ.cm) was used as subphase and in the

preparation of 0.2 M and 0.4 M NaCl solutions. Surface pressure-area isotherms and LB film deposition was carried out in a KSV 2000 Langmuir trough system (KSV Instruments). In all experiments, the subphase temperature was maintained at 25 ±1 ^{o}C using an external circulating water bath. Before each measurement, blank runs (compression of a freshly cleaned subphase surface) showed no appreciable change in surface pressure with compression. For Langmuir and LB film preparation, a 60 μL aliquot of surfactant solution was spread on the surface of the subphase using a micro-syringe. The solvent was allowed to evaporate for ten minutes prior to compression. The compression rate was 20 mm/min for isotherm experiments and 10 mm/min for film deposition. For each surfactant mixture, the π–*A* isotherm was repeated a minimum of three times and the isotherms showed no significant deviation between replicate measurements. Depositions were carried out at a surface pressure of 30 mN/m and the film was allowed to stabilize for 10 min before the mica substrate was pulled upward through the water-air interface in a single stroke. The film was left to dry in a clean environment (a clean plexiglass enclosure surrounding the trough) at room temperature for several hours before measurement in the AFM.

3.4.3.3 Atomic Force Microscope Measurements

A Dimension Hybrid Nanoscope system (Veeco Metrology Group) was used to image the LB films. The measurements were performed in contact mode using commercial non-conductive silicon nitride AFM probes (Veeco Metrology Group). Samples could be imaged repeatedly without observable tip-induced damage, though the film could be scratched off the substrate when desired ("scratching experiments") by repeatedly scanning the film at high operating forces with a stiff (~0.58 N/m) probe. Samples were typically imaged with a scan size of 20 μm x 20 μm, a scan rate of 1.00 Hz and a resolution of 512 pixels per line.

3.4.4 Results and Discussion

3.4.4.1 Compression Isotherm Measurements

Surface pressure-area (π-*A*) isotherms were obtained for monolayers of pure DPPC, C18F and their mixtures at 25^{o}C, using pure water, 0.2 M and 0.4 M NaCl solutions as a subphase. For the pH = 5.5 subphase used in these experiments, one can reasonably expect C18F (pKa ~3.8, reference [21]) to exist almost exclusively (~98%) in its negatively ionized form (R-COO^{-}) while the DPPC will exist as its neutral zwitterion.[27] Results for the isotherm experiments are shown in Figure 3-1(A-C). The isotherm for the pure DPPC film in water was typical of those reported elsewhere in the literature and consisted of a characteristic gaseous phase at low compression, a transition region between a liquid-expanded (LE) and liquid-condensed (LC) phases at ~13-15 mN/m and a collapse pressure of ~ 68 mN/m. There were no significant isotherm shifts or evidence of additional phase-transitions for the pure DPPC isotherms as a function of subphase salinity. These results are consistent with those reported by Sovago[28], who investigated the influence of subphase Na^{+} and Ca^{2+} on DPPC compression isotherms, and observed that Na^{+} had no significant effect on the compression behaviour. Association of the cation with the zwitterionic headgroup is minimal under these conditions, and it has additionally been proposed that at higher surface pressures (monolayer compressed beyond the LE phase), Na^{+} is actively "squeezed out" of the phospholipid headgroup region.

Isotherms for C18F consisted of a single, smooth curve which did not contain a LE-LC transition, and a film collapse pressure of ~65-68 mN/m, which is again consistent with isotherms we have reported previously in the literature.[11] As was the case with DPPC, there were no shifts or new phase-transitions observed for the pure C18F isotherm as a function of subphase salinity.

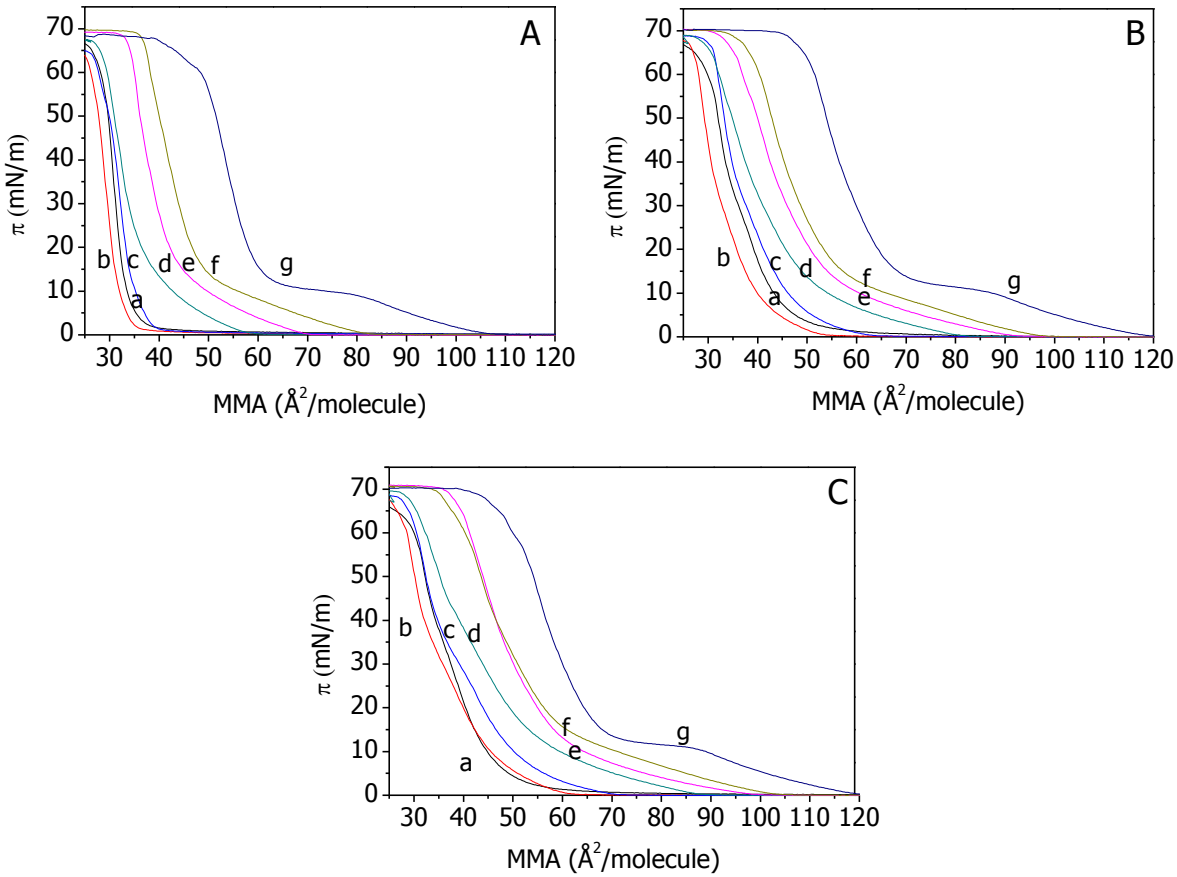

Figure 3-1 Surface–pressure area isotherms of pure and mixed monolayers at air-water interface. A. Water, B. 0.2 M NaCl, C. 0.4 M NaCl (a, C18F; b, 3:1; c, 2:1; d, 1:1; e, 1:2; f, 1:3; g, DPPC).

For the mixed component films, the π-*A* isotherms shifted markedly in comparison with the isotherms for the pure individual components. For the pure water subphase, the majority of the isotherms fell between the extremes defined by the two pure components. However, one of the mixtures (1DPPC:3C18F) displayed isotherms that were shifted to smaller mean molecular areas than the pure C18F alone, indicating the occurrence of a non-ideal mixing process. The LE-LC transition in DPPC becomes difficult to observe at even the largest DPPC:C18F ratios investigated, suggesting that the presence of the perfluorcarbon aids in the solubilization of DPPC as was reported previously in a closely-related system by Courrier et al.[13] While there were subtle shifts and shape variations in the isotherms as a function of salt concentration and film composition for the mixtures (explored in detail in the subsequent sections), the

disappearance of the LE-LC transition upon perfluorocarbon addition was found under all conditions that were investigated.

The miscibility of DPPC and C18F was studied in context of the additivity rule (equation (3.1)), which relates the measured mean molecular area of the mixed film to the areas and mole fractions of the individual film components.[29] For a binary film at a given surface pressure in which components are either completely immiscible or behave ideally and are completely miscible, the mixed film area (A_{12}) obeys the following:

$$A_{12} = A_1\chi_1 + A_2\chi_2 \qquad (3.1)$$

where A_1 and A_2 are the mean molecular areas of the pure, individual components and χ_1 and χ_2 are the mole fractions of the components present in the film.

Figure 3-2 (A-C) shows plots of experimentally determined mixed film areas as a function of film composition for two different surface pressures, 10 mN/m and 40 mN/m (other surface pressures gave comparable results). For comparison purposes, the ideal behavior predicted by equation (3.1) is also included, and appears as straight line. Measurements are plotted for three different subphase salinities (0-0.4 M NaCl). Under all salinity conditions examined, the systems exhibited strong negative deviations from ideality, manifesting as experimental points that fall below the line predicted by equation (3.1).

These results indicate that the cohesive interactions between DPPC and C18F are greater than those between the pure individual film components, with the molecules occupying a smaller mean molecular area than in the pure films, and that the monolayer components are partially miscible. Again, these results lend support to the evidence that suggests C18F mixes intimately with the DPPC and effectively dissolves the phospholipid. The negative deviations from ideality were marginally larger at low surface pressures (on the order of a few percent) than higher

pressures. This general result is similar to that observed by Hiranita et al. who attributed the attractive interactions between surfactant molecules at low pressures to the (presumably long-range) attraction between polar head-groups, balanced by a compensating repulsion between the fluorocarbon chains and the side-groups of the phospholipid as the surface pressure is increased.[25]

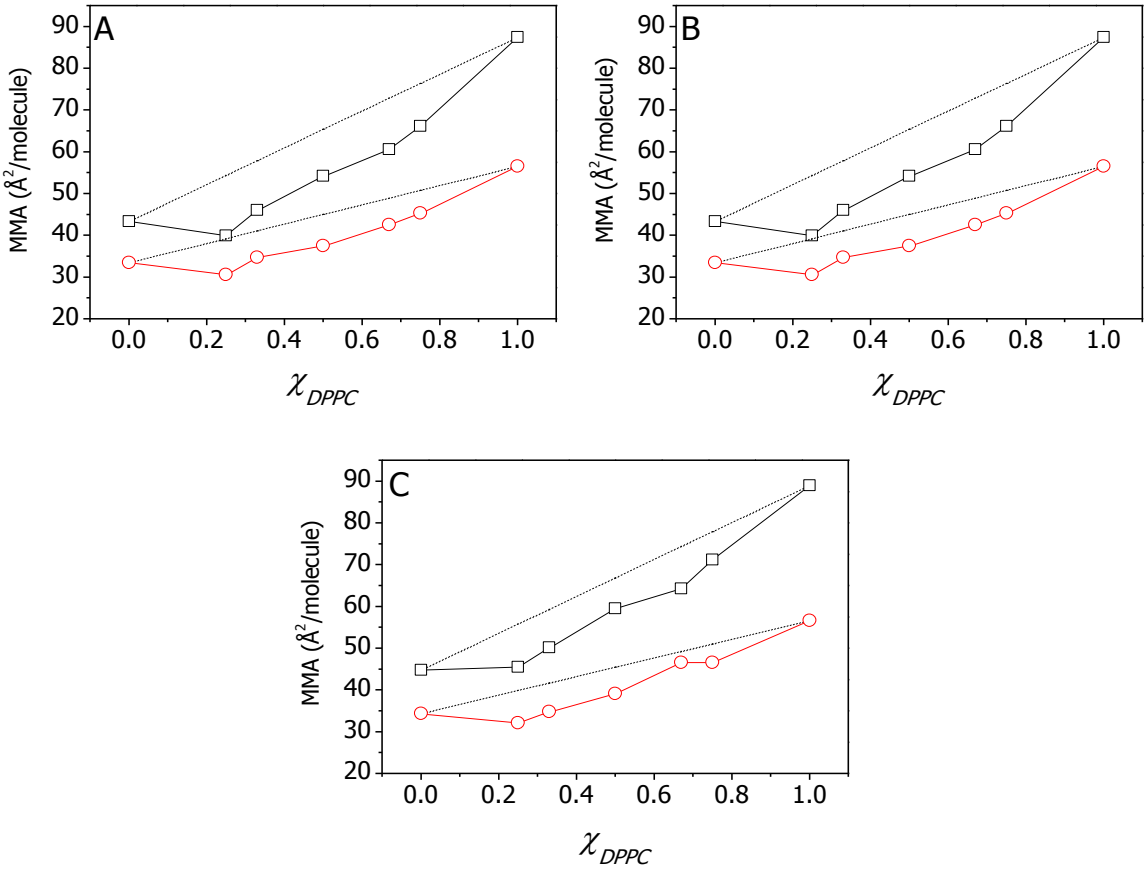

Figure 3-2 Mean molecular area as a function of mole fraction of DPPC. A. Water subphase, B. 0.2 M NaCl subphase, C. 0.4 M NaCl subphase. (□, 10mN/m; ○, 40mN/m, the dashed lines represents ideal behavior as dictated by the additivity relation, equation (3.1), solid lines are included as a guide to the eye).

It seems likely that a similar effect is in action here, and supporting data is discussed later in this manuscript. Furthermore, it was found that as the concentration of NaCl in the subphase was increased, the magnitude of the negative deviations decreased, and the mixed systems approached ideality. It is of value to consider the role played by the charge of the surfactant

headgroup in greater detail, and the expected effect of subphase salinity on surfactant interaction. As stated previously, the DPPC and C18F will be neutral (zwitterion) and negatively charged, respectively, at the subphase pH used here. Since the acyl side-chains of the phospholipid and the perfluorcarbon are highly immiscible, the overall miscibility of the system will be regulated by the nature of the interaction between the charged surfactant headgroups and any factors which affect this interaction. For the pure water subphase, the strong miscibility indicates that the net interaction between headgroups must be attractive (presumably electrostatic in nature, between the negatively charged carboxylic acid group and the positive charge of the zwitterionic phospholipid headgroup), which is consistent with the results described by Lehmler[23] and others on closely related phospholipid systems. Increasing the concentration of Na^+ in the subphase must then modulate the degree of interaction between the two different headgroups, likely through specific adsorption of the cation to the negatively charged perfluoroacid. We note that while the binding of Na^+ to carboxylate ion is typically weak in aqueous solution (values for equilibrium formation constants for insoluble perfluorinated fatty acid surfactants are not readily available in the literature, but the K_f for acetate-Na^+ binding (e.g. $CH_3COO^- + Na^+ = CH_3COONa$) which can be taken as a reasonable estimate of binding affinity, is on the order of 1[30]; other evidence for specific binding of Na^+ to acetate in aqueous solutions can also be found, for example Aziz et al.[31]), there is still abundant evidence in the literature for specific adsorption of Na^+ to carboxylate surfaces (for a review, see the book by Davies and Rideal[32]). For simple alkyl fatty-acid monolayer films on subphases with $pH > pK_a$, specific adsorption of mono- and divalent ions often leads to film stabilization through decreased dipole-dipole repulsion of the R-COO^- headgroups; for the mixed DPPC-C18F system, this effect is reversed because of the presence of opposite charges on the surfactant headgroups. In short, the primary role of the

subphase Na^+ appears to be to specifically adsorb to the negatively charged perfluoroacid and give a net decrease in the attractive interactions between headgroups of the two different surfactants.

3.4.4.2 Isothermal Elasticity Measurements

To further explore the influence of headgroup charge and subphase salinity on the mechanical properties of the mixed films, the isotherm data was analyzed in terms of isothermal elasticities (κ, the inverse of the isothermal compressibility, C_s), defined as:

$$\kappa = C_S^{-1} = -A\,(\frac{d\pi}{dA})_T \qquad (3.2)$$

Figure 3-3 shows the experimentally determined values of elasticities (measured at surface pressures of 10 and 40 mN/m, values that lie before and after the anticipated phase-transition in the pure DPPC film) as a function of mole fraction of DPPC at the three different subphase salinities (0 M, 0.2 M and 0.4 M NaCl). As an aside, we note that if the role of the salt in the subphase was simply to change the solubility of the surfactants in the subphase rather than to modulate interaction forces by binding to the charged surfactant headgroups, the relative position of the isotherms would shift with salt concentration due to the change in apparent mean molecular area, but the elasticities (slopes) would show minimal changes at these pressures. As is clear from Figure 3-3, the elasticities do change markedly with salt concentration, which we take as an indicator that specific ion adsorption to the monolayer rather than a simple change in solubility of the surfactants is at play here. Film elasticities for the mixed monolayers ranged from ~10-130 mN/m at the low surface pressure, to values of ~80-420 mN/m for the high surface pressure regime. While it is difficult to find published values for chemically comparable systems, we note that these values are generally higher than the elasticities reported by Hoda et al.[15] for

mixed DPPC / partially fluorinated "hybrid" phenylphosphate films, which were typically around 30-40 mN/m and 100-200 mN/m for comparable surface pressures.

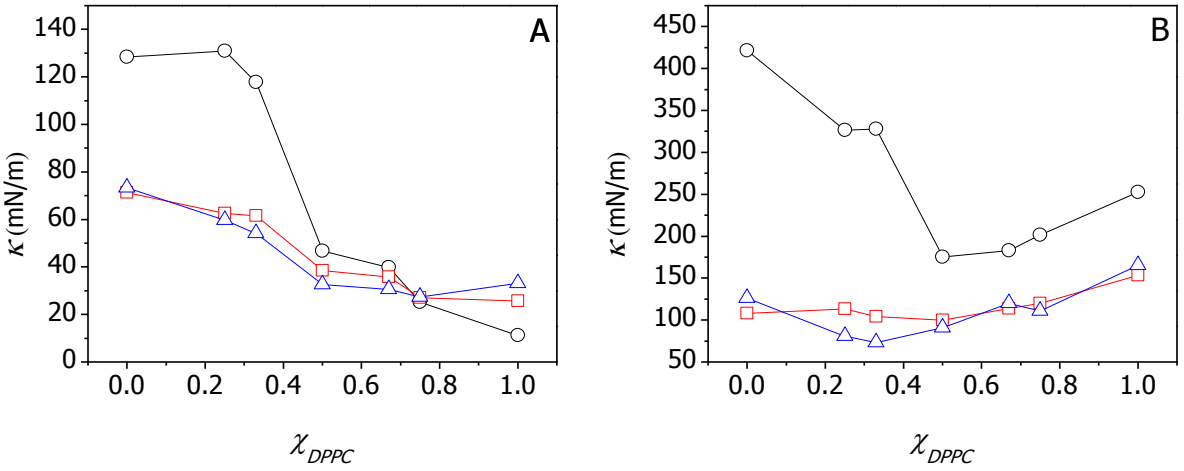

Figure 3-3 Elasticity of DPPC/C18F mixtures as a function of mole fraction of DPPC. A. Surface pressure of 10 mN/m B. Surface pressure 40 mN/m (○, water; □, 0.2 M NaCl; △, 0.4 M NaCl).

At π = 10 mN/m (DPPC is anticipated to be in the LE phase under these conditions), film elasticities generally decreased as a function of increasing χ_{DPPC}, indicating that under these conditions, pure C18F monolayers are relatively rigid, DPPC monolayers are relatively flexible, and mixing of the two components results in films of an intermediate rigidity. This is the expected result from combining the two highly miscible film components. The most extreme change in elasticity as a function of film composition occurred between the 1DPPC:2C18F and 1DPPC:1C18F, in which film elasticity decreased by ~50%, though the exact reason for this large change is presently unclear. In terms of the effect of subphase salinity, the film elasticities were generally larger in the pure water subphase than for the higher salt concentrations, regardless of film composition. There were minimal differences between the 0.2 M and 0.4 M NaCl subphase compositions in terms of elasticity values, suggesting that the specific adsorption of the Na^+ reaches saturation at or below a salt concentration of 0.2 M.

For measurements carried out at π = 40 mN/m (DPPC anticipated to be in the LC phase), elasticities were significantly greater than those observed at lower surface pressures, which is the expected result for more condensed films. We also note that high film elasticity (low compressibility) is a particularly desirable property for pulmonary lung surfactant applications[33] and the values reported here suggest that, at least in this regard, mixtures of DPPC and perfluorocarbons have some potential for such applications (for example, Panda et al. have reported elasticities of surfactant films from "normal", non-ventilated lungs of ~50 mN/m,[34] and the mixtures described in our study are superior in this regard). However, the response of film elasticity to subphase salinity might be of some concern, as it leads to a significant reduction in these values. As was the case for the low surface pressure regime, at low χ_{DPPC}, elasticities on a pure water subphase were greater than those for high salinity subphases. The most dramatic change in elasticity was observed between 3DPPC:1C18F and 2DPPC:1C18F in a pure water subphase, with the elasticity dropping from ~ 330 mN/m to ~ 175mN/m; this result is consistent with that observed for the lower pressure system shown in Figure 3-3A. Let us again consider these data in the context of specific ion adsorption to the negatively charged C18F headgroups, and the interaction of these with DPPC. For pure films of negatively-charged alkyl fatty acids, it is well-known that adsorption of ions (typically di- or trivalent alkaline cations) at the interface often results in the formation of highly rigid, insoluble soap-like films. This approach is often adopted to enhance the mechanical stability of monolayer films during deposition onto solid substrates.[35] However, the situation for the mixed DPPC-C18F system is quite different; as seen from the isotherm data, specific adsorption of cations to the negatively charged C18F headgroups leads to decreased attractive interactions between C18F and DPPC, and hence a net decrease in

mechanical stability (cohesion) of the monolayer. The system we describe here is unusual in that the addition of cations to the subphase leads to decreased overall film elasticity.

3.4.4.3 Gibbs Free Energy of Mixing Measurements

A quantitative examination of the energetics of the mixing process and the importance of subphase salinity on surfactant interaction can be obtained through evaluation of the excess Gibbs free energy of mixing for the system, ΔG_{ex}^{π}, defined as:

$$\Delta G_{ex}^{\pi} = \int_0^{\pi} [A_{12} - (\chi_1 A_1 + \chi_2 A_2)] d\pi \qquad (3.3)$$

Calculated ΔG_{ex}^{π} values are shown for a series of different isotherm pressures and subphase salinities in Figure 3-4 (A-D).

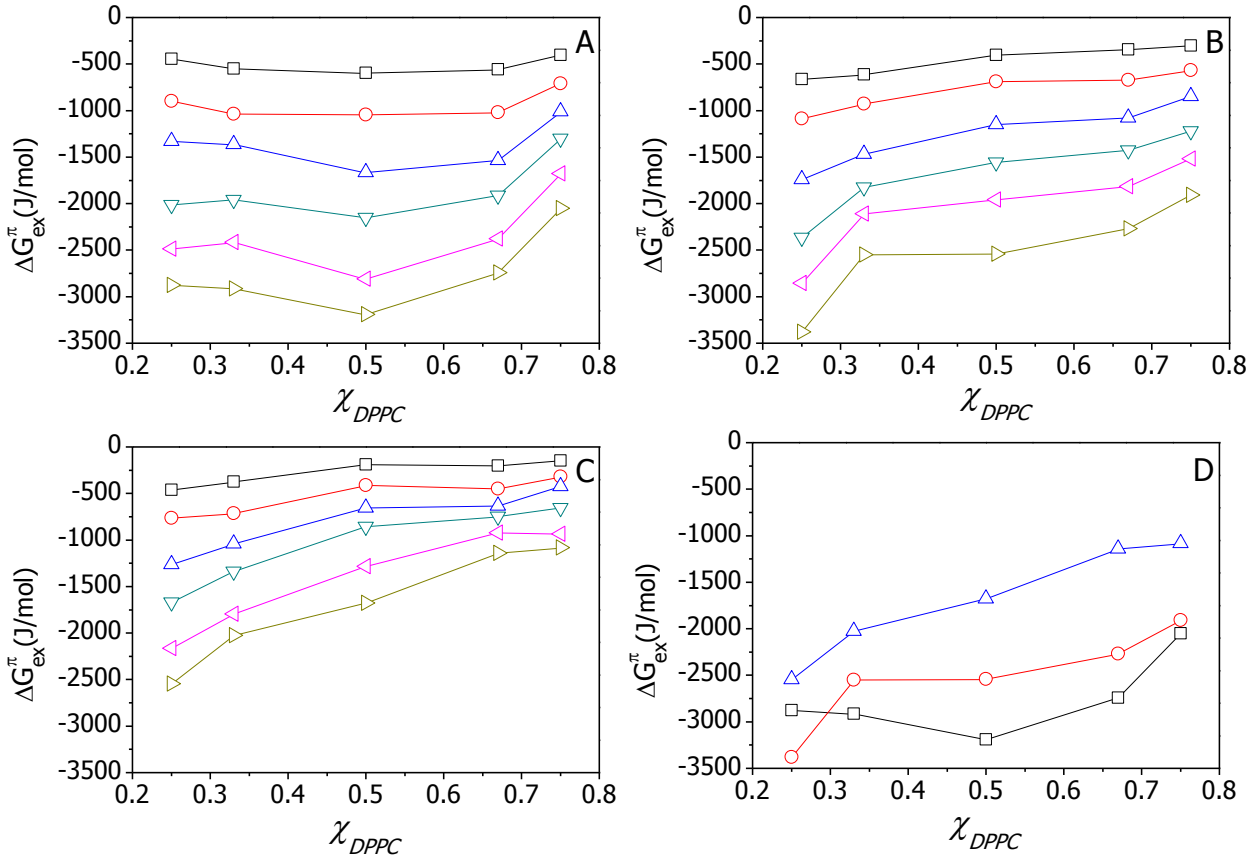

Figure 3-4 Excess Gibbs free energy as a function of mole fraction of DPPC. A. Water, B. 0.2 M NaCl, C. 0.4 M NaCl (□, 5 mN/m; ○, 10 mN/m; △, 20 mN/m; ▽, 30 mN/m; ◁, 40 mN/m; ▷, 50 mN/m). D. Excess Gibbs free energy at π = 50 mN/m for □, water; ○, 0.2 M NaCl; and △, 0.4 M NaCl.

The negative Gibbs mixing energy values verify that the films are indeed intimate mixtures of film components (cohesive films), and that the mixed films have greater thermodynamic stability than the pure components. Gibbs mixing energies became increasingly negative as a function of surface pressure, as expected from simply increasing the range of integration in equation (3.3). For a pure water subphase (Figure 3-4A), the Gibbs' energy reaches a minimum value at approximately equimolar composition for all of the surface pressures examined, and ranged in magnitude from -600 J/mol to -3200 J/mol (for reference, we compare this value against available thermal energy, RT ~ 2500 J/mol under the conditions used for these experiments, indicating the high degree of film stability for the mixed systems). Again, these values are strikingly different from those reported by Hoda for the mixed DPPC-hybrid amphiphile systems. The hybrid amphiphile systems exhibited Gibbs energies ranging from ~ -70 J/mol to 720 J/mol with values most typically being positive for $\pi > 5$ mN/m. The positive values were rationalized in terms of a short-range repulsive interaction between molecules, with the extent of repulsion depending on the chain length of the perfluorinated functional group on the amphiphile. The values measured in our fatty acid systems indicate that very strong film cohesion can be obtained through the use of simple perfluorinated fatty acids combined with DPPC in the absence of Na^+, and that tailoring such properties into applied surfactant mixtures such as pulmonary lung surfactants might not require the use of complex perfluorocarbons that are synthetically challenging to produce.

In terms of salinity dependence, the values of the excess Gibbs free energy generally became increasingly positive upon addition of NaCl (Figure 3-4 (A-C), with data from $\pi = 50$ mN/m summarized as a function of salinity to enable ease of comparison in Figure 3-4D; data at lower values of π were comparable), consistent with a net decrease in the magnitude of attraction

between film components upon salt addition. We do note that there was a slight anomaly in the trend of increasingly positive free energy values as a function of salt concentration; the Gibbs energies for 1DPPC:3C18F on the pure water subphase were marginally more positive than those observed for the high salinity subphases (observed for all values of π). However, this is consistent with the measurements of additivity and elasticity, which also change dramatically for these mixtures, indicating that film properties are particularly sensitive to salt concentrations at this particular composition.

3.4.4.4 Atomic Force Microscope Measurements

To assess surfactant film morphology for these systems, AFM imaging was used to characterize Langmuir-Blodgett (LB) films deposited onto solid mica substrates. Film deposition was carried out at π = 30 mN/m, in part because the films were both stable and reproducible at this pressure, but also to allow a reasonable comparison with other film morphologies reported in the literature which were deposited at comparable pressures. Film thicknesses were determined by either a "scratching experiment", in which a small area of the film (~2 μm x 2 μm) was removed from the underlying mica substrate by repeated scanning at a high operating force and subsequently measuring the height difference between the mica substrate and undamaged monolayer film surface, or by measuring the height difference between the film surface and the bottom of "pinhole" defects in the film. AFM images of LB films of DPPC, C18F and their mixtures using water and 0.4 M NaCl as subphase are shown in

Figure 3-5 (A-N), along with a cross-sectional analysis of the films (results for the 0.2 M subphase were comparable with the 0.4 M subphase and are not included here). Films deposited from high-saline subphases contained occasional nanometer-scale deposits, likely crystallized NaCl, but these were not so frequent as to significantly degrade image quality.

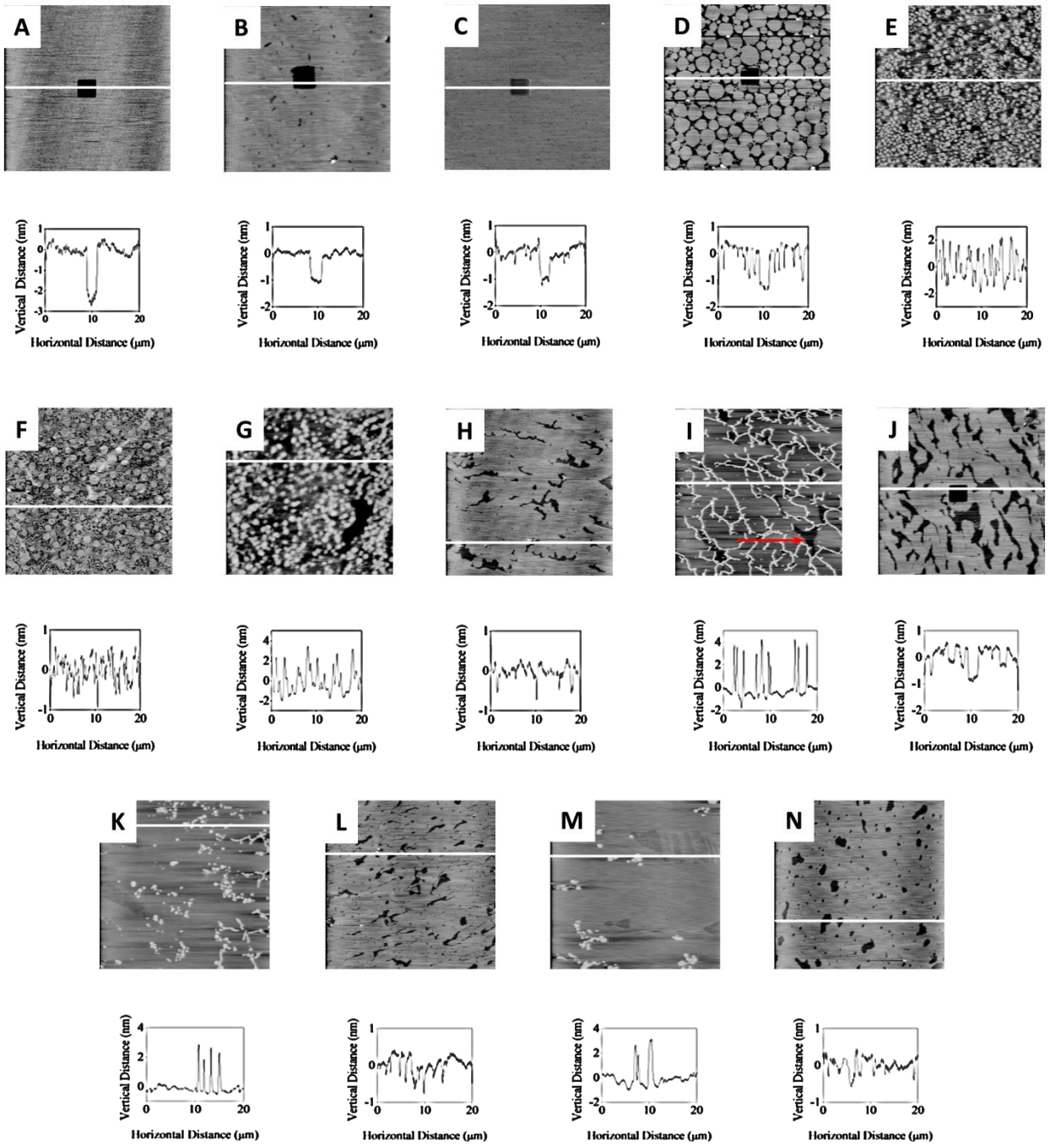

Figure 3-5 AFM height mode images (20μm x 20μm) and the cross sectional analysis of LB films deposited on mica using water and 0.4 M NaCl as a subphase. A. DPPC-water, B. DPPC-0.4 M NaCl, C. C18F-water, D. C18F-0.4 M NaCl, E. 1DPPC:3C18F-water, F. 1DPPC: 3C18F-0.4 M NaCl, G. 1DPPC:2C18F-water, H. 1 DPPC:2C18F-0.4 M NaCl, I. 1DPPC:1C18F-water (red arrow indicates "pinhole" defect in underlying monolayer), J. 1DPPC:1C18F-0.4 M NaCl, K. 2DPPC:1C18F-water, L. 2DPPC:1C18F-0.4 M NaCl, M. 3 DPPC:1C18F-water, N. 3DPPC:1C18F-0.4 M NaCl.

As shown in Figure 3-5 (A and B), the DPPC films were generally smooth and featureless, though films deposited from the NaCl subphase tended to contain a significantly greater number of "pinhole" defects than those deposited from the pure water subphase. The film thickness was ~2.7 $\pm$ 0.1 nm and ~1.2 $\pm$ 0.1 nm for DPPC films deposited using water and 0.4M NaCl respectively. Comparing these results to the molecular length of DPPC (2.8 nm,[36] and others) suggests that with a pure water subphase, DPPC deposits nearly normal to the mica surface but takes on an angle of ~60° from vertical upon deposition from a saline subphase. The precise explanation for the difference in tilt angle of the surfactants with salinity is presently unclear (C18F also adopts a significant tilt angle with respect to the solid substrate, as reported below), though DPPC adopting a significant tilt angle to the substrate normal is consistent with a number phospholipid systems, including those described by Schuy et al.[37] for DPPC and partially fluorinated DPPC, as well as those by Katsaras[38] for DPPC multilayers. Images of pure C18F films are shown in Figure 3-5 (C and D). Films of C18F consisted of closely packed circular domains (typically ~0.2 – 1.0 μm in diameter for the pure water subphase, ~0.5 – 2.5 μm for 0.4M NaCl) distributed over the mica surface, consistent with what we have reported previously.[11] Scratching tests showed that the depth of the deposited layer was ~1.1 $\pm$ 0.1 nm. The molecular length of C18F is 2.5 nm,[39] which suggests that C18F molecules are tilted by ~65^{o} from the vertical. Note, particular care must be taken when measuring monolayer film thicknesses using this "scratching" approach, as image flattening artifacts and the ability of the AFM tip to penetrate into small spaces can lead to underestimates of film thickness. We note, for example, that for the cross-sectional analysis in Figure 3-5D, the depth of the spaces between domains appears smaller than the depth of the scratched region. This is caused by the inability of the AFM probe tip to penetrate the small space between domains.

AFM images of the mixed LB films (1DPPC:3C18F – 3DPPC:1C18F molar ratio) deposited from pure water and the 0.4M subphase are shown in Figure 3-5 (E-N). In general, the morphology of films prepared from the pure water subphase differed significantly from those prepared from the high salinity subphases, with the difference in morphology becoming more pronounced as the relative mole fraction of DPPC increased. For 1DPPC:3C18F (Figure 3-5 (E and F)), the circular domains that were readily apparent in the pure films of C18F were still present, though the typical heights and diameters were ~3–4 nm and ~ 300 – 500 nm, respectively for water and ~ 1 nm and 0.7–1.0 μm for 0.4M salt. For the pure water subphase, the thickness measurements indicate that the film is no longer a simple, continuous monolayer but rather consists of a series of closely-packed multimolecular surfactant aggregates. This result is consistent with the highly cohesive nature of the films in the absence of Na^+, as reported in the preceding sections. It appears that the high degree of attraction between film components favours the production of multimolecular aggregates over a simple continuous monolayer on the mica substrate. It is also possible that the deposition process itself, along with interactions with the mica substrate may also play a role in inducing aggregate formation under these conditions (direct measurements of film structure at the air-water interface via Brewster angle or fluorescence microscopy may provide insight here, though we currently lack this technical capability). However, as noted previously, the addition of Na^+ to the subphase decreases overall film cohesion, and the film deposited under these conditions consisted of a mixed monolayer on the mica. Again, this is the expected result based on the isotherm and thermodynamic data.

At higher mole fractions of DPPC, the tendency towards forming aggregates in pure water versus continuous films in high subphase salinities continued. For the 1DPPC:2C18F mixtures in water, aggregates that were comparable to those found for 1DPPC:3C18F were

observed, whereas for saline subphase, a continuous film (with occasional "pinhole" defects) was formed, with film thickness of ~1.0 nm (Figure 3-5 (G and H)). The continuous, largely featureless films formed in salt are entirely consistent with an intimate monolayer mixture of perfluorocarbon and phospholipid oriented at ~65^{o} to the normal. Films produced at higher mole fractions of DPPC and 0.4M salt were comparable in structure (Figure 3-5 (J, L and N)) though the film thickness did decrease marginally, suggesting a slightly increased tilt angle (~70^{o}) of the surfactants adsorbed to the mica surface. A point worth considering is whether the mixing process itself might lead to a change in the lipid order parameter of the phospholipid and hence lead to an apparent change in film thickness. While our atomic force microscope measurements are insensitive to the lipid order parameter, it is worth noting that Böckmann et al.[40] have reported an increased lipid order parameter and accompanying membrane thickening in POPC bilayers systems upon addition of Na^{+} to the aqueous subphases. We take this result, in conjunction with the observation that the pure film components are also tilted relative to the substrate, as an argument against this possibility.

For the pure water deposited films, (Figure 3-5 (I, K and M)), more complex aggregates, including nanometer-scale filaments (Figure 3-5I, heights ~ 3-5 nm) and large spherical deposits were observed, though it should be noted that these filaments and deposits are lying on the surface of a continuous film that is again ~1.0 nm thick (a red arrow indicating a "pinhole" defect in the underlying film is included for reference in Figure 3-5I). Again, these results suggest a greater tendency for the mixtures in pure water to form aggregates versus the monolayer films deposited from the high salinity subphase.

In comparison with other related film structures found in the literature, the results obtained here are largely consistent. Addition of Hoda's hybrid phenylphosphate amphiphiles to

pure DPPC films resulted in a dispersion of ordered phospholipid domains, and the hybrid systems did not appear to form multimolecular aggregates when deposited from high salinity subphases.[15] There was no evidence for phase-separation or formation of more complex self-assembled structures, as has been demonstrated by Yoder in their investigations of mixed DPPC – DPPC fluorinated analog bilayer films,[24] or in the simple mixed fatty-acid systems that we have reported on previously.[5, 8, 10, 11] Yokoyama et al.[20, 21] have reported, for mixed films of dipalmitoylphosphatidylglycerol-C18F and dimyristoylphosphatidylethanolamine-C18F on high salinity subphases, the formation of multimolecular aggregates of C18F (two or three layers, in phase-separated domains), though the subphase pH was considerably lower from what we have used here (pH = 2.0), and the phospholipid headgroups also differ significantly. We also note that these previous systems tend to be highly immiscible and as such, considerable differences with the mixed films studied in this investigation might reasonably be anticipated.

3.4.5 Conclusions

The presence of sodium ions in the aqueous subphase of a Langmuir trough has been shown to play a major role in regulating the miscibility, and hence, mechanical properties and morphology of mixed DPPC-C18F Langmuir monolayer films. These results indicate that useful properties of mixed surfactant films can potentially be controlled via simple adjustment of subphase salinity. Film components for these systems were found to be miscible under all conditions examined, including a range of film compositions and sodium ion concentrations, though the degree of miscibility, manifested as negative deviations from the additivity rule, as well as large negative excess Gibbs free energies of mixing, could be decreased through the use of higher sodium-ion concentrations in the subphase. The effects observed here were attributed to the specific adsorption of sodium anion to the negatively-charged perfluoroacid. Furthermore,

high film elasticities, which indicated strong cohesion between film components were observed, could be significantly diminished through addition of sodium ion to the subphase. These results differ significantly for those typically observed in simple aliphatic fatty-acid systems, where addition of cations to the trough's subphase typically stabilize monolayer films, resulting in more rigid, inflexible films. Consistent with these observations, film morphology measurements indicated that on pure water subphase, there was a tendency for multimolecular aggregates to form over all film compositions, likely because of the strong film cohesion, though this effect could be diminished through the use of high salinity subphases.

3.4.6 Acknowledgements

The Natural Sciences and Engineering Research Council of Canada (NSERC), the Canada Foundation for Innovation (CFI), the Province of Saskatchewan and the University of Saskatchewan are acknowledged for the funding of this work.

3.4.7 References

1. Kissa, E., Ed.; In *Fluorinated Surfactants and Repellents, Second Edition;* Marcel Dekker Inc.: New York,USA, 1997; Vol. 97.

2. Kimura, H.; Watanabe, S.; Shibata, H.; Azumi, R.; Sakai, H.; Abe, M.; Matsumoto, M. Phase-Separated Structures of Mixed Langmuir-Blodgett Films of Fatty Acid and Hybrid Carboxylic Acid. *J Phys Chem B* **2008**, *112*, 15313-15319.

3. McConnell, H. M. Structures and transitions in lipid monolayers at the air-water interface. *Annu. Rev. Phys. Chem.* **1991**, *42*, 171-195.

4. Moehwald, H. Phospholipid and phospholipid-protein monolayers at the air/water interface. *Annu. Rev. Phys. Chem.* **1990**, *41*, 441-476.

5. Qaqish, S. E.; Paige, M. F. Rippled domain formation in phase-separated mixed Langmuir-Blodgett films. *Langmuir* **2008**, *24*, 6146-6153.

6. Broniatowski, M.; Dynarowicz-Latka, P. Interactions of a fluoroaryl surfactant with hydrogenated, partially fluorinated, and perfluorinated surfactants at the air/water interface. *Langmuir* **2006**, *22*, 6622-6628.

7. Matsumoto, Y.; Nakahara, H.; Moroi, Y.; Shibata, O. Langmuir monolayer properties of perfluorinated double long-chain salts with divalent counterions of separate electric charge at the air-water interface. *Langmuir* **2007**, *23*, 9629-9640.

8. Qaqish, S. E.; Paige, M. F. Mechanistic Insight into Domain Formation and Growth in a Phase-Separated Langmuir-Blodgett Monolayer. *Langmuir* **2007**, *23*, 10088-10094.

9. Shibata, O.; Krafft, M. P. Mixed Langmuir monolayers made from single-chain perfluoroalkylated amphiphiles. *Langmuir* **2000**, *16*, 10281-10286.

10. Qaqish, S. E.; Paige, M. F. Characterization of domain growth kinetics in a mixed perfluorocarbon-hydrocarbon Langmuir-Blodgett monolayer. *J. Colloid Interface Sci.* **2008**, *325*, 290-293.

11. Qaqish, S. E.; Urquhart, S. G.; Lanke, U.; Brunet, S. M. K.; Paige, M. F. Phase Separation of Palmitic Acid and Perfluorooctadecanoic Acid in Mixed Langmuir-Blodgett Monolayer Films. *Langmuir* **2009**, *25*, 7401-7409.

12. Arora, M.; Bummer, P. M.; Lehmler, H. Interaction of a Partially Fluorinated Heptadecanoic Acid with Diacyl Phosphatidylcholines of Varying Chain Length. *Langmuir* **2003**, *19*, 8843-8851.

13. Courrier, H. M.; Vandamme, T. F.; Krafft, M. P.; Nakamura, S.; Shibata, O. Mixed monolayers made from dipalmitoyl phosphatidylcholine and a fluorinated amphiphile. *Colloids and Surfaces A-Physicochemical and Engineering Aspects* **2003**, *215*, 33-41.

14. Garcia-Manyes, S.; Domenech, O.; Sanz, F.; Montero, M. T.; Hernandez-Borrell, J. Atomic force microscopy and force spectroscopy study of Langmuir-Blodgett films formed by heteroacid phospholipids of biological interest. *Biochimica Et Biophysica Acta-Biomembranes* **2007**, *1768*, 1190-1198.

15. Hoda, K.; Kawasaki, H.; Yoshino, N.; Chang, C.; Morikawa, Y.; Sugihara, G.; Shibata, O. Mode of interaction of two fluorinated-hydrogenated hybrid amphiphiles with dipalmitoylphosphatidylcholine (DPPC) at the air-water interface. *Colloids and Surfaces B-Biointerfaces* **2006**, *53*, 37-50.

16. Hoda, K.; Nakahara, H.; Nakamura, S.; Nagadome, S.; Sugihara, G.; Yoshino, N.; Shibata, O. Langmuir monolayer properties of the fluorinated-hydrogenated hybrid amphiphiles with dipalmitoylphosphatidylcholine (DPPC). *Colloids and Surfaces B-Biointerfaces* **2006**, *47*, 165-175.

17. Lehmler, H.; Bummer, P. Mixing of perfluorinated carboxylic acids with dipalmitoylphosphatidylcholine. *Biochimica Et Biophysica Acta-Biomembranes* **2004**, *1664*, 141-149.

18. Nakahara, H.; Nakamura, S.; Kawasaki, H.; Shibata, O. Properties of two-component Langmuir monolayer of single chain perfluorinated carboxylic acids with dipalmitoylphosphatidylcholine (DPPC). *Colloids and Surfaces B-Biointerfaces* **2005**, *41*, 285-298.

19. Nakamura, S.; Nakahara, H.; Krafft, M. P.; Shibata, O. Two-component Langmuir monolayers of single-chain partially fluorinated amphiphiles with dipalmitoylphosphatidylcholine (DPPC). *Langmuir* **2007**, *23*, 12634-12644.

20. Yokoyama, H.; Nakahara, H.; Nakagawa, T.; Shimono, S.; Sueishi, K.; Shibata, O. Miscibility behavior of two-component monolayers at the air-water interface: Perfluorocarboxylic acids and DMPE. *J. Colloid Interface Sci.* **2009**, *337*, 191-200.

21. Yokoyama, H.; Nakahara, H.; Shibata, O. Miscibility and phase behavior of DPPG and perfluorocarboxylic acids at the air-water interface. *Chem. Phys. Lipids* **2009**, *161*, 103-114.

22. Lehmler, H. J.; Bummer, P. M. Mixing of partially fluorinated carboxylic acids with their hydrocarbon analogs at the air-water interface. *J. Colloid Interface Sci.* **2002**, *249*, 381-387.

23. Lehmler, H. J.; Jay, M.; Bummer, P. M. Mixing of partially fluorinated carboxylic acids and their hydrocarbon analogues with dipalmitoylphosphatidylcholine at the air-water interface. *Langmuir* **2000**, *16*, 10161-10166.

24. Yoder, N. C.; Kalsani, V.; Schuy, S.; Vogel, R.; Janshoff, A.; Kumar, K. Nanoscale patterning in mixed fluorocarbon-hydrocarbon phospholipid bilayers. *J. Am. Chem. Soc.* **2007**, *129*, 9037-9043.

25. Hiranita, T.; Nakamura, S.; Kawachi, M.; Courrier, H. N.; Vandamme, T. F.; Krafft, M. P.; Shibata, O. Miscibility behavior of dipalmitoylphosphatidylcholine with a single-chain partially fluorinated amphiphile in Langmuir monolayers. *J. Colloid Interface Sci.* **2003**, *265*, 83-92.

26. Satoh, K. Determination of Binding Constants of Ca2+, Na+, and Cl(-)Ions to Liposomal Membranes of Dipalmitoylphosphatidylcholine at Gel Phase by Particle Electrophoresis. *Biochimica Et Biophysica Acta-Biomembranes* **1995**, *1239*, 239-248.

27. Jones, M. N. The Surface-Properties of Phospholipid Liposome Systems and their Characterization. *Adv. Colloid Interface Sci.* **1995**, *54*, 93-128.

28. Sovago, M.; Wurpel, G. W. H.; Smits, M.; Muller, M.; Bonn, M. Calcium-induced phospholipid ordering depends on surface pressure. *J. Am. Chem. Soc.* **2007**, *129*, 11079-11084.

29. Gaines, G. L. *Insoluble Monolayers at Liquid – Gas Interfaces*; Interscience Publishers: New York, USA, 1966.

30. Harris, D. C. *Quantitative Chemical Analysis, Eighth Edition*; W.H. Freeman: New York, USA, 2010.

31. Aziz, E. F.; Ottosson, N.; Eisebitt, S.; Eberhardt, W.; Jagoda-Cwiklik, B.; Vacha, R.; Jungwirth, P.; Winter, B. Cation-specific interactions with carboxylate in amino acid and acetate aqueous solutions: X-ray absorption and ab initio calculations. *J Phys Chem B* **2008**, *112*, 12567-12570.

32. Davies, J. T.; Rideal, E. K. *Interfacial Phenomena, Second Edition;* Academic Press: New York, USA, 1963.

33. Zuo, Y. Y.; Veldhuizen, R. A. W.; Neumann, A. W.; Petersen, N. O.; Possmayer, F. Current perspectives in pulmonary surfactant - Inhibition, enhancement and evaluation. *Biochimica Et Biophysica Acta-Biomembranes* **2008**, *1778*, 1947-1977.

34. Panda, A. K.; Nag, K.; Harbottle, R. R.; Rodriguez-Capote, K.; Veldhuizen, R. A. W.; Petersen, N. O.; Possmayer, F. Effect of acute lung injury on structure and function of pulmonary surfactant films. *American Journal of Respiratory Cell and Molecular Biology* **2004**, *30*, 641-650.

35. Petty, M. C. *Langmuir-Blodgett Films: An Introduction;* Cambridge University Press: New York, USA, 1996; .

36. Yang, X. M.; Xiao, D.; Xiao, S. J.; Wei, Y. Domain-Structures of Phospholipid Monolayer Langmuir-Blodgett-Films Determined by Atomic-Force Microscopy. *Applied Physics A-Materials Science & Processing* **1994**, *59*, 139-143.

37. Schuy, S.; Faiss, S.; Yoder, N. C.; Kalsani, V.; Kumar, K.; Janshoff, A.; Vogel, R. Structure and thermotropic phase behavior of fluorinated phospholipid bilayers: A combined attenuated total reflection FTIR spectroscopy and imaging ellipsometry study. *J Phys Chem B* **2008**, *112*, 8250-8256.

38. Katsaras, J. Structure of the Subgel (L(c')) and Gel (L(beta')) Phases of Oriented Dipalmitoylphosphatidylcholine Multibilayers. *J. Phys. Chem.* **1995**, *99*, 4141-4147.

39. Thunemann, A. F.; Schnablegger, H. Monodisperse disk-shaped micelles of perfluorooctadecanoic acid. *Langmuir* **1999**, *15*, 5426-5428.

40. Bockmann, R. A.; Hac, A.; Heimburg, T.; Grubmuller, H. Effect of sodium chloride on a lipid bilayer. *Biophys. J.* **2003**, *85*, 1647-1655.

CHAPTER 4 INFLUENCE OF FILM COMPOSITION ON THE MORPHOLOGY, MECHANICAL PROPERTIES, AND SURFACTANT RECOVERY OF PHASE-SEPARATED PHOSPHOLIPID-PERFLUORINATED FATTY ACID MIXED MONOLAYERS

4.1 Description

This chapter is a verbatim copy of a paper published in Langmuir. [Reproduced with permission from Langmuir, (28) 15150−15159, 2012.]

In this study, the molecular level organization of binary mixed monolayers prepared from the phospholipid 1,2-dipalmitoyl-sn-glycero-3-phosphocholine (DPPC) and the perfluorinated fatty acid perfluorooctadecanoic acid (C18F) was examined at the liquid-air and solid-air interfaces using surface pressure-area isotherms, Brewster angle microscopy (BAM), atomic force microscopy (AFM) and fluorescence microscopy (FM). The cumulative information provided by the isotherm measurements and the three imaging techniques indicated that the two film forming components were phase separated to form a series of discontinuous, circular domains enriched in C18F that were surrounded by a continuous domain comprised of DPPC. The quantitative assessment of surfactant recovery showed that the addition of C18F to DPPC enhanced its re-spreading capability. Consecutive BAM micrographs during a compression-expansion cycle suggested that C18F molecules were squeezed out of the surfactant film during compression and reintegrated back into the film during expansion. In summary, the enhanced *in vitro* effectiveness of DPPC in the presence of C18F suggests it has considerable promise as a pulmonary surfactant (PS) additive.

The experimental section for this study is provided in the paper. A detailed description of the techniques used is provided in Chapter 1.

4.2 Description of the Candidate's Contribution

For this contribution, I prepared the samples, performed the isotherm, Brewster angle microscopy and atomic force microscopy measurements, played a major role in interpreting the results, wrote the initial draft of the work and participated in the subsequent editing in response to collaborators and editors. Dr. Sophie Brunet carried out the confocal fluorescence measurements and was involved in editing the paper. Dr. Matthew Paige provided extensive guidance throughout the experimental work and was greatly involved in results interpretation, writing and editing the paper.

4.3 Relation of Contribution towards Research Objectives

This contribution was solely performed towards the objectives of the thesis research. In the preceding Chapters (2 and 3), we fully characterized mixed monolayers of phospholipid-perfluorocarbon in terms of surfactant miscibility, mechanical rigidity and morphology. We also discussed the effect of subphase sodium chloride concentration on the monolayer formation characteristics of DPPC-C18F mixed films. Despite the potential importance of this type of films for PS application, little is known about their morphology and phase behavior in an environment that mimics the alveoli aqueous hypophase. In this chapter, the surface characteristics of DPPC-C18F mixed monolayers have been explored using a highly simplified lung fluid. The addition of C18F to DPPC monolayer enhanced its spreading kinetics and improved its hysteresis response after repeated compression expansion cycles. These are important properties for exogenous surfactant replacement therapeutics. A full discussion of the results of this study and its implications for the thesis research as a whole of is provided in Chapter 8.

The influence of film composition on the morphology, mechanical properties and surfactant recovery of phase-separated phospholipid-perfluorinated fatty acid mixed monolayers

Ala'a F. Eftaiha[1], Sophie M.K. Brunet[2] and Matthew F. Paige[1]

[1]Department of Chemistry, University of Saskatchewan, 110 Science Place, Saskatoon, Saskatchewan, Canada, S7N 5C9

[2]Saskatchewan Structural Sciences Centre, University of Saskatchewan, 110 Science Place, Saskatoon, Saskatchewan, Canada, S7N 5C9

Received 3 July 2012, Revised 17 September 2012

4.4.1 Abstract

Monolayer surfactant films comprised of a mixture of phospholipids and perfluorinated (or partially fluorinated) surfactants are of potential utility for applications in pulmonary lung surfactant-based therapies. As a simple, minimal model of such a lung surfactant system, binary mixed monolayer films comprised of 1,2-dipalmitoyl-sn-glycero-3-phosphocholine (DPPC) and perfluorooctadecanoic acid (C18F) prepared on a simplified lung fluid mimic subphase (pH 7.4, 150 mM NaCl) have been characterized in terms of mixing thermodynamics and compressibility (measured through π–A compression isotherms), film morphology (via atomic force, fluorescence and Brewster angle microscopy), as well as spreading rate and hysteresis response to repeated expansion-contraction cycles for a variety of compositions of mixed films. Under all mixing conditions, films and their components were found to be completely immiscible and phase-separated, though there were significant changes in the aforementioned film properties as a function of composition. Of particular note was the existence of a maximum in the extent of immiscibility (characterized by ΔG_{ex}^{π} values) and enhanced surfactant recovery during hysteresis experiments at $\chi_{C18F} \geq 0.30$. The latter was attributed to the relatively rapid re-spreading rate

of the perfluorinated amphiphile in comparison with DPPC alone at the air-water interface, which enhances the performance of this mixture as a potential pulmonary lung surfactant. Further, monolayer film structure could be tracked dynamically as a function of compression at the air-water interface via Brewster angle microscopy, with the C18F component being preferentially squeezed out of the film with compression, but returning rapidly upon re-expansion. In general, addition of C18F to DPPC monolayers resulted in improvements to mechanical, structural and re-spreading properties of the film, indicating the potential value of these compounds as additives to pulmonary lung surfactant formulations.

4.4.2 Introduction

Pulmonary lung surfactant (PS), a complex mixture of surfactants and proteins found in the alveoli and affiliated bronchiol surfaces, plays a crucial role in regulating surface tension during normal respiration cycles.[1-3] Production of insufficient or faulty PS has been associated with a variety of disease states, most notably in infants as neonatal respiratory distress syndrome, and similar medical difficulties have been reported in adults following traumatic lung injury. While a complex mixture, the primary lipid component of native PS are phosphatidylcholines (PCs; ~ 80% of the total lipid content) such as DPPC, whose primary function is to generate stable, low surface tension PS films at the air-alveolar fluid interface, thereby decreasing work associated with lung expansion during respiration. However, this property alone is insufficient to ensure proper lung performance; functionally competent PS must also re-spread rapidly at the air-alveolar interface (with spreading rates on the same time-scale as respiration rates) and allow for rapid replenishment of the alveolar surfactant layer through formation of surfactant "reservoirs" in the bulk liquid phase.[3] DPPC typically has poor re-spreading characteristics and as such, cannot, alone, serve as a good PS material.

For *in vivo* PS, the necessary functionality is met through combining diverse types of lipids in addition to various surface-active proteins.[4] There is considerable interest in the development of artificial PS formulations for treatment of respiratory distress syndrome and a number of these formulations have been approved for medical applications (e.g. Survanta, Infosurf). While useful, many PS formulations are based on animal lung extracts which can suffer from large batch-to-batch variation as well as concerns over potential zoonotic diseases, and there is sufficient motivation to develop purely synthetic PS preparations. Efforts to date in this area have included PS formulations based on mixtures of PCs with various additives to improve surfactant re-spreading and other performance properties, with additives including primary alcohols, polymers (tyloxapol, dextran, polyethylene glycol) as well as a variety of synthetic or semi-synthetic peptides and proteins.[5-9] While the various peptides and proteins contained in PS play an invaluable role in enhancing the performance of PS, their use significantly increases material costs and creates handling challenges with these formulations.

Fluorinated and semi-fluorinated surfactant additives have recently been explored for applications in tailoring properties of potential PS mixtures.[10-13] Fluorinated surfactants are highly surface-active materials that can yield air-water surface tensions that are less than those obtained with conventional hydrocarbon-based surfactants. The compounds tend to be chemically stable over a wide range of conditions and are often used in combination with their hydrogenated counterparts to achieve lower surface tensions, and to improve liquid spreading and chemical robustness.[14,15] Fluorinated surfactants can be miscible, partially-miscible or entirely immiscible with hydrogenated surfactants, depending on the precise chemical nature of the chemical system, and while they can be useful additives for various surfactant applications, great care must be taken in order to fully-optimize the performance of mixed fluorocarbon-

hydrocarbon mixtures because of these miscibility issues. Further, for some fluorinated surfactants, there are significant concerns related to their toxicity and propensity for bioaccumulation, both of which are of particular importance for medical applications.[14,16] Nonetheless, fluorinated surfactants are technologically useful and potentially beneficial additive molecules for tailoring properties of PS formulations. As such, characterizing simple, minimal model monolayer systems comprised of PCs mixed with perfluorinated additives on lung fluid mimic subphases is of significant interest for formulating potential artificial PS mixtures.

Properties of mixed PC-fluorinated surfactant monolayer films have been investigated via Langmuir and Langmuir-Blodgett (LB) approaches by a number of groups and under various mixing conditions. Lehmler et al.[17,18] have investigated the miscibility and film-forming capabilities of monolayer mixtures of PCs and semifluorinated surfactants and found that the extent of surfactant miscibility depended strongly upon differences in surfactant chain lengths (increasing the length of constituent molecules above a certain size resulted in increased immiscibility), headgroup charge (opposite charges on head groups leads to increased miscibility) and surface pressure. Hoda et al.[19,20] have reported monolayer studies of the interaction between hybrid fluorinated-hydrogenated surfactants and DPPC, in which it was found that the hybrid amphiphiles were generally miscible with PC and could effectively fluidize and disperse liquid-condensed domains of the phospholipid. Similar results were described by Courier et al.[21] and Hiranita et al.[22] for closely-related systems.

Of particular interest to our research group have been efforts aimed at characterizing miscibility and monolayer structures of DPPC mixed with simple perfluorocarboxylic acids; Nakahara et al. [23,24] have surveyed the miscibility of a number of perfluorocarboxylic acids (CnF, n = 12, 14, 16, 18) with DPPC; while Yokoyama et al. have investigated

dipalmitoylphosphatidylglycerol (DPPG) and dimyristoylphosphatidylethanolamine (DMPE) phospholipids on a low pH, high salinity subphase (pH = 2.0, 150 mM NaCl). [25,26] Similar to the systems described above, the degree of miscibility depended strongly on the surfactant chain length as well as the relative mole fraction of perfluorocarboxylic acid; addition of C12F to DPPC resulted in efficient fluidization of the phospholipid, but the effect was reversed (domain solidification) for longer perfluorocarbon chains. In the case of DPPC-C18F, mixtures were found to be highly immiscible, resulting in phase-separated domains in both Langmuir and LB films as observed by fluorescence microscopy and atomic force microscopy. Research in our own laboratory has shown that the extent of miscibility of C18F and DPPC is a strong function of subphase pH and sodium ion concentration, with the system forming miscible, unstructured films at pH = 5.5 and ion concentrations ranging from nominal zero to 400 mM.[11] Specific adsorption of ions to the negatively charged headgroups of C18F under these conditions led to a decrease in the net attractive interactions between film components via headgroup interactions, resulting in a lessening of the cohesive force within the films.

While the combined works described above have provided valuable insight into basic thermodynamic and structural properties of mixed dialkylphosphatidylcholine-C18F monolayer films, there are many important issues relating to performance of these mixtures as potential PS replacement systems, even when considering these binary systems as simple minimal models. In this work, we present an in-depth investigation of the mixing thermodynamics, spreading kinetics, film morphology (at both the solid-air and liquid-air interfaces) and film hysteresis after multiple compression-expansion cycles for mixed monolayers comprised of DPPC and C18F (chemical structures shown in Scheme 4-1). Sample films have been prepared using a highly-simplified lung fluid (pH 7.4, 150 mM NaCl) as an aqueous subphase to mimic some of the

properties of alveoli and bronchial space, though we note that the actual *in vivo* environment will contain a significantly more complicated mixture of inorganic ions, proteins and affiliated chemical species. To our knowledge, this is the first report of a combined thermodynamic, kinetic and structural characterization of a mixed DPPC-C18F monolayer film under subphase conditions relevant to pulmonary lung surfactant applications. Results indicate that while the two film components are immiscible, addition of the perfluorocarboxylic acid can cause significant alterations (and in some cases, enhancements) to film properties that are useful in PS applications, including both unique structural changes and enhanced spreading kinetics that have not been previously reported, and that use of these perfluorinated amphiphiles holds some considerable potential as additives for these formulations.

A)

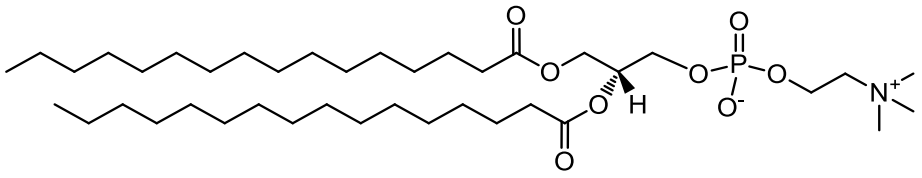

B)

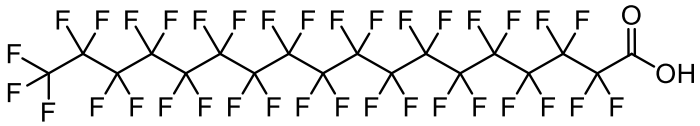

C)

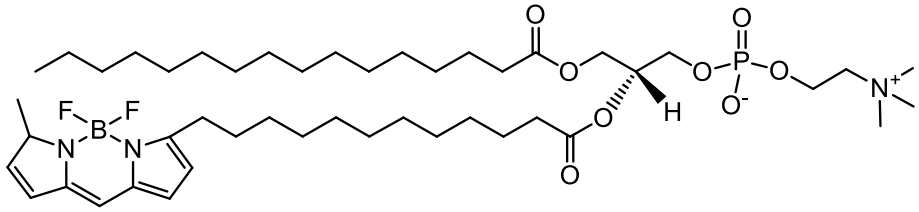

Scheme 4-1 Chemical structures of A) DPPC; B) C18F; and C) Bodipy-PC.

4.4.3 Materials and Methods

4.4.3.1 Chemicals

The surfactants DPPC and C18F were purchased from Avanti Polar Lipids and Alfa Aesar, respectively, and used as received. The fluorescent probe, 2-(4,4-difluoro-5-methyl-4-bora-3a,4a-diaza-s-indacene-3-dodecanoyl)-1-hexadecanoyl-sn-glycero-3 phosphocholine (Bodipy-PC; structure shown in Scheme 1C) was purchased from Invitrogen Corp. The n-hexane, methanol (MeOH) and sodium chloride were purchased from Fisher Scientific, while chloroform ($CHCl_3$) and sodium hydroxide was purchased from EMD Canada. Microscope cover glass and muscovite mica were from VWR International and Structure Probe Inc. respectively. Mica was freshly cleaved with adhesive tape prior to use, while the microscope cover glass was rinsed thoroughly with ethanol, dried under nitrogen gas and cleaned in a plasma cleaner (Harrick Plasma) to remove any residual contaminants.

4.4.3.2 Surface Pressure-Area Isotherms

Stock solutions of DPPC and C18F were prepared by dissolving the solid surfactants in 8:1:1 and 7:1:2 volume ratio of hexane: $CHCl_3$: MeOH, respectively. The solutions were combined in appropriate volumes to give the desired molar ratio of surfactants. Surface pressure-mean molecular area (π-*A*) isotherms were measured in a Langmuir trough (mini-trough, KSV NIMA), with surface pressure monitored using a Wilhelmy balance and paper Wilhelmy plate. A minimum of three independent isotherms were run for each composition of film, and the isotherms displayed in figures are the means of these experiments. Ultrapure water (Millipore, resistivity 18 MΩ·cm) was used to prepare a subphase of 150 mM NaCl. The pH of the subphase was adjusted with 70 mM NaOH to 7.4 ± 0.2. An aliquot of the amphiphile solution was spread on the subphase surface at 25 ± 1 °C, with temperature controlled using an external

circulating water bath. The solvent was allowed to evaporate for 10 min before the monolayer was compressed at a speed of 1000 mm·min^{-1} (570 Å^2·molecule^{-1}·min^{-1}). Film hysteresis and surfactant recovery was measured by recording 5 successive compression-expansion cycles with no lag time between consecutive cycles, with the expansion rate equal to the compression rate (1000 mm·min^{-1}).

4.4.3.3 Langmuir-Blodgett (LB) Film Deposition

LB films were prepared for a 0.5 C18F mole fraction (χ_{C18F}) mixture using a Langmuir trough (standard trough, KSV NIMA) and the subphase conditions described above. After surfactant spreading and solvent evaporation, films were compressed at a rate of 20 mm·min^{-1} (11.4 Å^2·molecule^{-1}·min^{-1}) until reaching a surface pressure of 2 mN/m. The film was allowed to stabilize for 10 min and the substrate (mica for AFM imaging or coverglass for fluorescence imaging) was pulled upward through the water–air interface in a single stroke. The film was left to dry in a clean environment at room temperature for several hours before measurements. For samples used in fluorescence imaging experiments, an aliquot of Bodipy-PC solution (fluorescent probe was dissolved in 8:1:1 volume ratio of hexane: $CHCl_3$: MeOH) was added to the surfactant mixture to give a final fluorescent probe concentration of 2.1 x 10^{-3} mole% (ratio of Bodipy-PC to the total amount of amphiphile).

4.4.3.4 Microscopy Measurements

For Brewster angle microscope (BAM) measurements, an aliquot of surfactant solution was spread over the subphase in a Langmuir trough and the solvent was allowed to evaporate. The monolayer was then compressed at 20 mm·min^{-1} (11.4 Å^2.molecule^{-1}·min^{-1}) to the desired surface pressure. The monolayer was measured using a KSV NIMA UltraBAM system (KSV NIMA). The microscope used a 50 mW, 658 nm *p*-polarized laser as an illumination source and

a CCD detector (collection rate of 20 frames per second). The lateral resolution of the instrument was 2 μm (based on the Rayleigh criterion) and the angle of the incident beam to the air-water interface was fixed to the Brewster angle (53.1°).

Atomic force microscope (AFM) measurements were carried out on a Dimension Hybrid Nanoscope system (Veeco Metrology Group), operating in contact mode in air using silicon nitride AFM probes (k ~0.1 $N \cdot m^{-1}$), a scan rate of 0.5 Hz and 512 pixels per line. Samples could be imaged repeatedly without apparent tip-induced damage.

Bodipy-PC doped films were imaged in a modified LSM-410 Zeiss laser scanning confocal microscope (LSM Tech), using the 457 nm excitation laser line of an argon ion laser. Fluorescence emission was filtered with a 500 nm longpass filter.

All microscope images shown are representative examples; measurements of different regions of the same film and different samples gave comparable results.

4.4.4 Results and Discussion

Surface pressure-area isotherms were measured at 25°C for the pure individual surfactants as well as their mixtures, with resulting isotherms shown in Figure 4-1. Isotherms for the pure components were consistent with those reported elsewhere in the literature, with the pure DPPC isotherm exhibiting characteristic gaseous, liquid-expanded (LE), liquid-condensed (LC) phases, with co-existence regions and a collapse plateau of ~66 mN/m, and the C18F isotherm exhibiting a single, smooth curve with collapse plateau of ~64 mN/m.[11,27] Limiting molecular areas (A_o) for the pure components, estimated by extrapolating the pseudo-linear portion of the liquid-condensed phase to the mean molecular area axis intercept, were ~61 $Å^2$/molecule and ~34 $Å^2$/molecule for DPPC and C18F, respectively. As an aside, Nakahara et al.[24] have commented that perfluorocarboxylic acids from commercial sources can contain

significant impurities (certified purity of C18F from Alfa Aesar used here was reported as ~ 97%) and have suggested that these impurities can result in A_o values that are unreasonably large in comparison with those estimated from the cross-section of a perfluorocarbon chain (~ 28 $Å^2$). Further, the authors suggest that multiple recrystallizations of these materials are necessary for meaningful quantitative measurements. In this work, π-*A* isotherms for commercial C18F gave $A_\circ$ values that were larger than those reported for Nakahara's highly purified compounds (34 $Å^2$/molecule vs. 29 $Å^2$/molecule), though careful inspection of the literature indicates that even for nominally purified C18F, a sizable range of A_o values can be found. We have measured isotherms after performing multiple recrystallizations (following a similar procedure to that described by Tsuji et al.[28]) of the commercial C18F, and the isotherms were, within error, the same as those from the commercial product. ^{19}F-NMR spectra for both the commercial and re-crystallized compound were the same and indistinguishable from those of a model compound perfluoroctanoic acid[29], and no spectral peaks that might be attributed to impurities were observed (see supplemental information). Finally, the melting point of the commercial C18F was 168^{o}C, in comparison with the range of 162-164^{o}C Nakahara has reported for impure surfactant. In combination, we take these measurements as indicating that the commercial C18F used in this study had an acceptably high degree of purity for quantitative measurements and further purification was not necessary.

Isotherms for the surfactant mixtures were similar in appearance to the pure C18F isotherms, and consisted of a single, smooth curve with no LE-LC co-existence regions. This is consistent with previous observations under different sub-phase conditions, in which the addition of perfluorocarboxylic acids to DPPC results in fluidization of LC domains, and it is likely that the same action is in effect under these conditions. Addition of C18F to DPPC resulted in a shift

in the isotherms at low pressures to a higher mean molecular area in comparison to DPPC alone, with the extent of the shift increasing as a function of the relative proportion of C18F.

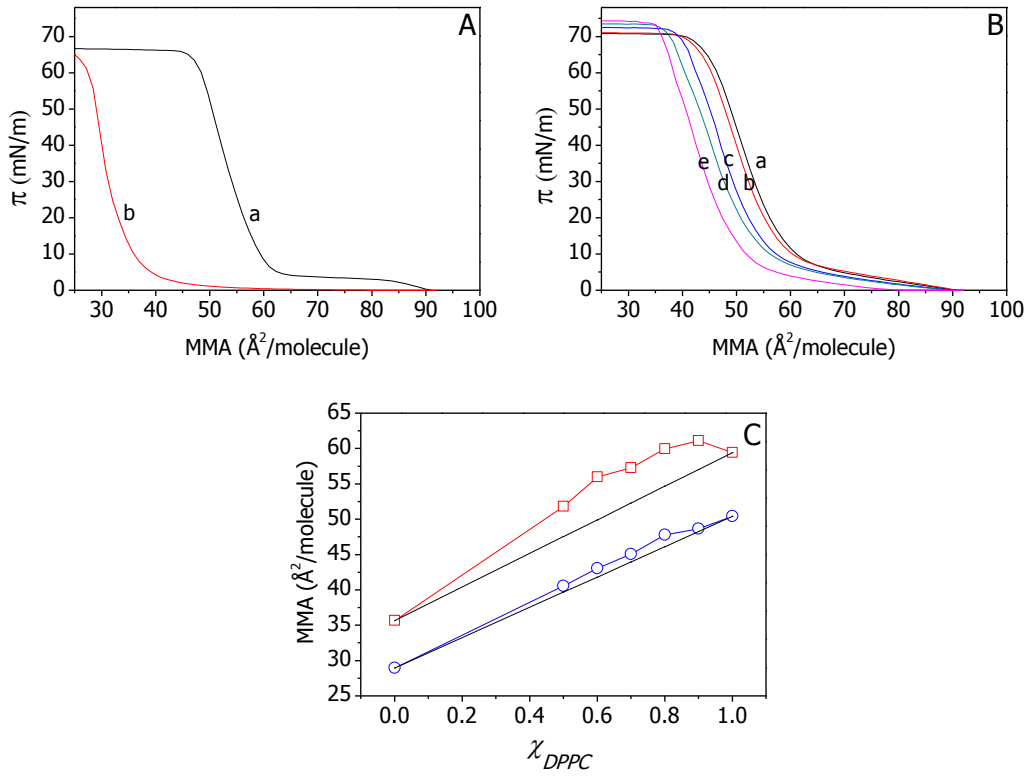

Figure 4-1 A) π-*A* isotherms for a, pure DPPC; and b, pure C18F monolayer films on pH 7.4, 150 mM NaCl subphase. B) π-*A* isotherms for a, χ_{C18F} = 0.1; b, χ_{C18F}= 0.2; c, χ_{C18F}= 0.3; d, χ_{C18F}= 0.4; and e, χ_{C18F}= 0.5 mixed monolayer films. C) Mean molecular area as a function of mole fraction of DPPC (□, 10 mN/m; ○, 50 mN/m). The dashed lines represent ideal mixing behavior as predicted by equation (4.1), and the solid lines are a guide to the eye.

Further, mixed monolayers showed significant positive deviations from ideal mixing (Figure 4-1C) predicted by the two-component additivity relationship described in equation (4.1)[30]:

$$A_{12} = A_1\chi_1 + A_2\chi_2 \qquad (4.1)$$

where A_1, A_2 are the mean molecular areas of the individual film components for a given surface pressure, A_{12} is the mean molecular area of the mixed film and χ_i is the mole fraction of the i^{th} component in the mixture.

All mixed films showed positive deviations from ideal mixing, indicating the existence of significant repulsive interactions between the film components,[30] though the extent of these deviations decreased significantly with increasing surface pressure. Relative uncertainties in these measurements were small and are documented in the Supplemental Information. Previous reports of DPPC-C18F miscibility by Nakahara et al.[23,24] and our group[11] under different subphase conditions (pH 2, 150 mM NaCl, pH 5.5, 0 – 400 mM NaCl, respectively), have observed negative deviations from ideality (attractive interactions between components), with the effect being ascribed to attractive interactions between the oppositely charged headgroups (zwitterionic choline headgroup for DPPC and negatively charged carboxylate for C18F) under the subphase conditions used.

It is instructive to consider the influence of pH on the extent of ionization of C18F for the different experimental conditions described above; the degree of ionization of C18F in the monolayer can be estimated through equation (4.2), based on the Boltzmann distribution of ions in an electric field and the Gouy-Chapman model of charged interfaces[24,30]:

$$pH_{bulk} = pK_a + log\frac{\propto}{1-\propto} + 0.87sinh^{-1}\left(\frac{1.37 \propto}{A\sqrt{c}}\right) \qquad (4.2)$$

where K_a is the acid dissociation constant, α is the fractional ionization of the acid, A is the surface film area on a per molecule basis, and c is the molar concentration of electrolyte.

Assuming a pK_a of 2.8 for C18F (estimated from affiliated compounds[14]), then a gaseous film of C18F has α ~ 99% at bulk subphase pH = 7.4 as compared to ~9% for pH = 2.0. One can reasonably argue that for a pH = 2.0 subphase, the small sub-population of negatively-charged C18F molecules will interact electrostatically with the zwitterionic headgroups of DPPC, resulting in the observed film stabilization. However, this cannot explain the results at elevated

pH because if this were the dominant effect, the film would be further stabilized, not destabilized. It appears that the principle source of this effect is the role played by sodium ion; we have previously demonstrated that sodium ion in the subphase decreases electrostatic interaction between the two film components through specific adsorption to the carboxylate headgroup[11], and this effect will be of even greater importance since the number of available sodium ion adsorption sites is approximately 10-fold larger at pH 7.4. Negation of the headgroup-headgroup stabilization interaction through specific ion-binding, in combination with repulsion between the alkyl and perfluorinated chains, results in a net repulsive interaction between components.

The extent of film stabilization (or destabilization) due to interactions between film components can be evaluated from the isotherm data by calculating excess Gibbs free energies of mixing (ΔG_{ex}^{π}) via equation (4.3):

$$\Delta G_{ex}^{\pi} = \int_0^{\pi} [\sigma_{12} - (\chi_1 \sigma_1 + \chi_2 \sigma_2)] d\pi \qquad (4.3)$$

where σ_{i} is the molar area of the pure film and σ_{ij} is the molar area of the mixed film.

Positive or negative excess values of the Gibbs excess function indicate either repulsive or attractive interactions. As shown in Figure 4-2 below, the mixed monolayer systems showed positive ΔG_{ex}^{π}, with values ranging from 0.1 kJ/mol to 0.9 kJ/mol, indicating a significant non-ideal repulsive interaction between components for all compositions. Values for ΔG_{ex}^{π} were found to increase as a function of increasing C18F, until reach a maximum at a mixing ratio of χ_{C18F} = 0.3, followed by a decrease in magnitude at greater C18F fraction, and also increased with increasing surface compression, which can be attributed to an increasing importance of short-range repulsive forces in close-packed films[19]. To provide a "calibration" scale, these are modestly small repulsive interactions in comparison with thermal energy (RT~ 2.5 kJ/mol), and

only slightly larger than the estimated contribution to film stabilization energy from the headgroup-headgroup interaction between DPPC and the perfluorcarboxylic acid (~ 0.25 kJ/mol).[31] Hoda et al.[20] have reported comparable magnitude (and sign) interaction energies (calculated via the Joos equation) between DPPC and hybrid fluorocarbon-hydrocarbon hexylphosphate surfactants, though negative ΔG_{ex}^{π} values on the order of -0.1 to -0.8 kJ/mol were reported by Nakamura et al.[32] for mixtures of DPPC with single-chain (perfluorooctyl)pentanol and (perfluorooctyl)pentylphosphocholine.

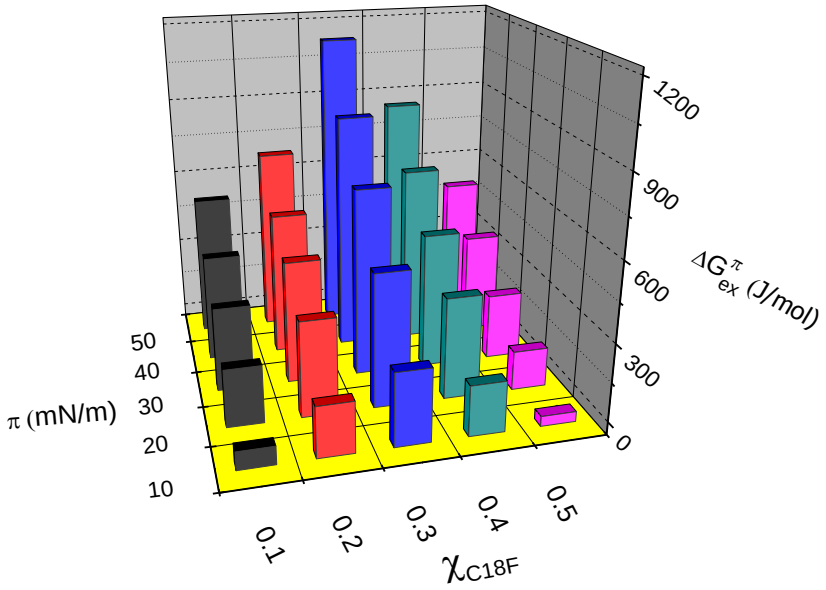

Figure 4-2 Plot showing excess Gibbs free energies of mixing (ΔG_{ex}^{π},) as a function of film composition and subphase pressure for the mixed monolayer films on pH 7.4, 150 mM NaCl subphase.

In short, significant changes to the chemical nature of the perfluorinated surfactant typically have modest, though significant effects upon overall film stability, allowing control over the film miscibility from being ideally to entirely non-ideally miscible. For the simple surfactants and lung surfactant mimicking subphase conditions used here, it appears that the repulsive contributions to overall film stability arising from hydrocarbon-perfluorocarbon tail group interactions dominate any net attractive interaction resulting from headgroups. The effect

is particularly important at χ_{C18F} ~ 0.3 which, as will be shown in upcoming sections, results in the formation of a highly structured surfactant film.

To assess mechanical properties of the mixed monolayer films at the air-water interface, isothermal compressiblities (C_s) have been determined via equation (4.4) and are summarized for control samples of pure DPPC, C18F and their mixed films (χ_{C18F} = 0.1 – 0.5) at four different surface pressures in Table 4-1:

$$C_s = -\left(\frac{1}{A}\right)\left(\frac{dA}{d\pi}\right)_T \qquad (4.4)$$

where A is the mean molecular area determined from the surface compression isotherms.

Isothermal compressibility values provide information on the degree of film elasticity; condensed, rigid DPPC films yield small values of C_s (a more elastic film), and as such the values can be used to assess the degree of monolayer elasticity upon addition of perfluorocarbons. Desirable compressibility values of PS films are typically < 0.01 $(mN/m)^{-1}$, meaning minimal lung compression (typically 20-30% area reduction[3]) is needed to affect a physiologically appropriate decrease in surface tension. Pure films of C18F gave larger C_s values than pure DPPC under all film compression values, though the difference was minimal at the highest extent of compression (40 mN/m; both films are in the condensed phase under these conditions). Mixtures of the two components gave C_s values that were comparable to those of pure C18F films for the majority of compositions measured. At each fixed surface pressure, there were some minor variations in C_s as a function of χ_{C18F}, but there was no readily discernible trend to the variations, and we simply report mean values of C_s for all mixtures at a fixed pressure here. The minimum values of C_s (the most elastic film) over the conditions explored were ~ 4×10^{-3} $(mN/m)^{-1}$, but overall, the elasticity was not particularly sensitive to the total amount of C18F in the mixture. In terms of absolute C_s values, Zuo et al.[33] have reported values

for bovine lipid extract surfactant (BLES; mixtures of native surfactants plus SP-B, SP-C, two principal surfactant protein) on the order of $1.5x10^{-2}$ $(mN/m)^{-1}$ over the surface pressure range studied here, while Wuestneck et al.[34] and Aydogan et al.[10] have reported minimum values of $3x10^{-3}$ $(mN/m)^{-1}$ for DPPC SP-C mixtures and DPPC mixed with a novel hydrocarbon-fluorocarbon hybrid cationic amphiphile, respectively (latter two groups measured values via pendant drop-surface dilational approaches). In the case of Aydogan's measurements, addition of low levels of fluorosurfactant significantly increased film elasticity of the mixed films over DPPC alone, though this was not the case here with C18F. It should also be noted for C18F, however, that while perfluorocarbon addition minimally alters C_s, absolute values are still well within the range required for a competent PS mixture, and mechanical properties of DPPC films at the air-water interface are not unduly perturbed by addition of the perfluorocarbon component.

Table 4-1 Isothermal compressibility $(mN/m)^{-1}$ values for pure and mixed surfactant monolayers on the pH 7.4, 150mM NaCl subphase at 25°C .

Surfactant	C_s $(mN/m)^{-1}$ at π = 10 mN/m	C_s $(mN/m)^{-1}$ at π = 20 mN/m	C_s $(mN/m)^{-1}$ at π = 30 mN/m	C_s $(mN/m)^{-1}$ at π = 40 mN/m
DPPC	$6.7 \pm (0.3) \times 10^{-3}$	$4.5 \pm (0.1) \times 10^{-3}$	$3.7 \pm (0.1) \times 10^{-3}$	$3.5 \pm (0.1) \times 10^{-3}$
C18F	$1.2 \pm (0.1) \times 10^{-2}$	$7.0 \pm (1) \times 10^{-3}$	$4.6 \pm (0.3) \times 10^{-3}$	$3.6 \pm (0.2) \times 10^{-3}$
$\chi_{C18F} = 0.1 - 0.5$	$1.4 \pm (0.2) \times 10^{-2}$	$6.8 \pm (0.5) \times 10^{-3}$	$5.1 \pm (0.5) \times 10^{-3}$	$4.5 \pm (0.3) \times 10^{-3}$

In addition to examining the effect of C18F addition upon the thermodynamic and mechanical properties of the DPPC monolayer, we have also carried out preliminary measurements of surfactant spreading rates on the simplified lung-fluid mimic subphase. This is a particularly important property for PS performance as noted above, as the surfactant needs to rapidly re-spread over alveolar surfaces during respiration cycles. Measurements were carried out using a modified version of Taeusch's approach,[35] in which a circular teflon dish (6 cm diameter) was filled with subphase, an aliquot of surfactant solution was deposited onto the subphase via microsyringe, and surface pressure was monitored as a function of time

immediately after deposition (distance between addition point and Wilhelmy plate was ~3 cm). Spreading data is shown in Figure 4-3 for the pure individual components as well as for a representative mixture (χ_{C18F} = 0.2). The rate of spreading for the C18F was faster than the time resolution of our measurements, with the film reaching its equilibrium spreading pressure (π_{eq} ~ 53 mN/m) almost immediately upon surfactant addition (< 10 s). DPPC films spread significantly more slowly than the C18F, attaining equilibrium (π_{eq} ~ 50 mN/m) in ~ 40 s. The rate of spreading of the pure DPPC on the lung mimic subphase is comparable though slightly faster than that reported for the spreading of several different aqueous surfactant suspensions (native and extracted porcine surfactant as well as the commercial clinical surfactants Curosurf, Survanta and Infasurf) in the presence of serum, which typically attain π_{eq} ~ 40 mN/m in approximately two minutes (with spreading rates a strong function of subphase conditions)[35]. Measurements were made for a variety of mixed films, and while addition of C18F to DPPC generally resulted in more rapid spreading (~ 20 s to reach equilibrium), there was significant variability in the data (possibly due to difficulties in adding the surfactant droplet to precisely the same position in the Teflon dish for each measurement). Because of this and the relatively modest time resolution of the measurements, we have not attempted a more quantitative evaluation of the kinetic data, but simply report that under subphase conditions that mimic lung surfactant fluid, the addition of C18F results in a more rapid (approximate doubling) decrease in surface tension over DPPC alone.

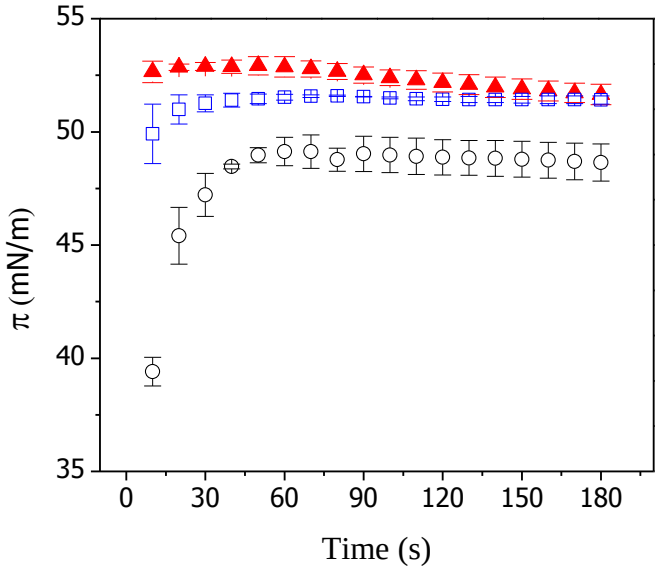

Figure 4-3 Surface pressure measured as a function of time for spreading of surfactants on the pH 7.4, 150 mM NaCl subphase (▲, C18F; □, χ_{C18F} = 0.2; ○, DPPC).

It is worth noting that one of the primary protein components of native PS, SP-C, likely working in conjunction with other peptides, is believed to play a key role in improving surfactant re-spreading rates for *in vivo* PS mixtures. Pastrana et al.[36] have reported that addition of bovine extracted SP-C to DPPC-DPPG surfactant mixtures results in 50-fold faster surfactant spreading rates (500 minutes improved to 10 minutes). Other additives (palmitic acid, hexadecanol) can have similar effects. While spreading rate improvements offered by C18F are significantly more modest than those offered by SP-C, they are nonetheless significant and the costs and handling issues associated with use of peptides or animal extracts are considerable. This suggests that addition of the perfluorinated surfactant to DPPC can improve not only overall surface tension values, but also kinetic performance of mixed surfactant films for PS applications, without the challenges associated with use of proteins and peptides. However, we note that caution must be taken when interpreting spreading data (measuring surface pressure after direct addition of surfactant to air-water interface) in the context of surfactant re-spreading after film collapse, which is a more appropriate descriptor of what takes place at the alveolar surface during

respiration. The latter likely requires fusion of surfactant bilayers or micelles to the interface,[3] and measuring simple spreading rates is clearly a crude approximation of a more complex kinetic process. Nonetheless, as will be shown below through BAM measurements, re-spreading of surfactants from collapsed films occur on the time-scale of seconds, suggesting that these measurements, while clearly approximations, are reasonable ones and capture the essence of the surfactant re-spreading process.

A combination of surface microscopy techniques, including BAM imaging, AFM imaging, and laser scanning confocal microscope imaging were used to structurally characterize the mixed film samples, and to probe dynamics of the films under compression. BAM images of the pure DPPC and mixed monolayer films at the air-water interface are shown in Figure 4-4. We note that the refractive index for typical perfluorocarbons is similar to pure water (at 25^{o}C, n_{water} ~ 1.33, $n_{perfluorocarbon}$ ~ 1.40[37]) and dark regions (low reflectivity) in BAM images correspond to water, perfluorocarbon or a mixture of both (images of pure C18F films are featureless). We further note that image morphology appears different for all three techniques, as they generate contrast by entirely different mechanisms (reflectivity, morphology and the presence of a fluorescent probe, respectively). As reported elsewhere (see McConnell [27] for example) images of low surface pressure DPPC films exhibited minimal features up to the coexistence LE-LC region (data not shown), whereupon characteristic multi-lobed, condensed domains were abundant (Figure 4-4A). Further film compression lead to an increase in the area occupied by these domains until spacing between domains could not be spatially resolved by the microscope and images appeared unstructured. Addition of C18F to the DPPC films lead to morphological variations in the mixed film structures. Films containing χ_{C18F} = 0.1 (Figure 4-4B), exhibited numerous condensed domains (diameter ~8 μm *vs.* 35 μm for pure

DPPC), with the characteristic lobe-structure of the LC domains being replaced with circular domains. The shift from lobed-structure to circles is consistent with the minimization of line-tension at the phase-boundary between co-existing perfluorocarbon and hydrocarbon phases, and is also consistent with the expected fluidization of the condensed DPPC described in the isotherm data.

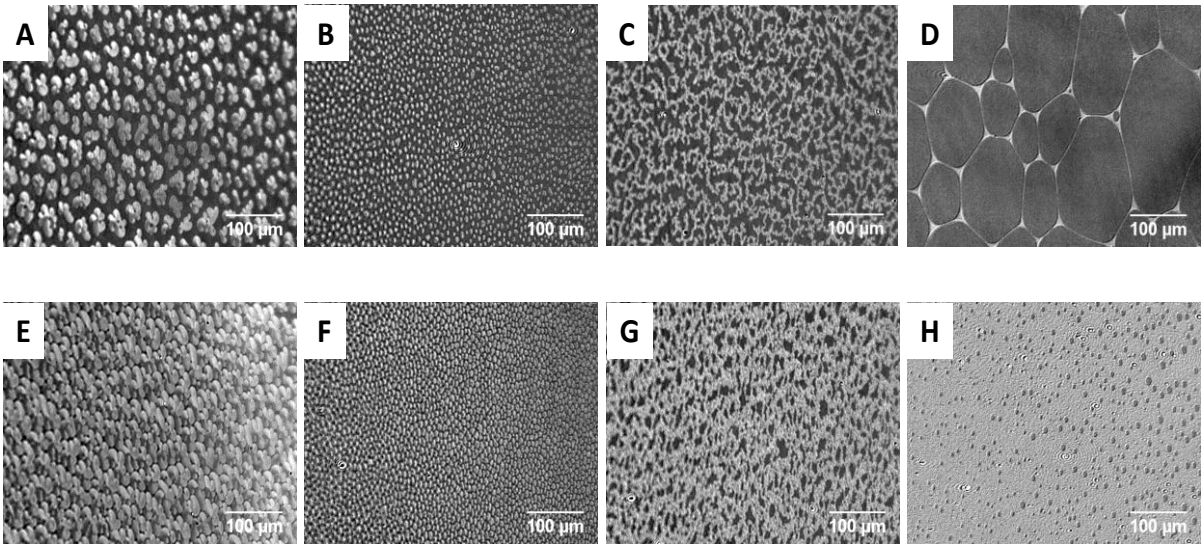

Figure 4-4 Brewster angle micrographs (620 µm x 340 µm) of monolayer films at the air-water interface; (A) DPPC; (B) χ_{C18F} = 0.1; (C) χ_{C18F} = 0.2; (D) χ_{C18F} = 0.5; (E) DPPC; (F) χ_{C18F} = 0.1; (G) χ_{C18F} = 0.2; and at 64Å^2/molecule; (H) χ_{C18F} = 0.5. Films in (A)-(D) were compressed to an area of 70Å^2/molecule, (E)-(H) were compressed to an area of 60 Å^2/molecule.

Morphologies continued to change with increasing χ_{C18F}. At χ_{C18F} = 0.2 (Figure 4-4C), extended interwoven strands were observed, with dark regions occupying the space between strands. The most dramatic morphological changes were observed for $\chi_{C18F} \geq$ 0.3 (representative image shown in Figure 4-4D; other values of χ_{C18F} gave comparable images). Films prepared with these compositions consisted of a mesh-like network of reflective surfactant (DPPC) surrounding dark, discrete, discontinuous domains. These are the same compositions at which maximum non-ideal mixing behavior was observed in the ΔG_{ex}^{π} values, and it is clear that the film components are fully phase-separated. Further compression of the films (Figure 4-4H)

results in a net decrease in separation of the highly-reflective domains, or in the case of $\chi_{C18F} \geq$ 0.3, a decrease in the total area occupied by the dark (perfluorocarbon) domains, and in subsequent sections, particular attention will be paid to the mesh-like network in terms of structure and hysteresis response to compression-expansion cycles. In combination, we take these results to mean the DPPC-C18F mixtures are fully immiscible over the composition ranges and subphase conditions measured here, with the degree of repulsive interactions between film components giving rise to significant alterations in overall film morphology at the air-water interface.

Further molecular-scale morphology and compositional information about the mixed films can be collected through AFM and laser scanning confocal measurements. We have chosen to focus attention on the most highly-structured, phase-separated films that form at $\chi_{C18F} \geq 0.3$. LB films of χ_{C18F} = 0.5 on mica were measured in the AFM, and are shown with a cross-sectional analysis in Figure 4-5. The image reveals the formation of well-defined domains that were roughly circular in shape, typically around 1-2 μm in diameter, surrounded by a continuous matrix that was lower in height than the circular domains by 2.0 – 2.5 nm. Nanometer-scale deposits, likely crystallized salt from the high salinity subphase, were occasionally observed, though these did not significantly obscure the underlying film morphology. The average difference in height between the circular domains and the surrounding matrix was comparable to the fully-extended molecular length of either DPPC (2.8 nm) or C18F (2.5 nm).[38,39] The BAM and AFM images show a film structure that consists of a continuous matrix and numerous discrete patches. The low reflectivities of the circular domains in the BAM images indicate that they are comprised of perfluorocarbon. In combination with the AFM, this suggests that the

circular domains are vertically adsorbed C18F, with the surrounding continuous matrix consisting of DPPC lying flat on the underlying substrate.

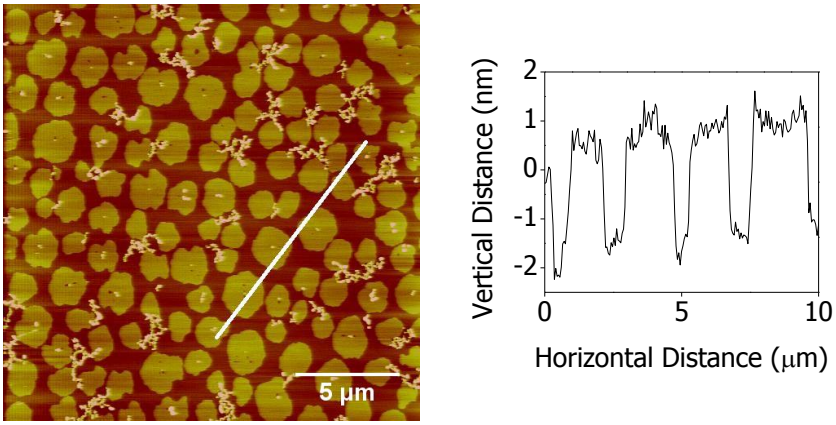

Figure 4-5 AFM height mode image (20 µm x 20 µm) and cross-sectional analysis of a χ_{C18F} = 0.5 mixed monolayer film deposited on a mica substrate (deposition pressure of π = 2 mN/m) from a subphase of 150 mM NaCl (pH 7.4) at 25°C.

This interfacial organization suggests the film components are fully separated. For additional verification of this assignment and molecular-level organization of the films, samples were doped with Bodipy-PC (Scheme 4-1C), a fluorescent DPPC analogue, and imaged using confocal fluorescence microscopy. Bodipy-PC partitions preferentially into the LE phospholipid phase (see, for example, Korlach et al.[40]), and we note that at the deposition pressures used here (π = 2 mN/m), the phospholipid film should consist almost exclusively of LE phase. Figure 4-6 shows a confocal fluorescent image of χ_{C18F} = 0.5 mixed film doped with Bodipy-PC and deposited on a glass substrate. Images showed the same characteristic surface patterns observed previously in the BAM and AFM images, consisting of a uniform bright background, with a series of discontinuous dark patches (1-2 µm in size).

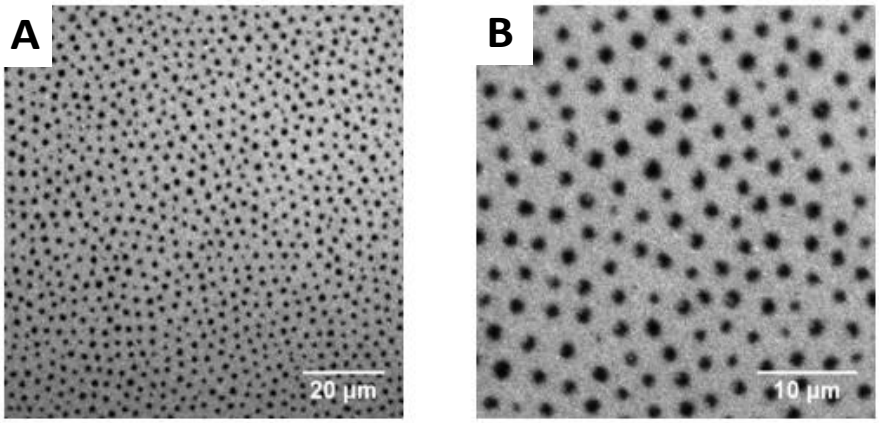

Figure 4-6 Confocal fluorescence images; A) 100 µm x 100 µm; and B) 40 µm x 40 µm of χ_{C18F}= 0.5 mixed film doped with Bodipy-PC and deposited onto a glass substrate (deposition pressure of π = 2 mN/m) from a subphase of 150 mM NaCl (pH 7.4) at 25°C.

Because of the preferential partitioning of Bodipy-PC to the LE phase, the highly-luminescent continuous matrix must consist of LE DPPC, which is again consistent with the AFM results; phospholipids in the LE phase do not adsorb vertically to the underlying substrate, but will rather lie flush with the surfaces, and the immiscible, phase-separated patches of C18F adopt a close-packed, vertical arrangement.

Surfactant recovery (monolayer hysteresis) of monolayer films after repeated compression-expansion cycles is an important property of PS, with the ability to rapidly and efficiently replenish the surface layer after film collapse being a key performance parameter for these mixtures. In brief, when films are compressed past the collapse pressure (or squeeze-out pressure for one particular component), surfactant is forced into the subphase, and may or may not be able to return to the air-water interface upon subsequent re-expansion. Monolayer hysteresis can be evaluated quantitatively by measuring the change in integrated area for π-*A* isotherms during repeated compression-expansion cycles performed on the Langmuir trough. In these experiments, films were compressed at a fixed rate (1000 mm·min^{-1}; five compression re-

expansion cycles in total) until film collapse (~ 70 – 75 mN/m; see Figure 4-1B), followed immediately by re-expansion at the same rate. Percentage surfactant recovery was defined as:

$$\%\ Recovery = \frac{area\ under\ isotherm\ curve\ for\ n^{th}\ compression\ cycle}{area\ under\ isotherm\ curve\ for\ 1^{st}\ compression\ cycle}\ x\ 100\% \quad (4.5)$$

Results of surfactant recovery measurements for the pure films and their mixtures are summarized in Table 4-2. While all films exhibited some irreversible loss of surfactant, both the pure C18F monolayer and the mixed monolayers with $\chi_{C18F} \geq 0.3$ showed superior percentage recovery in comparison with pure DPPC alone. The recovery data for pure DPPC films highlights one of the shortcomings of the phospholipid as a PS component: its substantial, irreversible loss after the first compression cycle. This effect is likely related to the inability of DPPC vesicles (formed after film collapse) to 'unzip' and rapidly re-adsorb to the liquid interface after re-expansion.[3]

Table 4-2 Percent recovery of mixed monolayers compressed past their collapse pressure as a function of consecutive compression-expansion cycles.

No. of compression cycles	***DPPC***	χ_{C18F} ***0.1***	χ_{C18F} ***0.2***	χ_{C18F} ***0.3***	χ_{C18F} ***0.4***	χ_{C18F} ***0.5***	***C18F***
2	34 (±2)%	35 (±2)%	38 (±2)%	77 (±2)%	80 (±3)%	80 (±3)%	70 (±1)%
3	30 (±1)%	33 (±1)%	36 (±3)%	65 (±3)%	66 (±4)%	66 (±3)%	58 (±2)%
4	30 (±1)%	32 (±1)%	35 (±2)%	55 (±2)%	55 (±3)%	57 (±3)%	51 (±2)%
5	29 (±1)%	31 (±1)%	34 (±2)%	49 (±2)%	49 (±3)%	51 (±1)%	46 (±2)%

*Uncertainty ranges calculated as standard deviations from a minimum of n = 5 independent measurements.

For C18F, it is reasonable to postulate that recovery is superior to pure DPPC because of the nature of the aggregates that form upon film collapse. Thunemann et al.[38] have estimated the critical micelle concentration of C18F at ~$8x10^{-5}$ M, which is several orders of magnitude larger than that for DPPC ($0.46x10^{-9}$ M, Avanti Polar Lipids). After film collapse, the C18F is not expected to form micelles and therefore can be re-integrated into air-water interface with greater efficiency than micellar DPPC. Increasing the amount of C18F in the mixed films will generally

result in increased overall recovery because of this effect. On the basis of the cumulative data, we propose the following model of film dynamics for the immiscible films during compression-expansion cycles: after initial spreading at constant surface area, the immiscible film components are phase-separated at the air-water interface. During compression, the phase-separated domains of C18F are reduced in area (as per Figure 4-4 D and H, for example) until the system approaches the collapse pressure for the film, at which point the C18F will be preferentially forced out of the monolayer (collapse pressure for C18F is marginally lower than that of the DPPC), leaving the film temporarily enriched in DPPC until it, too, is squeezed out into the underlying suphase. Upon re-expansion, the rapidly-spreading C18F component returns back first with reasonably high efficiency, followed, more slowly, by the DPPC component. As the film re-expands, both components are replenished at the air-water interface, though some fraction of both DPPC and C18F are permanently lost to the subphase. We note that this mechanism is consistent with the so-called "squeeze-out" hypothesis for PS operation,[3] in which fluid, non-DPPC PS components are squeezed out of the film during the course of film compression, leaving DPPC (with the assistance of the various protein components of PS) to maintain low π at low surface area values. While the squeeze-out hypothesis mechanism of operation for native PS is actively under debate, it appears that in the case of the minimal model used in this study, such a mechanism is plausible.

In support of this model, we have measured a continuous series of BAM images for a χ_{C18F} = 0.5 mixed film during a single compression-expansion cycle (compression rate and expansion rate were equal and had a value of 20 mm·min^{-1}). A series of still images showing the results of these measurements are provided in Figure 4-7. As observed previously, the mixed films initially consisted of large, low-reflectivity regions (assigned as C18F) separated by strands

of high-reflectivity (assigned as DPPC) material (Figure 4-7A). During compression, the relative size of the C18F domains decreased and the DPPC increased, corresponding to more close-packing of the different surfactant materials (Figure 4-7(B-C)). Ultimately, the C18F domains begin to vanish ("squeezed out"), leaving the film a uniform reflectivity (either the pure water subphase or a uniform layer of highly-compressed DPPC) (Figure 4-7D). Upon re-expansion, the original domain structures re-appear, and grow as a function of trough area, indicating the strong degree of reversibility of the cyclic process.

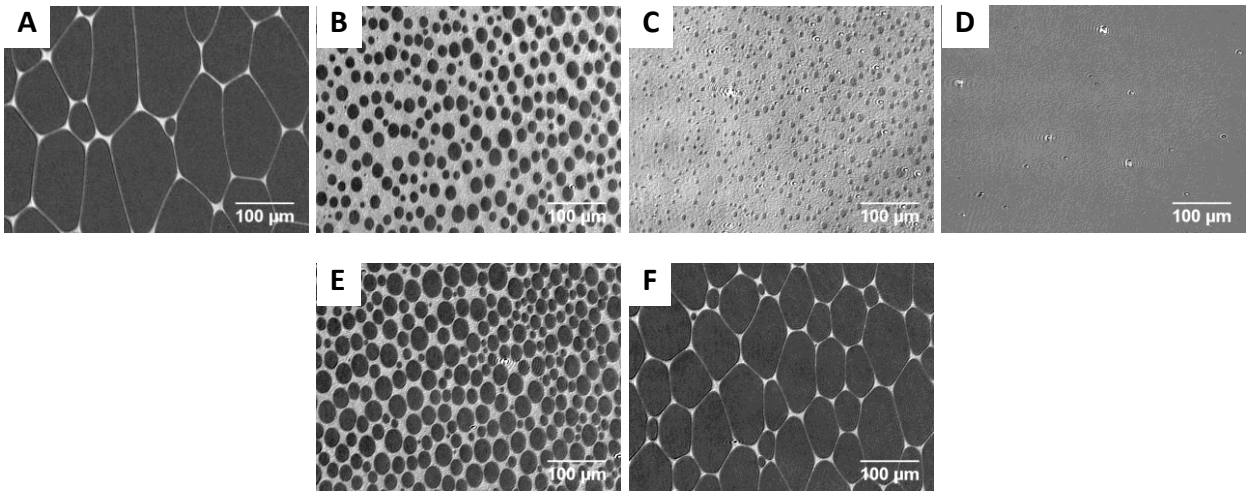

Figure 4-7 Series of consecutive Brewster angle micrographs (620 µm X 340 µm) of a χ_{C18F} = 0.5 mixed surfactant monolayer film collected during a compression-expansion cycle. A) π = 2 mN/m; B) π = 3 mN/m; C) π = 4 mN/m; D) π = 6 mN/m; E) π = 4 mN/m; F) π = 3 mN/m.

Further insight into both the time-scale of the surfactant re-spreading process and the extent of surfactant recovery can also be collected from these measurements. Upon film re-expansion after the initial compression, elapsed time between film collapse and the first appearance of circular domains was typically < 10 seconds (determined through the frame rate of the CCD camera used for image collection). While complicated by the fact that the barriers are in constant motion during these experiments, the results are in overall good agreement with the surfactant spreading rate data described previously, and further suggests that any differences

between the measured rates of surfactant spreading and surfactant re-spreading after compression are minimal for C18F. As an additional point, we note that the monolayer film structures in Figure 4-7 differ slightly for the compression and recompression at the same nominal trough area (e.g. Figure 4-7 (B and F) are for the same trough area but the images appear slightly different). This difference is the result of the irreversible loss of surfactant material during the re-expansion process.

In short, the results presented here suggest a mechanism of operation for this mixture that is consistent with the squeeze-out hypothesis, with the perfluorocarboxylic acid playing the role of the non-DPPC PS components, and the mixture as a whole exhibiting good surfactant recovery upon repeated cycling. While we emphasize that the system here is only intended as a simple, minimal model to describe behavior of mixed perfluorcarbon-DPPC PS films on a lung-fluid mimic subphase, the broad, general improvements in surfactant performance obtained through the use of perfluorinated surfactants suggests that this class of compounds holds significant potential for enhancing PS performance, and that further development and exploration of this class of additives for PS formulations is worthwhile.

4.4.5 Conclusions

The thermodynamic miscibility, film structures, spreading kinetics and hysteresis response for a binary mixed C18F-DPPC monolayer system was investigated on a model lung fluid mimic subphase, with a view towards characterizing potential improvements to PS performance brought about by addition of a perfluorinated surfactant to DPPC. Under the subphase conditions explored here, the mixed films were fully-immiscible, with the extent of miscibility depending modestly upon the composition of the mixed film. Comparison with related studies in the literature indicated that the subphase pH and salinity (via sodium ion

binding) play a key role in regulating miscibility and mechanical properties of the resulting films. Highly-structured, phase-separated monolayer films were observed at both the air-water and air-solid interface, and film compositions and the underlying molecular structure were determined through a combination of surface-sensitive microscopy techniques. With respect to performance of a potential PS mixture, addition of C18F to DPPC resulted in improved surfactant spreading rates and surfactant recovery, with minimal perturbations to overall film compressibility from the DPPC alone. The net overall improvement in performance resulting from the use of C18F in this model system suggests potential general utility of this class of molecules for enhancing PS performance in applied PS formulations.

4.4.6 Acknowledgments

Financial support has been provided by the Natural Sciences and Engineering Research Council of Canada, the Canadian Foundation for Innovation and the University of Saskatchewan. The Saskatchewan Structural Sciences Centre is acknowledged for providing access to confocal microscopy instrumentation. Dr. Keith Brown is acknowledged for assisting with NMR measurements.

4.4.7 Supporting Information Available

Standard deviations for mean molecular area measurements and excess Gibbs free energies of mixing are tabulated in the Supplemental Information section. Characterization information (^{19}F-NMR) for the commercial C18F used in these experiments, before and after recrystallization, is also included. A Brewster angle microscope "movie" showing the response of a mixed monolayer film (χ_{C18F} = 0.5, compression rate of 67 mm·min^{-1}) at the air-water interface to a compression-expansion cycle is also provided. This material is available free of charge via the Internet at http://pubs.acs.org.

4.4.8 References

1. Engelskirchen, S. The pseudo-binary pulmonary surfactant system. *Current Opinion in Colloid & Interface Science* **2007**, *12*, 68-74.

2. Rugonyi, S.; Biswas, S. C.; Hall, S. B. The biophysical function of pulmonary surfactant. *Respiratory Physiology & Neurobiology* **2008**, *163*, 244-255.

3. Zuo, Y. Y.; Veldhuizen, R. A. W.; Neumann, A. W.; Petersen, N. O.; Possmayer, F. Current perspectives in pulmonary surfactant - Inhibition, enhancement and evaluation. *Biochimica Et Biophysica Acta-Biomembranes* **2008**, *1778*, 1947-1977.

4. Serrano, A. G.; Perez-Gil, J. Protein-lipid interactions and surface activity in the pulmonary surfactant system. *Chem. Phys. Lipids* **2006**, *141*, 105-118.

5. Hall, S. B.; Venkitaraman, A. R.; Whitsett, J. A.; Holm, B. A.; Notter, R. H. Importance of Hydrophobic Apoproteins as Constituents of Clinical Exogenous Surfactants. *Am. Rev. Respir. Dis.* **1992**, *145*, 24-30.

6. Kobayashi, T.; Ohta, K.; Tashiro, K.; Nishizuka, K.; Chen, W. M.; Ohmura, S.; Yamamoto, K. Dextran restores albumin-inhibited surface activity of pulmonary surfactant extract. *J. Appl. Physiol.* **1999**, *86*, 1778-1784.

7. Lu, J. J.; Cheung, W. W. Y.; Yu, L. M. Y.; Policova, Z.; Li, D.; Hair, M. L.; Neumann, A. W. The effect of dextran to restore the activity of pulmonary surfactant inhibited by albumin. *Respiratory Physiology & Neurobiology* **2002**, *130*, 169-179.

8. Thomassen, M. J.; Antal, J. M.; Divis, L. T.; Wiedemann, H. P. Regulation of Human Alveolar Macrophage Inflammatory Cytokines by Tyloxapol - a Component of the Synthetic Surfactant Exosurf. *Clin. Immunol. Immunopathol.* **1995**, *77*, 201-205.

9. Yu, L. M. Y.; Lu, J. J.; Chiu, I. W. Y.; Leung, K. S.; Chan, Y. W. W.; Zhang, L.; Policova, Z.; Hair, M. L.; Neumann, A. W. Poly(ethylene glycol) enhances the surface activity of a pulmonary surfactant. *Colloids and Surfaces B-Biointerfaces* **2004**, *36*, 167-176.

10. Aydogan, N.; Uslu, B.; Tanaci, H. Biophysical investigation of the interfacial properties of cationic fluorocarbon/hydrocarbon hybrid surfactant: Mimicking the lung surfactant protein C. *J. Colloid Interface Sci.* **2011**, *360*, 163-174.

11. Eftaiha, A. F.; Paige, M. F. The influence of salinity on surfactant miscibility in mixed dipalmitoylphosphatidylcholine-perfluorooctadecanoic acid monolayer films. *J Colloid Interface Sci* **2011**, *353*, 210-219.

12. Krafft, M. P. Fluorocarbons and fluorinated amphiphiles in drug delivery and biomedical research. *Adv. Drug Deliv. Rev.* **2001**, *47*, 209-228.

13. Nakahara, H.; Lee, S.; Krafft, M. P.; Shibata, O. Fluorocarbon-Hybrid Pulmonary Surfactants for Replacement Therapy - A Langmuir Mono layer Study. *Langmuir* **2010**, *26*, 18256-18265.

14. Kissa, E., Ed.; In *Fluorinated Surfactants and Repellents, Second Edition;* Marcel Dekker Inc.: New York,USA, 1997; Vol. 97.

15. Krafft, M. P.; Goldmann, M. Monolayers made from fluorinated amphiphiles. *Current Opinion in Colloid & Interface Science* **2003**, *8*, 243-250.

16. Lau, C.; Anitole, K.; Hodes, C.; Lai, D.; Pfahles-Hutchens, A.; Seed, J. Perfluoroalkyl acids: A review of monitoring and toxicological findings. *Toxicological Sciences* **2007**, *99*, 366-394.

17. Lehmler, H. J.; Bummer, P. M. Mixing of partially fluorinated carboxylic acids with their hydrocarbon analogs at the air-water interface. *J. Colloid Interface Sci.* **2002**, *249*, 381-387.

18. Lehmler, H. J.; Bummer, P. M. Mixing of perfluorinated carboxylic acids with dipalmitoylphosphatidylcholine. *Biochimica Et Biophysica Acta-Biomembranes* **2004**, *1664*, 141-149.

19. Hoda, K.; Kawasaki, H.; Yoshino, N.; Chang, C.; Morikawa, Y.; Sugihara, G.; Shibata, O. Mode of interaction of two fluorinated-hydrogenated hybrid amphiphiles with dipalmitoylphosphatidylcholine (DPPC) at the air-water interface. *Colloids and Surfaces B-Biointerfaces* **2006**, *53*, 37-50.

20. Hoda, K.; Nakahara, H.; Nakamura, S.; Nagadome, S.; Sugihara, G.; Yoshino, N.; Shibata, O. Langmuir monolayer properties of the fluorinated-hydrogenated hybrid amphiphiles with dipalmitoylphosphatidylcholine (DPPC). *Colloids and Surfaces B-Biointerfaces* **2006**, *47*, 165-175.

21. Courrier, H. M.; Vandamme, T. F.; Krafft, M. P.; Nakamura, S.; Shibata, O. Mixed monolayers made from dipalmitoyl phosphatidylcholine and a fluorinated amphiphile. *Colloids and Surfaces A-Physicochemical and Engineering Aspects* **2003**, *215*, 33-41.

22. Hiranita, T.; Nakamura, S.; Kawachi, M.; Courrier, H. N.; Vandamme, T. F.; Krafft, M. P.; Shibata, O. Miscibility behavior of dipalmitoylphosphatidylcholine with a single-chain partially fluorinated amphiphile in Langmuir monolayers. *J. Colloid Interface Sci.* **2003**, *265*, 83-92.

23. Nakahara, H.; Nakamura, S.; Kawasaki, H.; Shibata, O. Properties of two-component Langmuir monolayer of single chain perfluorinated carboxylic acids with dipalmitoylphosphatidylcholine (DPPC). *Colloids and Surfaces B-Biointerfaces* **2005**, *41*, 285-298.

24. Nakahara, H.; Shibata, O. Langmuir Monolayer Miscibility of Perfluorocarboxylic Acids with Biomembrane Constituents at the Air-Water Interface. *Journal of Oleo Science* **2012**, *61*, 197-210.

25. Yokoyama, H.; Nakahara, H.; Nakagawa, T.; Shimono, S.; Sueishi, K.; Shibata, O. Miscibility behavior of two-component monolayers at the air-water interface: Perfluorocarboxylic acids and DMPE. *J. Colloid Interface Sci.* **2009**, *337*, 191-200.

26. Yokoyama, H.; Nakahara, H.; Shibata, O. Miscibility and phase behavior of DPPG and perfluorocarboxylic acids at the air-water interface. *Chem. Phys. Lipids* **2009**, *161*, 103-114.

27. McConnell, H. M. Structures and transitions in lipid monolayers at the air-water interface. *Annu. Rev. Phys. Chem.* **1991**, *42*, 171-195.

28. Tsuji, M.; Inoue, T.; Shibata, O. Purification and thermal analysis of perfluoro-n-alkanoic acids. *Colloids and Surfaces B-Biointerfaces* **2008**, *61*, 61-65.

29. Goecke, C. M.; Jarnot, B. M.; Reo, N. V. A Comparative Toxicological Investigation of Perfluorocarboxylic Acids in Rats by F-19 Nmr-Spectroscopy. *Chem. Res. Toxicol.* **1992**, *5*, 512-519.

30. Gaines, G. L. *Insoluble Monolayers at Liquid – Gas Interfaces*; Interscience Publishers: New York, USA, 1966; .

31. Eftaiha, A. F.; Brunet, S. M. K.; Paige, M. F. Thermodynamic and structural characterization of a mixed perfluorocarbon-phospholipid ternary monolayer surfactant system. *J. Colloid Interface Sci.* **2012**, *368*, 356-365.

32. Nakamura, S.; Nakahara, H.; Krafft, M. P.; Shibata, O. Two-component Langmuir monolayers of single-chain partially fluorinated amphiphiles with dipalmitoylphosphatidylcholine (DPPC). *Langmuir* **2007**, *23*, 12634-12644.

33. Zuo, Y. Y.; Keating, E.; Zhao, L.; Tadayyon, S. M.; Veldhuizen, R. A. W.; Petersen, N. O.; Possmayer, F. Atomic force microscopy studies of functional and dysfunctional pulmonary surfactant films. I. Micro- and nanostructures of functional pulmonary surfactant films and the effect of SP-A. *Biophys. J.* **2008**, *94*, 3549-3564.

34. Wustneck, R.; Perez-Gil, J.; Wustneck, N.; Cruz, A.; Fainerman, V. B.; Pison, U. Interfacial properties of pulmonary surfactant layers. *Adv. Colloid Interface Sci.* **2005**, *117*, 33-58.

35. Taeusch, H. W.; de la Serna, J. B.; Perez-Gil, J.; Alonso, C.; Zasadzinski, J. A. Inactivation of pulmonary surfactant due to serum-inhibited adsorption and reversal by hydrophilic polymers: Experimental. *Biophys. J.* **2005**, *89*, 1769-1779.

36. Pastrana, B.; Mautone, A. J.; Mendelsohn, R. Fourier-Transform Infrared Studies of Secondary Structure and Orientation of Pulmonary Surfactant Sp-C and its Effect on the Dynamic Surface-Properties of Phospholipids. *Biochemistry (N. Y.)* **1991**, *30*, 10058-10064.

37. Skoog, D. A.; Holler, J. F.; Nieman, T. A. *Principles of Instrumental Analysis, Fifth Edition;* Nelson Thomson Learning: Toronto, ON, 1998.

38. Thunemann, A. F.; Schnablegger, H. Monodisperse disk-shaped micelles of perfluorooctadecanoic acid. *Langmuir* **1999**, *15*, 5426-5428.

39. Yang, X. M.; Xiao, D.; Xiao, S. J.; Wei, Y. Domain-Structures of Phospholipid Monolayer Langmuir-Blodgett-Films Determined by Atomic-Force Microscopy. *Applied Physics A-Materials Science & Processing* **1994**, *59*, 139-143.

40. Korlach, J.; Schwille, P.; Webb, W. W.; Feigenson, G. W. Characterization of lipid bilayer phases by confocal microscopy and fluorescence correlation spectroscopy. *Proc. Natl. Acad. Sci. U. S. A.* **1999**, *96*, 8461-8466.

CHAPTER 5 PHASE-SEPARATION OF MIXED SURFACTANT MONOLAYERS: A COMPARISON OF FILM MORPHOLOGY AT THE SOLID–AIR AND LIQUID–AIR INTERFACES

5.1 Description

This chapter is a verbatim copy of a paper published in the Journal of Colloid and Interface Science. [Reproduced with permission from Journal of Colloid and Interface Science, (380) 105–112, 2012.]

The gross morphology of phase-separated fatty acid-perfluorocarbon mixed films was visualized in Langmuir monolayer and Langmuir-Blodgett (LB) films using atomic force microscopy (AFM) and Brewster angle microscopy (BAM). AFM images of films made of arachidic acid (C20) mixed with perfluorotetradecanoic acid (C14F) and palmitic acid (C16) mixed with perfluorooctadecanoic acid (C18F) gave rise to a series of discontinuous, polygonal domains that were consisted of C20 and C18F, and dispersed in a continuous matrix corresponded to C14F and C16 respectively. Real time BAM micrographs corroborated a similar structure deduced from the AFM measurements. This agreement in the film structures monitored by both BAM and AFM indicated that the deposition process minimally perturbed the film morphology. Further BAM measurements of mixed C20–C14F at air-water interface confirmed the domain growth mechanism deduced from the AFM data of mixed LB films.

The experimental section for this study is provided in the paper. A detailed description of the techniques used is provided in Chapter 1.

5.2 Description of the Candidate's Contribution

For this contribution, I prepared the samples, performed the isotherm, Brewster angle microscopy and atomic force microscopy measurements, played a major role in interpreting the results, wrote the initial draft of the work and participated in the subsequent editing in response

to collaborators and editors. Dr. Matthew Paige provided an extensive guidance throughout the experimental work and was greatly involved in results interpretation, writing and editing the paper.

5.3 Relation of Contribution towards Research Objectives

This contribution was solely performed towards the objectives of the thesis research. LB films provide simple model systems to examine both structures and domain growth kinetics in mixed perfluorocarbon-hydrocarbon mixed monolayers. They can be examined using surface characterization techniques that aren't accessible with Langmuir monolayers such as AFM. The most common concern associated with LB films is if surfactant deposition perturbs the overall film structure. This Chapter reports studies aimed at answering this question.

In this chapter we examined the morphology of mixed monolayer surfactant films at air-water and air-solid interfaces was examined using BAM and AFM respectively. A full discussion of the results of this study and its implications for the thesis research as a whole of is provided in Chapter 8.

The Phase-separation of mixed surfactant monolayers: A comparison of film morphology at the solid-air and liquid-air interfaces

Ala'a F. Eftaiha and Matthew F. Paige

Department of Chemistry, University of Saskatchewan, 110 Science Place, Saskatoon, Saskatchewan, Canada, S7N 5C9

Received 21 March 2012, Accepted 5 May 2012

5.4.1 Abstract

The morphologies of phase-separated monolayer films prepared from two different binary mixtures of perfluorocarbons and hydrocarbons have been examined and compared, for the first time, at the solid-air and liquid-air interfaces. Films were comprised of binary mixtures of arachidic acid ($C_{19}H_{39}COOH$) with perfluorotetradecanoic acid ($C_{13}F_{27}COOH$) and of palmitic acid ($C_{15}H_{31}COOH$) with perfluorooctadecanoic acid ($C_{17}F_{35}COOH$). For both mixed systems, Langmuir Blodgett films on mica substrates consisted of polygonal domains of one surfactant dispersed in a continuous matrix of the other (arachidic acid in perfluorotetradecanoic acid or perfluorooctadecanoic acid in palmitic acid, respectively), consistent with previous reports. Real-time imaging of the air-water interface via Brewster angle microscopy revealed that comparable film morphology was present at the air-water interface and the solid-air interface over a wide range of surface pressures, and that for the arachidic acid-based mixture, domain growth dynamics at the air-water interface is entirely consistent with that inferred from sequential "static" atomic force microscope images collected at the solid-air interface.

5.4.2 Introduction

The phase-separation of mutually immiscible surfactants in monolayer films is an important phenomenon, both for characterizing fundamental thermodynamics and kinetics of mixing processes, as well as for technological applications that require surface-patterning and the

tailoring of physical and chemical properties of solid-air and liquid-air interfaces. Our group and others have been systematically investigating the thermodynamics, kinetics and dynamics and surface morphology of mixed Langmuir and Langmuir-Blodgett (LB) monolayer films comprised of fluorinated and hydrogenated amphiphiles, with a view towards both understanding and controlling film morphology, composition, and mechanical properties.[1-5] Potential applications of these "bottom-up" assembly processes include the development of chemical and biological sensing platforms, surface passivation or functionalization and for preparing pulmonary lung surfactant therapeutics. Surfactant systems which have been investigated include binary mixtures of hydrogenated fatty acids with both perfluorinated and semi-fluorinated fatty acids;[3, 4, 6] binary and ternary phospholipid mixtures with perfluorinated amphiphiles;[7,8] and surfactant mixtures that contain both fluorocarbons and surface-active peptides that are commonly found in pulmonary lung surfactants,[9] to name a few.

A topic of intensive investigation in our group has been phase-separation in monolayer surfactant films prepared from mixtures of hydrogenated and perfluorinated fatty acids,[5, 10, 11] with binary mixtures of perfluorotetradecanoic acid ($C_{13}F_{27}COOH$; abbreviated C14F) with arachidic acid ($C_{19}H_{39}COOH$; abbreviated C20) and of perfluorooctadecanoic acid ($C_{17}F_{35}COOH$; abbreviated C18F) with palmitic acid ($C_{15}H_{31}COOH$; abbreviated C16) being of particular interest. Chemical structures of these surfactants are shown in Figure 5-1. The components of these mixed systems were found to be immiscible at the air-water interface, and the corresponding LB films deposited onto a variety of solid supports (muscovite mica, microscope coverglass, oxidized silicon) consisted of a mixture of polygonal structures ("discontinuous domains") that were highly-enriched in one surfactant, dispersed in a continuous matrix of the other surfactant. In the case of C20-C14F mixtures, the polygonal structures were

comprised of the hydrogenated surfactant whereas in the C16-C18F mixtures, the polygonal structures were comprised of the perfluorinated component. It was also inferred that dynamics of the surfactants at the air-water interface played a crucial role in controlling overall film morphology. For C20-C14F, it was found that domain size increased as a function of the time the surfactants remained at the air-water interface. This was attributed to the mechanism of domain growth (preliminary nucleation of the hydrogenated fatty acids, followed by diffusion-limited Ostwald ripening in conjunction with occasional domain coalescence). Some similarities in structure and interfacial behaviour can be found between the mixed hydrocarbon-perfluorocarbon systems and single-component semi-fluorinated alkanes ($C_nF_{2n+1}C_mH_{2m+1}$; often abbreviated F_nH_m), which also form complex self-assembled structures at the water-air interface under a variety of conditions.[12-15]

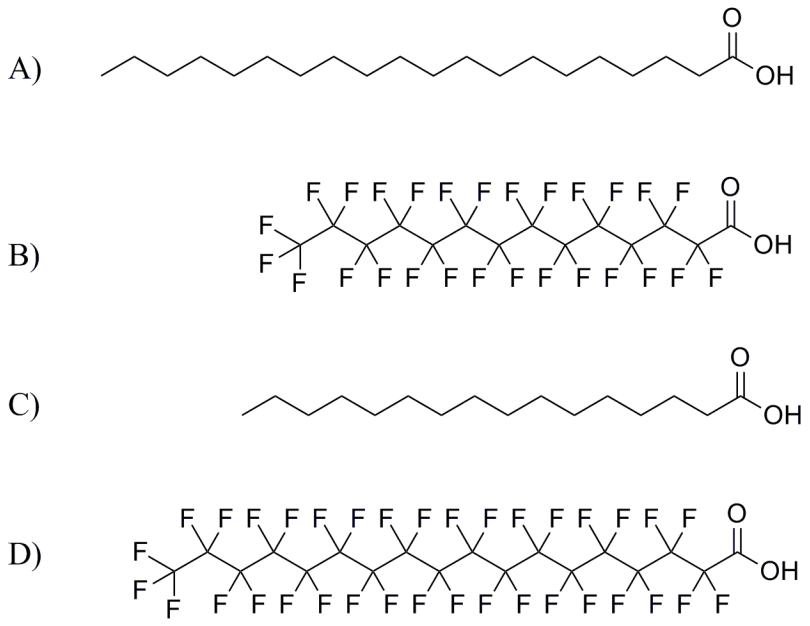

Figure 5-1 Chemical structures of A) arachidic acid ($C_{19}H_{39}COOH$; C20), B) perfluorotetradecanoic acid ($C_{13}F_{27}COOH$; C14F), C) palmitic acid ($C_{15}H_{31}COOH$; C16), and D) perfluorooctadecanoic acid ($C_{17}F_{35}COOH$; C18F).

Many of the studies described above, as well as others that can be found in the literature, have made use of atomic force microscope (AFM) imaging of solid-supported monolayer films

(Langmuir Blodgett) for morphological characterization. AFM is an invaluable tool for these studies, as the technique is surface-sensitive, non-destructive, provides high spatial resolution of non-conductive samples (nm and better) and, under suitable conditions, can provide both chemical and mechanical information about the sample of interest. However, AFM imaging is only useful for investigating solid-supported films and it is the air-water interface (typically an aqueous subphase contained in a Langmuir trough) that is of primary importance when assessing dynamics and kinetics of phase-separation and domain growth. In effect, AFM images are merely static "snapshots" of the dynamic liquid surface, and when assessing film morphology from these images, one necessarily assumes that the deposition process minimally perturbs film structure and that the AFM images are a true representation of the film morphology at the liquid-air interface. However, this may not be the case, and there are well-documented situations in which the interaction of film materials and the solid substrate plays a crucial role in controlling film morphology. An example of this has been provided by Gleiche et al.[16], in which deposition of a single-component phospholipid film onto mica gave rise to highly parallel nanoscale lines because of dynamic wetting instabilities during film transfer. Similar effects, though with different underlying mechanisms, have also been reported by Moraille et al.[17,18] for the deposition of multi-component phospholipid films.

To assess the role, if any, played by the deposition process on film morphology in both the mixed C20-C14F and C16-C18F systems (2:1 and 1:1 mole ratio compositions, respectively, were chosen to allow comparison of results with previous data), we have directly measured monolayer film structure at the air-water interface with a Brewster angle microscope (BAM), a refractive-index-reflectance-based optical microscopy technique that can directly image structures at the liquid-air interface, and compared the results with those obtained with AFM

imaging of solid-supported films. We have also completed a series of qualitative observations of domain growth dynamics for the C20-C14F mixtures under a variety of film conditions, and compared the results with those obtained in earlier studies.[5, 10, 11, 19] In all cases, film morphology and growth dynamics observed directly at the liquid-air interface were consistent with those measured (or inferred) using the AFM, indicating that for these systems, deposition effects on morphology are minimal and that meaningful inferences about film morphology and composition can be taken from films deposited at the solid-air interface. Of particular interest was the fact that the polygonal structures observed in the solid films were also observed at the liquid-air interface. These results observation defy conventional intuition which suggests domain structures at the liquid-air interface should be circular in order to minimize overall line-tension. These results are discussed in context of closely-related chemical systems which show similar domain structures at the solid-air and liquid-air interfaces, and the potential existence of a common underlying nanoscale structure in various mixed perfluorocarbon-hydrocarbon systems is discussed.

5.4.3 Materials and methods

5.4.3.1 Chemicals

Arachidic acid (C20), palmitic acid (C16) and perfluorotetradecanoic acid (C14F) were purchased from Sigma-Aldrich Corp., while perfluorooctadecanoic acid (C18F) was purchased from Alfa Aesar. Tetrahydrofuran (THF), hexane and absolute ethanol were purchased from Merck EM Science, EMD and Greenfield Ethanol Inc., respectively. Mica was purchased from Structure Probe Inc., and was freshly cleaved with adhesive tape prior to use.

5.4.3.2 Langmuir–Blodgett (LB) Film Deposition

Stock solutions of C20 and C14F were prepared in a 9:1 volume ratio of hexanes:THF, while solutions of C16 and C18F were prepared in a 9:1 volume ratio of hexane:THF and

hexane:ethanol, respectively. The solutions were combined in appropriate volumes to give the final mixed solutions. LB films were prepared using a standard Langmuir-Blodgett trough system (KSV Instruments, Helsinki, Finland), with surface pressure measured using a Wilhelmy balance equipped with a paper Wilhelmy plate. The baseline of nominal zero surface pressure was set by zeroing the Wilhelmy balance when the plate was in contact with a freshly cleaned water subphase and the barriers were fully extended. For deposition experiments, the mica substrate was immersed in ultrapure water (Millipore, resistivity 18.2 MΩ·cm), and aliquots of the surfactant mixtures were spread on the water surface. The spreading solvent was allowed to evaporate for 10 minutes and the film was compressed to the desired surface pressure (see text) with a compression rate of 10 $mm \cdot min^{-1}$. Upon reaching the selected surface pressure, the film was left to stabilize for 10 min, followed by withdrawing the mica substrate through the subphase at a rate of 5 $mm \cdot min^{-1}$.

5.4.3.3 Atomic Force Microscopy

AFM measurements were carried out on a Dimension Hybrid Nanoscope system (Veeco Metrology Group). Measurements were performed in contact mode in air, at a scan rate of 0.5 Hz using silicon nitride probes with nominal spring constant of ~0.1 $N \cdot m^{-1}$. Samples were typically imaged with a resolution of 512 pixels per line. Samples could be imaged repeatedly without causing detectable tip-induced damage.

5.4.3.4 Brewster Angle Microscopy

The BAM experiments were carried out at the water-air interface using a KSV-NIMA BAM system (KSV-NIMA, Biolin Scientific) equipped with a 658 nm illumination laser and a CCD camera detector. As with LB film deposition, aliquots of surfactant solution were spread over the subphase in a Langmuir trough and the solvent was allowed to evaporate. The

monolayer was then compressed at 10 mm·min^{-1} to the desired surface pressure and real-time images of the surface (200 μm x 200 μm, 20 frames per second) were collected.

5.4.4 Results and Discussion

5.4.4.1 Atomic Force Microscopy

AFM images of a C20-C14F and a C16-CF18 film deposited at π = 1 mN/m (26.5 Å^2/molecule) and nominal π = 0 mN/m (56.5 Å^2/molecule) are shown in Figure 5-2 (A and B), along with an appropriate cross-sectional analysis. We note that the deposition pressures used in this study are significantly lower than those used previously,[5, 11, 20] because at higher pressures it is not possible to spatially resolve adjacent domain structures in the BAM and comparing film structures between the solid-air and water-air interface under these exact conditions is not possible (*vide infra*). For both compositions, films consisted of elevated polygonal domains (discontinuous domains) that were polydisperse in size, surrounded by a lower, continuous matrix (continuous domain).

For C20-C14F monolayers (Figure 5-2A), the discontinuous domains were ~ 2.0 nm in height above the continuous matrix and had diameters ranging from ~ 2-20 μm (the latter necessarily being an estimate because of the irregular domain shape and high polydispersity). Deposition experiments at higher pressures (π = 20 mN/m; see Supplemental Figure 5-1 for image) gave comparable gross film morphology, though some subtle structural differences were observed (at the higher pressure, domains were ~1.0 nm high, diameters ~ 1-2 μm and spacing between adjacent domains was on the order of tens of nanometers). While we have not previously reported film structures at low deposition pressures, the film structure observed for π = 1 mN/m (gaseous phase; see π-*A* isotherm for both C20–14F and C16–C18F monolayers in Supplemental Figure 5-2) is entirely consistent with the formation of vertically-oriented C20

domains, with a surrounding matrix of C14F which is oriented with a tilt angle to the surface normal (the expected result for a loosely-packed perfluorinated surfactant film). This film structure has previously be ascribed to discontinuous domains comprised of vertically-oriented C20 (labeled with an '**a**' in Figure 5-2A) adsorbed to the substrate, surrounded by a continuous C14F matrix (labeled with a '**b**' in Figure 5-2A). A "scratch test" (results not shown), in which the surfactant film was removed by scanning with the AFM at high operating forces confirmed this result, with the discontinuous domains ~ 2.5 nm in height (approximately the length of an individual C20 molecule) above the underlying mica substrate, and the continuous domain ~ 1.0 nm above the mica.

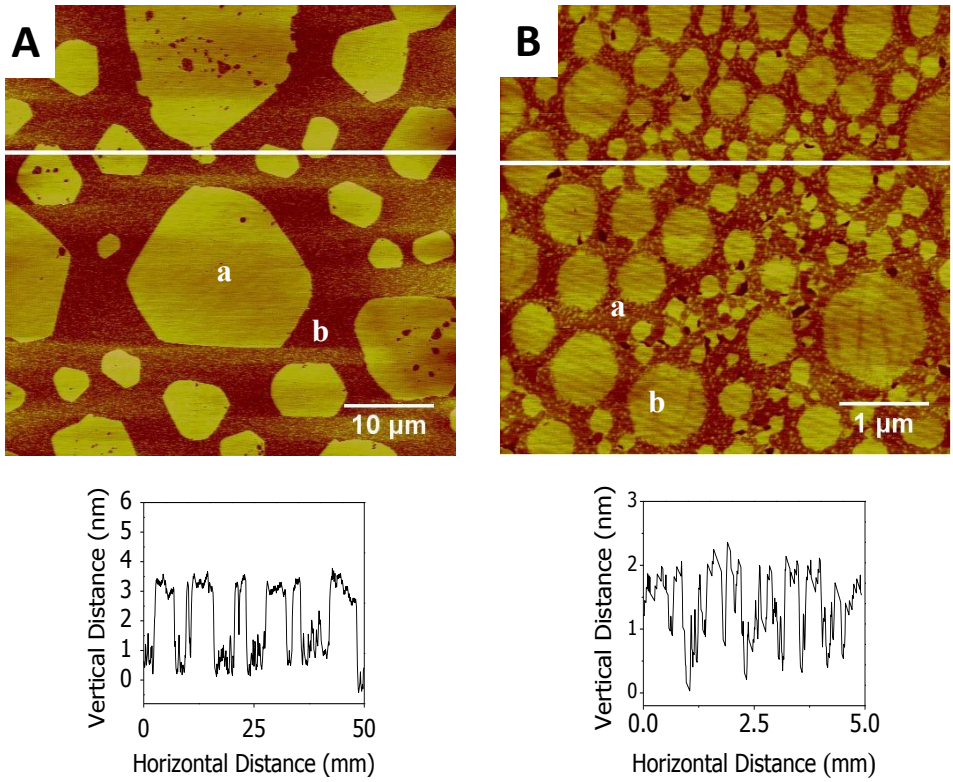

Figure 5-2 AFM images and cross-sectional analysis of: A) 2:1 C20-C14F film (50µm x 50µm) deposited at a surface pressure of π = 1 mN/m; the labels 'a' and 'b' indicate regions of the film occupied by C20 and C14F, respectively; and (B) 1:1 C16-C18F film (5 µm x 5 µm) deposited at a surface pressure of π = 0 mN/m; the labels 'a' and 'b' indicate regions of the film occupied by C16 and C18F, respectively.

Monolayers of C16-C18F (Figure 5-2B) consisted of polygonal discontinuous domains of ~ 0.5 – 2.0 μm in diameter and ~ 3.4 nm in height above the surrounding matrix. Consistent with the C20-C14F monolayer system, these heights are slightly larger than those observed at π = 20 mN/m,[11] as is expected for less condensed monolayers, though again, the gross morphological features of the film are the same as reported at π = 20 mN/m. X-ray photoemission electron microscopy measurements, in conjunction with confocal fluorescence microscopy imaging of fluorescent-probe doped films have been used previously to assign the continuous matrix (labeled '**a**' in Figure 5-2B) and the discontinuous domains (labeled '**b**' in Figure 5-2B) as C16 and C18F, respectively.[11, 20]

5.4.4.2 Brewster Angle Microscopy at Fixed Surface Pressure

To compare the deposited film structures with those present at the liquid-air interface, BAM images were taken for the two different compositions of films (Figure 5-3 and Figure 5-4). As an aside, we note that the refractive index of perfluorocarbons is comparable with that of pure water (verified by control samples of pure C14F films on water, which showed negligible contrast), and as such, reflective (bright) regions in the BAM images can, fortuitously, be attributed almost exclusively to the presence of the hydrogenated film component.

For C20-C14F mixtures at surface pressure π = 1 mN/m, BAM images show that the films consisted of a series of interconnected domains, giving rise to an overall mesh-like (percolated) structure. The interconnected domains were typically tens of microns in size, and adjacent domains often met at a sharp asperity. Because of the similar refractive indices of the perfluorocarbon and the underlying water subphase, dark regions in the BAM images can be ascribed to the presence of water, perfluorocarbon, or both, whereas the reflective regions must consist of the hydrogenated surfactant. The hydrogenated domains often contained a number of

pinhole defects (one such defect is indicated with an arrow in Figure 5-3), which were also observed (albeit at a smaller length scale) in the corresponding AFM images shown in Figure 5-2A. There was no tendency for the pin-hole defects to anneal or otherwise change shape during the course of the BAM measurements.

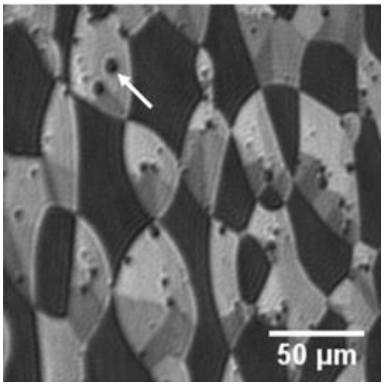

Figure 5-3 Representative BAM image of 2:1 C20-C14F mixed film at the air-water interface (π = 1 mN/m, 26.5 $Å^2$/molecule). The arrow highlights a pin-hole defect as described in the text.

We have not previously observed these mesh-like structures in solid-supported films, regardless of deposition conditions. It is possible that these structures are not sufficiently stable to maintain structural integrity during film transfer to a solid substrate, and fracture to give discrete domains. However, a more likely explanation is that while the mesh-like network in Figure 5-3 appears to be entirely continuous, the spatial resolution of our microscope is simply insufficient to distinguish sub-micrometer separations between domains (the smallest resolvable distance between points as defined by the Rayleigh criterion is ~2 µm for the wavelength of light and numerical aperture of the collection lens used here) and many of the regions between domains that are readily apparent in the AFM images are simply not resolvable in the BAM. Closer inspection of Figure 5-3 (and similar images in subsequent experiments, Figure 5-5) suggests the interconnected mesh-like structure is actually comprised of closely-spaced geometric (polygonal) structures which are comparable with those observed in Figure 5-2A. We further note that contrast in the polygonal structures of Figure 5-3 (and in other BAM images

described subsequently) is not uniform, but rather consists of several distinct and well-separated shades of grey. In general, several different parameters contribute to image contrast in BAM images of monolayer films, including molecular tilt and film thickness, azimuthal tilt, roughness of the underlying substrate, as well as instrumental factors such as fluctuations in illumination intensity and detector noise.[21] Deconvolving these effects is often problematic, though there are several reports in the literature which describe some viable approaches (typically based on the 4x4 matrix formalism) to solving this issue (see Tabe et al.[22] and Tsao et al.[23]). While a more in-depth analysis is beyond the scope of this study, we note that similar distinct grey-shaded domains have been reported by Brezensinski et al.[24] for BAM images of 1-monopalmitoyl-*rac*-glycerol monolayers. In these systems, disk-like domains of surfactant were found to consist of seven well-defined segments each with different contrasts (reflectivities), and contrast differences between the segments was attributed to each having slightly different surfactant tilt azimuths. Subtle structural differences of this type would be difficult to resolve in AFM images and are certainly not apparent in Figure 5-2A, and it is certainly possible that the polygonal domains contain some subtle structural variations in terms of alkyl chain tilt, both within and between different domains. During the time period that the domains remained in the microscope's field of view, there were no significant changes in grey-levels (pixel intensities) for the domains, suggesting that the tilt azimuths remained at fixed values on this time scale. Regardless, accounting for the spatial resolution limits of the optical technique, the BAM data agrees well with the AFM data, indicating that similar domain structures can be found at both the liquid-air and solid-air interfaces.

In the case of the C16-C18F system, film morphology was somewhat more difficult to investigate via BAM imaging because of the intrinsically smaller domain sizes that were formed

(see Figure 5-2B) and the spatial resolution limit described above. BAM images of films collected at π = 1 mN/mshowed negligible contrast, suggesting that the spacing between close-packed domains was too small to be spatially resolved. This result is consistent with the AFM images in Figure 5-2B, in which the space between domains is sub-micron in size. However, film structures could be observed at lower pressures (nominally π = 0 mN/m, 56.5 Å^2/molecule), where the inter-domain spacing is expected to be larger, and a typical image of such a film is shown in Figure 5-4. To aid in visualization, the BAM image has also been converted into a false colour scheme that correlates with that used to display the AFM data.

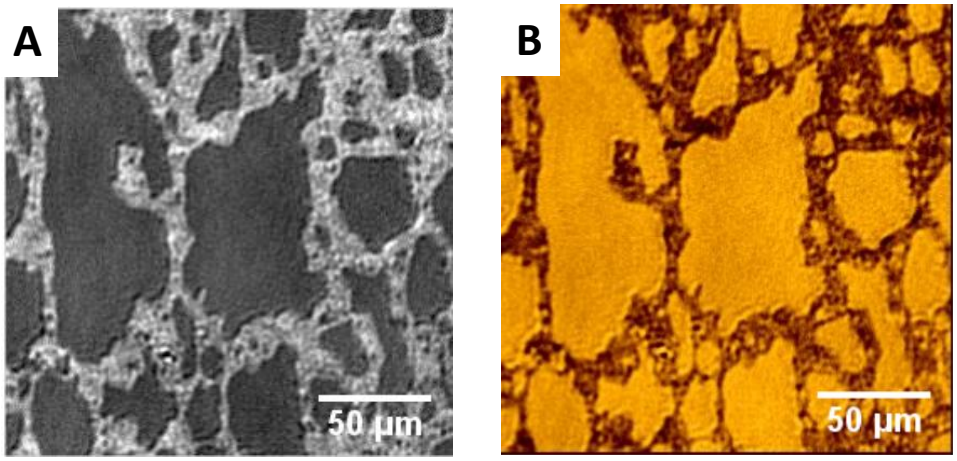

Figure 5-4 A) BAM image of a 1:1 C16-C18F mixed film at the air water interface (π = 0 mN/m, 56.5 Å^2/molecule); B) Modified BAM image with false color scheme. Color contrast has been adjusted such that the bright regions correspond to areas of negligible refractive index difference with the subphase and hence, correspond to the hydrogenated film component (C16).

Again, the gross film structure at the liquid-air interface is entirely consistent with that expected from the AFM measurements at the solid-air interface, with the dark regions in the BAM images (C18F) corresponding to the polygonal domains in the AFM images and the bright regions (C16) correspond to the continuous matrix. We note that the sizes of the structures in the BAM images are, on average, larger than those in AFM images and it is likely that there is a built-in bias in the data collection due to the different length-scales over which the two methods

intrinsically operate; in larger scale AFM images (~ 100 μm x 100 μm; data not shown) occasional large scale domains comparable with those seen in Figure 5-4 are observed.

Smaller structures at the resolution limit of the instrument can just be detected in Figure 5-4A, and larger scale AFM images reveal occasional large domains which are comparable in size to those in Figure 5-4A. Because of the resolution limitations imposed by the small domain sizes in the C16-C18F system, the remainder of this study focused on a more in-depth investigation of the morphology and film dynamics of the C20-C14F system.

5.4.4.3 Brewster Angle Microscopy under Conditions of Varying Pressure

To further characterize film morphology at the air-water interface for the C20-C14F system, BAM images (Figure 5-5 (A-D)) have been collected during film compression (compression rate of 10 $mm \cdot min^{-1}$), with pressures varying from π = 1 mN/m - 20 mN/m (gaseous through solid phases in the compression isotherm; isotherm shown in Supplemental Figure 5-2A). An evolution of film structures can be seen as a function of surface pressure, and in general, as surface pressure was increased, the resolvable distance between domains decreased, which is the expected result for discrete domains which are gradually being compressed together by the trough barriers.

At the initial pressure of π = 1 mN/m, the mesh-like network described previously was readily apparent. As the surface pressure increases (Figure 5-5 (B and C)), individual polygonal domains become more clearly resolved, with the shapes of the domains being entirely consistent with those observed in the AFM images. It was common to observe fused clusters of domains (one such cluster is indicated with an arrow in Figure 5-4C) in the BAM images, but the sharp, well-defined edges that are apparent in the AFM experiments are still readily detectable under all imaging conditions. Again, a distribution of contrast levels (grey levels) in the polygonal

domains is observable, suggesting the presence of small variations in alkyl chain tilt angles. At sufficiently high pressures (π = 20 mN/m), the images contain a smaller number of large domains, though empty space between domains is still resolvable.

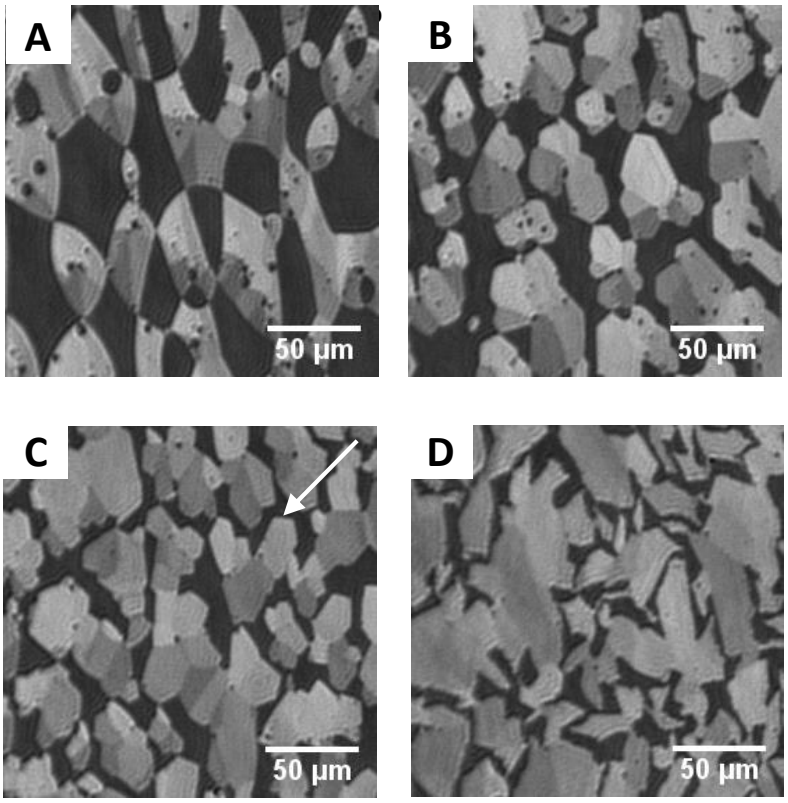

Figure 5-5 BAM images (200 µm X 200 µm) of 2:1 C20-C14F film (total surfactant concentration = 6.92 mM, compression rate = 10 mm·min^{-1}, temperature = 25°C) measured at a surface pressure of A) π = 1 mN/m, B) π = 5 mN/m, C) π = 10 mN/m and D) π = 20 mN/m. The arrow in C) indicates a highly-aggregated cluster of polygonal domains.

Researchers in this discipline have taken a great interest in the molecular-scale structure of the phase-separated domains, particularly because the sharp edges observed in the polygonal structures suggests an underlying crystalline nature. For phase-separated surfactant systems, domain morphology arises from a complex interplay of interactions, including (but not limited to) long-range repulsive interactions between similarly charged head groups which lead to complex, extended domains, line tension between different phases which leads to circular shapes, as well as kinetic trapping of metastable structures and, for solid-supported samples,

substrate interaction effects in conjunction with fluid-flow (film draining). Potentially useful insight into the overall domain morphology observed in the binary systems studied here can be gained from review of the affiliated literature associated with single-component semifluorinated alkane monolayers. Huang et al.[13] have made use of grazing incidence X-ray diffraction at the air-water interface to examine $F_{12}H_{18}$ monolayer film structure, and results from these experiments indicated that the fluorinated blocks of the molecules packed in a highly-organized hexagonal lattice, oriented on a hydrocarbon block that was in contact with the water subphase. Kato et al.[14] and Maaloum et al.[25] have independently reported the observation of ~ 30 nm diameter nanodomains in AFM images of deposited semi-fluorinated fatty acids ($C_nF_{2n+1}C_mH_{2M}$-COOH) and F_8H_{16} monolayers, respectively, and Fontaine et al.[26] have used grazing incidence small angle X-ray scattering experiments measurements to support a model suggesting the domains consist of a crystallized, hexagonal network of these ~30 nm nanodomains. Very recently, Bardin et al.[12] have demonstrated this result to be more general through a combination of BAM and X-ray scattering measurements, with similar domains (and underlying nanodomains) being formed by a wide range of semifluorinated alkanes (F_8H_m, m = 14, 16, 18 and 20).

While the semifluorinated alkane systems described in the literature differ significantly from the binary perfluorocarbon-hydrocarbon surfactant mixtures studied here, there are clearly many structural similarities in terms of micron-scale film morphology, and we speculate that there are underlying structural features that are common to both as well. Following the analysis of Bardin et al.[12], typical angles observed for the higher-pressure polygonal domains in the BAM images (~ 60^o, 90^o, 120^o) are consistent with what is expected from an underlying 2D hexagonal crystallinity. Furthermore, and also consistent with the semifluorinated alkane systems, while

BAM data alone cannot definitively explain why polygonal structures are observed, one can now effectively rule out the possibility that when films are deposited onto solid substrates, the underlying solid substrate may be acting as a template for polygonal domain formation. We are presently investigating the possibility of carrying out synchrotron-based X-ray scattering diffraction experiments to investigate the detailed molecular scale structure of the polygonal domains, and speculate that the underlying hexagonal symmetry may be a common structural motif found in many mixed fluorocarbon-hydrocarbon systems.

5.4.4.4 Brewster Angle Microscopy as a Function of Time

Previous measurements of the C20-C14F system have examined domain growth dynamics,[19] though the analysis has again suffered from the potential problem of the deposition altering overall domain morphology. While the results described above now suggest that this effect is negligible, BAM images have also been collected as a function of time (at fixed π = 20 mN/m) to directly assess growth dynamics at the water-air interface, and are shown in Figure 5-6 (A-C). Note, under these experimental conditions, growth of domains cannot be observed for more than several seconds because they do not remain in the illumination region for longer than this (residence time is strongly affected by diffusion rates as well as by convection and air currents). Further, at this high of a compression pressure, individual domains are so closely packed that they cannot be resolved and bright regions in the images correspond to large numbers of domains that are either tightly-packed (closer than 2 μm) or fused together. Because of this, BAM does not allow for the nanometer-length scale imaging of domains (for example, observing individual domains undergoing ripening is not detectable) but rather a gross assessment of micrometer-scale film morphology. With these caveats, we show representative images collected at three different stages of film growth.

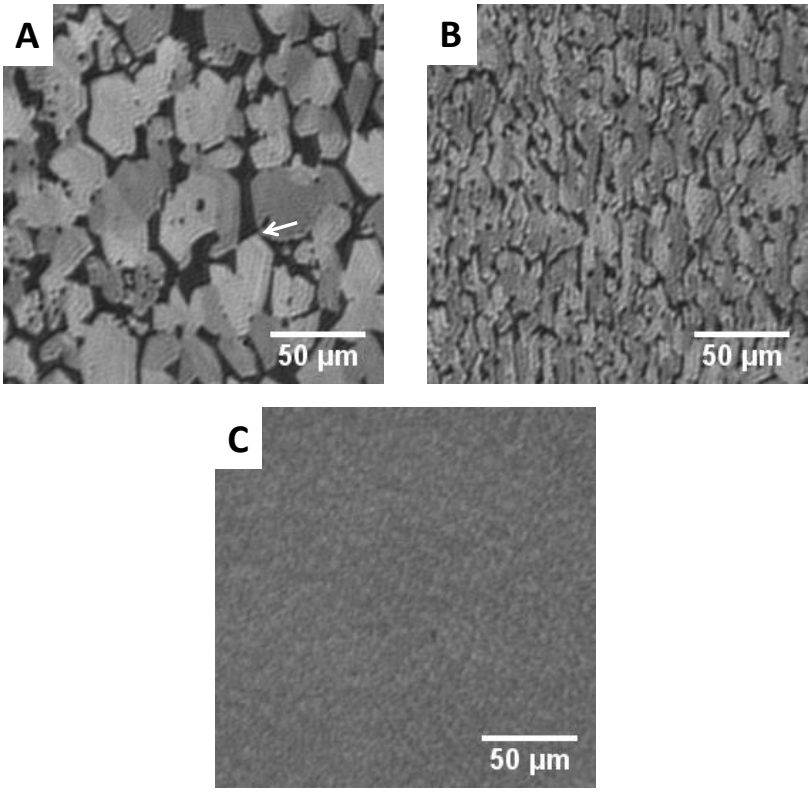

Figure 5-6 BAM images (200 µm x 200 µm) of a 2:1 C20-C14F film (compressed to a constant pressure of π = 20 mN/m, temperature = 25°C) after A) 100s, B) 400s, C) 500s. The arrow in A) indicates a hexagonal asperity at the edge of one highly-reflective surfactant region.

Initially, images of films collected at π = 20 mN/m consisted of highly-reflective regions (closely-packed and fused domains) with well-defined gaps between different regions. At the edges of these regions, one occasionally observes the characteristic hexagonal asperities and domain angles observed under other film preparation conditions (an arrow in Figure Figure 5-6A highlights one such asperity). As the observation period increased, the overall distance between the highly-reflective regions decreased until after ~ 500 s the entire film assumed an essentially featureless grey appearance, indicating that the separation between all domains in the film was no longer resolvable. The amount of time required for the film features to become unresolvable was a function of the pressure at which the films were maintained; at pressures of π = 1 mN/m,

features were resolvable for ~ 5000 s, with the length of time decreasing with increasing surface pressure.

Although precisely reconciling the images collected here with those from AFM experiments is problematic because of differences in spatial resolution and sensitivity of the two methods, both approaches are consistent with the proposed underlying growth mechanism (Ostwald ripening of domains in conjunction with domain fusion). Again, we note that the BAM provides micron-scale surface morphology information; while the highly-reflective regions in the BAM images may show a wide variety of sizes (and in the images shown in Figure 5-6, may actually appear to decrease in size with time), this does not mean that the domains that comprise them are decreasing in size. At early stages of this experiment, the domains are, on average, small but polydisperse; as the individual domains grow larger with time, spacing between adjacent domains becomes smaller and the ability to resolve the domains decreases until, ultimately, the entire film appears homogeneous in the BAM. While this gross morphological assessment of film structure at the liquid-air interface is useful, the ability to track individual domains, though technically challenging, would clearly be an asset. In the future, attempts will be made to significantly increase the residence time of the domains in the illumination area through reduction of trough size, temperature control and minimization of convection, with an ultimate goal of tracking the time-evolution and dynamics of isolated domains and obtaining a detailed, real-time visualization of the domain growth mechanism.

5.4.5 Conclusions

Film structures for mixed, phase-separated monolayer films were measured and compared at the liquid-air and solid-air interfaces for two different immiscible perfluorocarbon-hydrocarbon ($C_{13}F_{27}COOH$ with $C_{19}H_{39}COOH$; and $C_{17}F_{35}COOH$ with $C_{15}H_{31}COOH$) surfactant

systems. Parallel use of AFM and BAM imaging allows, for the first time, an assessment of the role played by deposition on the morphology and composition of these important mixed monolayer films. For the two different mixed films, gross film morphology and composition was, to within the resolution and sensitivity capabilities of the two microscopy approaches, comparable, indicating that deposition onto solid substrates minimally perturbs the overall film structure and that the underlying solid substrate is not templating or otherwise affecting the observed structures as has been reported for other monolayer film systems.[16-18] Further, for the mixed arachidic acid – perfluorotetradecanoic acid system, domain growth kinetics observed at the liquid-air interface was consistent with that inferred previously from static AFM images of solid-deposited films.[19]

An important implication of this work is that, for these systems, inferences about domain morphology and composition at the liquid-air interface can reasonably be made based upon data gathered at the solid-air interface alone. Further, we note that domain morphology for the mixed perfluorocarbon-hydrocarbon systems reported here is consistent with that observed for the closely-related semifluorinated alkane surfactant systems,[12, 14, 25, 26] suggesting the existence of a common underlying nanoscale surface structure for hydrocarbon-perfluorocarbon surfactant monolayers.

5.4.6 Acknowledgements

Funding for this work was provided by the Natural Sciences and Engineering Research Council of Canada (NSERC), the Canada Foundation for Innovation (CFI), the Province of Saskatchewan and by the University of Saskatchewan. We thank Professor Ian Burgess for insightful discussions and comments.

5.4.7 Appendix A. Supplementary material

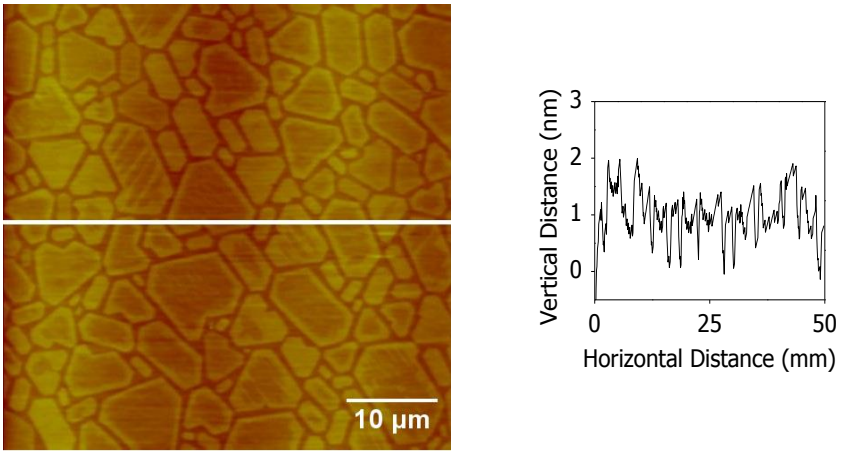

Supplemental Figure 5-1 Atomic force microscope image and cross-sectional analysis of a C20–C14F monolayer film prepared at a deposition pressure of π = 20 mN/m.

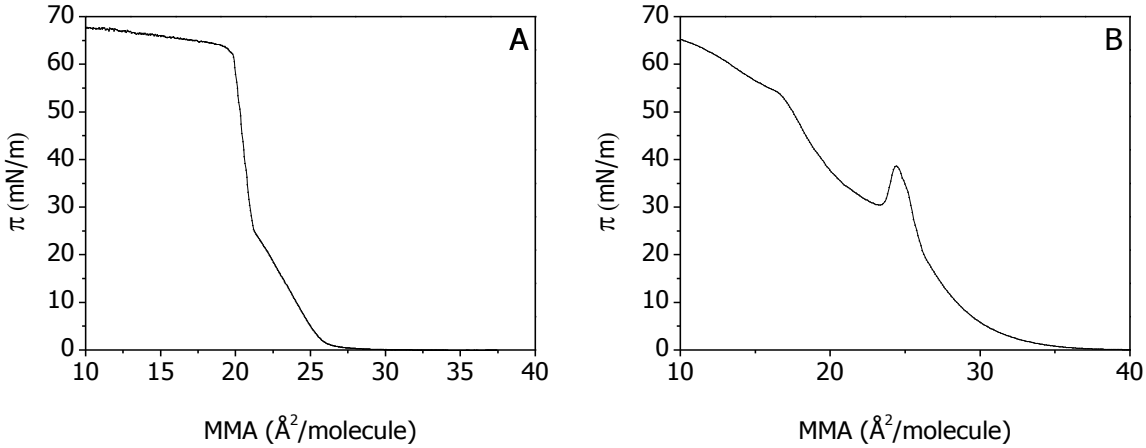

Supplemental Figure 5-2 Surface pressure-area (π vs. mean molecular area) compression isotherms for (A) C20–C14F monolayer film, (B) C16–C18F monolayer film. For the C16–C18F film, the peak at ~ 24 Å^2/molecule corresponds to the collapse of the C16 component.

5.4.8 References

1. Broniatowski, M.; Dynarowicz-Łątka, P. Semifluorinated chains at the air/water interface: Studies of the interaction of a semifluorinated alkane with fluorinated alcohols in mixed langmuir monolayers. *Langmuir* **2006**, *22*, 2691-2696.

2. Krafft, M. P.; Riess, J. G. Chemistry, physical chemistry, and uses of molecular fluorocarbon-hydrocarbon diblocks, triblocks, and related compounds-unique "apolar" components for self-assembled colloid and interface engineering. *Chem. Rev.* **2009**, *109*, 1714-1792.

3. Lehmler, H. -.; Bummer, P. M. Mixing of partially fluorinated carboxylic acids with their hydrocarbon analogs at the air-water interface. *J. Colloid Interface Sci.* **2002**, *249*, 381-387.

4. Matsumoto, M.; Watanabe, S.; Tanaka, K. -.; Kimura, H.; Kasahara, M.; Shibata, H.; Azumi, R.; Sakai, H.; Abe, M.; Kondo, Y.; Yoshino, N. Control of two-dimensional nanopatterns by adjusting intermolecular interactions. *Adv Mater* **2007**, *19*, 3668-3671.

5. Qaqish, S. E.; Paige, M. F. Mechanistic insight into domain formation and growth in a phase-separated Langmuir-Blodgett monolayer. *Langmuir* **2007**, *23*, 10088-10094.

6. Matsumoto, M.; Tanaka, K. -.; Azumi, R.; Kondo, Y.; Yoshino, N. Structure of phase-separated Langmuir-Blodgett films of hydrogenated and perfluorinated carboxylic acids investigated by IR spectroscopy, AFM, and FFM. *Langmuir* **2003**, *19*, 2802-2807.

7. Eftaiha, A. F.; Brunet, S. M. K.; Paige, M. F. Thermodynamic and structural characterization of a mixed perfluorocarbon-phospholipid ternary monolayer surfactant system. *J. Colloid Interface Sci.* **2012**, *368*, 356-365.

8. Gerber, F.; Krafft, M. P.; Vandamme, T. F.; Goldmann, M.; Fontaine, P. Fluidization of a dipalmitoyl phosphatidylcholine monolayer by fluorocarbon gases: Potential use in lung surfactant therapy. *Biophys. J.* **2006**, *90*, 3184-3192.

9. Nakahara, H.; Lee, S.; Krafft, M. P.; Shibata, O. Fluorocarbon-Hybrid Pulmonary Surfactants for Replacement Therapy - A Langmuir Monolayer Study. *Langmuir* **2010**, *26*, 18256-18265.

10. Christensen, S.; Lanke, U. D.; Haines, B.; Qaqish, S. E.; Paige, M. F.; Urquhart, S. G. Structural and compositional mapping of a phase-separated Langmuir-Blodgett monolayer by X-ray photoelectron emission microscopy. *Journal of Electron Spectroscopy and Related Phenomena* **2008**, *162*, 107-114.

11. Qaqish, S. E.; Paige, M. F. Structural and compositional mapping of a phase-separated langmuir-blodgett monolayer by atomic force microscopy. *Langmuir* **2007**, *23*, 2582-2587.

12. Bardin, L.; Fauré, M. -.; Limagne, D.; Chevallard, C.; Konovalov, O.; Filipe, E. J. M.; Waton, G.; Krafft, M. P.; Goldmann, M.; Fontaine, P. Long-range nanometer-scale organization of semifluorinated alkane monolayers at the air/water interface. *Langmuir* **2011**, *27*, 13497-13505.

13. Huang, Z.; Acero, A. A.; Lei, N.; Rice, S. A.; Zhang, Z.; Schlossman, M. L. Structural studies of semifluorinated hydrocarbon monolayers at the air/water interface. *Journal of the Chemical Society - Faraday Transactions* **1996**, *92*, 545-552.

14. Kato, T.; Kameyama, M.; Ehara, M.; Iimura, K. -. Monodisperse two-dimensional nanometer size clusters of partially fluorinated long-chain acids. *Langmuir* **1998**, *14*, 1786-1798.

15. Mourran, A.; Tartsch, B.; Gallyamov, M.; Magonov, S.; Lambreva, D.; Ostrovskii, B. I.; Dolbnya, I. P.; De Jeu, W. H.; Moeller, M. Self-assembly of the perfluoroalkyl-alkane F 14H 20 in ultrathin films. *Langmuir* **2005**, *21*, 2308-2316.

16. Gleiche, M.; Chi, L. F.; Fuchs, H. Nanoscopic channel lattices with controlled anisotropic wetting. *Nature* **2000**, *403*, 173-175.

17. Moraille, P.; Badia, A. Highly parallel, nanoscale stripe morphology in mixed phospholipid monolayers formed by Langmuir-Blodgett transfer. *Langmuir* **2002**, *18*, 4414-4419.

18. Moraille, P.; Badia, A. Nanoscale stripe patterns in phospholipid bilayers formed by the Langmuir-Blodgett technique. *Langmuir* **2003**, *19*, 8041-8049.

19. Qaqish, S. E.; Paige, M. F. Characterization of domain growth kinetics in a mixed perfluorocarbon-hydrocarbon Langmuir-Blodgett monolayer. *J. Colloid Interface Sci.* **2008**, *325*, 290-293.

20. Qaqish, S. E.; Urquhart, S. G.; Lanke, U.; Brunet, S. M. K.; Paige, M. F. Phase separation of palmitic acid and perfluorooctadecanoic acid in mixed langmuir-blodgett monolayer films. *Langmuir* **2009**, *25*, 7401-7409.

21. Hénon, S.; Meunier, J. Microscope at the Brewster angle: Direct observation of first-order phase transitions in monolayers. *Rev. Sci. Instrum.* **1991**, *62*, 936-939.

22. Tabe, Y.; Yokoyama, H. Fresnel formula for optically anisotropic Langmuir monolayers: An application to Brewster angle microscopy. *Langmuir* **1995**, *11*, 699-704.

23. Tsao, M.; Fischer, T. M.; Knobler, C. M. Quantitative analysis of Brewster-angle microscope images of tilt order in Langmuir monolayer domains. *Langmuir* **1995**, *11*, 3184-3188.

24. Brezesinski, G.; Scalas, E.; Struth, B.; Mohwald, H.; Bringezu, F.; Gehlert, U.; Weidemann, G. Relating Lattice and Domain-Structures of Monoglyceride Monolayers. *J. Phys. Chem.* **1995**, *99*, 8758-8762.

25. Maaloum, M.; Muller, P.; Krafft, M. P. Monodisperse surface micelles of nonpolar amphiphiles in langmuir monolayers. *Angewandte Chemie - International Edition* **2002**, *41*, 4331-4334.

26. Fontaine, P.; Goldmann, M.; Muller, P.; Fauré, M.; Konovalov, O.; Krafft, M. P. Direct evidence for highly organized networks of circular surface micelles of surfactant at the air-water interface. *J. Am. Chem. Soc.* **2005**, *127*, 512-513.

CHAPTER 6 THE IMPACT OF TAIL POLARITY ON PHASE SEPARATION IN MIXED LIPID MONOLAYERS: A MOLECULAR DYNAMICS STUDY

6.1 Description

This chapter is a copy of a manuscript that is in preparation.

Coarse grained (CG) molecular dynamics (MD) simulations of mixed surfactant monolayers is an active area of research. It provides an approach to examine monolayer films with high temporal and resolutions (tens of nm and μs). MARTINI force field (one of the most used CG force fields for studying biomolecular systems) was used to explore mixed monolayers comprised of surfactant molecules with different tail polarities such as hydrogenated and fluorinated surfactants. In this context, we investigated surfactant aggregation in response to variations in lipid hydrocarbon tail polarity as a simplified model for perfluorocarbon-hydrocarbon mixed films using 1,2-dipalmitoyl-sn-glycero-3-phosphocholine (DPPC) monolayers and monolayers containing different polarity species. Simulated surface pressure-area isotherms, the radial distribution function (RDF) and tilt angle measurements of single component DPPC monolayers indicated the formation of more expanded and disordered systems with increasing tail polarity. The time dependency of RDFs and cluster size data of mixed monolayer systems indicated that the lateral organization of the film forming components is a function of tail polarity differences encountered within the monolayer system.

The theoretical section for this study is provided in the manuscript. A detailed description of the techniques used is provided in Chapter 1.

6.2 Description of the Candidate's Contribution

For this contribution, I performed the computer simulation measurements, played a major role in interpreting the results, wrote the initial draft of the work except the methods section and participated in the subsequent editing in response to collaborators. Dr. Surajith Wanasundara provided a major contribution to this work. He wrote the computer code needed throughout the project, the majority of the methods section in the manuscript and was involved in editing the manuscript. Both Dr. Richard Bowles and Dr. Matthew Paige provided an extensive guidance throughout the experimental work and were greatly involved in results interpretation, writing and editing the manuscript.

6.3 Relation of Contribution towards Research Objectives

This contribution was solely performed towards the objectives of the thesis research. As shown in the previous Chapters (2-5), we have used different surface sensitive techniques (atomic force microscopy, confocal fluorescence microscopy and Brewster angle microscopy) to get information about the morphology of mixed monolayer films comprised of hydrogenated and perfluorinated surfactants at the micrometer and nanometer length scale. Computer simulation provides an access to high-resolution molecular-scale information. In this chapter, we have used CG-MD simulation to study the lateral organization of mixed monolayer systems comprised of MARTINI model DPPC molecules with different tail polarities. Results indicated that the molecules tend to separate with increasing the polarity difference between the monolayer forming components. This revealed that the MARTINI force field can be used to examine mixed monolayers made of surfactant molecules of different tail polarities such as hydrogenated and semi or fully fluorinated surfactants. A full discussion of the results of this study and its implications for the thesis research as a whole of is provided in Chapter 8.

The Impact of Tail Polarity on Phase Separation of Mixed Lipid Monolayers: A Molecular Dynamics Study

Ala'a F. Eftaiha, Surajith N. Wanasundara, Richard K. Bowles and Matthew F. Paige

Department of Chemistry, University of Saskatchewan, 110 Science Place, Saskatoon, Saskatchewan, Canada, S7N 5C9

6.4.1 Abstract

Coarse-grained molecular dynamics simulations have been used to investigate the effect of dipalmitoylphosphatidylcholine (DPPC) tail group polarity on the structural and phase behavior of both single component and binary mixed monolayers using the MARTINI force field. The mixed monolayer systems with components of different polarity were selected such that they may be viewed as a simple model system for mixed hydrogenated and semi- or perfluorinated surfactant monolayer systems. Surface pressure-area isotherms of single component systems indicate that DPPC monolayers become more expanded with increasing degree of polarity of the hydrophobic tail groups. A combination of radial distribution function values and tilt angle measurements indicate the formation of an increasingly disordered monolayer as a function of increasing tail group polarity. For the mixed monolayer systems, the time dependence of the radial distribution function as well as average and maximum cluster size measurements indicate that phase separation takes place between components of sufficiently different tail group polarity and that this is accompanied by a phase transition into a more disordered phase. Further, the extent of surfactant segregation and their tendency to remix upon monolayer compression can be tuned by altering the degree of polarity of the hydrophobic chains. It is proposed that this is a simple and useful approach to predict the phase behavior and

spatial distribution of surfactants in mixed hydrogenated and semi- or perfluorinated surfactant monolayer systems.

6.4.2 Introduction

Mixed monolayer films of surfactants at the air-water interface are invaluable systems for probing numerous important physical and chemical phenomena, ranging from phase-separation and intermolecular interactions, to dynamics of surface processes and a host of others. The spatial distribution and organization of surfactants in mixed films is a key area of interest, in part because mixed monolayers (and bilayers) are excellent, albeit highly simplified model systems for biological membranes, which exhibit complex spatial distribution of surface active species. Significant efforts have been made to understand and control factors that regulate intermolecular interactions between film components in complex mixed films, though many of these factors are still poorly understood.

Our research group and others are particularly interested in understanding factors that regulate the organization and distribution of surfactants in mixed monolayers comprised of hydrogenated and semi- or perfluorinated surfactants at the air-water interface.[1-4] Interest in these mixtures is substantial because of their potential applications for industrial and biomedical applications, including, for example, their use as fire-fighting foams in the former and for pulmonary lung surfactant mixtures in the latter.[5,6] Mixed monolayer films of fluorinated and hydrogenated surfactants (most commonly mixtures of fluorinated fatty acids with hydrogenated fatty acids or phospholipids) are often heterogeneous, with the intrinsic lipophobicity of the fluorinated surfactant contributing significantly to this effect (see the works by Kimura et al. and Kraft et al.[7,8] for overviews of this topic). However, a variety of additional intermolecular interactions also influence the spatial distribution of film constituents; for example, the influence

of hydrophobic-lipophobic interactions between surfactant tail groups are a strong function of surface pressure of the monolayer, as is the electrostatic interaction between head groups. The latter can also be heavily modulated by binding of ions (including protons) present in the underlying aqueous subphase. Structures of phase-separated domains in surfactant monolayer films and the intermolecular interactions which regulate them have been reviewed in detail by McConnell.[9] In general, structures are controlled by competition between dipole-dipole interactions of polar (or charged) head-groups which tend to favor formation of extended structures, and line tension, which favors round, compact domains with minimal interfacial area. In addition to these factors, structures of mixed hydrocarbon-perfluorocarbon films which exhibit phase-separation are also affected by kinetic factors (e.g. kinetically trapped structures have been observed for these systems).[10] As a consequence of these factors, a diverse range of surfactant distributions for mixed monolayer film structures have been reported in the literature, ranging from completely phase-separated domains of various geometries and sizes, to intimate mixtures of the film components.

The development of a simple, minimal model for predicting the spatial distribution of surfactants based on the chemical identity and the composition of the film constituents is important but challenging research goal because of the combination of effects which contribute to the final surfactant distribution. As an initial step towards this, we wish to explore the influence of one readily identifiable and isolatable parameter, the polarity of the surfactant tail group, on surfactant distribution through the use of molecular dynamics (MD) simulations. MD simulations have proven to be a useful computational approach for investigating various properties of lipid monolayers (see the work by Nielsen et al.[11] and others[12-13], for example). The traditional methodology employed to simulate lipid systems is based on an atomistic

approach,[14,15] with every atom in the system represented as a point mass and interactions between atoms described by a simple empirical potential function or force field. While useful, these simulations are computationally expensive and are typically limited to a time scale of tens of nanoseconds, which is often insufficient to explore important phenomena in complex surfactant systems. To overcome these limitations, coarse-grained (CG) force fields have been developed.[16-19] The general strategy used with CG force fields is to represent approximately four, non-hydrogen, heavy atoms by single super-sites (a CG bead), with CG beads interacting through a simple potential function. In addition to the reduced number of degrees of freedom, the simplified interactions make CG MD attractive for studying larger time-scale processes often seen in biological and surface phenomena. In particular, the MARTINI CG force field[18,19] has proven to be especially useful, and has been used to study the microsecond time-scale behavior of lipid systems. A detailed description for the MARTINI force field used in this study is presented in the Methods section.

In this study, MARTINI-based MD simulations have been used to study the effect of surfactant tail polarity on the phase behavior of single component and mixed Langmuir monolayers. As a simple model system, monolayer films comprised of either pure dipalmitoylphosphatidylcholine (DPPC; chemical structure and the corresponding CG model representation are shown in Figure 6-1) or mixtures of two “variants" DPPC, each with different tail polarity, have been examined. DPPC has been chosen because MARTINI force field calculations yielded surface pressure-area isotherms (π-A) in reasonable agreement with experimental measurements.[20] Results indicated that the single component monolayers became more expanded and disordered as the tail group polarity was increased and phase separation in mixed monolayer films was a function of polarity differences between surfactant tail groups. To

the best of our knowledge, this is the first report that systematically explores the impact of tail polarity on surfactant miscibility in mixed monolayer systems using MARTINI force field.

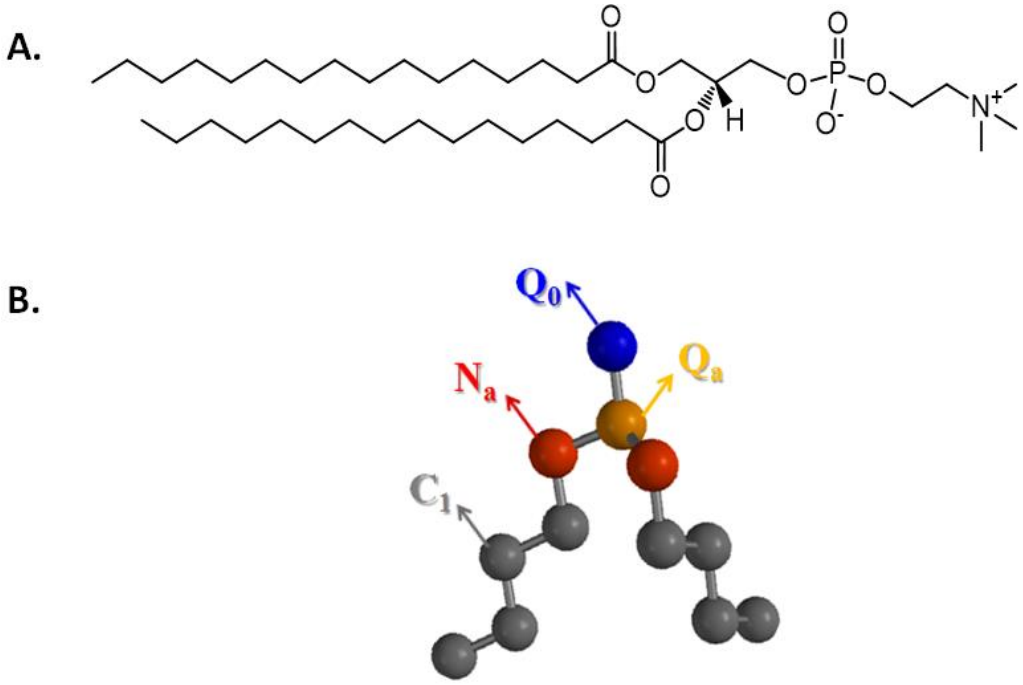

Figure 6-1 Schematic representation of DPPC molecule in A: atomistic and B: Coarse grain models. (Q_0, Q_a, N_a and C_1 correspond to the MARTINI bead types of DPPC).

6.4.3 Methods

6.4.3.1 MARTINI Coarse-Grained Force Field

The MARTINI force field is a biomolecular CG simulation model developed by Marrink and co-workers.[18,19] In the MARTINI CG force field, there are only four main types of interaction sites, referred to as polar (P), nonpolar (N), apolar (C), and charged (Q). Each particle type has a number of subtypes that are either distinguished by a letter denoting the hydrogen-bonding capabilities (d = donor, a = acceptor, da = both and 0 = none), or by a number indicating the degree of polarity starting from 1 (low polarity) to 5 (high polarity). These subtypes allow fine-tuning of interactions on the basis of the chemical nature of the atoms.[19] DPPC is represented by a positively charged choline ($N(CH_{3)3}^{+}$), negatively charged phosphate (PO_4^{-}),

non-polar glycerol and apolar hydrocarbon tail groups. The MARTINI force field classifications of these groups are Q_0, Q_a, Na and C1, respectively. The CG representation of the DPPC molecule is shown in Figure 6-1B.

Bonded interactions between groups are described by a sum of bond stretching and anglepotentials that are described by weak harmonic potentials. Non-bonded interactions are described by sum of Lennard-Jones (LJ) and Coulomb potential functions given by[19]

$$V_{nb} = 4\varepsilon_{ij}[(\frac{\sigma_{ij}}{r_{ij}})^{12} - (\frac{\sigma_{ij}}{r_{ij}})^{6}] + \frac{q_i q_j}{4\pi\varepsilon_o\varepsilon_r r_{ij}} \qquad (6.1)$$

in which σ_{ij} is the closest distance of approach between bead *i* and *j*, ε_{ij} is the strength of their interaction, r_{ij} is distance between bead *i* and *j*, ε_o is the dielectric constant in vacuum and ε_r is the relative dielectric constant. Here, q_i and q_j are charges carried by bead *i* and *j*, respectively. Generally, MARTINI force field defines ten levels (0 - 9) of LJ interactions between the beads based on their chemical identity. The strength of each level is determined by the value of ε_{ij}. The most polar interactions of compounds in the solid state at room temperature are described by level I, corresponds to strong polar interactions as in bulk water. More volatile liquids are described by level II and III and the nonpolar interactions in aliphatic chains are described by level IV. Various degrees of hydrophobic repulsion between polar and nonpolar phases are described by levels V-VIII. The interaction between charged particles and a very apolar medium is described by level IX. Strengths of LJ interactions between CG sites in DPPC-water system are listed in Table 6-1. Furthermore, the value of the ε_{ij} respect to each level is given in Table 6-2.

Table 6-1. The level of interactions between the different polarity C_n beads, head group beads and water beads (each four water molecules are represented by one CG bead (P_4 type).[19]

	P_4	Q_0	Q_a	N_a	C_1	C_2	C_3	C_4	C_5
P_4	I	O	O	III	VIII	VII	VI	VI	V
Q_0	O	IV	II	III	IX	IX	VII	VI	V
Q_a	O	II	III	III	IX	IX	VII	VI	V
N_a	II	III	III	III	VI	VI	VI	V	VI
C_1	VIII	IX	IX	VI	IV	IV	IV	V	V
C_2	VII	IX	IX	VI	IV	IV	IV	V	V
C_3	VI	VII	VII	VI	IV	IV	IV	IV	IV
C_4	VI	VI	VI	V	V	V	IV	IV	IV
C_5	V	V	V	IV	V	V	IV	IV	IV

Table 6-2 The interaction strength (ε) of the C_n-DPPC interaction levels.[19]

Interaction Level	O	I	II	III	IV	V	VI	VII	VIII	IX
ε (kJ/mol)	5.6	5.0	4.5	4.0	3.5	3.1	2.7	2.3	2.0	2.0

6.4.3.2 Molecular Dynamics Simulation Details

The DPPC-water system consists of two DPPC monolayers (256 molecules in each layer) separated by a water slab between the head groups. The simulation box is expanded to 25 nm in the direction normal to the water-DPPC interfaces in order to create a vacuum region in both DPPC tail regions. These vacuum regions prevent the interaction between DPPC hydrocarbon chains in different monolayers when periodic boundary conditions are applied.

The MARTINI 2.1 CG force field[18,19] was used to model the DPPC monolayers-water system. All MD simulations were performedusing the Gromacs 4.0.5 software package[21,22] with a time step of 30 fs. All non-bonded interactions were treated using the standard shiftfunction of Gromacs with a cut-off distance of 1.2 nm. The temperature during simulation was kept constant at 298.15 K by Berendsen thermostat. Surface tension coupling was applied by using the Berendsen pressure coupling algorithm in Gromacs.[22] In this case, surface tension applied to the x/y-plane (parallel to the bilayer surface) and the z component (parallel to the membrane normal)

of the pressure is coupled to a pressure bath. Periodic boundary conditions were applied in all directions.

To remove unfavorable contacts between beads, the initial structure of the DPPC-water system was first relaxed by energy minimization, followed by a 1 μs equilibration run with a negative surface tension of 50 mN/m to create a highly ordered monolayer system as a starting configuration. The trajectory at the end of the equilibration was then used to performed MD simulations with zero surface tension for 1 μs. A final trajectory was then used to performed another 1 μs simulation at a surface tension of 10 mN/m. This was repeated up to the largest surface tension value that maintains a stable simulation box. After that, the surface tension values were decreased back to zero. This process, namely cycling CG MD simulation, was repeated for DPPC monolayers with other tail polarity beads (C_2, C_3, C_4 and C_5). This methodology was repeated again for 3:1 mixtures of C_1-C_2, C_1-C_3, C_1-C_4 and C_1-C_5 mixed monolayers.

6.4.4 Results and Discussion

6.4.4.1 Single Component Monolayers

Figure 6-2 shows π-*A* expansion-compression isotherms of C_n-DPPC monolayers that weregenerated by a cycling CG MD simulation at 25°C from an initially ordered configuration as described previously. The calculated isotherm for DPPC (or C_1-DPPC) was consistent with that reported previously by Duncan et.al.[20] In comparison with the experimentally measured isotherms reported elsewhere in the literature,[23,24] the simulated isotherm was shifted to higher pressures, and the LE-LC coexistence region (the red plateau in Figure 6-2A) took place over a smaller range of mean molecular areas. This difference between the computational and experimental results might be explained by the lower number of degrees of freedom adopted by MARTINI force field, since four heavy atoms were grouped into a single interaction center.[19] In

general, the comparison between simulated and experimentally generated isotherms is not common in the literature. Simulated isotherms can be affected by the selection of force field parameters,[25] while the experimentally measured isotherms are constructed under different conditions which would result in a large variation between these isotherms. As shown in Figure 6-2 (A-D), the area per molecule in the highly ordered monolayers increased as the surface pressure was decreased. This took place until a substantial change in the monolayer area occurred, described here by a phase transition from a highly ordered to disordered monolayer. The surface pressure continued to increase until reaching the largest possible value that maintain a stable simulation box, after which the process is reversed, with the system reaching a surface pressure of ~ 72 mN/m. The expansion-compression isotherms of the higher polarity DPPC monolayers (Figure 6-2 (B-E)) were shifted to higher surface pressure as the polarity designation changed from C_2 to C_5. In addition, the LE-LC phase transitions of the compression isotherms disappeared completely for C_3, C_4 and C_5 systems and the isotherms of both C_3 and C_4-DPPC monolayers were superimposed.

As shown in Table 6-1 and Table 6-2, the level of interaction between C_n beads is equal, i.e., the interaction between C_1-C_1 is the same as C_2-C_2, etc. Therefore, the interaction between C_n and (N_a, Q_a and Q_0) beads governs the phase behavior of the C_n-DPPC monolayers. For each polarity level, both Q_0 and Q_a has the same level of interaction with each C_n bead, they interact more favorably with higher polarity C_n beads and they are more repulsive than C_n-N_a interactions. This suggests lower cohesion forces within the high polarity monolayers, and disordered monolayers were expected at higher surface pressures as the C_n beads became more polar.

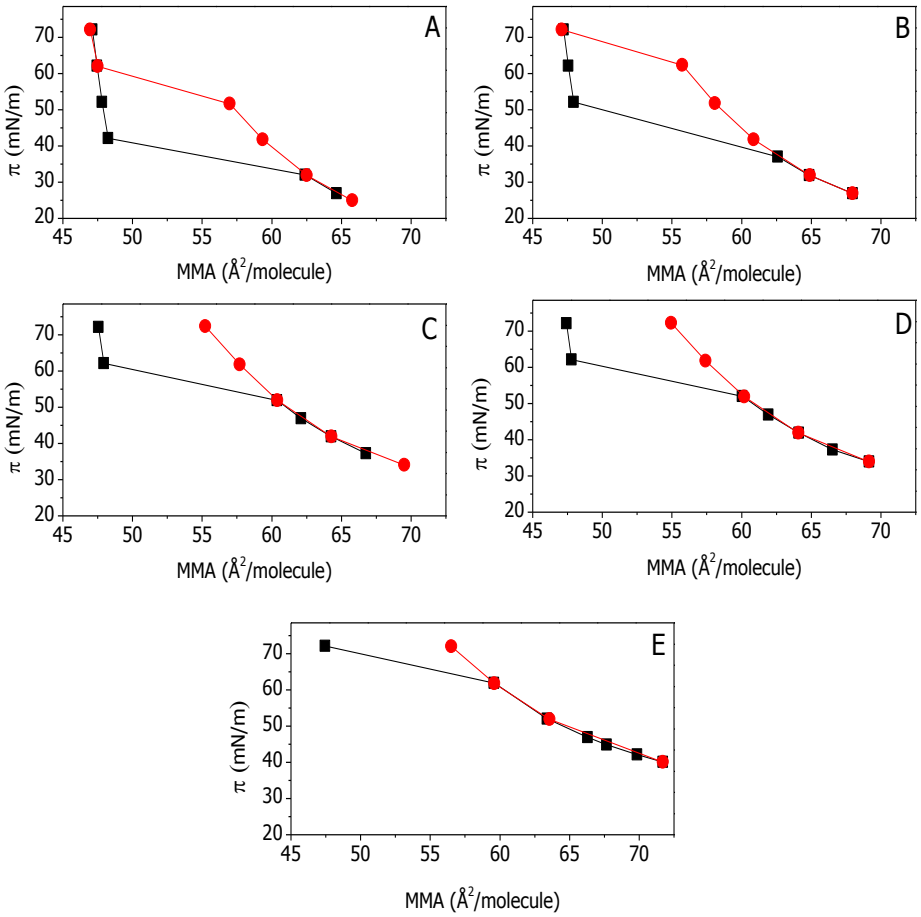

Figure 6-2 Surface pressure-area, expansion (black) – compression (red) isotherms of, A: C_1-DPPC, B: C_2-DPPC, C: C_3-DPPC, D: C_4-DPPC and E: C_5-DPPC generated by CG simulation at 25°C.

The disappearance of the LE-LC phase transition (the compression isotherm of C_3, C_4 and C_5) might be explained by the lower van der Waals forces between the C_n bead as the polarity is increased. This is consistent with the behavior of simple long chain amphiphilic compounds, where the reduction in the van der Waals forces between the hydrophobic chains (either for shorter hydrophobic chain or at higher temperature) causes the formation of highly condensed films which shorten and shift the LE-LC phase transition to a higher surface pressure.[26] This agreed with the experimental results reported by Toimil et al.[27] They reported that the LE-LC coexistence region was shifted upwards for mono-fluorinated DPPC (an example of high polarity species) compared to the fully hydrogenated phospholipid.

In order to investigate the onset of the phase transition upon monolayer expansion, radial distribution functions (RDFs) of C_n-DPPC monolayers have been calculated from the centers of mass of different polarity DPPC molecules at different surface pressure by averaging over 1 μs of the simulation time. The RDF, $g_{nAB}(r)$, between particles of type A and B is defined by[22]

$$g_{nAB}(r) = V \sum_{i \in A}^{N_A} \sum_{i \in B}^{N_B} P(r) \qquad (6.2)$$

in which *V* is the system volume and *P(r)* is the probability of finding an atom of type *B* at distance *r* from a type *A* atom. Figure 6-3 shows the RDF's of C_n-DPPC – C_n-DPPC i at different surface pressures. Herein, at π = 72 mN/m, all films consisted of a highly-ordered monolayer with a sharp peak at 0.5 nm followed by a second peak with lower intensity at 1 nm. Duncan et.al[28] has calculated RDFs for DPPC- palmitoyloleoylphosphatidylcholine mixed monolayers, and reported similarly-shaped functions. It appears that these peaks are characteristic of lipid monolayers regardless of the degree of surfactant polarity. Upon monolayer expansion (Figure 6-3B), the RDF of C_5-DPPC film showed a rapid decay in the lateral order within about 1.5 nm. This indicated a disordered film structure at lower surface pressures. This agreed with the phase transition exhibited by the π-*A* expansion isotherm of the C_5-DPPC monolayer (π = 62 mN/m). At this point, the RDF's for the other monolayer films showed no appreciable change in the peak positions and intensities with decreasing the surface pressure. Further film expansion (Figure 6-3C) led to a decay of all higher-order peaks of the RDF's of C_3 and C_4-DPPC monolayers, similarl to C_5-DPPC at π = 62 mN/m. This revealed the significant influence of the surface pressure on the lateral distribution of the C_n-DPPC molecules and coincided with the phase transition that already shown by expansion isotherms at π = 52 mN/m for both C_3 and C_4-DPPC films. The decay of the fine structure of the RDF of C_2-DPPC monolayer expanded at π =

42 mN/m (Figure 6-3D), indicated the formation of disordered and loosely packed C_2-DPPC monolayer. Further, the decay in the RDF of C_n-DPPC monolayer films suggested the formation of loosely packed surfactant film upon monolayer expansion is a function of both surface pressure and tail polarity.

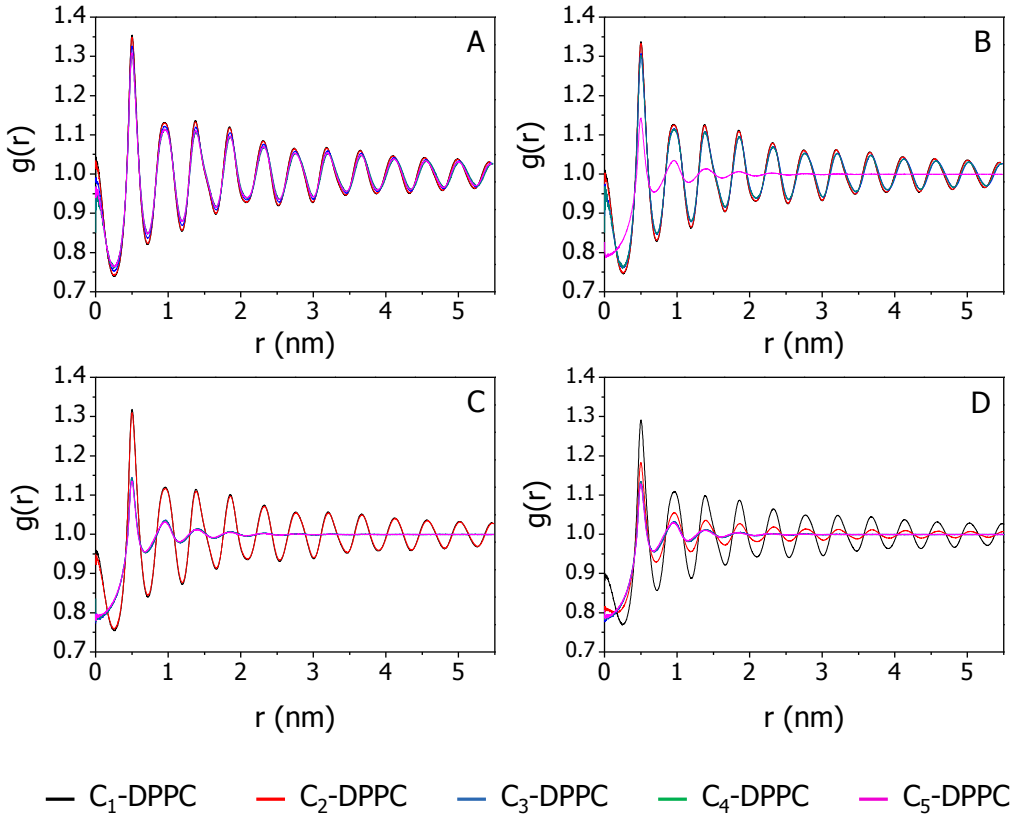

Figure 6-3 Radial distribution functions ($g(r)$) of C_n-DPPC – C_n-DPPC molecules generated by coarse grained simulation and averaged over 1 μs at A: π = 72 mN/m, B: π = 62 mN/m, C: π = 52 mN/m and D: π = 42 mN/m.

To gain more insight into the lateral ordering of monolayers comprised of surfactants with different polarities, tilt angle (defined by the angle between the surface normal and any two beads of C_n-DPPC molecule) for both N_a-C_n and C_n-C_n beads, namely head-tail (H-T) and tail-tail (T-T) respectively, was averaged over a 1 μs time interval and presented in Figure 6-4.

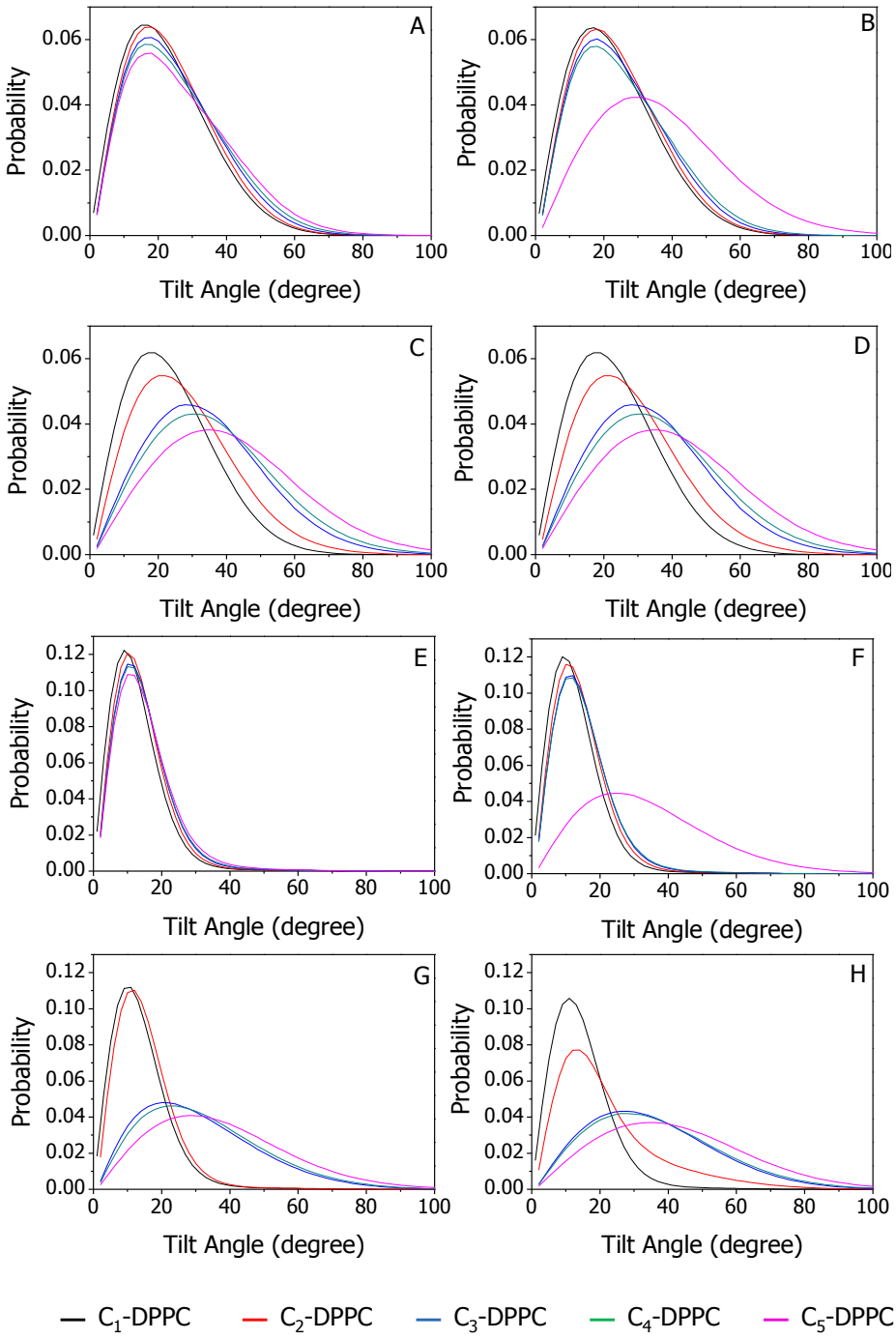

Figure 6-4 Tilt angle distribution measured from π-*A* expansion isotherms of C_n-DPPC monolayers. (A-D): Head-Tail and (E-H): Tail-Tail tilt angle measured at: π = 72, 62, 52 and 42 mN/m respectively.

The H-T and T-T tilt angle distributions (Figure 6-4 (A and E)) showed that C_n-DPPC molecules were almost vertically oriented to the surface film at π = 72 mN/m. The distributions of the T-T beads were much narrower compared to the H-T beads. This might be explained by

the more favorable interaction between the glycerol and water beads (N_a-P_4) compared to C_n- N_a. The former represents the polar interaction between the interacting sites, while the later indicates either a nonpolar interaction within aliphatic chains or various degrees of hydrophobic repulsion between polar and nonpolar phases.[19] These data were consistent with X-ray measurements reported by Ma and Allen[29] that indicated C_1-DPPC molecules tend to be tilted by 25° with respect to the surface normal to compensate the head-tail area mismatch (50 $Å^2$/molecule for the head group and 38 $Å^2$/molecule for the tail). These distributions became broader and shifted to larger tilt angles as the surface pressure was decreased. This indicated that the surfactant film underwent a transition to a disordered configuration upon monolayer expansion. This took place at π = 62, 52 and 42 mN/m for C_5, (C_4 and C_3) and C_2-DPPC monolayers, respectively. This was consistent with the results of π-*A* expansion isotherms and RDF calculations.

6.4.4.2 Mixed Monolayers

π-*A* expansion-compression isotherms for a series of mixed 3:1 C_1-C_n DPPC films are shown in Figure 6-5. The incorporation of C_2 and C_3-DPPC species into C_1-DPPC monolayer did not result in a significant change in the expansion-compression behavior in comparison to that of C1-DPPC isotherm (Figure 6-2A). This can be explained by the identical level of interaction between the tail beads (both C_1-C_2 and C_1-C_3) and between the C_1, C_2, C_3 and the glycerol beads.

A further increase in the tail polarity, i.e. going for C_4 and C_5 beads, caused the isotherms to shift markedly upwards in comparison to that of C_1-DPPC and resulted in smaller hysteresis loops. This agrees with the results reported by Shibata and co-workers who's measurements indicated that the LE-LC phase transition of C_1-DPPC monolayer was shifted to a higher surface pressure after incorporating (perfluorooctyl)pentanol.[3] The similarity between the isotherms of C_1-C_2 and C_1-C_3 and that of C_1-DPPC monolayer might indicate an ideal mixing behaviour with

the aforementioned mixed monolayer. However, the upward shift in the C_1-C_4 and C_1-C_5 isotherms might reveal a non-ideal mixing between both C_4 and C_5 with C_1 species.

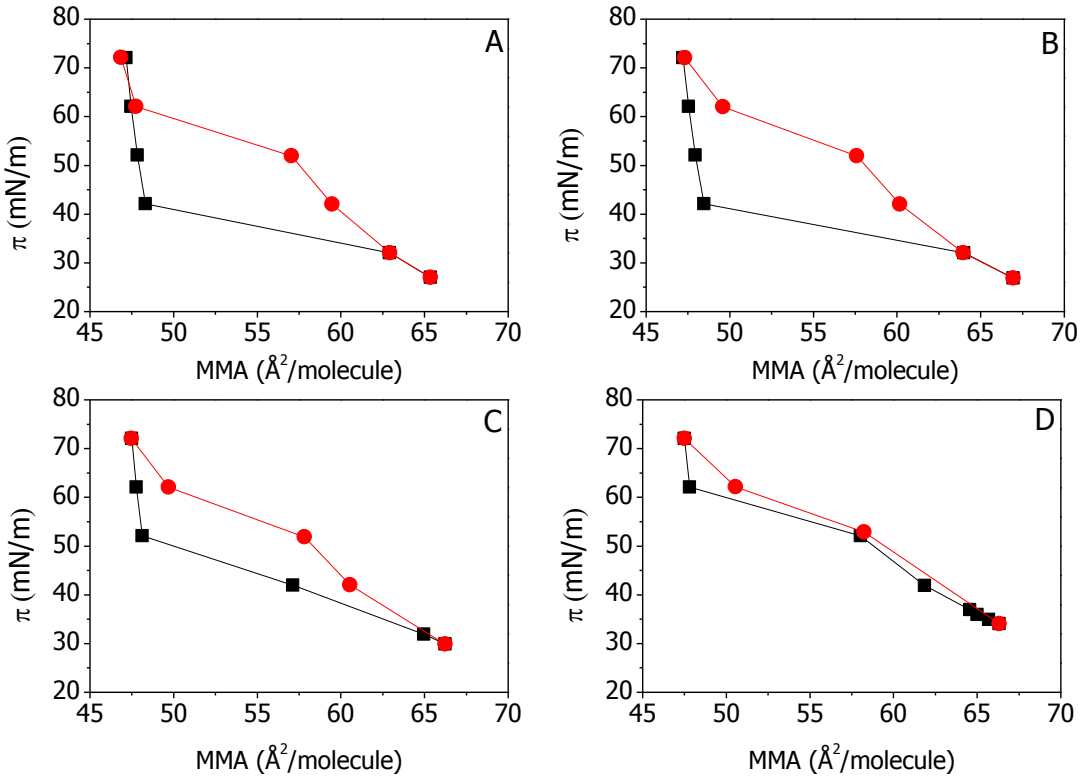

Figure 6-5 Surface pressure-area expansion (black) – compression (red) isotherms of 3:1 C_1-C_n mixed monolayers, A: C_1-C_2, B: C_1-C_3, C: C_1-C_4, D: C_1-C_5, generated by CG simulation at 25ºC for a system made of 256 molecules/monolayer.

To more closely characterize the degree of mixing and the spatial distribution of surfactants in the mixed monolayer system, we calculated the RDFs for C_1-C_n mixed systems between the centers of mass of C_n-C_n species as a function of time and surface pressures, before the occurrence of the phase transition during monolayer expansion. Results are presented in Figure 6-6. The RDF's of C_1-C_2 and C_1-C_3 mixed films (Figure 6-6 (A – D)) were time independent for both the highly compressed (π = 72 mN/m) and expanded (π = 42 mN/m) monolayers. This suggests either an intimate association or ideal mixing behavior within the C_1-C_2 and C_1-C_3 mixed monolayers.

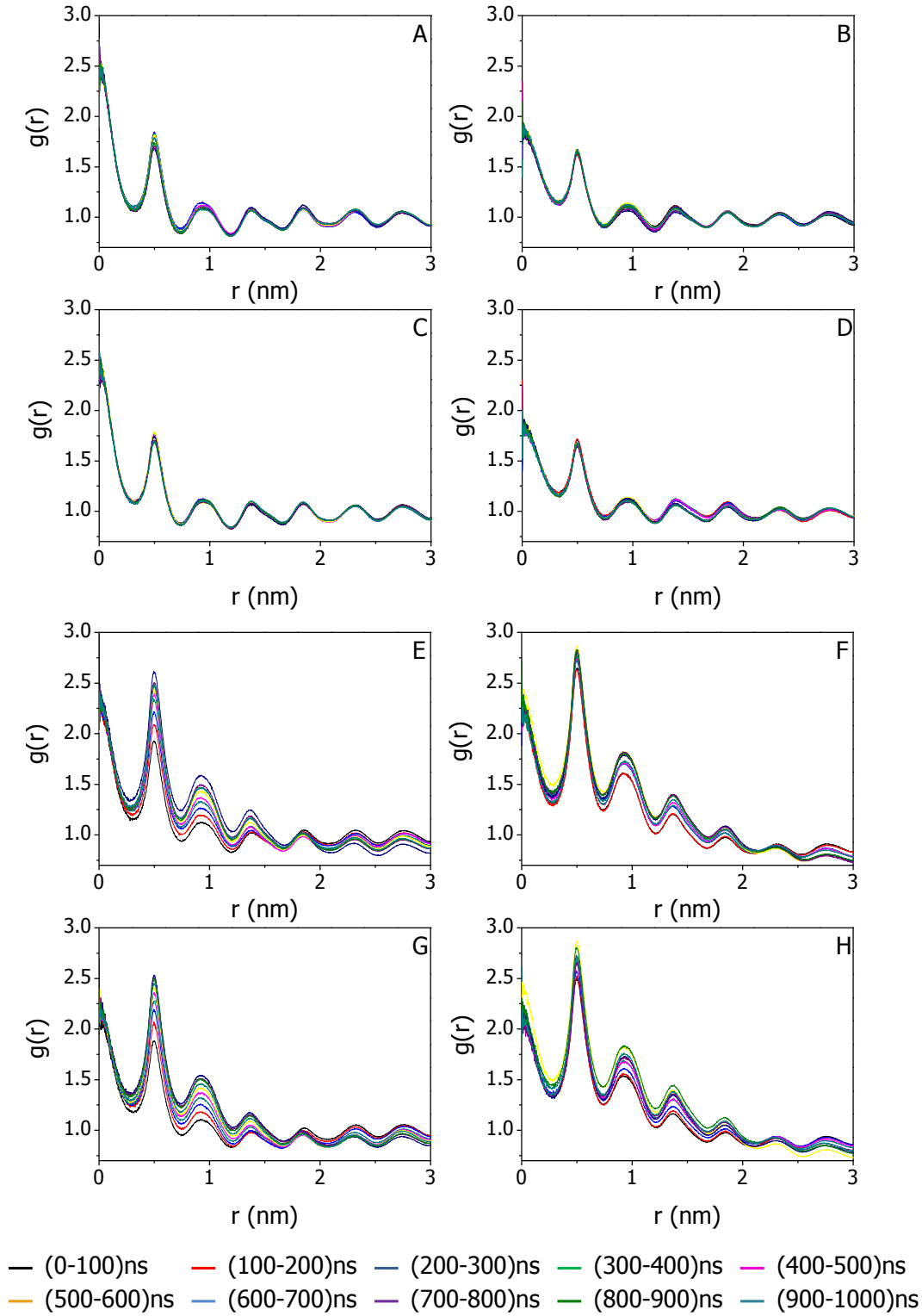

Figure 6-6 Radial distribution functions as a function of time for C_n-C_n species in 3:1 C_1-C_n DPPC mixed monolayers of the following C_n and surface pressure: (A and B): C_1-C_2, π = 72 and 42 mN/m respectively, (C and D): C_1-C_3, π = 72 and 42 mN/m respectively, (E and F): C_1-C_4, π = 72 and 62 mN/m respectively and (G and H): C_1-C_5, π = 72 and 42 mN/m respectively.

At π = 72 mN/m (Figure 6-6 (E and G)), the intensity of the RDF's of C_1-C_4 and C_1-C_5 mixtures increased as a function of time, indicating that the C_n-DPPC domains are highly dynamic on the time scale of the simulation. These domains tend to be surrounded preferentially by other molecules of the same kind with the progress of the time, which indicated that C_n molecules tend to segregate on the examined time scale. The crowding within the mixed lipid systems continued to decrease by lowering the surface pressure to 62 mN/m (Figure 6-6 (F and H)). Although the intensity of the RDFs for the C_1-C_4 and C_1-C_5 mixed systems didn't change significantly as noted before at π = 72 mN/m. The time dependency of the RDFs showed that the lipid molecules of the same kind continued to cluster with each other.

The time dependency of the RDF`s of C_4 and C_5 containing system implied that the C_n clusters grew as a function of time and surface pressure. To confirm this conclusion, we have calculated the average number of molecules per cluster, namely the average cluster sizes (ACS), of Cn species as a function of time and surface pressure in order to provide support for the RDF measurements. As presented in Figure 6-7 (A-D), ACS measurements for C_1-C_2 and C_1-C_3 mixed monolayers showed that Cn species tend to form small clusters (mostly trimers, tetramers and pentamers) for all of the investigated surface pressure values through the expansion-compression cycle. This agreed with the previously examined RDF measurements and provided evidence that both C_2 and C_3 species were either mixed ideally or were fully miscible with the C_1 molecules regardless of the surface pressure.

ACS measurements for C_1-C_4 and C_1-C_5 mixed monolayer showed cluster growth as a function of time and surface pressure. As shown in Figure 6-7 (E and G), at π = 72 mN/m, the ACS increased from 5 to 10 C_n molecules per cluster during the 100 ns to 1000 ns time interval

for both the C_1-C_4 and C_1-C_5 systems. A further decrease in the surface increased the ACS up to 15 molecules per cluster for both mixtures.

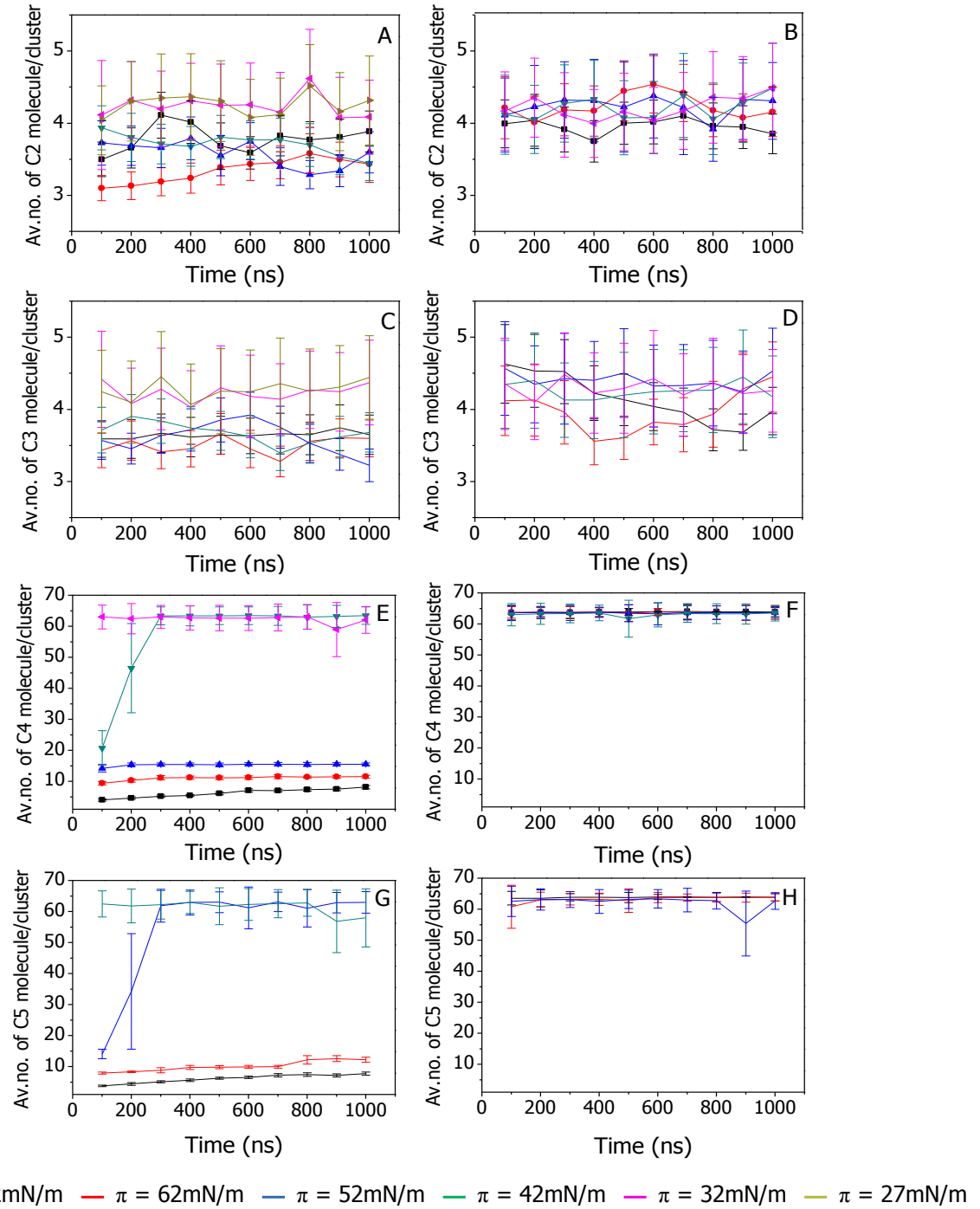

Figure 6-7 Average cluster size as a function of time and surface pressure of (A and B): 3-1 C_2-C_1, (C and D): C_3-C_1, (E and F): C_4-C_1, (G and H): C_5-C_1. The left and the right columns correspond to expansion and compression, respectively.

At π = 62 mN/m, which corresponds to the phase transition at the π-A expansion isotherm of the 3:1 C_1-C_5 mixed system, the ACS increased rapidly in the first 200 ns, to form one cluster made of 64 species. Similar behavior was noticed for the C_1-C_4 mixed system at π = 42 mN/m. These clusters were maintained during monolayer compression back to π = 72 mN/m (Figure 6-7 (F and H)).

Top views of the 3:1 C1-Cn DPPC monolayers illustrating the lateral distribution of the C_n molecules in the mixed monolayers at different surface pressures are shown in Figure 6-8.

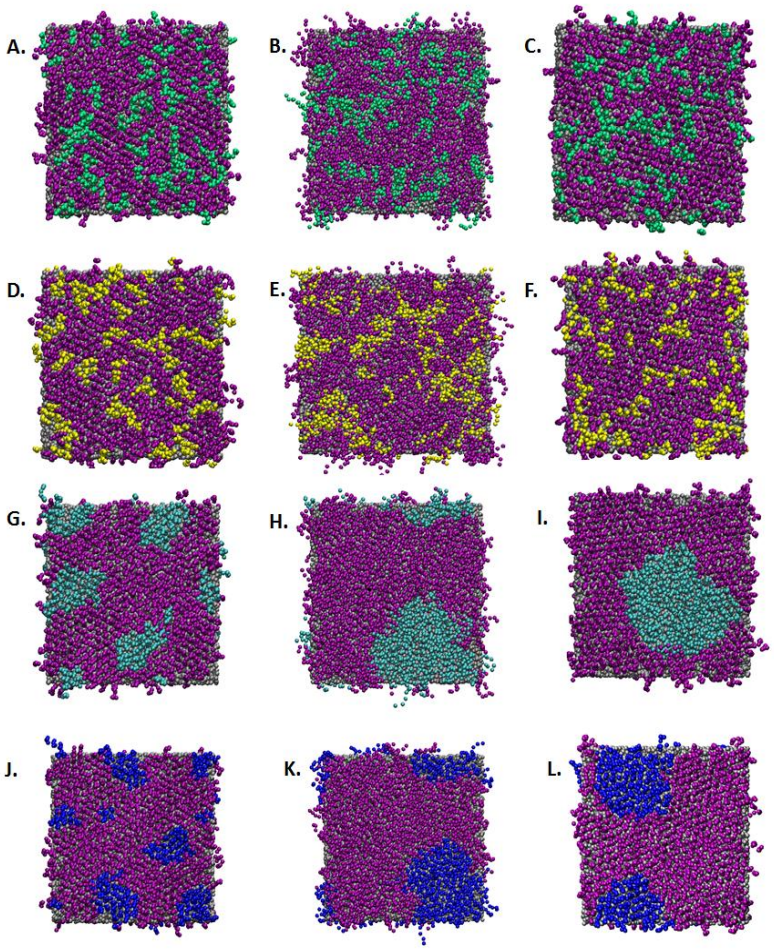

Figure 6-8 Top views of the lateral distribution for C_n-DPPC molecules in mixed monolayer made of: (A, B and C) C_2-C_1 mixed monolayer at π = 42, 32 (expansion) and 72 (compression) mN/m respectively. (D, E and F) C_3-C_1 mixed monolayer at π = 42, 32 (expansion) and 72 (compression) mN/m respectively. (G, H and I) C_4-C_1 mixed monolayer at π = 52, 42 (expansion) and 72 (compression) mN/m respectively. (J, K and L) C_5-C_1 mixed monolayer at π = 62, 52 (expansion) and 72 (compression) mN/m respectively.

The images in each row of Figure 6-8 shows the lateral structure of the mixed systems before and after the phase transition into the disordered monolayer during expansion in addition to the re-compressed structure at π = 72 mN/m. The structures of the C_1-C_2 and C_1-C_3 mixed monolayers (Figure 6-8 (A-F)) was the same both below and above the phase transition surface pressure, indicating that these systems are fully miscible, which is consistent with the ACS measurements. For the C_4 and C_5 containing systems, these molecules formed several clusters just before the appearance of the disordered configuration (Figure 6-8 (J and I)). The occurrence of the phase transition upon monolayer expansion induced the lateral phase separation as ended by the formation of one cluster composed of 64 molecules (Figure 6-8 (H and K)). It seems the phase separated structures were thermodynamically stable since they persisted even after compressing the fully expanded monolayer to π = 72 mN/m (Figure 6-8 (I and L)).

The importance of this study is that it provided a simple approach to understand surfactant miscibility in mixed monolayers made of surfactants with different tail polarities such as semi or perfluorinated amphiphiles with hydrogenated surfactants (fatty acids or phospholipid). The miscibility of such systems has been investigated extensively using Langmuir and Langmuir-Blodgett (LB) monolayers.[23,30-39] It has been demonstrated that surfactant miscibility in these systems was highly dependent of the subphase conditions that may modulate surfactant head-head interaction, thereby contributes more significantly to surfactant miscibility than surfactant tails interactions.

6.4.5 Conclusions

It has been demonstrated that the lateral organization of C_n species in mixed C_1-C_n monolayers was a function of both tail polarity and surface pressure. The components of these mixed systems were found to be increasingly immiscible as the difference in the tail polarities

between surfactant molecules is increased in the expanded monolayers. Moreover, it has been shown that increasing the tail polarity shifts the LE-LC coexistence region to a higher surface pressure. This has been examined by the π-*A* compression-expansion isotherms, the RDF`s measurements as a function of time and the average cluster size calculations.

This study provided a potentially useful approach to predict the phase behavior and the lateral distribution of mixed monolayers made of amphiphilic molecules with different tail polarities such as hydrogenated and semi or perfluorinated fluorinated mixed films.

6.4.6 Acknowledgments

Funding for this work was provided by the Natural Sciences and Engineering Research Council of Canada (NSERC), the Canada Foundation for Innovation (CFI). All computations were performed using computing resources provided by WestGrid (www.westgrid.ca) and Compute/ Calcul Canada.

6.4.7 References

1. Broniatowski, M.; Dynarowicz-Latka, P. Interactions of a fluoroaryl surfactant with hydrogenated, partially fluorinated, and perfluorinated surfactants at the air/water interface. *Langmuir* **2006**, *22*, 6622-6628.

2. Matsumoto, M.; Watanabe, S.; Tanaka, K.; Kimura, H.; Kasahara, M.; Shibata, H.; Azumi, R.; Sakai, H.; Abe, M.; Kondo, Y.; Yoshino, N. Control of two-dimensional nanopatterns by adjusting intermolecular interactions. *Adv Mater* **2007**, *19*, 3668-+.

3. Nakahara, H.; Lee, S.; Krafft, M. P.; Shibata, O. Fluorocarbon-Hybrid Pulmonary Surfactants for Replacement Therapy - A Langmuir Mono layer Study. *Langmuir* **2010**, *26*, 18256-18265.

4. Qaqish, S. E.; Paige, M. F. Structural and compositional mapping of a phase-separated Langmuir-Blodgett monolayer by atomic force microscopy. *Langmuir* **2007**, *23*, 2582-2587.

5. Kissa, E., Ed.; In *Fluorinated Surfactants and Repellents, Second Edition;* Surfactant Science Series; Marcel Dekker, Inc.: New York, USA, 2001; Vol. 79.

6. Krafft, M. P. Large Organized Surface Domains Self-Assembled from Nonpolar Amphiphiles. *Acc. Chem. Res.* **2012**, *45*, 514-524.

7. Kimura, H.; Watanabe, S.; Shibata, H.; Azumi, R.; Sakai, H.; Abe, M.; Matsumoto, M. Phase-Separated Structures of Mixed Langmuir-Blodgett Films of Fatty Acid and Hybrid Carboxylic Acid. *J Phys Chem B* **2008**, *112*, 15313-15319.

8. Krafft, M. P.; Riess, J. G. Chemistry, Physical Chemistry, and Uses of Molecular Fluorocarbon-Hydrocarbon Diblocks, Triblocks, and Related Compounds-Unique "Apblar" Components for Self-Assembled Colloid and Interface Engineering. *Chem. Rev.* **2009**, *109*, 1714-1792.

9. McConnell, H. Structures and Transitions in Lipid Monolayers at the Air-Water-Interface. *Annu. Rev. Phys. Chem.* **1991**, *42*, 171-195.

10. Qaqish, S. E.; Paige, M. F. Characterization of domain growth kinetics in a mixed perfluorocarbon-hydrocarbon Langmuir-Blodgett monolayer. *J. Colloid Interface Sci.* **2008**, *325*, 290-293.

11. Nielsen, S.; Lopez, C.; Moore, P.; Shelley, J.; Klein, M. Molecular dynamics investigations of lipid Langmuir monolayers using a coarse-grain model. *J Phys Chem B* **2003**, *107*, 13911-13917.

12. Baoukina, S.; Monticelli, L.; Marrink, S. J.; Tieleman, D. P. Pressure-area isotherm of a lipid monolayer from molecular dynamics simulations. *Langmuir* **2007**, *23*, 12617-12623.

13. Rose, D.; Rendell, J.; Lee, D.; Nag, K.; Booth, V. Molecular dynamics simulations of lung surfactant lipid monolayers. *Biophys. Chem.* **2008**, *138*, 67-77.

14. Feller, S. Molecular dynamics simulations of lipid bilayers. *Current Opinion in Colloid & Interface Science* **2000**, *5*, 217-223.

15. Scott, H. Modeling the lipid component of membranes. *Curr. Opin. Struct. Biol.* **2002**, *12*, 495-502.

16. Shelley, J.; Shelley, M. Computer simulation of surfactant solutions. *Current Opinion in Colloid & Interface Science* **2000**, *5*, 101-110.

17. Muller, M.; Katsov, K.; Schick, M. Coarse-grained models and collective phenomena in membranes: Computer simulation of membrane fusion. *Journal of Polymer Science Part B-Polymer Physics* **2003**, *41*, 1441-1450.

18. Marrink, S.; de Vries, A.; Mark, A. Coarse grained model for semiquantitative lipid simulations. *J Phys Chem B* **2004**, *108*, 750-760.

19. Marrink, S. J.; Risselada, H. J.; Yefimov, S.; Tieleman, D. P.; de Vries, A. H. The MARTINI force field: Coarse grained model for biomolecular simulations. *J Phys Chem B* **2007**, *111*, 7812-7824.

20. Duncan, S. L.; Larson, R. G. Comparing experimental and simulated pressure-area isotherms for DPPC. *Biophys. J.* **2008**, *94*, 2965-2986.

21. Berendsen, H.; Vanderspoel, D.; Vandrunen, R. Gromacs - a Message-Passing Parallel Molecular-Dynamics Implementation. *Comput. Phys. Commun.* **1995**, *91*, 43-56.

22. Van der Spoel, D.; Lindahl, E.; Hess, B.; Van Buuren, A. R.; Apol, E.; Meulenho Gromacs User Manual, Version 4.5.4. **2010**.

23. Eftaiha, A. F.; Brunet, S. M. K.; Paige, M. F. Influence of Film Composition on the Morphology, Mechanical Properties, and Surfactant Recovery of Phase-Separated Phospholipid-Perfluorinated Fatty Acid Mixed Monolayers. *Langmuir* **2012**.

24. Eftaiha, A. F.; Brunet, S. M. K.; Paige, M. F. Thermodynamic and structural characterization of a mixed perfluorocarbon-phospholipid ternary monolayer surfactant system. *J. Colloid Interface Sci.* **2012**, *368*, 356-365.

25. Mohammad-Aghaie, D.; Mace, E.; Sennoga, C. A.; Seddon, J. M.; Bresme, F. Molecular Dynamics Simulations of Liquid Condensed to Liquid Expanded Transitions in DPPC Monolayers. *J Phys Chem B* **2010**, *114*, 1325-1335.

26. Petty, M. C. *Langmuir-Blodgett Films: An Introduction;* Cambridge University Press: New York, USA, 1996.

27. Toimil, P.; Prieto, G.; Minones, J., Jr.; Sarmiento, F. A comparative study of F-DPPC/DPPC mixed monolayers. Influence of subphase temperature on F-DPPC and DPPC monolayers. *Physical Chemistry Chemical Physics* **2010**, *12*, 13323-13332.

28. Duncan, S. L.; Dalal, I. S.; Larson, R. G. Molecular dynamics simulation of phase transitions in model lung surfactant monolayers. *Biochimica Et Biophysica Acta-Biomembranes* **2011**, *1808*, 2450-2465.

29. Ma, G.; Allen, H. C. DPPC Langmuir monolayer at the air-water interface: Probing the tail and head groups by vibrational sum frequency generation spectroscopy. *Langmuir* **2006**, *22*, 5341-5349.

30. Shibata, O.; Yamamoto, S.; Lee, S.; Sugihara, G. Mixed monolayer properties of tetradecanoic acid with n-perfluorocarboxylic acids with 10, 12, 14, 16, and 18 carbon atoms. *J. Colloid Interface Sci.* **1996**, *184*, 201-208.

31. Imae, T.; Takeshita, T.; Kato, M. Phase separation in hybrid Langmuir-Blodgett films of perfluorinated and hydrogenated amphiphiles. Examination by atomic force microscopy. *Langmuir* **2000**, *16*, 612-621.

32. Qaqish, S. E.; Paige, M. F. Mechanistic insight into domain formation and growth in a phase-separated langmuir-blodgett monolayer. *Langmuir* **2007**, *23*, 10088-10094.

33. Qaqish, S. E.; Urquhart, S. G.; Lanke, U.; Brunet, S. M. K.; Paige, M. F. Phase Separation of Palmitic Acid and Perfluorooctadecanoic Acid in Mixed Langmuir-Blodgett Monolayer Films. *Langmuir* **2009**, *25*, 7401-7409.

34. Eftaiha, A. F.; Paige, M. F. Phase-separation of mixed surfactant monolayers: A comparison of film morphology at the solid-air and liquid-air interfaces. *J. Colloid Interface Sci.* **2012**, *380*, 105-112.

35. Yokoyama, H.; Nakahara, H.; Nakagawa, T.; Shimono, S.; Sueishi, K.; Shibata, O. Miscibility behavior of two-component monolayers at the air-water interface: Perfluorocarboxylic acids and DMPE. *J. Colloid Interface Sci.* **2009**, *337*, 191-200.

36. Yokoyama, H.; Nakahara, H.; Shibata, O. Miscibility and phase behavior of DPPG and perfluorocarboxylic acids at the air-water interface. *Chem. Phys. Lipids* **2009**, *161*, 103-114.

37. Nakahara, H.; Nakamura, S.; Kawasaki, H.; Shibata, O. Properties of two-component Langmuir monolayer of single chain perfluorinated carboxylic acids with dipalmitoylphosphatidylcholine (DPPC). *Colloids and Surfaces B-Biointerfaces* **2005**, *41*, 285-298.

38. Eftaiha, A. F.; Paige, M. F. The influence of salinity on surfactant miscibility in mixed dipalmitoylphosphatidylcholine-perfluorooctadecanoic acid monolayer films. *J Colloid Interface Sci* **2011**, *353*, 210-219.

39. Lehmler, H.; Bummer, P. Mixing of perfluorinated carboxylic acids with dipalmitoylphosphatidylcholine. *Biochimica Et Biophysica Acta-Biomembranes* **2004**, *1664*, 141-149.

CHAPTER 7 THE IMPACT OF AN α-HELICAL PEPTIDE ON THE INTERFACIAL BEHAVIOR OF DIPALMITOYLPHOSPHATIDYL-CHOLINE AT LOW PEPTIDE SURFACE CONCENTRATION

7.1 Description

This is an unpublished work that was carried out to study lipid-protein interactions between 1,2-dipalmitoyl-sn-glycero-3-phosphocholine (DPPC), the most abundant pulmonary surfactant (PS) phospholipids and the peptide Hel 13-5 (consisting of 12 leucine, 1 cystine and 5 lysine residues) that functionally mimics pulmonary surfactant protein. The surface behavior of the peptide containing monolayers was studied in Langmuir monolayers using a normal saline subphase (150 mM NaCl, pH 7.4) at the air-liquid interface. Surface thermodynamic parameters evaluated from the surface pressure-area isotherms (the additivity data and the excess Gibbs free energy values) indicated a repulsive interaction between the peptide and the DPPC. The morphology of mixed films, explored by Brewster angle microscopy (BAM) and confocal fluorescence microscopy (CFM), indicated that addition of peptide resulted in the fluidization of the phospholipid monolayer. This was further verified from the cyclic compression-expansion measurements that indicated addition of the peptide to DPPC resulted in improved surfactant recovery.

The experimental section for this study is provided in the manuscript. A detailed description of the techniques used is provided in Chapter 1.

7.2 Description of the Candidate's Contribution

For this contribution, I prepared the samples, performed the isotherms and Brewster angle microscopy measurements, played a major role in interpreting the results, wrote the initial draft of the work and participated in the subsequent editing in response to collaborators. Our collaborators Dr Jan Rainey and Marie Laurence-Tremblay (Dalhousie University) synthesized

the peptide, while Ken Thoms characterized the peptide via mass spectrometric methods. Dr. Matthew Paige carried out the confocal fluorescence microscopy measurements with the assistance of Mr Jason Maley, provided extensive guidance throughout the experimental work and was greatly involved in results interpretation, writing and editing the manuscript.

7.3 Relation of Contribution towards Research Objectives

This contribution was solely performed towards the objectives of the thesis research. As shown in the previous Chapter (2-4), we have examined the interaction of perfluorooctadecanoic acid (C18F) and DPPC with an ultimate view toward characterizing the potential utility of C18F as PS additive. The attractive interaction between C18F and DPPC led to formation of multimolecular aggregates that can be considered as surfactant reservoirs of potential importance to PS application. Using a highly simplified mimic fluid, C18F enhanced the recovery of DPPC films after repeated compression expansion cycles.

To assess the performance of C18F in comparison with Hel 13-5, as a pulmonary surfactant mimicking peptide, we have explored the interaction of Hel 13-5 and DPPC at air-water and air-solid interface. The result revealed that Hel 13-5 fluidized the phospholipid films and improved its re-spreading properties. A full discussion of the results of this study and its implications for the thesis research as a whole of is provided in Chapter 8.

The Impact of an α-Helical Peptide on the Interfacial Behavior of Dipalmitoylphosphatidylcholine at Low Peptide Surface Concentration

Ala'a F. Eftaiha[1], M-L. Tremblay[2], J. K. Rainey[2] and Matthew F. Paige[1]

[1]Department of Chemistry, University of Saskatchewan, 110 Science Place, Saskatoon, Saskatchewan, Canada, S7N 5C9

[2]Department of Biochemistry and Molecular Biology, Dalhousie University, Halifax, NS B3H 1X5

7.4.1 Abstract

Artificial PS formulations contain simplified peptides that fully or closely mimic the biophysical properties of endogenous surfactant proteins. These formulations can be superior to both animal-derived products and protein-free synthetic surfactants. Herein, Langmuir monolayers and Langmuir-Blodgett films have been used to examine the surface behavior and morphology of binary mixed films comprised of 1,2-dipalmitoyl-sn-glycero-3-phosphocholine (DPPC), the major component of endogenous lung surfactant, and an 18 amino acid amphiphilic α-helical peptide (Hel 13-5), a monomeric synthetic peptide that mimics surfactant protein B. The studies made use of a highly simplified lung fluid mimic subphase (pH 7.4, 150 mM NaCl). Surface pressure-area isotherm measurements of the mixed monolayers showed that the film forming components were immiscible for all compositions investigated. Both the additivity rule and excess Gibbs free energy of mixing indicated that the extent of immiscibility increased significantly with increasing the peptide mole fraction. Both *in situ* Brewster angle microscopy and *ex situ* fluorescence microscopy measurements indicated that the addition of Hel 13-5 to the DPPC monolayer increased the contribution of dipole-dipole repulsive interaction to the system. Successive compression-expansion cycles revealed that the incorporation of Hel 13-5 into the

DPPC monolayer decreases the substantial and irreversible loss of the phospholipid molecules after the first compression cycle. This is important characteristic of potential additive molecules in exogenous PS formulations.

7.4.2 Introduction

Endogenous lung surfactant is a lipid-protein mixture that forms a thin film at the air-alveolar interface. The lipids are mainly composed of phospholipids, with small amounts of other lipids, primarily cholesterol. Phosphatidylcholines (PCs) are the prevalent phospholipid. Half of the PC is DPPC, which is the main phospholipid component responsible for reducing surface tension during respiration. The surfactant proteins (SPs) are categorized into four types, namely A, B, C and D. SP-A and D are hydrophilic and are the first line of defense againstinhaled pathogens. SP-B and C are hydrophobic and dominate the surface activity of lung surfactant.[1]

Among the many lung diseases found in mammals, two are directly related either to surfactant deficiency, primarily respiratory distress syndrome (RDS), or dysfunction such as acute lung injury (ALI) and the acute respiratory distress syndrome (ARDS).[2] Surfactant replacement therapies are the most efficient interventions for such diseases. Effective therapeutic mixtures should be able to achieve low surface tension, to adsorb rapidly at the air-water interface and to replenish surface film effectively during compression-expansion cycles. It has been suggested that replacement exogenous surfactants (natural, modified or artificial) that are compositionally analogous to the endogenous surfactant may exhibit physiological activity. This makes the content of both lipids and proteins in exogenous lung surfactants highly important.[3]

The content of hydrophobic proteins (SP-B and C) in animal-derived surfactant preparations such as Survanta and Curosurf varies from batch to batch and is significantly lower than the content of endogenous surfactant.[4] This has led to a new class of replacement surfactants

that contain simplified peptides designed to mimic the biophysical properties of the endogenous surfactant.[3] Various studies have concluded that the secondary structure of SP-B contains α-helices that contribute to the biophysical function of that protein.[5-7] This suggests that synthetic peptides with a sequence corresponding to those helical regions are potentially useful additives for replacement therapeutics.

Cochrane and Revak[8] found that a peptide sequence made of 21 amino acids, consisting of positively charged lysine (K) residues interspaced with hydrophobic leucine (L) residues according to the following sequence [lysine-$(leucine)_4]_4$-lysine (abbreviated by KL_4), had equal activity to that of SP-B upon mixing with DPPC, palmitoyl-oleoyl phosphatidylglycerol (POPG) and palmitic acid. Recently, Lucinactant (Surfaxin) became the first FDA approved synthetic surfactant based on KL_4. It shows superiority over protein-free synthetic surfactants and it is effective as animal-derived surfactants in treatment and prevention of RDS in premature infants.[9]

Sugihara and co-workers[10] synthesized an α-helical peptide, namely Hel 13-5, composed of five lysine, twelve leucine and one tryptophan (W) residues, with the following overall amino acid sequence: KLLKLLLKLWLKLLKLLL. The tryptophan residue was introduced to allow detection of the peptide by means of fluorescence microscopy. It was found that the hydrophobic and the hydrophilic residues tend to be fully separated in the secondary structure and form polar and non-polar faces. This complete separation generates an ideal helical structure, unlike KL_4, which shows a disheveled helical configuration. This separation led to an increased affinity for lipid binding (compared to other helical peptides with similar hydrophobic-hydrophilic properties), promotes the peptide self-assembly and enhances its interfacial properties.[11] The potential use of Hel 13-5 as an SP-B analogue has been investigated extensively at air-water and air-solid interfaces.[6,11-18] Kinetic measurements indicated that Hel 13-5 enhanced the adsorption

of sub-surface DPPC molecules to the air-water interface.[11] *In situ* fluorescence images revealed that the interaction of Hel 13-5 with PCs depends strongly on the degree of phospholipid saturation.[11,12] It was found that Hel 13-5 promoted the nucleation of ordered DPPC domains, while it induced the shrinkage of the liquid condensed domains in PCs mixtures. Surface pressure-area isotherm measurements of PCs-Hel 13-5 mixed monolayers suggested that Hel 13-5 was squeezed out of the film once the collapse pressure had been passed.[11-13] This was confirmed by atomic force microscopy measurements that indicated the formation of peptide protrusions above and beneath the monolayer.[11] Moreover, it has been reported that Hel 13-5 plays a major role in refining the composition of surface films by promoting the exclusion of anionic phosphatidylglycerols out of the monolayer during monolayer compression.[13] This is of great importance for lung surfactant functions as it leaves behind a surfactant film that is highly enriched with PCs to reach very low surface tension values. Moreover, the influence of different lung surfactant additives such as fatty acids, hydrogenated and semi-fluorinated alcohols on a mixture consisting of DPPC and Hel 13-5 have been investigated extensively.[17,18] While the previously described studies provided important information about mixed phospholipids-Hel 13-5 monolayers, a major drawback of most of those studies, particularly those related to the PCs-Hel 13-5 mixtures, is the excessive amount of the added peptide in comparison with that found in endogenous lung surfactant). This may alter and (or) eliminate some important aspects of the lipid-peptide interaction. In fact, endogenous pulmonary surfactant contains about 6–8% by weight of SPs.[18] It has been reported previously that high concentration of SP-B and SP-C were found to influence the surface activity of phospholipids in a concentration-dependent fashion and to perturb membrane packing.[19-21] This suggests that it would be instructive to investigate the

properties of potential lung surfactant mixtures that are compositionally analogous to the endogenous surfactant.

In this work, we investigated the mixing thermodynamics, film morphology (at the air-water and air-solid interfaces) and film hysteresis after repeated compression-expansion cycles of binary mixtures made of DPPC and Hel 13-5 containing about ~ 1.4 to 9.5% by weight of the peptide on a highly simplified lung fluid (pH 7.4, 150 mM NaCl) mimic subphase. Results indicated that the two film components were immiscible. The addition of Hel 13-5 induced some morphological variation of the DPPC monolayer and enhanced its re-spreading, which is highly desirable for lung surfactant applications.

7.4.3 Materials and Methods

7.4.3.1 Chemicals

DPPC (semisynthetic, 99%) was purchased from Sigma–Aldrich Corporation. The fluorescent probe, 2-(4,4-difluoro-5-methyl-4-bora-3a,4a-diaza-s-indacene-3-dodecanoyl)-1-hexadecanoyl-sn-glycero-3- phosphocholine (Bodipy-PC) was purchased from Invitrogen Corp, sodium chloride and n-hexane were purchased from Fisher Scientific, absolute ethanol (99%) was purchased from Greenfield Ethanol Inc., chloroform was purchased from Merck KGaA, methanol was purchased from Sigma–Aldrich and sodium hydroxide was purchased from EMD. All reagents were used as received without additional purification. Hel 13-5 (MW: 2119.9 Da) was synthesized by Dr. Jan Rainey's laboratory (Dept. of Biochemistry and Molecular Biology) and the composition was confirmed by electrospray ionization mass spectrometry measurements. It should be noted that the fluorescent amino acid tryptophan was replaced with a cysteine residue in this peptide.

Microscope cover glass (No. 1.5, VWR International) was rinsed thoroughly with ethanol and dried under nitrogen gas. The slides were then placed in a plasma cleaner (PDC-32G, Harrick Plasma) for ~20 min at high power to remove any residual contaminants.

7.4.3.2 Surface Pressure-Area Isotherms and Langmuir–Blodgett Film Deposition

Stock solutions of DPPC (1.25 mM) and Hel 13-5 (0.1 mM) were prepared by dissolving the solid compounds in 9:1 and 4.5:5.5 volume ratio of n-hexane:ethanol respectively. The solutions were combined in appropriate volumes to give the following mole fraction (and the equivalent weight percentages) of Hel 13-5:

Mole fraction (χ)	0.005	0.010	0.015	0.020	0.025	0.030	0.035
Wt%	1.4%	2.8%	4.2%	5.6%	6.9%	8.2%	9.5%

Surface pressure-mean molecular area (π-*A*) isotherms were measured in a Langmuir mini-trough and LB films were prepared using a standard Langmuir trough (KSV NIMA). A subphase of 150 mM NaCl was prepared using ultrapure water (Millipore, resistivity 18 MΩ·cm). The pH was adjusted to 7.4 ± 0.2 using NaOH. The subphase temperature was controlled using an external circulating water bath at 25 ± 1 °C and the surface pressure was monitored using a Wilhelmy balance equipped with platinum plate. An aliquot of the amphiphile solution was spread on the subphase surface and the solvent was allowed to evaporate prior to compression. Hysteresis measurements were performed by recording five successive compression-expansion cycles with no lag time between consecutive cycles. For the fluorescent probe-doped samples, stock solutions of the Bodipy-PC was prepared in 8:1:1 volume ratio of n-hexane:chloroform:methanol. Aliquots of the fluorescent probe solutions were added to the surfactant mixtures to prepare 2.5×10^{-3}% Bodipy-PC (moles of dye per 100 moles of total surfactant). The glass substrate was immersed in the subphase prior spreading the amphipile

solution and the film was compressed to a surface pressure of 10 mN/m. The film was allowed to stabilize for 10 minutes before the glass substrate was pulled upward through the water-air interface in a single stroke. The film was left to dry at room temperature.

7.4.3.3 Brewster Angle Microscopy

The monolayer was measured using a KSV NIMA UltraBAM system (KSV NIMA) equipped with a 658 nm illumination laser and a CCD camera (collection rate of 20 frames/s). As with LB film deposition, the monolayer was compressed to the desired surface pressure and real time images of the surface were collected. The angle of the incident beam to the air-water interface was fixed to the Brewster angle (53.1°).

7.4.3.4 Fluorescence Microscopy

Bodipy PC doped LB films were imaged using a modified laser scanning confocal microscope (LSM Tech). Samples were excited at 457 nm using a laser line obtained from argon ion. Fluorescence emission was filtered with a 500 nm long-pass filter.

7.4.4 Results and Discussion

Surface pressure-area isotherms of DPPC, Hel 13-5 and their mixtures measured at 25°C using a 150 mM NaCl subphase of pH 7.4 are shown in Figure 7-1 (A and B). The isotherm of pure DPPC was consistent with those reported elsewhere in the literature.[22-25] The isotherm consisted of a liquid expanded phase (LE), liquid condensed phase (LC), a LE-LC coexistence region between 8.5 and 10 mN/m and a collapse plateau at about 71 mN/m. The limiting area ($A_\circ$) of DPPC molecules under close-packed conditions obtained by extrapolating the mean molecular area of the LC phase to zero surface pressure was 56 $Å^2$/molecule. The isotherm of Hel 13-5 reflects the formation of a highly expanded monolayer in comparison of DPPC, with no LE-LC phase transition and a collapse plateau at ~ 35 mN/m. The extrapolated area, which was

265 Å^2/molecule, was in good agreement with that reported previously by Nakahara et.al.[11] This indicates that the replacement of tryptophan with cysteine does not significantly alter the surface properties of the peptide.

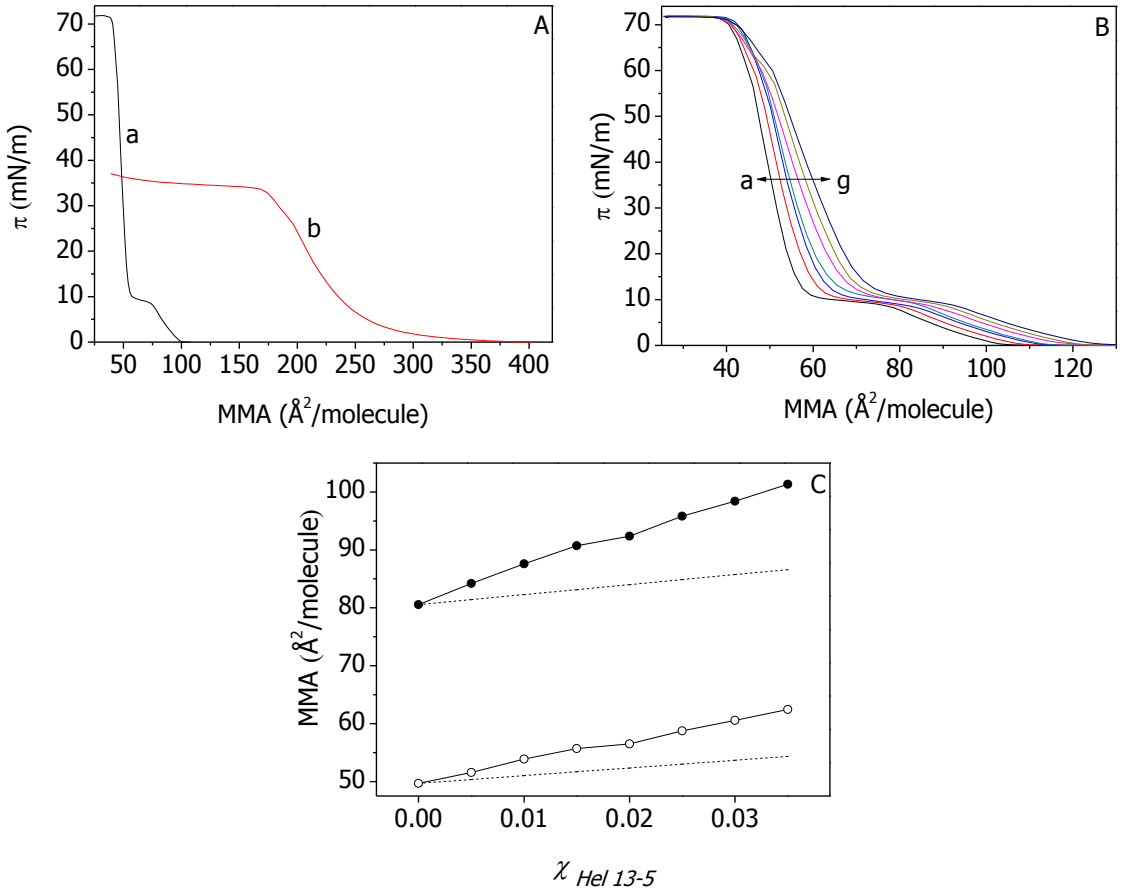

Figure 7-1 (A) Surface pressure-mean molecular area isotherms of pure components, a: DPPC, b: Hel 13-5. (B) Surface pressure-mean molecular area isotherms of a: χ_{Hel} = 0.005, b: χ_{Hel} = 0.01, c: χ_{Hel} = 0.015, d: χ_{Hel} = 0.02, e: χ_{Hel} = 0.025, f: χ_{Hel} = 0.03 and g: χ_{Hel} = 0.035. (C) Mean molecular area as a function of mole fraction of Hel 13-5. Filled (●) and empty (○) circles corresponds to experimental mean molecular area measured at 6 and 30 mN/m respectively. The dashed line represents the ideal behavior predicted by the additivity relationship. The percentages correspond to the area occupied by the LC domains.

The isotherms for the mixed monolayers (Figure 7-1B) fell in between tp=hose of the pure components. They were shifted laterally to a higher mean molecular area and vertically to a higher surface pressure as the mole fraction of the peptide was increased. While the lateral shift is expected from the expanded peptide monolayer, the increase in the LE-LC transition pressure indicates that the area occupied by the LC-DPPC domains is decreased with increasing mole

fraction of Hel 13-5, i.e., the monolayer becomes more fluid in the presence of the peptide. Moreover, the mixed monolayers retained a constant collapse pressure (equal to that of pure DPPC) regardless of the amount of peptide.

Herein, it was assumed that the collapse pressure of Hel 13-5 was too small to be detected because small amounts of Hel 13-5 (χ_{Hel} range between 0.005 and 0.035) have been used. The constant collapse pressure indicates that the monolayer components are immiscible.

Monolayer miscibility was further examined using the additivity rule, which relates the experimental mean molecular area obtained from surface pressure-area isotherms and those of the pure component according to the following equation:

$$A_{12} = A_1\chi_1 + A_2\chi_2 \qquad (7.1)$$

where A_{12} represents the mean molecular area of the mixed film at a specific surface pressure, A_i and χ_i are the molecular area and the corresponding molar fraction of the i^{th} component respectively. A detailed discussion of equation (7.1) has been provided in Chapter 2. Figure 7-1C shows both the experimental mean molecular area and the ideal behavior predicted by the additivity rule before and after the occurrence of the phase transition. The two sets of data indicated positive deviations from ideality. This deviation became more pronounced with increasing mole fraction of the peptide. Such behavior can be explained by the repulsive interaction between the positively charged lysine amino acid located at the lower part of the helix and the positively charged choline group of the DPPC. These data are consistent with the conclusion derived from the collapse pressure values obtained from the isotherm measurements, which indicated that the film forming components were immiscible.

The extent of the lipid-peptide interaction was evaluated quantitavely through the excess Gibb's energy of mixing, ΔG_{ex}^{π}. This excess function was calculated by measuring the area under

curve of the surface pressure-area isotherm for the mixed monolayer film (σ_{12}) up to a specific surface pressure and subtracting this value from the integrated area of the surface pressure-area isotherm of the pure components (σ_i) at the same surface pressure multiplied by the corresponding molar fraction, according to the following equation:

$$\Delta G_{ex}^{\pi} = \int_0^{\pi} [\sigma_{12} - (\chi_1\sigma_1 + \chi_2\sigma_2)]d\pi \qquad (7.2)$$

Again, a detailed explanation of equation (7.2) has been provided in Chapter 2. ΔG_{ex}^{π} values of the lipid-peptide mixed monolayers as a function of the peptide mole fraction are presented in Figure 7-2. The excess energy values were positive over the entire range of both surface pressures and composition. This agreed with the previous measurements (both the additivity and isotherm) and indicated that the repulsive forces between the positive charge of the zwitterionic DPPC and the lysine amino acids molecules increases as intermolecular distances between the lipid and peptide were decreased upon compression.

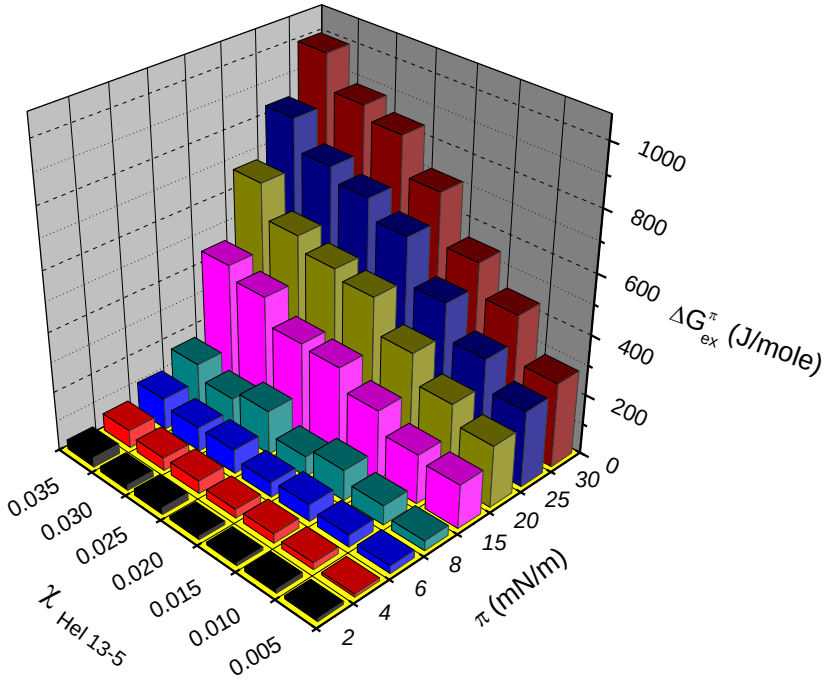

Figure 7-2 Plot of excess Gibbs free energies of mixing of DPPC-Hel 13-5 mixed monolayer as a function of film composition and surface pressure.

The excess energy values increased from a few tens of joules per mole in the LE phase up to ~ 1000 J/mol in the LC phase. These values are much larger than the ideal Gibbs free energy of mixing (ranges from ~ -78 to -378 J/mol for mixtures under investigation) and smaller than the thermal energy (RT ~ 2500 J/mol). This indicates that the enthalpic contribution due to repulsive interactions dominates over the entropic contribution over the entire range of compositions measured. So, it is anticipated that the peptide component will be phase separated with the phospholipid component until it is expelled out of the monolayer at surface pressures above the collapse plateau of the Hel 13-5. Shibata and co-worker[18] reported that the addition of either fatty acids or fatty alcohols to DPPC-Hel 13-5 mixed monolayer enhanced the squeezing-out of the peptide. This indicated that the attractive interaction between both the acid and alcohol with Hel 13-5 was enough to compensate the modest repulsive interaction between the peptide and the phospholipid.

Brewster angle microscopy (BAM) was used to visualize the influence of Hel 13-5 on the morphology of DPPC film in situ at the air-water interface. BAM micrographs of pure DPPC and DPPC-Hel 13-5 mixed monolayers are shown in Figure 7-3. In the LE phase, DPPC monolayer appeared as a featureless, dark gray background (images are not shown) up to the LE-LC coexistence region, after which the LC domain started to form small (ranged from 2 to 58 μm), bright structures dispersed in a continuous dark background. The nucleation of such structures led to the characteristic multi-lobed LC domains (Figure 7-3A).[26] Further compression increased the percentage surface area occupied by LC domains (Figure 7-3A'), until the microscope could no longer resolve the spacing between them. The addition of Hel 13-5 to DPPC monolayer caused both the shape and surface density of LC domains to change dramatically. As shown in Figure 7-3 (B and C), the molecular density of the LC domains decreased, especially at χ_{Hel} =

0.005 and 0.01. This is expected from both the highly expanded Hel 13-5 monolayer (deduced from the isotherm measurements) and the vertical shift of the mixed monolayer isotherms to a higher surface pressure. However, the accompanied lateral shift to higher mean molecular area became more pronounced at higher peptide fraction. This made the onset of the LE-LC coexistence region domains take place at larger area and leads to a larger number of LC domains to appear in the BAM micrographs (Figure 7-3 (D, D', E and E')).

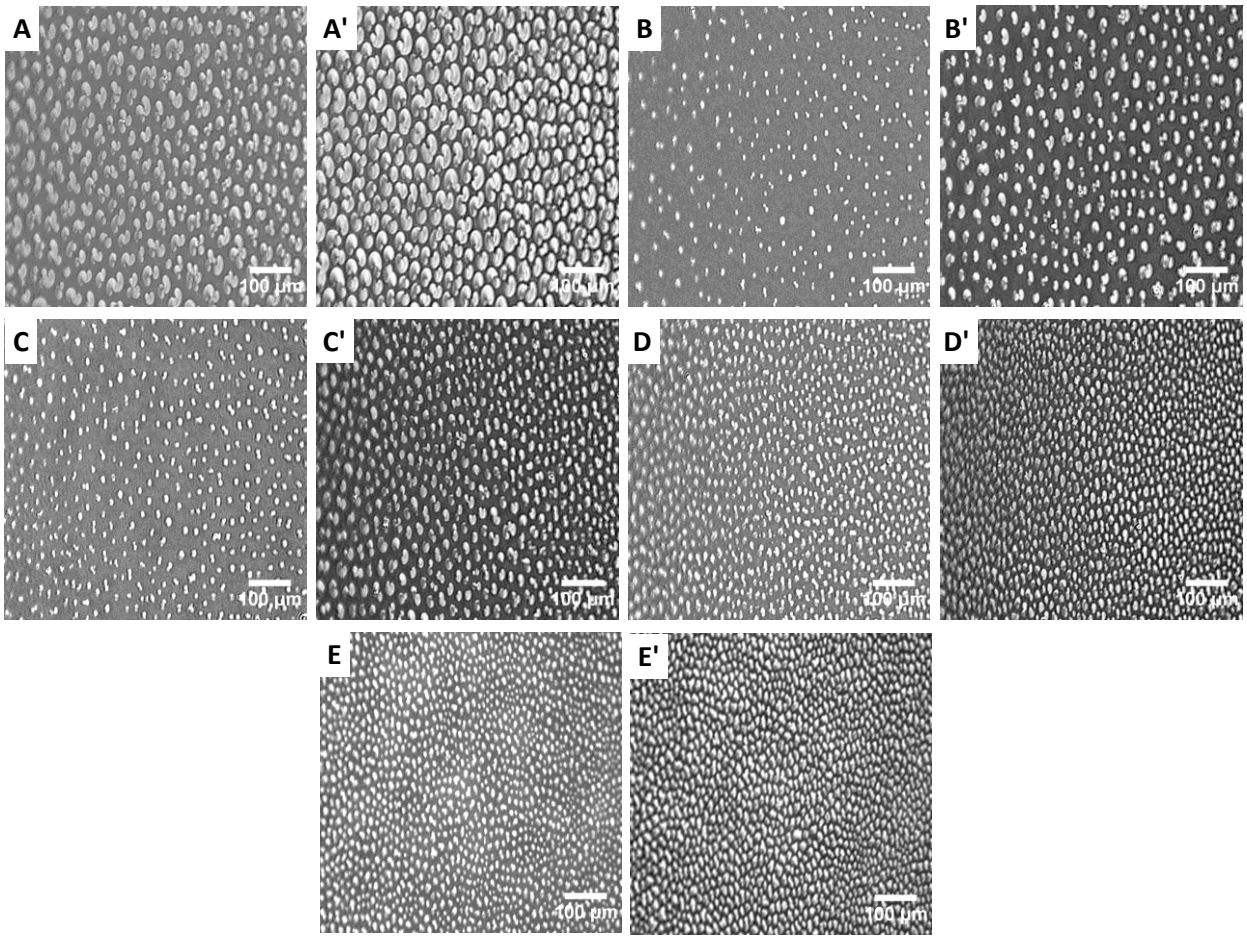

Figure 7-3 Brewster angle micrographs at the air-water interface of (A, A'): DPPC (at 9.7 and 10.1 mN/m), (B, B'): χ_{Hel} = 0.005 (at 9.7 and 10.1 mN/m), (C, C'): χ_{Hel} = 0.01 (at 9.7 and 10.1 mN/m), (D, D'): χ_{Hel} = 0.015 (at 9.7 and 10.1 mN/m) and (E, E'): χ_{Hel} = 0.03 (at 9.7 and 10.1 mN/m).

The shape of the DPPC-LC domains is mainly governed by the line tension of phase boundaries and repulsive dipolar interactions.[27,28] The former provides a driving force to form

large, often circular domains to decrease the total boundary length between coexisting phases in a given system. Long-range electrostatic repulsive interaction favors to form small and or elongated domains to decrease repulsion between molecular dipoles. The addition of Hel 13-5 led to morphological variations in the mixed film structures. At χ_{Hel} = 0.005-0.01, the characteristic multi-lobed structures of the DPPC-LC domains could still be observed. A further increase in peptide concentration led to small, roughly circular in shape domains instead of the characteristic lobe-structure (Figure 7-3 (D, D', E and E')). The circular shapes imply that line tension dominates the phase boundaries between the coexisting phases. However, the minimum overall repulsive interaction between the peptide polar amino acid and the choline group of the DPPC was achieved by disintegrating the large domains into smaller ones. i.e., dipolar repulsion is the dominant interaction.

To gain more insight into the morphology of the mixed monolayer films, Langmuir-Blodgett films were prepared, doped with Bodipy-PC, a fluorescently labeled DPPC analogue, transferred from the air-water onto glass substrate and imaged using confocal fluorescence microscopy (CFM). Bodipy-PC tends to partition itself preferentially in the LE phase and it is excluded from the LC phase.[29] This means the bright regions in the CFM images correspond to both DPPC-LE phase and Hel 13-5 as it tends to form homogeneous, disordered films. The dark regions correspond to the LC phase. Figure 7-4 shows CFM images of LB films doped with Bodipy-PC. Figure 4A indicates that the DPPC-LC domains occupied most of the available space with small voids that correspond to the LE phase. The characteristic lobed domains found previously at the same surface pressure can no longer be observed. This may be caused by weak dipole–dipole repulsions or instability of the lobed structures that tend to fuse together upon transfer to the glass substrate. A similar trend was demonstrated by 2-hydroxyethyl laurate

monolayers at air-water interface.[30,31] Hossain and Kato reported that at low temperature, line tension lead to formation of large, circular LC domains.[30] Decreasing the line tension by increasing the temperature would result in dendritic patterns that tend to fuse with each other by the progress of time.[31]

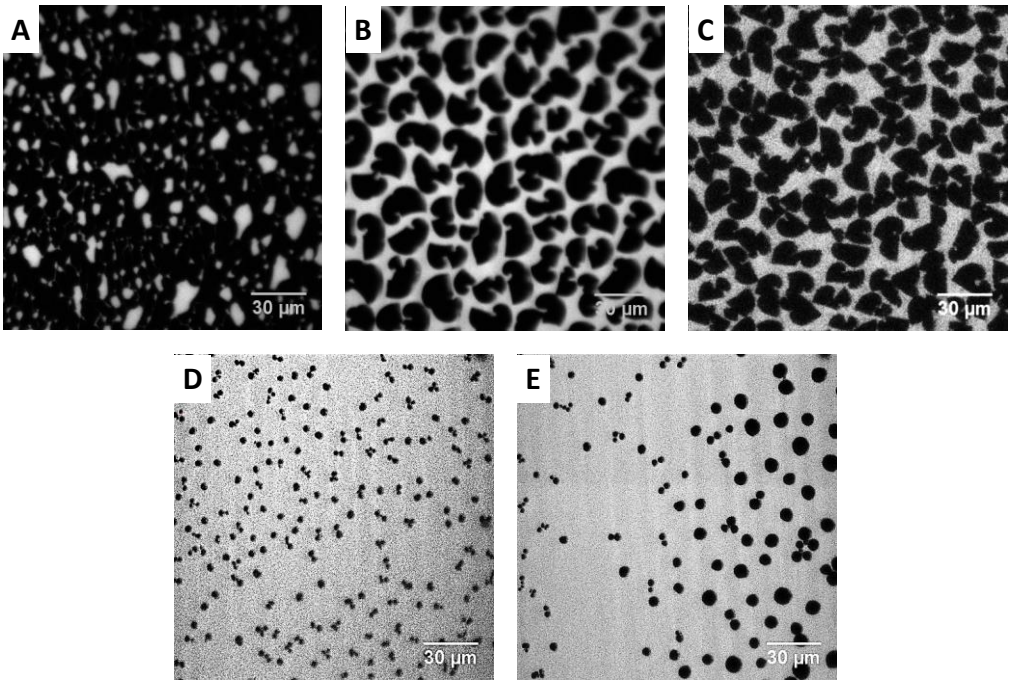

Figure 7-4 Confocal fluorescence images of LB films doped with Bodipy-PC and deposited on glass substrate at 10 mN/m, A: DPPC, B: χ_{Hel} = 0.01, C: χ_{Hel} = 0.015, D and E: χ_{Hel} = 0.03.

The addition of Hel 13-5 (χ_{Hel} = 0.01 and 0.015, Figure 7-4 (B and C)) to the DPPC monolayer hindered domain fusion and the lobed structure was retained. This appears to be a direct consequence of the long-range repulsive forces established between the peptide and the phospholipid that tend to keep the LC domains well-separated. At χ_{Hel} = 0.03 (Figure 7-4D), the dipolar repulsion induced the DPPC-LC patches into small circular domains. This is consistent with the morphology demonstrated by BAM. However, the formation of large circular domains was also observed (Figure 7-4E). This suggests that during the LB film deposition, the small domains underwent coalescence.

Repeated compression-expansion cycles of DPPC-Hel 13-5 mixed monolayers were performed in order to evaluate the influence of Hel 13-5 on the re-spreading ability of DPPC. The extent of isotherm displacement to a lower mean molecular area reflects the tendency of both the squeezed out molecules to re-integrate into the monolayer film upon subsequent re-expansion. Monolayer hysteresis can be described quantitatively by comparing the area under the curve of each compression isotherm with respect to that of the first compression cycle according to the following formula:

$$\%\, Recovery = \frac{area\ under\ isotherm\ curve\ for\ n^{th}\ compression\ cycle}{area\ under\ isotherm\ curve\ for\ 1^{st}\ compression\ cycle}\ x\ 100\% \qquad (7.3)$$

Although the hysteresis of DPPC-Hel 13-5 mixed monolayers has been studied extensively by Nakahara et.al.[11,12], the minimum amount of the incorporated peptide was three times larger the maximum amount used in this study (χ_{Hel} = 0.1 compared to 0.035). This corresponds to ~25% by weight compared to endogenous protein content of about 6–8%.

Table 7-1 represents percent hysteresis of the mixed monolayers for n = 5 compression cycles. The hysteresis response of the DPPC monolayer is consistent with the previously reported values[26] and suggests the irreversible loss of DPPC molecules from the surface monolayer compressed past the collapse plateau. However, the incorporation of Hel 13-5 into the monolayer film improved the re-spreading of DPPC films even after the fifth compression. According to the isotherm measurements, the repulsive interaction between the peptide and the DPPC suggest the exclusion of Hel 13-5 beyond ~37 mN/m. This will lead to formation of both surface and sub-surface aggregates. The ability of Hel 13-5 to interact with the sub-surface phospholipid aggregates and its tendency to re-spread back to the interface upon the sub-sequent expansion (see [13] for further details) will induce the sub-surface phospholipid molecules to re-integrate themselves to the surface film.

Table 7-1 Hysteresis response of pure DPPC and DPPC-Hel mixed monolayers as a function of consecutive compression-expansion cycles.

No. of compression cycles	***DPPC***	χ_{Hel} ***0.005***	χ_{Hel} ***0.010***	χ_{Hel} ***0.015***
2	*41% (±1%)*	*48% (±3%)*	*55% (±2%)*	*56% (±2%)*
3	*33%(±2%)*	*41% (±1%)*	*47% (±2%)*	*47% (±1%)*
4	*28% (±1%)*	*38% (±3%)*	*42% (±1%)*	*43% (±2%)*
5	*25% (±1%)*	*37% (±3%)*	*39% (±2%)*	*40% (±1%)*
	χ_{Hel} ***0.020***	χ_{Hel} ***0.025***	χ_{Hel} ***0.030***	χ_{Hel} ***0.035***
2	*63% (±2%)*	*64% (±2%)*	*65% (±0%)*	*65% (±2%)*
3	*54% (±1%)*	*58% (±2%)*	*58% (±0%)*	*57% (±1%)*
4	*50% (±1%)*	*53% (±2%)*	*54% (±0%)*	*53% (±0%)*
5	*46% (±0%)*	*49% (±1%)*	*50% (±1%)*	*50% (±1%)*

7.4.5 Conclusions

The thermodynamic measurements and film structures of Langmuir monolayers and LB films indicated that Hel 13-5 was immiscible with DPPC and improved the phospholipid re-spreading at mass fraction comparable to SP's content in the endogenous lung surfactants. These findings are consistent with the previously reported results indicating the potential application of Hel 13-5 as a lung surfactant additive. The importance of this study comes from the necessity of using a minimum amount of Hel 13-5 to evaluate its potential utility of the peptide for enhancing performance properties of DPPC in exogenous lung surfactant formulations.

7.4.6 References

1. Notter, R. H. *Lung Biology in Health and Disease;* Lung surfactants: Basic Science and Clinical Applications; Marcel Dekker: New York, USA, 2000; Vol. 149.

2. Willson, D. F.; Notter, R. H. The Future of Exogenous Surfactant Therapy. *Respir. Care* **2011**, *56*, 1369-1386.

3. Zuo, Y. Y.; Veldhuizen, R. A. W.; Neumann, A. W.; Petersen, N. O.; Possmayer, F. Current perspectives in pulmonary surfactant - Inhibition, enhancement and evaluation. *Biochim. Biophys. Acta, Biomembr.* **2008**, *1778*, 1947-1977.

4. Bernhard, W.; Mottaghian, J.; Gebert, A.; Rau, G.; von der Hardt, H.; Poets, C. Commercial versus native surfactants - Surface activity, molecular components, and the effect of calcium. *American Journal of Respiratory and Critical Care Medicine* **2000**, *162*, 1524-1533.

5. Kang, J.; Lee, M.; Kim, K.; Hahm, K. The relationships between biophysical activity and the secondary structure of synthetic peptides from the pulmonary surfactant protein SP-B. *Biochem. Mol. Biol. Int.* **1996**, *40*, 617-627.

6. Nakahara, H.; Lee, S.; Shibata, O. Specific interaction restrains structural transitions of an amphiphilic peptide in pulmonary surfactant model systems: An in situ PM-IRRAS investigation. *Biochimica Et Biophysica Acta-Biomembranes* **2010**, *1798*, 1263-1271.

7. Dohm, M. T.; Seurynck-Servoss, S. L.; Seo, J.; Zuckermann, R. N.; Barron, A. E. Close Mimicry of Lung Surfactant Protein B by "Clicked" Dimers of Helical, Cationic Peptoids. *Biopolymers* **2009**, *92*, 538-553.

8. Cochrane, C.; Revak, S. Pulmonary Surfactant Protein-B (Sp-B) - Structure-Function-Relationships. *Science* **1991**, *254*, 566-568.

9. Piehl, E.; Fernandez-Bustamante, A. Lucinactant for the Treatment of Respiratory Distress Syndrome in Neonates. *Drugs of Today* **2012**, *48*, 587-593.

10. Kiyota, T.; Lee, S.; Sugihara, G. Design and synthesis of amphiphilic alpha-helical model peptides with systematically varied hydrophobic-hydrophilic balance and their interaction with lipid- and bio-membranes. *Biochemistry (N. Y.)* **1996**, *35*, 13196-13204.

11. Nakahara, H.; Nakamura, S.; Hiranita, T.; Kawasaki, H.; Lee, S.; Sugihara, G.; Shibata, O. Mode of interaction of amphiphilic alpha-helical peptide with phosphatidylcholines at the air-water interface. *Langmuir* **2006**, *22*, 1182-1192.

12. Nakahara, H.; Nakamura, S.; Lee, S.; Sugihara, G.; Shibata, O. Influence of a new amphiphilic peptide with phospholipid monolayers at the air-water interface. *Colloids and Surfaces A-Physicochemical and Engineering Aspects* **2005**, *270*, 52-60.

13. Nakahara, H.; Lee, S.; Sugihara, G.; Shibata, O. Mode of interaction of hydrophobic amphiphilic alpha-helical peptide/dipalmitoylphosphatidylcholine with phosphatidylglycerol or palmitic acid at the air-water interface. *Langmuir* **2006**, *22*, 5792-5803.

14. Nakahara, H.; Lee, S.; Sugihara, G.; Chang, C.; Shibata, O. Langmuir monolayer of artificial pulmonary surfactant mixtures with an Amphiphilic peptide at the Air/Water enterface: Comparison of new preparations with surfacten (Surfactant TA). *Langmuir* **2008**, *24*, 3370-3379.

15. Nakahara, H.; Dudek, A.; Nakamura, Y.; Lee, S.; Chang, C.; Shibata, O. Hysteresis behavior of amphiphilic model peptide in lung lipid monolayers at the air-water interface by an IRRAS measurement. *Colloids and Surfaces B-Biointerfaces* **2009**, *68*, 61-67.

16. Nakahara, H.; Lee, S.; Shibata, O. Pulmonary Surfactant Model Systems Catch the Specific Interaction of an Amphiphilic Peptide with Anionic Phospholipid. *Biophys. J.* **2009**, *96*, 1415-1429.

17. Nakahara, H.; Lee, S.; Krafft, M. P.; Shibata, O. Fluorocarbon-Hybrid Pulmonary Surfactants for Replacement Therapy - A Langmuir Mono layer Study. *Langmuir* **2010**, *26*, 18256-18265.

18. Nakahara, H.; Lee, S.; Shoyama, Y.; Shibata, O. The role of palmitic acid in pulmonary surfactant systems by Langmuir monolayer study: Lipid-peptide interactions. *Soft Matter* **2011**, *7*, 11351-11359.

19. Shiffer, K.; Hawgood, S.; Haagsman, H.; Benson, B.; Clements, J.; Goerke, J. Lung Surfactant Proteins, SP-B and SP-C, Alter the Thermodynamic Properties of Phospholipid-Membranes:A Differential Calorimetry Study. *Biochemistry* **1993**, *32*, 590-597.

20. Perezgil, j.; casals, C.; Marsh, D. Interactions of Hydrophobic Lung Surfactant Proteins Sp-B and Sp-C with Dipalmitoylphosphatidylcholine and Dipalmitoylphosphatidylglycerol Bilayers Studied by Electron-Spin-Resonance Spectroscopy. *Biochemistry* **1995**, *34*, 3964-3971.

21. Cabre, E. J.; Loura, L. M. S.; Fedorov, A.; Perez-Gil, J.; Prieto, M. Topology and lipid selectivity of pulmonary surfactant protein SP-B in membranes: Answers from fluorescence. *Biochimica Et Biophysica Acta-Biomembranes* **2012**, *1818*, 1717-1725.

22. Duncan, S. L.; Larson, R. G. Comparing experimental and simulated pressure-area isotherms for DPPC. *Biophys. J.* **2008**, *94*, 2965-2986.

23. Eftaiha, A. F.; Paige, M. F. The influence of salinity on surfactant miscibility in mixed dipalmitoylphosphatidylcholine-perfluorooctadecanoic acid monolayer films. *J Colloid Interface Sci* **2011**, *353*, 210-219.

24. Eftaiha, A. F.; Brunet, S. M. K.; Paige, M. F. Thermodynamic and structural characterization of a mixed perfluorocarbon-phospholipid ternary monolayer surfactant system. *J. Colloid Interface Sci.* **2012**, *368*, 356-365.

25. Eftaiha, A. F.; Brunet, S. M. K.; Paige, M. F., Eds.; In *A Comparison of Atomic Force Microscopy,Confocal Fluorescence Microscopy and Brewster Angle Microscopy for Characterizing Mixed Monolayer Surfactant Films;* Méndez-Vilas, A., Ed.; Current Microscopy Contributions to Advances in Science and Technology; Formatex: Spain, 2012; Vol. 2.

26. Eftaiha, A. F.; Brunet, S. M. K.; Paige, M. F. Influence of Film Composition on the Morphology, Mechanical Properties, and Surfactant Recovery of Phase-Separated Phospholipid-Perfluorinated Fatty Acid Mixed Monolayers. *Langmuir* **2012**.

27. McConnell, H. Structures and Transitions in Lipid Monolayers at the Air-Water-Interface. *Annu. Rev. Phys. Chem.* **1991**, *42*, 171-195.

28. Sriram, I.; Schwartz, D. K. Line tension between coexisting phases in monolayers and bilayers of amphiphilic molecules. *Surface Science Reports* **2012**, *67*, 143-159.

29. McConnell, H.; Tamm, L.; Weis, R. Periodic Structures in Lipid Monolayer Phase-Transitions. *Proceedings of the National Academy of Sciences of the United States of America-Physical Sciences* **1984**, *81*, 3249-3253.

30. Hossain, M.; Yoshida, M.; Iimura, K.; Suzuki, N.; Kato, T. Phase transition in adsorbed monolayers of 2-hydroxyethyl laurate at the air-water interface. *Colloids and Surfaces A-Physicochemical and Engineering Aspects* **2000**, *171*, 105-113.

31. Hossain, M.; Kato, T. Line tension induced instability of condensed domains formed in adsorbed monolayers at the air-water interface. *Langmuir* **2000**, *16*, 10175-10183.

CHAPTER 8 RESEARCH WRAP UP: CONCLUSIONS AND FUTURE WORK

8.1 Conclusion

Despite the significant concerns related to the long-term bioaccumulation and potential toxicity of some fluorinated molecules,[1] fluorinated amphiphiles have potential biomedical applications such as diagnostic agents, oxygen carriers and exogenous lung surfactant additives.[2-4]

The difference in bulkiness and cohesive interaction between perfluorinated and hydrogenated surfactant tail groups promote phase separation in mixed surfactant systems.[4-6] This provides the ability to design two dimensional structures with a high level of control over the molecular-level composition. Mixed surfactant monolayers provide model systems to elucidate the interfacial properties and miscibility of fluorinated surfactants with biological membrane constituents, particularly phospholipids. Although mixed monolayers comprised of hydrogenated and fluorinated amphiphiles, particularly phospholipids and perfluorinated carboxylic acids (CnF's) have been studied extensively, the majority of these studies have been conducted using a highly acidic subphase conditions (pH ~1-2) that were far away from physiological conditions.[7-10, 11]

For fatty acid surfactants, if the subphase pH is kept above the pK_a value, a large fraction of the surfactant head groups will be ionized to form a negatively charged carboxylate. Adjusting the pH of the subphase using either acids or bases will change the net charge carried by the ionized monolayers. This change is a function of both identity and concentration of the added counter ion(s).[12]

In order to evaluate the utility of fluorinated fatty acids for biomedical applications such as pulmonary surfactant (PS) replacement therapy, it is important to measure the interfacial behavior of phospholipids and CnF's under the physiological conditions prevalent in the lung alveolar lining layer. To the best of our knowledge, none of the previously reported studies have been conducted in an environment relevant to pulmonary lung surfactant applications.

In the first study described in this thesis, the mutual interaction between a perfluorinated fatty acid (C18F) and the two prevalent PS phospholipids (phosphatidylcholine and phosphotidylglycerol) was explored in Langmuir monolayer and Langmuir-Blodgett (LB) films using an ion-free water subphase (Millipore water, resistivity = 18 MΩ.cm and pH ~ 5.5). This research was important to understand the elementary interactions that exist between the surfactant pairs and to establish a basis for future research, as it may ultimately lead to control over the surface patterning of perfluorinated carboxylic acid-phospholipids mixed films. One of the major findings in this manuscript was the significant film stabilization imparted by head group attractive interaction between DPPC and C18F that led to formation of micro- and nanometer size phospholipid-rich domains. These domains are of potential importance for PS applications as they represent surfactant reservoirs that can promote surfactant re-spreading during film expansion. This will ensure that sufficient surfactant is available to lower surface tension during subsequent expansion cycles.[13] This might mimic one of the biophysical functions of pulmonary surfactant protein A (SP-A) that promotes the association of phospholipids sub-surface aggregates that showed excellent adsorption and dynamic surface tension lowering ability. It is important to recall that due to immunological considerations, none of the modified natural surfactant mixtures used as therapeutic agents contain hydrophilic surfactant proteins (like SP-A), because they are removed during purification processes.[14]

Addition of perfluorinated surfactants to DPPC resulted in efficient solubilisation and dispersion of liquid-condensed domains (LC) in phospholipid monolayers. It is anticipated that this may inhibit the formation of crystalline DPPC films upon monolayer compression, thereby enhancing its re-spreading ability during successive compression expansion cycles. It seems C18F is functionally equivalent to gaseous fluorocarbons that prevented the formation of LC-DPPC domains upon film compression under an atmosphere saturated with fluorocarbon vapors.[15,16]

It has been reported that surfactant head group interactions are highly affected by ion binding.[12,17] Therefore, it was deemed important to explore the effect of subphase salinity on the miscibility of DPPC-C18F mixed monolayers as a minimal PS mixture, especially because potential biomedical surfactant mixtures will be used in a high ionic strength environment. Extracellular fluid is characterized by a large concentration of both sodium (Na^+) and chloride (Cl^-) ions (140 and 110 mM respectively) and relatively small concentration of potassium (K^+, 4 mM), calcium (Ca^{2+}, 2.5 mM) and magnesium (Mg^{2+}, 1mM).[18] To gain a better understanding of surfactant's interfacial behavior, the effect of varying the concentration of sodium chloride in the underlying subphase (0-400 mM NaCl, pH ~ 5.5) on surfactant miscibility, compressibility and morphology of LB films was investigated in the second manuscript to definitely map ion-surfactant interactions at both air-water and air-solid interfaces. It was found that the addition of NaCl to the aqueous subphase reduced the attractive interactions between the phospholipid and the fluorinated fatty acid head group, due to the specific adsorption of Na^+ to the negatively charged carboxylate group of C18F. This had a negative impact on the multimolecular aggregates described previously, as they vanished at high salt concentration. The disappearance of the liquid expanded (LE) – LC phase transition of the DPPC isotherms continued to take place

the presence of the perfluorcarbon even at high subphase salinity, indicating that it aided the solubilization of the phospholipid regardless of the subphase salinity.

To gain insight into basic thermodynamics, structural and performance properties of DPPC-C18F mixed monolayers at more prevalent physiological conditions, a highly simplified lung mimic fluid (pH 7.4, 150 mM NaCl) was used in the third paper. Thermodynamic and microscopy measurements indicated that DPPC and C18F were completely immiscible and phase-separated. Monolayer compression led to preferential squeezing-out of the C18F molecules to form either surface or sub-surface aggregates. This is thought to be functionally important for PS films as it leaves behind a monolayer that is highly enriched with DPPC. This is necessary for real-life applications because non-DPPC components don't have the ability to lower surface tension as effectively as DPPC. Upon the subsequent expansion, the C18F molecules returned back into the surface film. Monolayer hysteresis measurements indicated that the incorporation of C18F into DPPC monolayer reduced the surfactants losses after repeated expansion-compression cycles. This might be explained by the lower tendency of the C18F molecules to form sub-surface aggregates compared to DPPC. For example, the critical micelle concentration of C18F is several orders of magnitude larger than that for DPPC. This mimics the biophysical function of both SP-B and SP-C as they facilitate phospholipids insertion into surface film though there interaction with the phospholipid headgroups and hydrophobic chains. Moreover, the addition of C18F to DPPC improved its spreading kinetics continued to solubilise the LC domains of the phospholipid, likely in the same manner under the previously examined conditions. The presence of compounds that disrupt packing of DPPC molecules in the highly compressed monolayer is important for enhanced surface film replenishment. This effect is

imparted by some endogenous PS constituents such as cholesterol or unsaturated phospholipids like dioleoyl phosphatidylcholine.[14]

As shown in the previous chapters (2-4), mixed lipid monolayers provide a simple model system to investigate interfacial behavior in biological interfaces such as the air-alveoli interface in the lungs. From this perspective, Langmuir monolayers and LB films are basic tools to examine surfactant assembly, phase transitions and phase separation at both air-water and air-solid interfaces. It has been recognized that the structure of the transferred film is influenced by a number of factors including the substrate interaction with amphiphilic molecules. The displacement of the aqueous subphase by a solid substrate changes the free energy of the monolayer, thereby creating morphological changes during after deposition. Möhwald and co-workers[19] suggested that strong intermolecular interactions between surfactant chains (particularly those with more than one tail group) tend minimize surfactant–substrate interactions. The main objective in Chapter 5 was to assess the effect of deposition process on the morphology of phase-separated mixed monolayer films comprised of hydrogenated and perfluorinated fatty acids at the solid-air and liquid–air interfaces using atomic force microscopy (AFM) and Brewster angle microscopy (BAM). Gross morphological assessment of the film structures indicated that the deposition process minimally perturbed the overall film structure. This means that the underlying solid substrate has not changed the observed films structures. Moraille and Badia [20] reported that the deposition of films made of DPPC and dilauroyl-*sn*-glycero-3-phosphocholine onto mica substrates resulted in the formation of nanoscale stripe patterns consisting of two lipids in different phases. The difference between the two phase separated mixed monolayers (i.e., the fully hydrogenated and the hydrogenated-fluorinated systems) might be explained by the strong sidechain interaction (the repulsive interaction

between alkyl and perfluorinated surfactant chains) that dominated over substrate-head groups interactions.

The combination of interaction between hydrophobic chains and polar head groups control the miscibility of hydrogenated and fluorinated surfactant mixed films. In chapters (2 – 4), the role played by surfactant head groups in controlling miscibility of mixed monolayer systems was explored. To elucidate the effect of atomic-level differences between hydrophobic chain lengths on the phase behavior of mixed monolayer films, MARTINI[21,22] coarse grained molecular dynamics (CG-MD) simulations were used to establish a link between phase separation and differences in surfactant tail polarities. Surfactant headgroup interactions have been negated by examining mixed monolayers made of amphiphilic molecules with the same head groups and different tail polarities. These can be changed easily using the MARTINI force field as it provides apolar beads with different degrees of polarity. To enlarge small differences between surfactant tail polarities, a film forming component made of two nonpolar tails instead of surfactants that have one nonpolar tail was used. DPPC was selected as a test molecule because its MARTINI force field description showed good agreement with experimentally measured isotherms.[23]

One of the major findings in this study was that the isotherms for single component monolayers were shifted to a higher surface pressure with increasing tail polarity. This is consistent with the results reported by Sarmiento and co-worker[24] who reported that the LE-LC coexistence region of the mono-fluorinated DPPC isotherms took place at higher pressures than that of fully hydrogenated DPPC. This means the high polarity beads provided by MARTINI force field represents a reasonable approximation of the fluorine atom. The agreement between simulation and experimental results of the single component monolayer indicated that the

MARTINI force field is of significant potential value for calculating properties related to the mixing behavior of fully hydrogenated and semi or perfluorinated surfactant (this can be achieved by investigating amphiphilic molecules of hydrophobic tails made of one or more high polarity beads). The measurements of the mixed monolayers made of two DPPC molecules with different tail polarities revealed the tendency of the film forming components to phase separate as a function of time and surface pressure. This chapter work showed that the MARTINI force field was able to reproduce the expected phase separation behavior between mixed monolayers comprised of surfactant molecules with different tail polarities. To the best of our knowledge this is the first time that the MARTINI force field has been used to investigate mixed monolayer composed of surfactant molecules of varying tail polarity. This provided a fast computational routine that has enabled the investigation of mixed surfactant monolayers on a microsecond timescale.

In Chapter 7, the impact of an α-helical peptide (Hel 13-5) that mimics the structural and functional aspects of SP-B, on the phase behavior of DPPC in Langmuir monolayers and LB films was examined. Although phospholipid-Hel 13-5 mixed monolayers have been studied extensively,[25-29] the majority of these studies incorporated a large amount of Hel 13-5 in comparison to the endogenous protein content. Results indicated that the two film components were immiscible and the addition of the Hel 13-5 to DPPC monolayers enhanced the phospholipid recovery during successive compression expansion cycles. This study is of particular importance to the research results discussed in Chapters (2-4) as it provided the necessary information to compare the effect of two potential PS additives, the perfluorinated fatty and the synthetic peptide on the performance characteristics of DPPC monolayers. Results indicated that both Hel 13-5 and C18F were immiscible with DPPC, they solubilized the LC

domains of the phospholipids and they enhanced the re-spreading properties of the DPPC monolayer after repeated compression expansion cycles. These findings reinforced the conclusions drawn from the previous studies (Chapters 2-4). Although the addition of the C18F to DPPC monolayers led to a high percentage recovery comparable to that obtained for the Hel 13-5 containing monolayers, the amount of C18F required was much higher than that of the peptide. This may highlight the importance of developing surfactant preparations containing inexpensive potential additives like perfluorocarboxylic acids compared to the relatively high cost associated with use of synthetic peptides and/or animal extracts.

8.2 Future Work

It is important to understand the biophysical characteristics of mixed phospholipid-fluorinated monolayers in order to tailor the structure, composition and mechanical properties of surfactant films at solid-air and liquid-air. This will help in accomplishing an ultimate goal of developing synthetic surfactant preparations that fully or closely mimic the biophysical properties of the endogenous surfactant. To achieve this goal, it is necessary to screen a wide range of fluorinated surfactants that show strong repulsive interactions with hydrogenated surfactants, have a relatively low collapse pressure, have a low tendency to form sub-surface aggregates and bear a negatively charged head group to be able to disrupt and fuse phospholipid sub-surface aggregates such as bilayers or vesicles to promote the adsorption of the phospholipid insertion into surface films. I suggest to explore the impact of a series of shorter CnF's molecules (particularly n = 16 and 14) on the interfacial behavior of DPPC monolayers, because they are anticipated to obey the above mentioned properties and they are more acceptable in the clinical field than long and perfluorinated surfactant chains.[30]

Moreover, it is important to measure the impact of progressive fluorination on the surface characteristic of a series of hydrogenated fatty acid to determine the percentage of fluorination at which surfactant tail interaction is sufficiently strong to overcome attractive interactions with the DPPC choline group head group. The results provided by the MARTINI force field CG simulation (Chapter 6) will be invaluable in this regard. However, it is important to first develop a new parameter to represent fluorinated beads explicitly (instead of using the high polarity beads) to investigate the surface behavior of a more realistic systems which allow to map the surfactants tail interaction precisely. Once this has been accomplished, the predictive powers given by the CG simulations can be used to guide optimal selection of the CnFs used for these works.

8.3 References

1. Riess, J. G. Highly fluorinated amphiphilic molecules and self-assemblies with biomedical potential. *Current Opinion in Colloid & Interface Science* **2009**, *14*, 294-304.

2. Krafft, M. P. Highly fluorinated compounds induce phase separation in, and nanostructuration of liquid media. Possible impact on, and use in chemical reactivity control. *Journal of Polymer Science Part A-Polymer Chemistry* **2006**, *44*, 4251-4258.

3. Nakahara, H.; Lee, S.; Krafft, M. P.; Shibata, O. Fluorocarbon-Hybrid Pulmonary Surfactants for Replacement Therapy - A Langmuir Monolayer Study. *Langmuir* **2010**, *26*, 18256-18265.

4. Krafft, M. P.; Riess, J. G. Chemistry, Physical Chemistry, and Uses of Molecular Fluorocarbon-Hydrocarbon Diblocks, Triblocks, and Related Compounds-Unique "Apblar" Components for Self-Assembled Colloid and Interface Engineering. *Chem. Rev.* **2009**, *109*, 1714-1792.

5. Krafft, M.; Goldmann, M. Monolayers made from fluorinated amphiphiles. *Current Opinion in Colloid & Interface Science* **2003**, *8*, 243-250.

6. Nakahara, H.; Shibata, O. Langmuir Monolayer Miscibility of Perfluorocarboxylic Acids with Biomembrane Constituents at the Air-Water Interface. *Journal of Oleo Science* **2012**, *61*, 197-210.

7. Lehmler, H.; Bummer, P. Mixing of perfluorinated carboxylic acids with dipalmitoylphosphatidylcholine. *Biochimica Et Biophysica Acta-Biomembranes* **2004**, *1664*, 141-149.

8. Nakahara, H.; Nakamura, S.; Kawasaki, H.; Shibata, O. Properties of two-component Langmuir monolayer of single chain perfluorinated carboxylic acids with dipalmitoylphosphatidylcholine (DPPC). *Colloids and Surfaces B-Biointerfaces* **2005**, *41*, 285-298.

9. Yokoyama, H.; Nakahara, H.; Shibata, O. Miscibility and phase behavior of DPPG and perfluorocarboxylic acids at the air-water interface. *Chem. Phys. Lipids* **2009**, *161*, 103-114.

10. Yokoyama, H.; Nakahara, H.; Nakagawa, T.; Shimono, S.; Sueishi, K.; Shibata, O. Miscibility behavior of two-component monolayers at the air-water interface: Perfluorocarboxylic acids and DMPE. *J. Colloid Interface Sci.* **2009**, *337*, 191-200.

11. Shibata, O.; Yamamoto, S.; Lee, S.; Sugihara, G. Mixed monolayer properties of tetradecanoic acid with n-perfluorocarboxylic acids with 10, 12, 14, 16, and 18 carbon atoms. *J. Colloid Interface Sci.* **1996**, *184*, 201-208.

12. Petty, M. C. *Langmuir-Blodgett Films: An Introduction;* Cambridge University Press: New York, USA, 1996; .

13. Zuo, Y. Y.; Veldhuizen, R. A. W.; Neumann, A. W.; Petersen, N. O.; Possmayer, F. Current perspectives in pulmonary surfactant - Inhibition, enhancement and evaluation. *Biochimica Et Biophysica Acta-Biomembranes* **2008**, *1778*, 1947-1977.

14. Notter, R. H. *Lung Biology in Health and Disease;* Lung surfactants: Basic Science and Clinical Applications; Marcel Dekker: New York, USA, 2000; Vol. 149.

15. Gerber, F.; Krafft, M.; Vandamme, T.; Goldmann, M.; Fontaine, P. Preventing crystallization of phospholipids in monolayers: A new approach to lung-surfactant therapy. *Angewandte Chemie-International Edition* **2005**, *44*, 2749-2752.

16. Gerber, F.; Krafft, M.; Vandamme, T.; Goldmann, M.; Fontaine, P. Fluidization of a dipalmitoyl phosphatidylcholine monolayer by fluorocarbon gases: Potential use in lung surfactant therapy. *Biophys. J.* **2006**, *90*, 3184-3192.

17. Satoh, K. Determination of Binding Constants of Ca^{2+}, Na^{+}, and Cl^{-} Ions to Liposomal Membranes of Dipalmitoylphosphatidylcholine at Gel Phase by Particle Electrophoresis. *Biochimica Et Biophysica Acta-Biomembranes* **1995**, *1239*, 239-248.

18. Raff, H. *Physiology Secrets, Second Edition;* Hanley & Belfus, Inc.: Philadelphia, USA, 2002; .

19. Leporatti, S.; Brezesinski, G.; Mohwald, H. Coexistence of phases in monolayers of branched-chain phospholipids investigated by scanning force microscopy. *Colloids and Surfaces A-Physicochemical and Engineering Aspects* **2000**, *161*, 159-171.

20. Moraille, P.; Badia, A. Highly parallel, nanoscale stripe morphology in mixed phospholipid monolayers formed by Langmuir-Blodgett transfer. *Langmuir* **2002**, *18*, 4414-4419.

21. Marrink, S.; de Vries, A.; Mark, A. Coarse grained model for semiquantitative lipid simulations. *J Phys Chem B* **2004**, *108*, 750-760.

22. Marrink, S. J.; Risselada, H. J.; Yefimov, S.; Tieleman, D. P.; de Vries, A. H. The MARTINI force field: Coarse grained model for biomolecular simulations. *J Phys Chem B* **2007**, *111*, 7812-7824.

23. Duncan, S. L.; Larson, R. G. Comparing experimental and simulated pressure-area isotherms for DPPC. *Biophys. J.* **2008**, *94*, 2965-2986.

24. Toimil, P.; Prieto, G.; Minones, J.,Jr.; Sarmiento, F. A comparative study of F-DPPC/DPPC mixed monolayers. Influence of subphase temperature on F-DPPC and DPPC monolayers. *Physical Chemistry Chemical Physics* **2010**, *12*, 13323-13332.

25. Nakahara, H.; Nakamura, S.; Lee, S.; Sugihara, G.; Shibata, O. Influence of a new amphiphilic peptide with phospholipid monolayers at the air-water interface. *Colloids and Surfaces A-Physicochemical and Engineering Aspects* **2005**, *270*, 52-60.

26. Nakahara, H.; Nakamura, S.; Hiranita, T.; Kawasaki, H.; Lee, S.; Sugihara, G.; Shibata, O. Mode of interaction of amphiphilic alpha-helical peptide with phosphatidylcholines at the air-water interface. *Langmuir* **2006**, *22*, 1182-1192.

27. Nakahara, H.; Lee, S.; Sugihara, G.; Shibata, O. Mode of interaction of hydrophobic amphiphilic alpha-helical peptide/dipalmitoylphosphatidylcholine with phosphatidylglycerol or palmitic acid at the air-water interface. *Langmuir* **2006**, *22*, 5792-5803.

28. Nakahara, H.; Lee, S.; Sugihara, G.; Chang, C.; Shibata, O. Langmuir monolayer of artificial pulmonary surfactant mixtures with an Amphiphilic peptide at the Air/Water enterface: Comparison of new preparations with surfacten (Surfactant TA). *Langmuir* **2008**, *24*, 3370-3379.

29. Nakahara, H.; Lee, S.; Shibata, O. Pulmonary Surfactant Model Systems Catch the Specific Interaction of an Amphiphilic Peptide with Anionic Phospholipid. *Biophys. J.* **2009**, *96*, 1415-1429.

30. Riess, J. G. Highly fluorinated amphiphilic molecules and self-assemblies with biomedical potential. *Current Opinion in Colloid & Interface Science* **2009**, *14*, 294-304.